NSSDC
WDC-A-R&S
National Space Science Data Center
World Data Center A For Rockets and Satellites
81-01

Coordinated Ionospheric and Magnetospheric Observations from the ISIS 2 Satellite by the ISIS 2 Experimenters

(NASA-TM-84022) LARGE STORMS: AIRGLOW AND RELATED MEASUREMENTS. VLF OBSERVATIONS, VOLUME 4 (NASA) 180 p HC A09/MF A01 CSCL 04A G3/46 N81-33717 Unclas 27613

Volume 4

A. Large Storms
B. Airglow and Related Measurements
C. VLF Observations

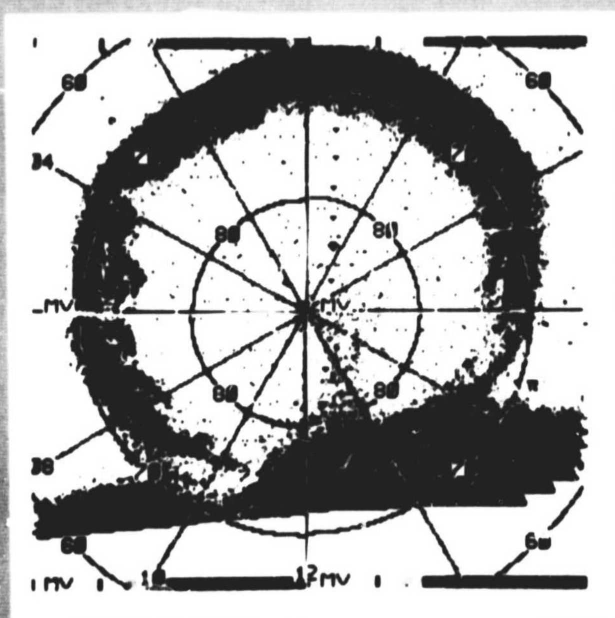

June 1981

COORDINATED IONOSPHERIC AND MAGNETOSPHERIC OBSERVATIONS FROM THE ISIS 2 SATELLITE BY THE ISIS 2 EXPERIMENTERS

VOLUME 4

A. LARGE STORMS

B. AIRGLOW AND RELATED MEASUREMENTS

C. VLF OBSERVATIONS

Coordinators:

A -- J. R. Burrows
National Research Council, Ottawa, Canada

B -- L. L. Cogger
University of Calgary, Alberta, Canada

C -- H. G. James
Communications Research Centre, Ottawa, Canada

June 1981

The Experimenters are grateful to the National Space Science Data Center, Greenbelt, Maryland, for making this publication possible.

This Data Book is dedicated

to the memory of John H. Chapman,

through whose efforts the Alouette-ISIS

satellite program became a reality.

TABLE OF CONTENTS

TABLE OF CONTENTS (continued)

I. INTRODUCTION

ISIS 2 is the fourth and final satellite launched in the Alouette/ISIS series. In this International Satellites for Ionospheric Studies program, Canada provided the spacecraft, data acquisition, and satellite control. The USA provided the launch capability, tracking, and data acquisition. Satellite instruments and data processing support were provided by both countries. During the course of the program these countries contributed telemetry support and collaborative data analysis: Australia, Finland, France, India, Japan, New Zealand, Norway, and the United Kingdom.

Alouette 1 won recognition mainly through the success of the topside sounder, but subsequent evolution led to a highly coordinated ISIS 2 satellite, having the capability for both direct measurements and remote sensing. Launched on April 1, 1971, into a near-circular near-polar orbit at 1400 km, it was essentially an observatory-type satellite with the potential of making fundamental measurements of both the ionosphere and magnetosphere, thereby yielding important information on the coupling processes between these regions.

At the time the program was planned, no provision was made for the generation or presentation of uniform and coordinated data sets, as this concept did not emerge until much later. This work has been done, for a selected number of passes, by the ISIS Experimenters Committee, and this publication is the result of their coordinated efforts.

The purpose of this work is to provide at the end of the data acquisition phase of the ISIS program, a representative set of data from ISIS 2 covering a range of operating modes and geophysical conditions. The data presented here show the typical values and range of ionospheric and magnetospheric characteristics, as viewed from 1400 km with the ISIS 2 instruments. For any scientist using ISIS data, this book should give a useful background and helpful perspective as to what is available. For others, this publication should be helpful in providing typical and extreme values of ionospheric and magnetospheric parameters, or may even provide research material. Anyone making serious quantitative use of these data may wish to contact the experimenters themselves. Original data from the instruments have been deposited in the National Space Science Data Center (NSSDC), NASA/GSFC, Greenbelt, Maryland 20771.

The overall publication comprises seven data sets in four volumes. The definition of each data set depends partly on geophysical parameters and partly on satellite operating mode. Preceding the data set is a description of the organizational parameters and a review of the objectives and general characteristics of the data set. The data are shown as a selection from 12 different data formats. Each data set has a different selection of formats, but uniformity of a given format selection is preserved throughout each data set. A description of how to interpret each format is given in the introductory sections. Most of the data that are plotted linearly in time are on one of two possible scales, corresponding to either 12 min/page or 20 min/page. Thus easy comparison of data is made possible. To summarize, each data set consists of a selected number of passes, each comprising a format combination that is most appropriate for the particular data set. Following this introduction is a list of ISIS 2 experimenters, with addresses and telephone numbers, then a brief description of the ISIS 2 satellite, followed by more detailed instrument descriptions, format descriptions, data set descriptions, and the data themselves. At the end of Volume 1 is a bibliography of ISIS 2 published papers. This bibliography was produced from a computerized technical reference file at the National Space Science Data Center. Comprehensive bibliographies for the other satellites of the Alouette-ISIS program also are available from NSSDC.

II. LIST OF ISIS 2 EXPERIMENTERS (as of 1980)

Communications Research Centre - Department of Communications P.O. Box 11490, Station "H", Ottawa, Ontario, Canada K2H 8S2

H. G. James - Topside sounder, VLF, Cosmic Noise (613-596-9279)
D. Muldrew - Topside sounder (613-596-9101)
J. H. Whitteker - " " "
J.D.R. Boulding - Satellite controller (613-596-9539)

Goddard Space Flight Center, Greenbelt, MD, USA 20771

L. H. Brace - Cylindrical electrostatic probe, Code 961 (301-344-8575)
E. J. Maier - Retarding potential analyzer, Code 963 (301-344-8912)
C. Freeman - Data analyst (301-344-6374)

National Research Council - Herzberg Institute of Astrophysics, Ottawa, Ontario, Canada K1A OR6 (613-992-2734)

I. B. McDiarmid
J. R. Burrows
D. D. Wallis
M. D. Wilson

Energetic Particle Detector and Fluxgate Magnetometer

University of Calgary, Physics Department, Calgary, Alberta, Canada T2N 1N4 (403-284-6340)

C. D. Anger
L. L. Cogger
J. S. Murphree

Auroral Scanning Photometer

University of Texas at Dallas, Center for Space Sciences, MS F02.2, P.O. Box 688, Richardson, TX, USA 75080

W. J. Heikkila
J. D. Winningham
D. M. Klumpar

Soft Particle Spectrometer (214-690-2835)

J. H. Hoffman - Ion Mass Spectrometer (214-690-2840)
W. H. Dodson - " " " "

York University, Centre for Research in Experimental Space Science, 4700 Keele Street, Downsview (Toronto), Ontario, Canada M3J 1P3 (416-667-3221)

G. G. Shepherd - Red Line Photometer
F. W. Thirkettle - Data Analyst

III. SATELLITE DESCRIPTION

ISIS 2 (Figure 1) was launched from the Western Test Range, California on April 1, 1971 (Franklin and Maclean, 1969; Daniels, 1971). The orbital parameters are: apogee 1423 km, perigee 1356 km, inclination 88.16°, and period 113.55 min. ISIS 2 carries 12 instruments (Figure 2), 10 of which are described in detail below. The other two are the Beacon experiment for measuring ionospheric irregularities and the Cosmic Noise experiment for measuring the cosmic or natural background noise level.

The satellite is an approximate oblate spheroid with a height of 119 cm, a diameter of 127 cm, and a weight of 260 kg. Its attitude is controlled by torquing coils and is measured by a 6-probe fluxgate magnetometer and a solar aspect sensor. The spin rate varies between about 2.5 and 3.5 rpm and can be changed by about 0.10 - 0.15 rpm/orbit. The spin axis is normally kept in the orbital plane (orbit-aligned) or at right angles to the orbital plane (cartwheel). For the orbit-aligned configuration the attitude can be changed by 2.0° - 2.5°/orbit and in the cartwheel configuration, by about 0.5°/orbit. The spacecraft contains about 11,000 solar cells and 3 Ni-Cd batteries. It was capable of operating for about 9 hours/day at launch and presently (1980) is capable of operating for about 2.5 hours/day. It has 3 telemetry transmitters at 136.08, 136.59, and 401.75 MHz and a tracking beacon at 136.41 MHz. Data are telemetered to several ground stations situated around the world. The spacecraft has a tape recorder and clock, but these failed in 1971 and 1974, respectively.

IV. INSTRUMENT DESCRIPTION AND DATA PROCESSING

AURORAL SCANNING PHOTOMETER (ASP)

The ISIS 2 dual wavelength auroral scanning photometer (Anger et al, 1973) is designed to map the distribution of auroral and airglow emissions at 5577Å and 3914Å over the portion of the dark Earth visible to the spacecraft.

Franklin, C. A., and M. A. Maclean, The design of swept-frequency topside sounders, Proc. IEEE, 57, 897-929, June 1969.

Daniels, F., The ISIS-II spacecraft, Communications Research Centre Report No. 1218, Department of Communications, Ottawa, March 1971.

Anger, C. D., T. Fancott, J. McNally, and H. S. Kerr, ISIS 2 scanning auroral photometer, App. Optics, 12, 1753-1766, Aug. 1973.

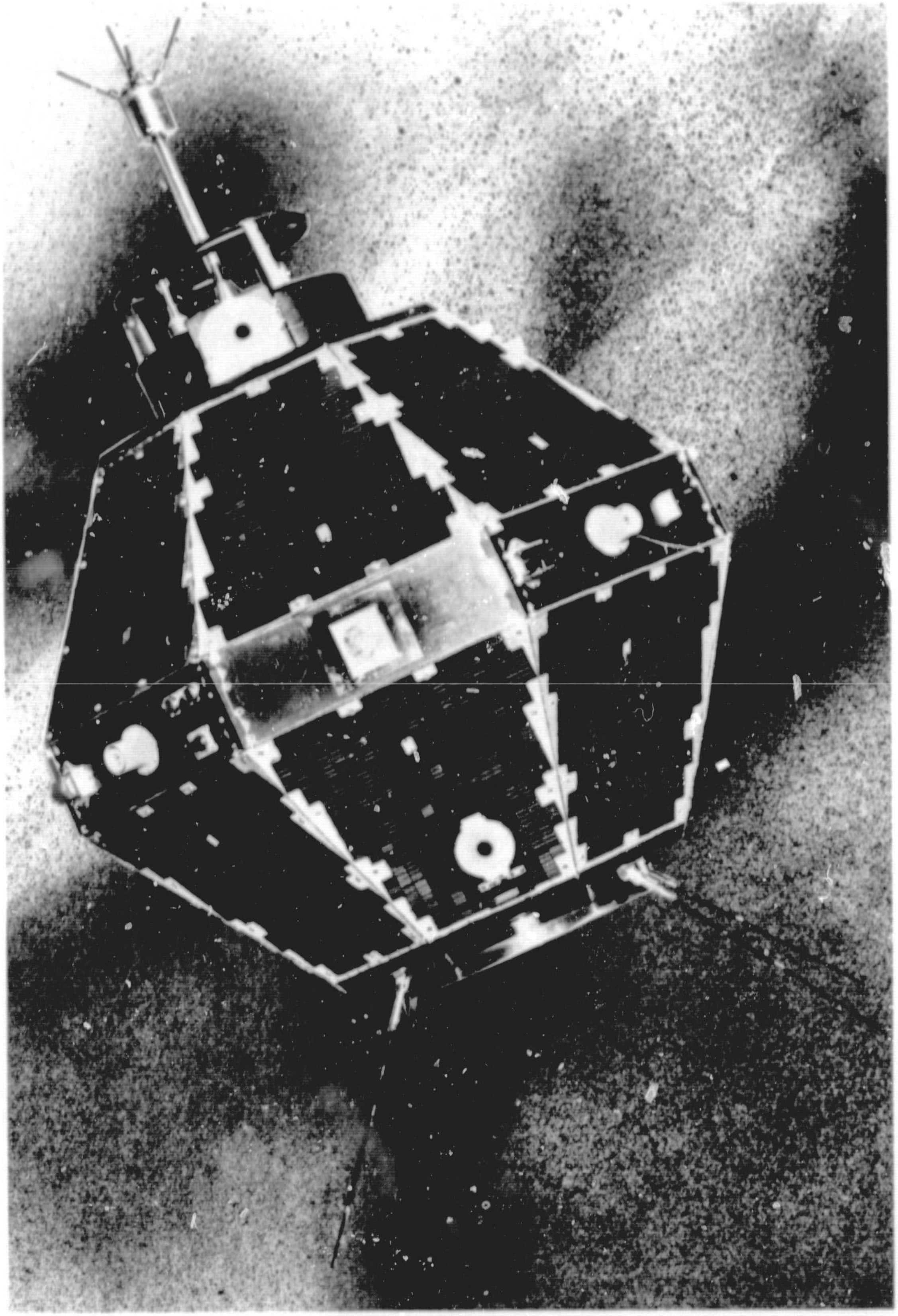

Figure 1. ISIS 2 Spacecraft.

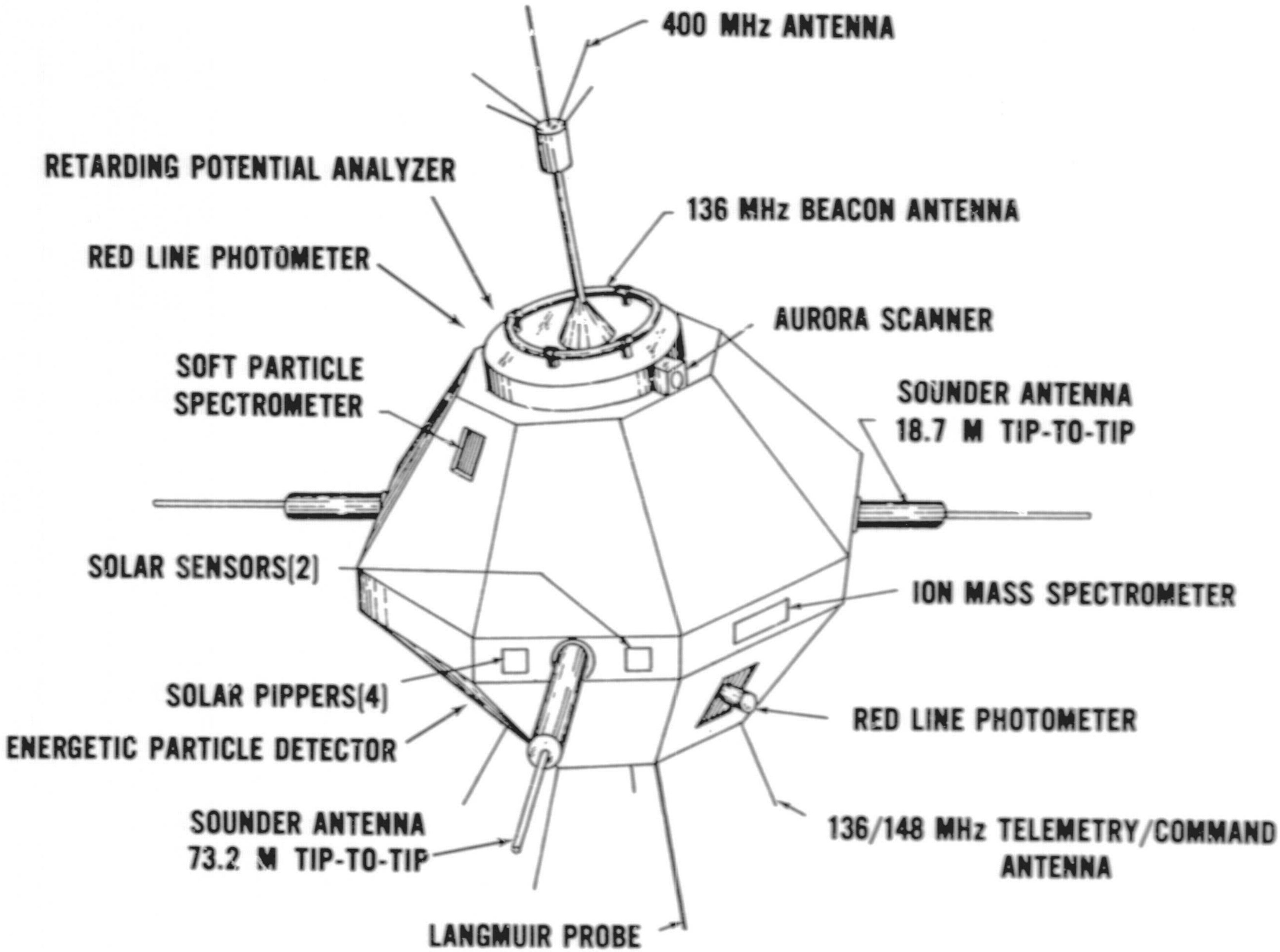

Figure 2. ISIS 2 Instrumentation.

Meaningful optical observations are possible at angles between the viewing direction of the instrument and the Sun direction of >60° and <120° due to a two-stage baffle system which shields the optics. The optical system consists of two separate barrels which are 180° apart so that only one barrel can look at the Earth at a time. The light from each of the barrels passes through its own interference filter (5581 ± 9Å or 3914 ± 13Å), lens, and mirror, and then is focused at a common point on a single-image dissector photomultiplier tube. This tube is similar to an ordinary photomultiplier tube except that an electrostatic imaging system and aperture are interposed between the cathode and first dynode. At any instant, only those photoelectrons from a small region of the cathode can pass through the aperture and be multiplied. This region is scanned across the photocathode by a magnetic scanning coil, thus generating a 13-element linear scan which is oriented at 90° to the direction of motion produced by rotational motion of the spacecraft (see Figure 3). The instantaneous field of view of each of these elements is 0.4° x 0.4°, resulting in an average output of one photoelectron pulse for ~250 rayleighs (R) from each point viewed, and hence a signal to noise ratio of one. The spatial resolution at 100 km directly under the spacecraft is ~8 km for each element.

Each photoelectron passing through the imaging electron optics and aperture of the image dissector tube is multiplied by about 10^7 by the dynode chain. The resulting output pulse is amplified by a pulse preamplifier, which produces standard pulses suitable for driving high-speed digital logic. Pulses from the preamplifier are accumulated in a digital logarithmic accumulator, the seven-bit output of which is transferred to a buffer and shifted out in standard PCM format at 630 words per second. As one frame of data consists of the 13 elements in a scan plus a frame synchronization word, there are 45 frames of data output per second.

The photometer scans the Earth by a combination of the rotational and translational motions of the spacecraft together with the internal electronic scanning performed by the image dissector (see Figure 3). The spacecraft spin axis and orbital plane remain essentially fixed in space as the spacecraft orbits the Earth, and, therefore, each rotation of the spacecraft results in the scanning of a strip, which, for the orbit-aligned mode of the spacecraft, is at right angles to the orbital plane. The width of the strip (5°) is chosen so that it will just join onto the strip scanned during the previous rotation. The image dissector repetitively scans at high speed across the narrow dimension of each strip, dividing it into 13 separately resolved regions (0.4° x 0.4°). Similar strips are scanned at each of the two wavelengths, although they differ in time by half the rotation period.

RED LINE PHOTOMETER (RLP)

The RLP (Shepherd et al, 1973) was designed to measure the emission of 6300Å aurora and airglow from the F-region of the Earth's ionosphere. It has two optical inputs, 180° apart and at 90° to the satellite spin axis. One input is characterized by a 10Å bandwidth filter and the other by an 88Å bandpass. They have roughly equal responses to white light, but the responses to

Shepherd, G. G., T. Fancott, J. McNally, and H. S. Kerr, The ISIS-II atomic oxygen red line photometer, Appl. Opt. 12, 1767 (1973).

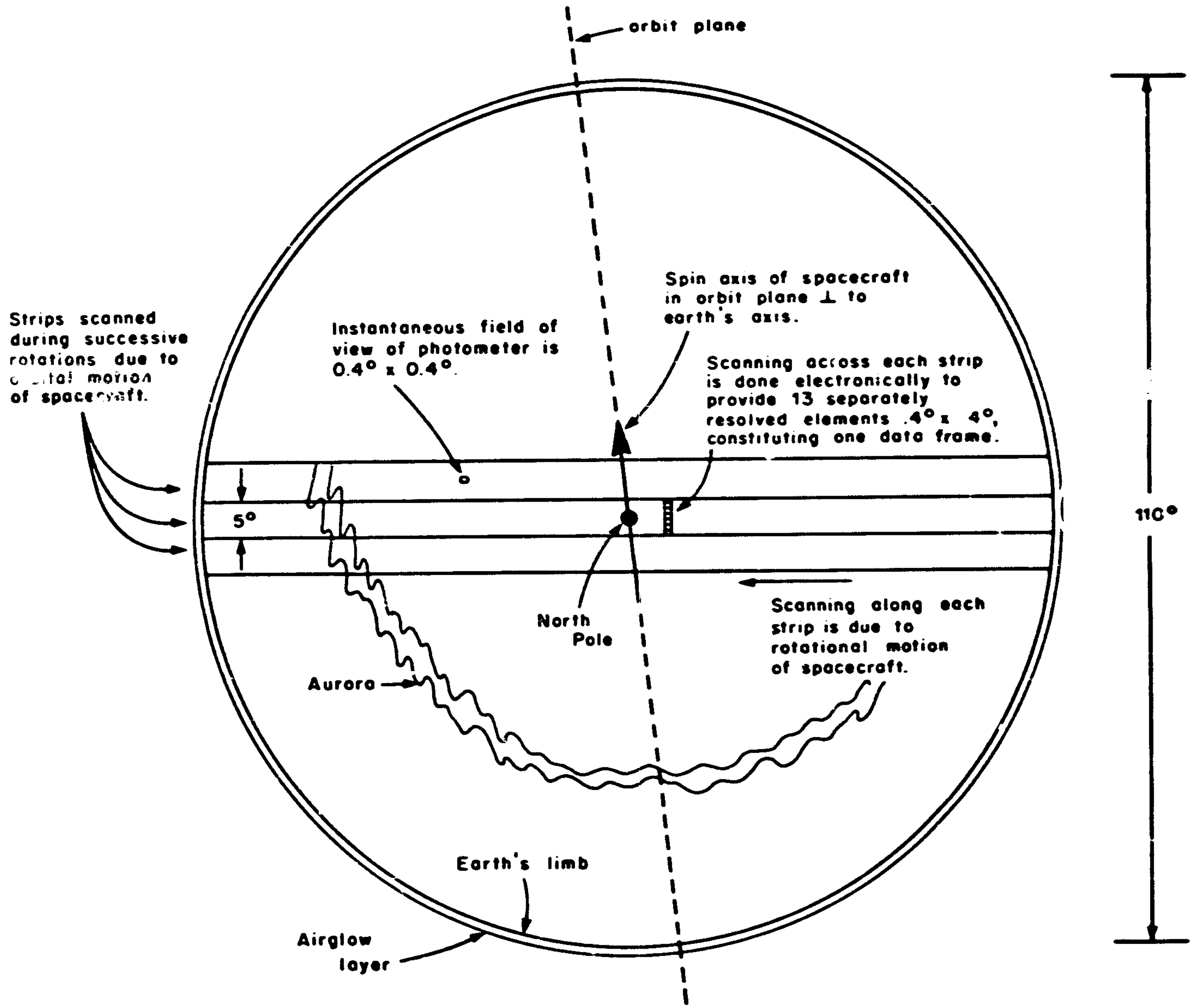

Figure 3. The Earth as it would appear from the spacecraft 1400 km above the pole, with scanning pattern of photometer superimposed.

6300Å emission are in the ratio of 9:1. The field of view of both is 2.5° in diameter. These optical inputs enter the same telescope system, and the intensities are summed onto one photomultiplier detector. As one input views the Earth the other views the dark sky, allowing the signals to be separated. Corrections for the starlight background intensity are made in data analysis. Intensities are measured at a rate of 30 samples/sec.

With the satellite spin axis in the plane of the orbit, the Earth scans caused by satellite rotation (19-second period, normally) form a raster-like scan pattern, generating two pictures per orbit; one as seen through the 10Å filter, the other by the 88Å filter. These pictures are combined to eliminate the white light background, leaving the 6300Å intensities. These intensity values are contoured in "spin coordinates," and then transformed to magnetic invariant coordinates using the method of Boyd (1977) . The details are described under Format 8.

When the spin axis is perpendicular to the orbit plane (cartwheel configuration), the RLP scans repeatedly along the satellite track. The output in this case is presented as intensity along the spacecraft track as a function of spacecraft time. The details are described under Format 1.

SWEPT-FREQUENCY SOUNDER

The sounder is essentially a radar, operating between 0.1 and 20 MHz, which transmits pulses approximately 100 μs in duration, and then listens for reflected signals. The pulses are repeated at the rate of 45 per second, as the frequency is gradually swept through its range. The received signal is displayed in the form of an ionogram, in which the density of the display at any point depends on the signal level.

An ionogram is shown in Figure 4. In a well-behaved (horizontally stratified) ionosphere, there will be at most two echoes for a given frequency. For each echo, the time delay is determined by the electron density (N) as a function of altitude (h). The delay-time scale is marked in units of distance (apparent range), corresponding to a signal propagating at the speed of light. In a plasma, the signal travels more slowly than this, and the delay time depends on an integral of group refractive index along the path. The ionogram provides apparent range as a function of frequency, and with this information, the integral can be inverted to give the vertical electron density profile N(h). A procedure for this inversion is described by Jackson (1969).

The trace in the lower portion of the ionogram represents the automatic gain control (AGC) voltage. Zero voltage is given by the horizontal line that is designated 2800 km apparent range, and the maximum AGC voltage of 5 volts is shown by the 2400 km apparent range marker. The AGC voltage can be used as a measure of the background noise level at the satellite.

Boyd, J. S., Invariant geomagnetic coordinates for epoch 1977.25, Planet. Space Sci. 25, 411 (1977).

Jackson, J. E., The reduction of topside ionograms to electron-density profiles. Proc. IEEE, 57, 960-976, June 1969.

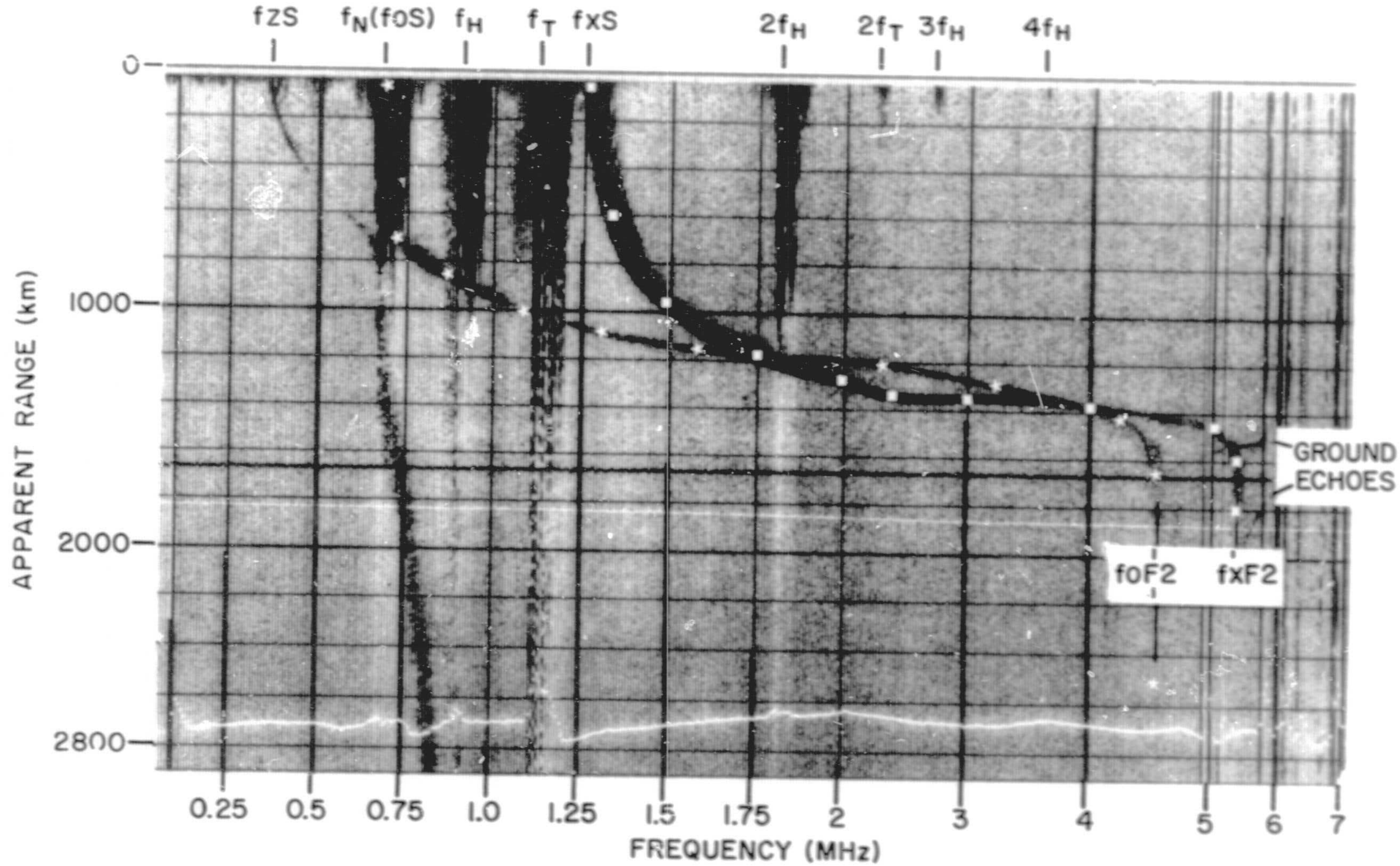

Figure 4. ISIS 2 Ionogram.

The sounder is described in more detail by Franklin and Maclean (1969). In the same issue of Proc. IEEE, there are several other articles on topside sounding. A short review on topside sounding is given by Jackson et al (1980).

CYLINDRICAL ELECTROSTATIC PROBE (CEP)

The CEP is a Langmuir probe instrument which measures the electron density (N_e) and temperature (T_e) of the ionospheric plasma. The instrument consists of a pair of thin wire collectors projecting from the spacecraft spin axis at both ends. The two collectors are operated independently in a time-shared fashion by a common electronic unit which applies an appropriate voltage waveform and measures the resulting volt-ampere characteristics of the collectors. Details of similar instruments used on the Alouette 2 and Explorer 31 satellites are discussed elsewhere (Findlay and Brace, 1969).

A typical CEP plot of N_e and T_e is shown in Figure 5. The plot format reflects the details of the instrument design. Points are shown at 6-second intervals, reflecting the repetition rate of the sweep voltage waveform. Each collector is assigned to the electronics during alternate 30-second intervals, thus alternate groups of five measurements are derived from different probes. Owing to damage of one of the probes at launch, which introduced a spin modulated error in its N_e measurement, only one probe is employed for N_e measurements. Both probes are capable of good T_e measurements, although wake effects on one or the other may cause slight disagreement in their T_e measurements at certain points in the orbit. This will be evident as an offset in alternate groups of five T_e points in the plots. The T_e values are given either by solid points or by question marks (?) in the case of poor curves caused by ionospheric irregularities, as discussed later.

The N_e measurements are made in the range of about 10^2 to $10^5/cm^3$. The lower limit arises from electrostatic shielding by the spacecraft sheath which grows out over the collectors at very low densities.

The T_e measurements can be made when N_e exceeds about $200/cm^3$ when the collectors are not in sunlight. When in sunlight, photoelectrons leaving the collectors prevent a proper ion current reference to be established until N_e exceeds about $10^3/cm^3$. T_e may be resolved between 500°K and 15,000°K when the above N_e conditions are attained.

Franklin, C. A. and M. A. Maclean, The design of swept-frequency topside sounders, Proc. IEEE, 57, 897-929, June 1969.

Jackson, J. E., E. R. Schmerling, and J. H. Whitteker, Mini-review on topside sounding, IEEE Transactions on Antennas and Propagation, Vol. AP-28, No. 2, 284-288, March 1980.

Findlay, J. A. and L. H. Brace, Cylindrical electrostatic probes employed on Alouette 2 and Explorer 31 satellites, Proc. IEEE, 57, 1054-1056, June 1969.

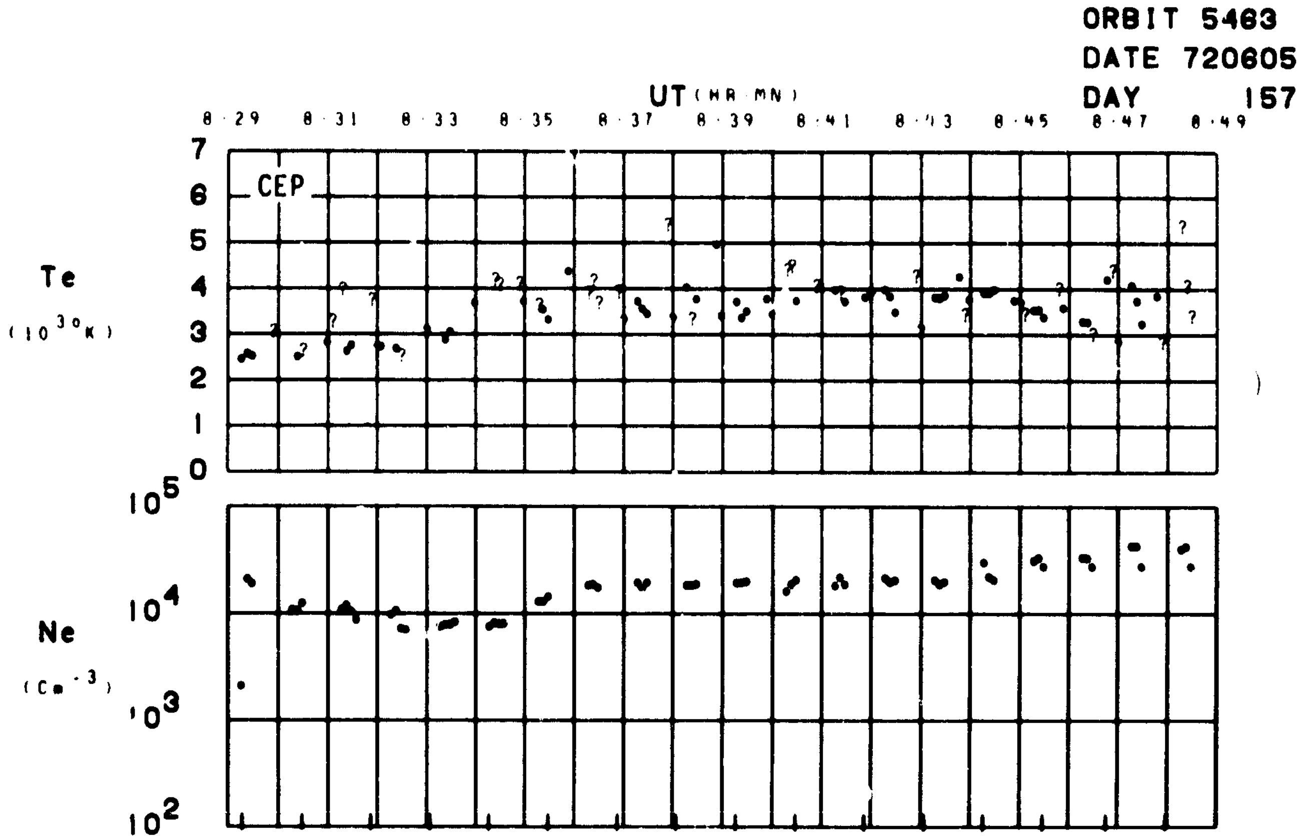

LAT	42	45	50	54	57	61	66	69	73	77	81	85	87	86	82	78
LONG	-155	-155	-155	-155	-155	-154	-154	-154	-153	-151	-147	-136	-84	-7	5	9
LT	22:10	22:11	22:12	22:13	22:15	22:17	22:20	22:23	22:28	22:36	22:54	23:37	3:07	8:17	9:09	9:27
DIP	73	75	77	78	80	81	83	84	85	86	88	88	88	88	86	85
DIPLAT	59	62	66	68	71	74	77	79	81	84	86	88	88	86	84	82
L	2.1	2.4	2.8	3.3	4.0	4.9	6.7	9.1	13.1	20.3	37.5	64.3	80.9	59.8	32.7	19.6
INVLAT	46	49	53	56	59	63	67	70	73	77	80	82	83	82	79	76
ZA	110	107	103	100	96	93	89	86	82	70	75	72	68	65	61	58

Figure 5. Example of CEP data.

The main sources of error in N_e are wake effects and inadequacies of the theory for the conversion of electron current to density. Comparisons with the sounder and the other direct measurements on ISIS 2 show that the errors seldom exceed a factor of two, even when wake effects are ignored. Thus we have not eliminated N_e data on the basis of spacecraft orientation.

The main source of error in T_e arises from the irregular structure of the high-latitude ionosphere which introduces distortions in the volt-ampere characteristics. When a solid point is employed to plot T_e, the error is probably less than 10 percent. Larger errors may be expected when question marks are used. No T_e value is plotted if the plasma is so structured as to distort the curve beyond recognition to the curve fitting program. In general, question mark symbols should be used only when solid T_e points are not available, and then only as an estimate of T_e.

ENERGETIC PARTICLE DETECTOR (EPD)

The EPD instrument was designed to provide directional flux measurements of electrons (from 0.15 keV to 2 MeV) and positive ions (from 2 keV to 20 MeV with some gaps). A diversity of sensors are used. A stepped electrostatic analyzer provides an 8-point electron spectrum ($0.15 < E < 10$ keV) and an 8-point positive ion spectrum ($2.0 < E < 26$ keV), each once per second. However, only three of these electron differential channels are displayed in the normal EPD format. Geiger counters and solid state detectors provide integral flux measurement at 12 different threshold energies starting at $E >$ 22 keV for electrons and $E >$ 150 keV for protons. Only three of these integral channels are included in Format 3, averaged to one second time resolution. The instrumental time resolution is $\sim$1/4 second. The energy bandpass ($\Delta E/E$) of the electrostatic analyzer is 30 percent for electrons and 15 percent for positive ions.

All of the sensors but one have the axis of their fields of view fixed in the same direction in the plane perpendicular to the spacecraft's spin axis. One geiger counter axis is along the spin axis. The fields of view of the integral detectors are conical. The electrostatic analyzer differential spectrometer has a rectangular field of view defined by a collimator with half angles 1.5° x 1.7°.

The electron differential channels are unaffected by positive ion fluxes but do give spurious counts due to solar ultraviolet light when viewing the Sun. The integral channels respond to both electrons and protons in general at different threshold energies. In Format 3, channel I(210) has had the positive ion flux removed. The $I_{\parallel}(40)$ channel includes both electron ($E >$ 40 keV) and positive ions ($E >$ 150 keV) fluxes. The latter flux is negligible except during solar proton events. Both I(40) and $I_{\parallel}(40)$ also sometimes have spurious Sun counts.

The gain of the differential spectrometers' channeltron detector decreased quickly between April and October 1974 and should be regarded as quantitatively inaccurate after April 1974. The geiger counter, $I_{\parallel}(40)$, failed in June 1973.

The instrumentation and detector characteristics are more fully described by Venkatarangan et al, 1975. Some relevant EPD detector characteristics are tabulated below.

Detector	Type	Energy Threshold keV	Geometric Factor cm^2 ster	Collimator Half-Angle
I(210)	solid state	e^- 210	8.15×10^{-3}	7.0°
I(40)	solid state	e^- 40 p^+ 150	7.84×10^{-3}	6.8°
$I_{\parallel}$(40)	geiger	e^- 40 p^+ 600	1.03×10^{-3}	5.6°
I(22)	geiger	e^- 22 p^+ 240	8.83×10^{-4}	5.5°
Ip(750)	solid state	$750<p^+<4000$	4.9×10^{-2}	11.3°

ION MASS SPECTROMETER (IMS)

The ion mass spectrometer (Hoffman et al, 1974) is a magnetic sector type mass spectrometer with two electron multiplier detectors located on two different radii within the sector. The incoming ions are accelerated by a potential that makes a complete sweep in 1 second such that the mass range 1 to 9 AMU is sampled on one channel and, simultaneously, the mass range 8 to 64 AMU is sampled on the other channel. Thus the mass spectrum from 1 to 64 AMU is sampled each second. The output current from the electron multipliers is then converted to an ion concentration using conversion constants determined by in-flight calibration using the electron density obtained from the topside sounder also located on the ISIS satellite.

The ion concentration is given in number of ions per cubic centimeter of the five dominant ions found at 1400 km, each plotted as a function of time in 20-minute segments. Each data point has been obtained by curve fitting the spacecraft spin-modulated cartwheel data and determining the maxima and time of maxima of the fitted curve. Thus the absence of data for a given ion may indicate that a good curve fit was not possible; this generally occurs at concentrations less than 10 ions/cm^3.

Venkatarangan, P., J. R. Burrows, and I. B. McDiarmid, On the angular distributions of electrons in 'inverted V' substructures, J. Geophys. Res. 80, 66-72, Jan. 1975.

Hoffman, J. H., W. H. Dodson, C. R. Lippincott, and H. D. Hammack, Initial ion composition results from the ISIS 2 satellite, J. Geophys. Res. 79, 4246, 1974.

RETARDING POTENTIAL ANALYZER (RPA)

The retarding potential analyzer (Kayser et al, 1978) is a planar multigrid instrument designed to measure ionospheric density and temperature parameters over the range 10 to 10^6 ions/cm^3 and 500-10,000°K, respectively. This is accomplished by performing an electrostatic retardation of the ions flowing into the instrument at the spacecraft velocity when the instrument is oriented in the nearly forward direction. The instrument is mounted in the equatorial plane of the spacecraft, with the sensor normal directed radially outward. Thus the viewing angle scans a variety of directions as the spacecraft rotates at the nominal 3-rpm spin rate. In the cartwheel mode, in which the spacecraft spin axis is perpendicular to the orbit plane, the sensor scans the full angle range 0° to 360° between the sensor normal and the velocity vector every (nominally) 20 seconds. In the orbit aligned mode, in which the spacecraft spin axis is in the orbit plane, the sensor cannot scan the forward direction at all latitudes. In particular, at high latitudes, the sensor normal is almost perpendicular to the velocity vector, thus precluding data collection when the optical instruments are obtaining "spin scan" images. Thus only the cartwheel data sets contain results from the RPA.

Plasma analysis is performed by applying programmed voltages to the various grids within the ion trap and measuring the current transmitted to the collector as a function of the applied potentials (Moss and Hyman, 1968). The resulting current voltage (I-V) response is fitted to a predicted response to provide the estimates of the ambient parameters. Results presented in this data book are based on the assumptions that the ions present in significant concentrations (>1 percent of the total) may be H^+, He^+, and O^+, all assumed to be at a common temperature T. Useful data are obtained only when the sensor normal is within 35° of the spacecraft velocity vector. The combination of the 3-second instrument program cycle and the 20-second spacecraft spin period yields a limit of 1 or 2 plasma analyses per 20-second interval. This nominal rate of 3 per minute may not be attained for several reasons. (1) Operation of the sounder transmitter sometimes perturbs the local plasma, yielding non-geophysical results. (2) Photoemission effects within the instrument sometimes preclude analysis of the I-V curve when the Sun is within the field of view of the instrument. This is most significant in regions of low plasma density. (3) Highly structured plasma often cannot be analyzed if the local plasma variations are fast on the 1-second time scale on the instrument. This is usually the reason for the apparent data gaps in the auroral zone. (4) Extreme spacecraft potentials are sometimes encountered, exceeding the range of the applied sweep voltages. For all of these cases, appropriate tests are used to delete, or correct, data points before analysis and to select results based on the quality of their fit to the theoretical I-V curve.

Kayser, S. E., E. J. Maier, and L. H. Brace, Quiet time plasma irregularities at 1400 km in the cleft region, J. Geophys. Res. 83, 2533, 1978.

Moss, S. J., and E. Hyman, Minimum variance technique for the analysis of ionospheric data acquired in satellite retarding potential analyzer experiments, J. Geophys. Res. 73, 4315, 1968.

SOFT PARTICLE SPECTROMETER (SPS)

The ISIS 2 Soft Particle Spectrometers measure the fluxes and energy spectra of electrons and positive ions over the energy range from 5 eV to approximately 15 keV.

There are two independent electrostatic analyzers (SPS's) on the ISIS 2 satellite, each of which is capable of measuring electrons and/or positive ions in either an energy step dwell mode or a spectral sweep mode. Each of the spectrometers, referred to as "top beam" and "bottom beam," are mounted looking in identical directions perpendicular to the satellite spin axis. The top detector is normally operated in an electron sweep mode and as such has a geometric factor of 4.95 x 10^{-4} cm^2 ster and an energy bandpass ($\Delta E/E$) of 24.7 percent with center energies from 13.15 keV to 5.5 eV in 38 levels. The bottom detector is normally operated in a positive ion sweep mode and in this mode has a geometric factor of 1.27 x 10^{-3} cm^2 ster and an energy bandpass ($\Delta E/E$) of 35.5 percent with center energies from 14.675 keV to 5.0 eV in 39 levels. Both spectrometers have rectangular fields of view with a full width of 5 degrees by 25 degrees for the top beam (electron mode) and 10 degrees by 25 degrees for the top beam (ion mode) and the bottom beam in both electron and ion modes. In both cases the long dimension of the field of view is parallel to the spin axis and the short dimension is in the equatorial plane. A similar instrument flown on ISIS 1 is described by Heikkila et al (1970).

VERY LOW FREQUENCY RECEIVER (VLF)

The center of the VLF instrument is a broadband receiver covering the frequency range from 50 Hz to 30 kHz (Franklin et al, 1960). A receiving antenna connects to the receiver through a protective low pass filter. Normally, the antenna is the 73.2-m dipole shared with the topside sounder. Also, the receiver input can be connected instead to the spacecraft torquing coils used for attitude adjustment; however, the torquing coils have not produced meaningful data. VLF emissions are observed over a wide amplitude range and consequently the receiver has been designed with a dynamic range of 68 dB, most of which is achieved by use of automatic gain control (AGC).

Output from the receiver directly modulates an FM telemetry transmitter and has a dynamic range of 3 dB above the AGC threshold. The AGC is sampled 60 times per second and telemetered to ground via the PCM data channel. The receiver threshold is 20 μV across an input impedance of 16 kΩ.

On ISIS 2 the VLF experiment also includes an exciter connected to the short (18.7 m) sounder dipole. It sweeps logarithmically from 15 to 0.05 kHz

Heikkila, W. J., J. B. Smith, J. Tarstrup, and J. D. Winningham, The soft particle spectrometer in the ISIS 1 satellite, Rev. Sci. Instr. 41, 1393, 1970.

Franklin, C. A., T. Nishizaki, and W. E. Mather, A wideband VLF Receiver for the Alouette II and ISIS-A satellites, DRTE Technical Memorandum 522, Department of National Defence, Ottawa, Canada, May 1960.

once every 5 or 10 seconds. In addition, the short-dipole impedance can be measured by recording the amplitude and phase of the current drawn by the dipole in response to the VLF exciter. These data are telemetered via the PCM system.

TRIAXIAL FLUXGATE MAGNETOMETER

The orthogonal set of magnetometers (McDiarmid et al, 1978) is mounted in the body of the spacecraft with one component oriented along the spin axis (designated the z-magnetometer) and the other two in the plane perpendicular to the spin axis (designated x-y plane). The x-and z-magnetometers each have two ranges, ± 60,000 nT (± 600 milligauss) and ± 20,000 nT. The former range has digitization steps of 480 nT while the latter has 160 nT. The y-magnetometer has only the ± 60,000 nT range. All components are sampled at the rate of 1 sample/sec. There is no in-flight calibration capability. There is an induced field due to the surrounding spacecraft mass and wiring harness which is of the order of 1 percent of the external field. This field and some other periodic sources of interference from spacecraft equipment are removed in the data processing.

In this data book, only data from the axial (z) component are presented since its processing is more straightforward than for the spinning components. Only data sets in which the spin axis is nearly perpendicular to the orbit plane (i.e., cartwheel) have magnetometer measurements included, since it is desirable to use the higher sensitivity (± 20,000 nT) range. In cartwheel, the axial component is aligned approximately in the East-West direction when crossing the auroral ovals.

V. DATA FORMAT DESCRIPTIONS

The data most appropriate, and available, for a particular study are presented in formats selected from the following list. A format may contain data from a single instrument or from several instruments. A description of the information provided by each instrument is provided in this section. The following table specifies what instrument and quantities are plotted in each format. Unless otherwise specified all quantities plotted are profiles along the spacecraft track.

McDiarmid, I. B., J. R. Burrows, and M. D. Wilson, Comparison of magnetic field perturbation at high latitudes with charged particle and IMF measurements, J. Geophys. Res. 83, 681, 1978.

Format Number	Instrument	Quantity Plotted
1	Auroral Scanning Photometer	5577Å, 3914Å intensity
	Red Line Photometer	6300Å intensity
	Soft Particle Spectrometer	Electron energy flux
2	Topside Sounder	Electron density contours at different altitudes
	Magnetometer	Magnetic field deviation
3	Energetic Particle Detector	Electron and proton flux/energy
4	Cylindrical Electrostatic Probe	Electron density and temperature
	Ion Mass Spectrometer	Concentration of H^+, He^+, O^{++}, N^+, O^+
5	Retarding Potential Analyzer	Concentration of H^+, O^+, He^+ and ion temperature
6	Soft Particle Spectrometer	Electron and positive ion spectrograms
7	Auroral Scanning Photometer	Grey-scale two dimension co-ordinate transform of 5577Å, 3914Å intensities and the 5577Å/3914Å ratio
8	Red Line Photometer	Contour plot of 6300Å intensity
9	Auroral Scanning Photometer	5577Å E and F region latitude profiles
	Red Line Photometer	6300Å latitude profile
10	Cylindrical Electrostatic Probe	Electron density and temperature
	Topside Sounder	Electron density contours at different altitudes
11	VLF	VLF spectra
12	Auroral Scanning Photometer	Height profiles of 5577Å slant intensity

FORMAT 1 (ASP, RLP and SPS)

The sample of Format 1 shown in Figure 6 has been retouched for clarity, but it corresponds to the direct computer plot reproduced in the ISIS 2 data book. This format contains a combination of Soft Particle Spectrometer (SPS) electron data and optical data from the Auroral Scanning Photometer (ASP) and Red Line Photometer (RLP). A minimum-time-delay algorithm is used, in which the time delay between the satellite crossing of a particular field line and the optical viewing of the emission from the foot of the field line is minimized. This delay can be kept to within one-half of a spin period, by selecting optical data from the most appropriate spin for a given latitude range, and splicing it together to form a continuous sequence. For this data set the satellite has its spin axis perpendicular to the orbit plane and the optical scans are repeatedly along the spacecraft track. Thus, there is adequate redundancy for the above procedure.

The electron data and optical data are then plotted as a function of Universal Time, corresponding to the time of the spacecraft motion (the time of the SPS measurement), which will be somewhat different from the optical viewing time as described above. The start time is shown at the lower left and minute values are given on the horizontal axis. The atomic oxygen 6300Å emission intensity from the RLP and the atomic oxygen 5577Å and N_2^+ 3914Å emission intensities from the ASP are plotted in kR on a logarithmic scale at the bottom. These intensities have not been corrected for airglow background or albedo. The SPS electron energy fluxes have been integrated over four energy bands as shown on Figure 6: 5 -60 eV, 60 -300 eV, .3 -1. keV, 1 -15 keV and plotted on vertically separated scales, with the ordinate labeled in units of the logarithm of the energy flux in erg cm^{-2} sr^{-1} sec^{-1}.

The modulation that appears on these fluxes results from the rotation of the spacecraft. The detectors look outward in the equatorial planes, sweeping through a pitch angle coverage shown by the sawtooth at the top of the plot. A downward sawtooth corresponds to downward-going particles.

At the top of Figure 6 the following geophysical quantities are indicated along the horizontal axis: INVL - invariant latitude, INVT - invariant time, SDEP - local solar depression angle at the location of the viewed emission, CDEP - solar depression angle at the magnetic conjugate point to the viewed emission.

The 5577Å and 3914Å data plotted are derived from the slow-speed PCM data link, the same as used for the 6300Å data, but not the same as the high speed data link employed for the high-resolution ASP photos. To achieve this reduced data rate the intensity across a 13-element scan is averaged into essentially a single value by filtering. Because of this, the PCM data should be used with caution when accurate intensities are desired. Optical observations from satellites (and rockets) include in addition to the real emission intensity, a variable contribution from ground scattering. In principle this contamination can be quantitatively removed using the method of Hays and Anger (1978) assuming

Hays, P. B. and C. D. Anger, Influence of ground scattering on satellite auroral observations, Appl. Opt. 17, 1898-1904, June, 1978.

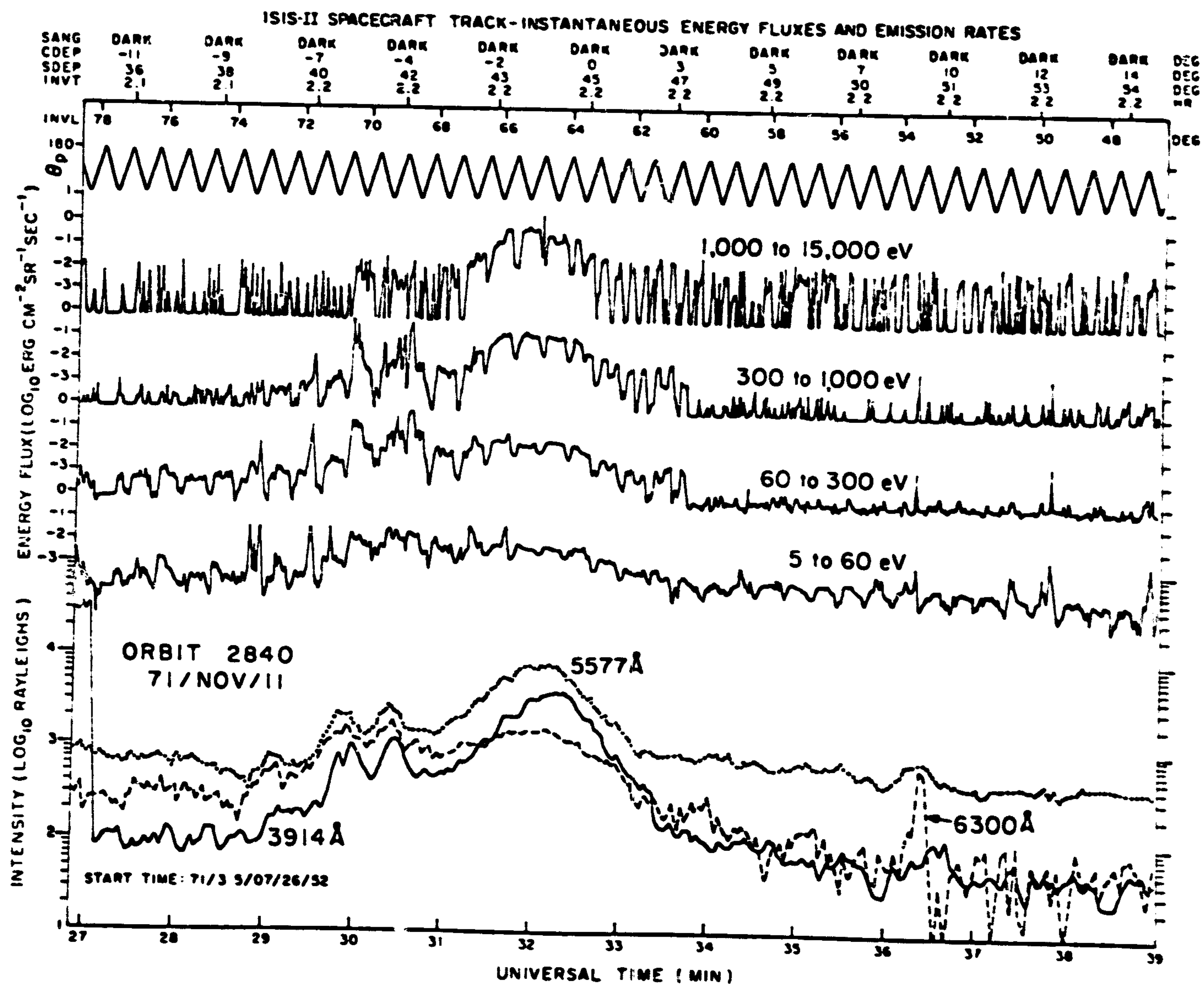

Figure 6. Example of Format 1 (Optical data and SPS).

the altitude of the emission and the spectral albedo of the surface are known. Practical experience has shown that the factor by which to divide an observed intensity (5577Å or 3914Å) varies from 2 for a large-scale, reasonably uniform region to 1 (i.e., no correction) for thin discrete arcs (Murphree et al, 1978). This correction factor is not as serious for the 6300Å emission because of its higher altitude and consequently lower susceptibility to contamination.

FORMAT 2, TOP (MAGNETOMETER)

The axial magnetometer plot is Format 2, combined on the same page with the sounder isodensity height profile plot. They have a common abscissa labeled in minutes of Universal Time. The orbit number and Universal Time at the beginning of the plot appear at the bottom. The ordinate is in units of nanoteslas (nT). The quantity plotted is the residual deviation of the filtered axial component from the GSFC 06/74* model field computed in the direction of the inferred spacecraft spin axis orientation. The residual baseline is offset from zero by an amount of the order of 400 to 1000 nT, in different orbits, depending on field contributions from electrical subsystems in the spacecraft. The offset from these sources remains unchanged for the duration of any plot. The data are low pass filtered with a 9-point filter and plotted at 1 point/sec. The principal source of noise is the digitization step size. After filtering, the typical RMS noise from this source is ~40 nT. Where deviations exceed the statistical fluctuations, negative-trending deviations correspond to Birkeland currents flowing into the ionosphere and positive-trending deviations correspond to Birkeland currents flowing out of the ionosphere.

FORMAT 2, BOTTOM (SOUNDER)

For each chosen value of electron density, the altitude at which that density was observed to occur is plotted as a function of UT. The values chosen for these plots are powers p of 10 such that 4p is integral, e.g., p= 3.0, 3.25, 3.5, 3.75, 4.0, etc. Units are cm^{-3}. Data points are indicated by * symbols on the contours for integral powers of 10, and by + symbols on the others. All the symbols in a vertical line represent the density information obtained from one ionogram.

The broken line at the top of the plot represents the position of the spacecraft (for ISIS 2 this line is straight and horizontal). The broken line at the bottom represents the lowest altitude from which density information was obtained. In favorable cases, this will be close to the peak of the F layer, but it can be any distance above the peak.

The altitudes are obtained under the assumption that the radio propagation from the topside sounder was vertical. At high latitudes, the propagation is more likely to be along the magnetic field. When this occurs, the altitudes shown are too low. At very high latitudes, the difference is small, but close to 60° magnetic latitude, it can amount to 50 km.

Murphree, J. S., I. W. H. Robertson, C. D. Anger, and L. L. Cogger, Rocket observations of auroral albedo over snow, Appl. Opt. 17, 1849-1850, June 1978.

*Cain, J. C., private communication, 1974.

The usual sampling rate for the topside sounder is about 4 per minute. On many passes, two consecutive samples are taken, then two missed. This mode was chosen on most cartwheel passes to provide the ion probes with interference-free intervals. Where data points are missing at irregular intervals, it is because some ionogram traces were too weak or too irregular to be scaled properly.

FORMAT 3 (EPD)

With two exceptions, the traces represent electron fluxes as a function of time. Those labeled D are differential channels while those labeled I are integral channels. The number in parentheses indicates the detected energy (keV) for the differential channels or the threshold energy for the integral detectors. Units are designated by R for 'counts per second' and I for 'electrons cm^{-2} sec^{-1} $ster^{-1}$ keV^{-1}'.

All of the above vertical scales are logarithmic.

The bottom trace, $\bar{E}$, indicates the average energy (keV) computed from the complete electrostatic analyzer energy range (0.15 to 9.6 keV); it does not include the integral detectors. The vertical scale is linear.

The top trace, I(22)/I(40), shows the ratio of geiger counter flux (electrons E > 22 keV and protons E > 240 keV) to the solid state detector flux (electrons E > 40 keV and protons E > 150 keV). Since the electron fluxes are normally greater than the positive ion fluxes, the ratio normally exceeds unity. However, when the proton flux between 150 and 240 keV predominates, the ratio is less than unity.

Shown across the bottom of each plot are the Universal Time (minutes), Invariant Latitude (degrees), magnetic local time (hours), B - the intensity of the magnetic field measured at the spacecraft (gauss), and Theta z - the angle between the spacecraft spin axis and the local magnetic field vector (degrees). Theta z (θ_z) is defined to be zero in both hemispheres for downward-coming field-aligned particles.

Detector $I_{\parallel}$(40) thus looks at θ_z to the local magnetic field while all other detectors execute pitch angle scans from $90°-\theta_z$ to $90°+\theta_z$. Consequently, fluxes are often modulated at twice the spin frequency for anisotropic fluxes or at the spin frequency in regions of isotropic precipitation. The nominal spacecraft spin frequency is 3 rpm.

The integral channels record a small component of background counts due to penetrating electron flux (e.g., outer zone electrons near invariant latitude of 60°) or due to penetrating proton flux in the inner zone and during solar flare events, over the polar cap. At other places, the penetrating background counts are negligible relative to the directional flux entering the collimator.

FORMAT 4, TOP (CEP)

CEP measurements of electron density, N_e, and temperature, T_e, are plotted independently. T_e is plotted either as a point or a question mark (?) depending upon the quality of fit of the exponential portion of the volt-ampere characteristic, as described in the CEP instrument description. T_e measurements of highest reliability are plotted as points, and those of lower reliability are plotted with question marks. If the plasma is highly structured or too low in density, no T_e measurement will be made.

The values of N_e are plotted as solid points. The points come in groups of five during alternate 30-second intervals as discussed in the instrument description.

Universal Time is given at 2-minute intervals and is represented by vertical lines at 1-minute intervals.

FORMAT 4, BOTTOM (IMS)

The date and time of the start of the frame are given in the upper left hand corner. The date is given in day, month, year, and Julian day in brackets. The time is given in hours, minutes, seconds, and second of day. The orbit number is given in the upper right hand corner and is the orbit number of the start of the data frame. The orbit is incremented on the north-bound crossing of the geographic equator. The orbital data at the bottom of the plot has been interpolated to an even 2-minute point on the plot. The description and units of the orbital data are given below:

	Description	Units
UT	Universal Time	HH:MM
LAST	Local apparent solar time	HH:MM
MLT	Magnetic local time	HH:MM
DLAT	Dip latitude	Degrees
INVL	Invariant latitude	Degrees
GLAT	Geodetic latitude	Degrees
GLNG	Geodetic longitude	Degrees
SZEN	Solar Zenith Angle	Degrees
ALT	Height above the geoid	Kilometers

The ion species are identified as follows:

Symbol	Species	Mass	Units
H	H^+	1	cm^{-3}
+	He^+	4	cm^{-3}
Δ	O^{++}	8	cm^{-3}
N	N^+	14	cm^{-3}
O	O^+	16	cm^{-3}

FORMAT 5 (RPA)

Geophysical parameters deduced from the RPA as described in the instrument section are plotted on two graphs using the standard 20-min. abscissa. The lower frame shows the H^+ (symbol H) and O^+ (symbol O) densities plotted against a logarithmic ordinate scale. The density grid shown is usually over the range 10 to 10^5 cm^{-3}, but occasionally is truncated if there are no data to allow more space for an extended scale on the second plot. The upper frame shows the ion temperature on a linear scale (symbol T) and the He^+ density (symbol 4) on a logarithmic scale. The temperature scale is usually 0° to 5000°K, but occasionally may be truncated at the lower limit (if no data are present) to permit extension of the upper limit. The scale factor in the plot (degrees/cm) is constant, regardless of scale truncation.

Universal Time is used for the standard 20-min. long linear abscissa, with a vertical line every 2 minutes. Additional abscissa values are shown to identify the local time, magnetic local time, dip latitude, invariant latitude, geodetic latitude, geodetic longitude, solar zenith angle, and altitude of the spacecraft as defined under Format 4, IMS.

FORMAT 6 (SPS)

Data from these instruments are displayed as energy versus time grey-shaded spectrograms where the plotted grey-scale intensity is proportional to the log of the instrument count rate at each energy level. Due to the operational characteristics of the instrument, the count rate at a particular energy, and thus the grey-scale intensity, is an indicator of the directional energy flux per unit energy at the measured energy. In the mode of operation for data presented here, one complete electron spectrum and one complete positive ion spectrum are obtained each second.

The upper and center panels of the plot contain the electron and positive ion spectrograms, respectively. The vertical scales are logarithmic in energy from 1 eV to over 10^4 eV. The lower panel contains pitch angle information and average energies. The pitch angle denotes the instrument look direction such that 0° refers to downward-moving particles, 90° to locally mirroring particles, and 180° refers to particles coming from below the spacecraft. Note that the range of pitch angles sampled by the detectors, which look radial to the spacecraft spin axis, depends upon the angle between the spacecraft spin axis and the local magnetic field. This angle is denoted by θ_z and appears along the upper edge of the electron spectrogram. For θ_z=90° the spin axis is perpendicular to the magnetic field, and all pitch angles from 0° to 180° are sampled each half spin period. The average energies in the lower panel are computed once each second for electrons and for positive ions and represent the average energy per particle over the range 5 eV to approximately 15 keV. The horizontal axis is time ordered with the beginning Universal Time printed at the lower left hand corner. Each succeeding minute of Universal Time is indicated along each horizontal axis. Geographic latitude, geographic longitude, and local time are given at the bottom of the plots for the first and last data points. The quantities called "ECAL" are calibration indicators for internal use. The spacecraft location in Magnetic Local Time and Invariant Latitude at 1-minute intervals appears along the top horizontal axis. Orbit number and satellite altitude also are shown above the plots.

FORMAT 7 (ASP)

Because of the large dynamic range of the Auroral Scanning Photometer (ASP), it is necessary to use a grey-scale representation and a sequence of varying upper and lower intensity limits to display the data. An example of the plotted data is shown in Figure 7. The data are plotted on an electrostatic dot matrix plotter and arranged in three independent rows with the leftmost picture in each row containing the coordinate system. There is, in addition, header information at the top of the page giving basic information about the pass and how the data were transformed. In all cases, the coordinates are corrected geomagnetic latitude (CGL) (Hakura, 1965) and time (see Murphree and Anger, 1980, for a description of the transform procedure). This magnetic coordinate system is denoted by the "M" in the lower left-hand corner of each coordinate picture. The accompanying "V" indicates that the intensity data have been corrected for look direction, i.e., van Rhijn effect. However, the data are not corrected for ground scattering and thus real intensity levels will be less depending on the spectral albedo of the surface under the auroral emissions. Latitudes are labeled in general every 10° and the Magnetic Local Time (MLT) every 6 hours. The geomagnetic pole is represented by a " + ".

The spacecraft track projected down to 100 km along magnetic field lines is given by the sequence of triangles, the approximate orbital motion being defined as the direction of the apex of the triangle. The triangles represent the position of the spacecraft exactly on the minute, the particular minute being derivable from the sequence of triangle shapes as follows. The basic shape

---

Hakura, Y., Tables and maps of geomagnetic coordinates corrected by the higher order spherical harmonic terms, Rep. Ionosph. Space Res., Japan, 19, 121, 1965.

Murphree, J. S., and C. D. Anger, An observation of the instantaneous optical auroral distribution, Can. J. Phys., 58, No. 2, 214-223, Feb. 1980.

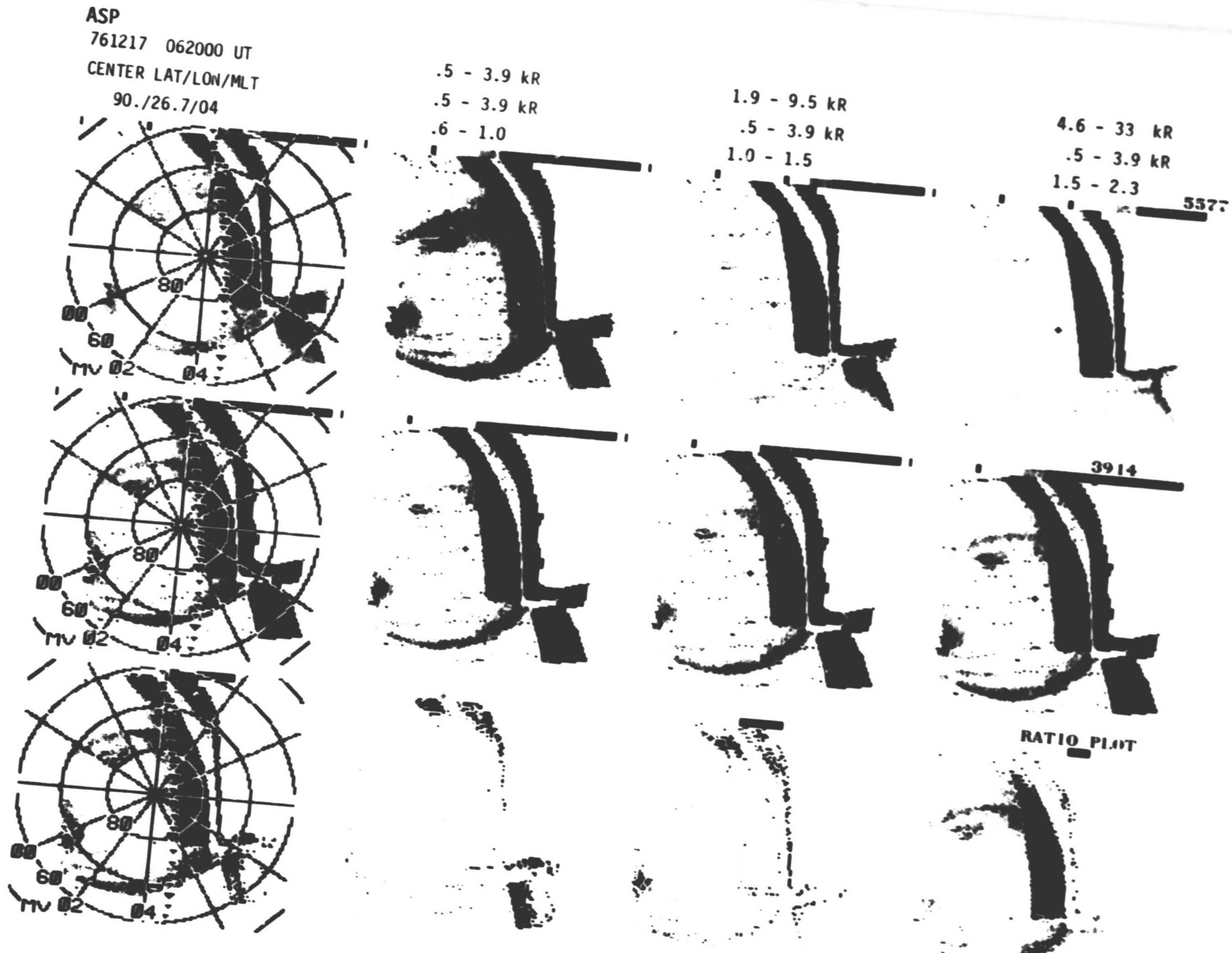

Figure 7. Example of Format 7 (ASP).

consists of filled (or a blank, depending on the surrounding background) blocks denoted below by "x":

```
  x
 xxx - represents any minute not specified in the following


  x
 xxx - one of the following:  5, 15, 25, 35, 45, 55 UT minute
xxxxx


  x
 xxx  - UT minute 10 or 50
xxxxx
  x



  x
 xxx
xxxxx  - UT minute 20 or 40
 xxx


  x
 xxx  - UT minute 0 or 30
xxxxx
xxxxx
```

The actual time values can be obtained by noting the start time in the header and identifying the first time symbol in the coordinate picture.

The start and/or end of a pass may or may not be apparent in the given transform, depending on the range (in degrees) to which it was desired to transform the data, but the spacecraft track indication will continue to the end of the coordinate system. If start or end does occur within the range of the transform, the data will be truncated in a straight line. In contrast to this, the limit of optical observations at 90° to the spacecraft track (its limbs) will form a pair of irregular lines parallel to and equidistant from the spacecraft track.

The data appearing in each picture in each row are a grey-scale representation of the intensity for the appropriate wavelength. Each picture element is represented by a 3 x 3 square matrix of dots and anywhere from 0 (at or below the bottom of the desired intensity range) to 9 (at or above the top of the range) of the dots are blackened so as to provide a grey scale. For example, if the picture is labeled .6 - .95 (the numbers representing kR for intensities and ratio values for ratio plots), then any points with intensities less than or equal to .6 kR will be white while any elements greater than or equal to .95 kR will be black. The three rows of pictures represent 5577Å intensity, 3914Å intensity and the ratio I(5577Å)/I(3914Å), respectively. In general, the 5577Å data are displayed in the three rightmost pictures of the first row with three different intensity ranges (in kR), e.g., .5 - 3.9, 1.9 - 9.5, 4.6 - 33, while 3914Å uses a single range for all three pictures, this range being the same as that for the lowest 5577Å range. The picture onto which the coordinate system is overlayed has a range equal to the entire range of intensities covered by all of the pictures in the row. For example, in the above 5577Å ranges, the coordinate picture would contain .5 - 33 as the kR range.

In the pass shown in Figure 7, the 5577Å and 3914Å data illustrate the northern hemisphere polar cap on 761217 at 0620 UT. The satellite track is basically from 16 MLT to 5 MLT as the data show well-defined auroral emissions in the evening (16 - 21 MLT) and morning (00 - 07 MLT) sectors. The midnight sector of the auroral emissions was beyond the limb on this pass as indicated by the irregular boundary of the data in that MLT sector. The dayside is contaminated by scattered sunlight as is illustrated by the high intensity, regular feature in both wavelengths. This is a common feature because of the difficulty in combining the correct satellite altitude with both time of year and UT to optimize dayside viewing conditions. Such features are usually easily distinguished from auroral emissions because they are aligned with the spacecraft track rather than with the magnetic coordinate system.

Because of contrast problems, it is necessary to approach the ratio in a different manner. Each of the three pictures in the ratio plot row represents different ratio ranges which are always chosen to be: 0.6 - 1.0, 1.0 - 1.5, 1.5 - 2.3. The ratio for each element (i.e., position in the coordinate system) in each picture is calculated. If it falls within the specified range as given above, then the 3914Å <u>intensity</u> at the point is plotted based upon the 3914Å intensity thresholds in the same column of the previous row (this is why all 3914Å thresholds are identical). The result is three pictures which show where 3914Å emissions are observed (and their intensity) for the three ratio ranges. The composite (i.e., the leftmost picture with the superimposed coordinate grid) then should be similar to the composite 3914Å given in the previous row. Any missing points in the composite picture will correspond to ratio values outside the range 0.6 - 2.3.

FORMAT 8 (RLP)

In this format the isointensity contours of atomic oxygen 6300Å emission are shown, obtained with the Red Line Photometer (RLP) and plotted in a polar invariant projection. The perimeter corresponds to 50° invariant, and dashed circles indicate 60°, 70°, and 80° invariant. Invariant noon is at the top and morning (06 h) on the right. The intensities corresponding to the contours selected are listed on the upper right, and the contours themselves are labeled in units of tens of rayleighs (25 = 250R). The orbit number, date, day number, and Universal Time for the first and last spins of the pass are given on the upper left. The hatched line shows the track of the spacecraft traced down to the 250 km level, the height assumed for the altitude of emission; each hatch mark indicates one rotation (spin) of the spacecraft, and every tenth spin is labeled. The spin axis is nearly parallel to the orbit plane. The Universal Times that correspond to each spin number are given on the far right-hand side.

The intensities given are not corrected for albedo and so over regions of widespread emission they may be too large by a factor of two. If the label at the top reads "6300 angstrom intensity" then a correction for white light background has been applied. If it reads "10 angstrom bandpass intensity" then there has been difficulty with white light subtraction in part of the picture and the 10Å channel data are shown uncorrected. The intensities shown for these cases will be less accurate than for the others.

The example shown in Figure 8 illustrates some aspects of the data and some of the peculiarities. The features discussed below correspond to contours that have been labeled, A → G.

A. These contours arise from sunlight scattered from the Earth. They can be recognized by their proximity to noon and by their steep gradient.

B. These linear contours are caused by scattering in the RLP baffle system, and the steep gradient is caused by one critical baffle element. When the solar illumination leaves this element the baffle scattering falls rapidly and the auroral contours become visible.

C. These linear contours, having a steep gradient, are generated by the passage of the spacecraft from sunlight into darkness, with the cessation of baffle scattering. These contours are perpendicular to the spacecraft track, and the rectangular pattern of B/C normally can be recognized readily.

D. Dayside auroral contours. The morning extension of the dayside auroral contours are evident here, extending from the region of baffle scattering. When baffle scattering is not present this pattern is normally roughly symmetric about noon.

E. Night auroral contours. These contours define the region of brighter nightside aurora.

F. Equatorward auroral boundary. These contours define the equatorward boundary of 6300Å aurora. The termination after midnight is caused by the scans reaching the "edge" of the Earth; i.e., the limb.

G. Poleward auroral boundary. These contours define the poleward auroral boundary and normally form a near-circular region in the polar cap.

FORMAT 9 (ASP AND RLP)

This format provides latitude profiles of airglow emission rate at 5577Å and 6300Å obtained from the ASP and RLP. In the cartwheel mode of operation, the fields of view of the photometer sweep along the path of the orbit to provide data over a large range of latitudes but a very small range of longitudes. Pole-to-pole coverage can be achieved in a time interval of about 30 minutes.

The latitude profiles are based on airglow limb data which result in a measurement at the leading and trailing limb for each limb. This ensures that the data are free from cloud and ground albedo effects and contamination by other sources of light. It also permits the separation of the 5577Å airglow into the E- and F-region components (see Format 12), both of which are plotted. The maximum of the E region airglow is defined to occur at 95 km for the 5577Å data and the F region is then referenced to that level. The emission rates given correspond to what would be observed in the zenith from below at the location of the airglow limbs. The plots therefore represent the vertical

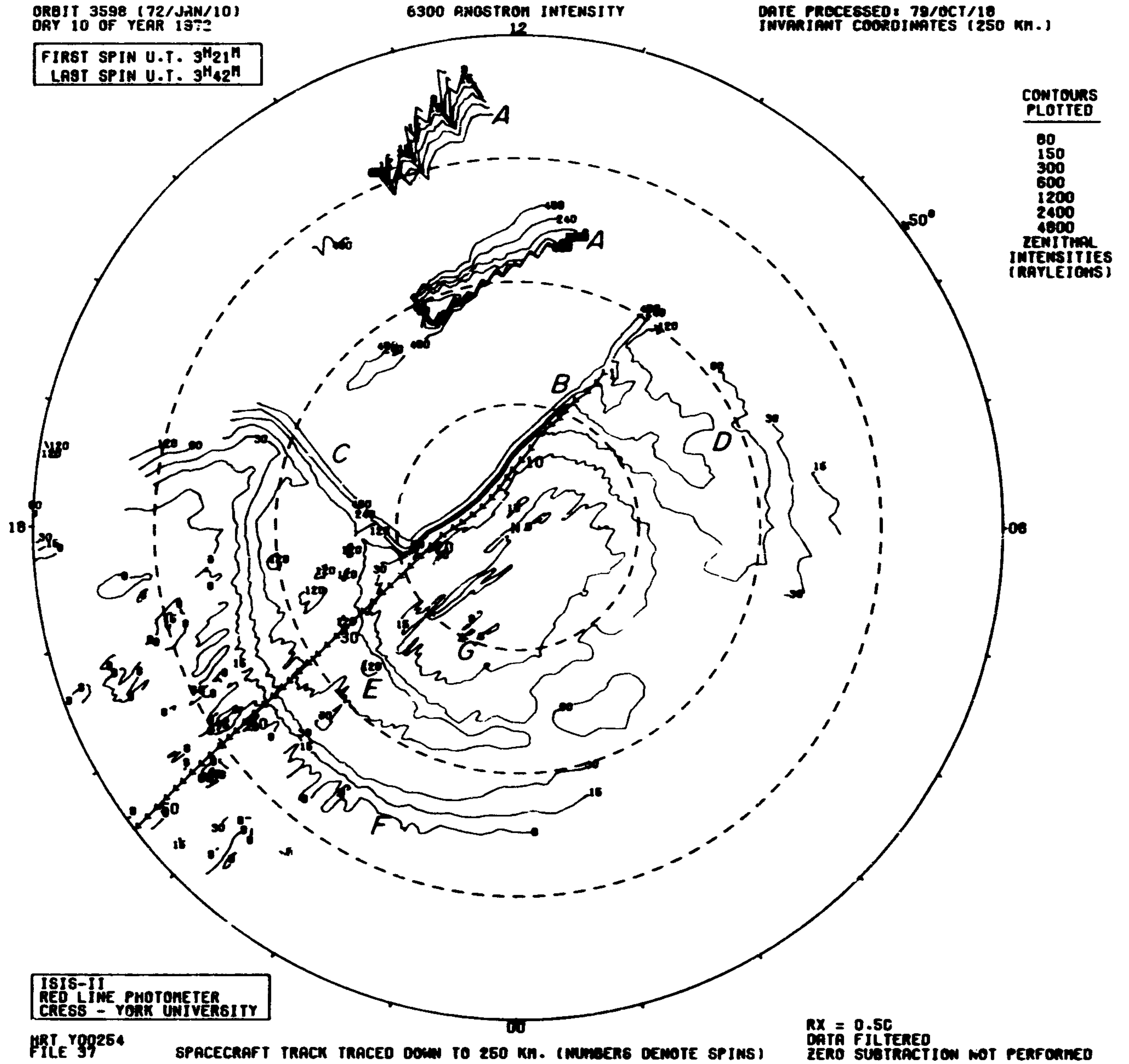

SPACECRAFT INFORMATION

SPIN NUMBER	ORBIT TIME (HRMNSC)	INVARIANT LATITUDE (DEGREES)
1	032159	76.3
2	032223	77.3
3	032247	78.3
4	032311	79.3
5	032335	80.2
6	032353	80.9
7	032417	82.0
8	032441	82.9
9	032505	83.6
10	032529	84.0
11	032553	84.2
12	032611	84.3
13	032635	84.3
14	032659	84.3
15	032723	84.3
16	032747	84.3
17	032811	84.2
18	032829	83.9
19	032853	83.5
20	032917	82.8
21	032941	81.9
22	033005	80.8
23	033029	79.8
24	033053	78.8
25	033111	78.1
26	033135	77.1
27	033159	76.0
28	033223	75.0
29	033247	73.9
30	033305	73.1
31	033329	72.1
32	033353	71.0
33	033417	69.9
34	033441	68.8
35	033505	67.7
36	033523	66.9
37	033547	65.8
38	033611	64.7
39	033635	63.6
40	033659	62.5
41	033723	61.3
42	033741	60.5
43	033806	59.4
44	033829	58.3
45	033853	57.2
46	033917	56.0
47	033941	54.9
48	033959	54.1
49	034023	53.0
50	034047	51.9
51	034111	50.8
52	034135	49.7
53	034159	48.6
54	034217	47.7
55	034241	46.7

Figure 8. Exa⁊ple of Format 8 (RLP) with the events A through G.

emission rate in rayleighs as a function of geographic latitude. The points are not independent due to the fact that the optical viewing path in the atmosphere is longer than the spatial sample interval which is determined by the orbital speed of the satellite. As a consequence the plots correspond to a running mean of the emission rate.

In practice, the latitude range is restricted to low and mid-latitudes due to the presence of aurora at higher latitudes. The difference between leading and trailing limb values when they overlap in the plot is due either to the small difference in longitude or to temporal variation in the airglow.

FORMAT 10, TOP (CEP)

See Format 4 (Top) description. The latitude, longitude, local time, dip angle, dip latitude, L value, invariant latitude, and solar zenith angle are given below the graphs.

FORMAT 10, BOTTOM (SOUNDER)

See Format 2 (Bottom) description.

FORMAT 11 (VLF)

VLF data published herewith are presented in the conventional amplitude-frequency-time display wherein signal corresponds to the dark parts of the display. These data are from routine 35-mm records having the frequency axis across the film and the time along the film. This data book has room only for interesting excerpts of the receiver film record. In data set C of Volume 4 the VLF film has been printed at 2X magnification to illustrate the details of a variety of typical phenomena observed by ISIS 2. In the other data sets, film is printed at 1X magnification. The VLF receiver was off during the majority of the passes. Excerpts of the VLF record for receiver-on passes have been chosen to show the highlights of those passes. In many cases, the VLF exciter was on and its periodic frequency downsweeps can be seen.

The example of the data format given in Figure 9 shows the frequency axis running linearly from 0 to 21 kHz, and the Universal Time axis running linearly from 06:41:10 to 06:41:39 (hours:minutes:seconds). Both the frequency and time limits are to be associated with the extremes of the film. In the example given, the broad diffuse patches are a natural emission, VLF hiss. The record also contains four instances of the received exciter signal. Two of these are on the fast duty cycle, at 06:41:15 and 06:41:21, and two on the slow cycle, at 06:41:23 and 06:41:34.

FORMAT 12 (ASP)

This format provides examples of the 5577Å airglow limb profiles obtained during a pass. The selection was made to demonstrate the variation of the two components of the airglow. The vertical axis gives the tangential height. In all cases the reference height of 95 km has been arbitrarily assigned to the maximum of the E- region airglow response. The slant intensity in kilorayleighs (kR) is plotted along the horizontal axis. The profiles, obviously broadened by the finite field of view of the instrument, do not give information about the detailed vertical distribution; they merely demonstrate the resolution of the main components.

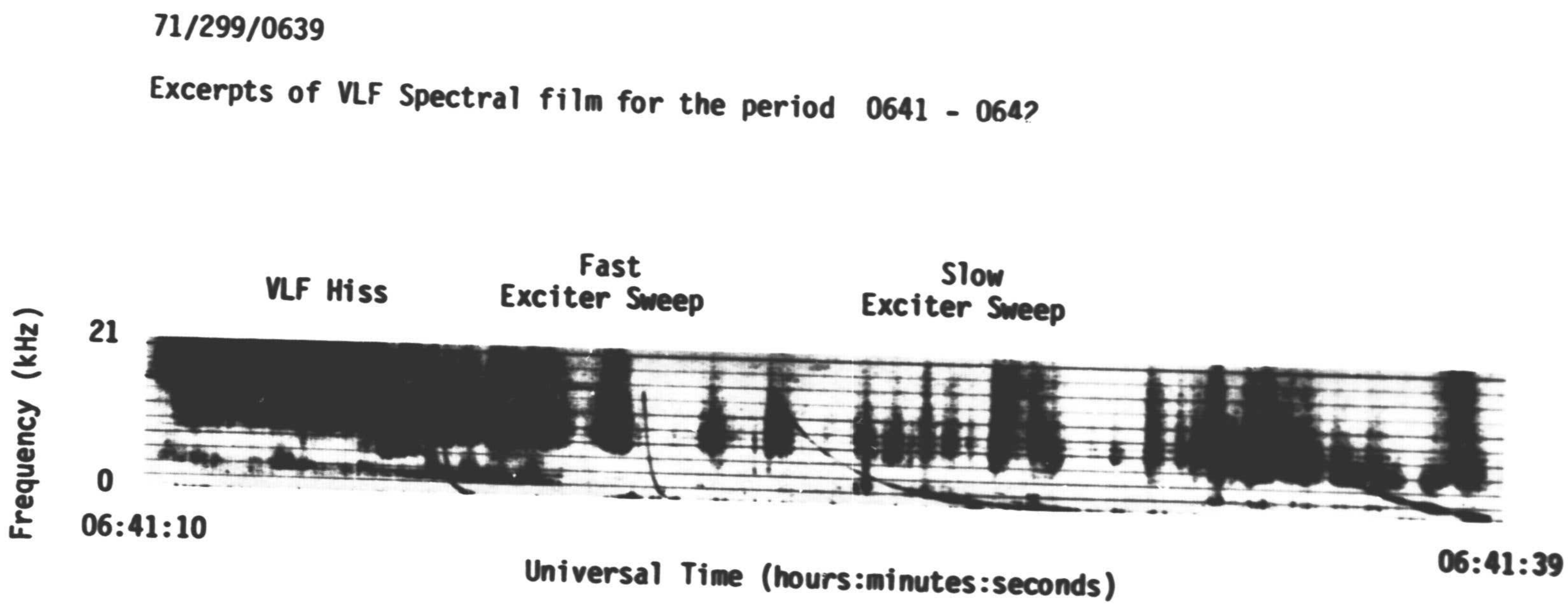

Figure 9. Example of Format 11 (VLF).

VI-A. GEOPHYSICAL DATA SET: LARGE STORMS

DATA SET DESCRIPTION

The large storm data set was selected to illustrate auroral conditions prior to, during and following a major magnetic storm. The ISIS 2 satellite is capable of being placed in two distinct modes as it orbits the Earth. First, the satellite spin axis may lie in the plane of the orbit such that instruments perpendicular to the spin axis rotate at 90° to the orbital motion. This is called the orbit-aligned mode. Second, the spin axis may be perpendicular to the orbit plane such that the resulting rotation of the instrument view directions is confined within the orbit plane. This is called the cartwheel mode. It is the orbit-aligned mode which is of interest here, as in this mode side-to-side scanning of the optical instruments is produced by the satellite rotation.

In the orbit-aligned mode, the two optical instruments, the Auroral Scanning Photometer (ASP) and the Red Line Photometer (RLP), sweep out fixed angular strips perpendicular to the direction of orbital motion of the satellite (see Figure 3 in the Instrument description of the ASP). These strips can be combined during data processing to provide grey-scale geomagnetic transforms (ASP) and contour plots (RLP), both of which illustrate the full remote sensing capabilities of the optical instruments. This remote sensing capability poses strict constraints first of all upon viewing conditions and also upon coordination with other satellite instruments which make direct (i.e., along the satellite path) measurements. The constraint on viewing conditions limits this data set to a magnetic storm which occurs when a significant fraction of the high latitude auroral region is dark. The latter constraint occurs because some instruments (e.g., ion mass spectrometer, retarding potential analvzer) require measurements to be made in the direction of the velocity of the satellite. Therefore, in this data set, only the following instruments (in the order of presentation for each pass) are used:

1. Auroral Scanning Photometer, Format 7
2. Red Line Photometer, Format 8
3. Energetic Particle Detector, Format 3
4. Soft Particle Spectrometer, Format 6
5. Cylindrical Electrostatic Probe, Format 10

   Topside Sounder, Format 10

Magnetic storms may or may not be simply an extreme case of the much more common magnetic substorm which is characterized by a brightening and poleward expansion of discrete arc systems. It is assumed that a magnetic storm may be coarsely identified by the occurrence of high Kp values; i.e., greater than 5.

This in itself is relatively uncommon; for example, for the years 1972-1975 inclusive Kp was greater than 4+ only ~ 9% of the time. Thus the combination of occurrence frequency and viewing conditions limits this data set to observations of the magnetic storm of 17-18 December 1971.

The data taken during this magnetic storm period are listed in Table 1. The peak in activity as defined by Kp occurred in the 18-21 UT interval on 17 December 1971. It should be stressed that the observations presented here are not typical auroral conditions, but rather represent some of the most extreme distortions of the optical aurora which have been observed. Perhaps the most interesting optical observation of the period is the destruction of any well defined oval even well after the peak in activity. Examples of this are the 0556 UT pass on 18 December, and the 0324 and 0518 passes on 20 December. Note that the concept of the classical polar cap must be significantly modified to account for observations such as these.

Table 1 Data Set Pass List

Date	UT	Kp	Page	Data Set
711217	0518	5+	35	1
711217	0705	4+	38	2
711217	0717	4+	41	3
711218	0207	4-	44	4
711218	0402	4	49	5
711218	0556	4	54	6
711219	0246	1-	59	7
711220	0324	0	64	8
711220	0518	0	69	9
711221	0402	1	74	10

ORBIT 3295 (71/DEC/17)
DAY 351 OF YEAR 1971

FIRST SPIN U.T. $5^{H}19^{M}$
LAST SPIN U.T. $5^{H}39^{M}$

6300 ANGSTROM INTENSITY

DATE PROCESSED: 80/AUG/14
INVARIANT COORDINATES (250 KM.)

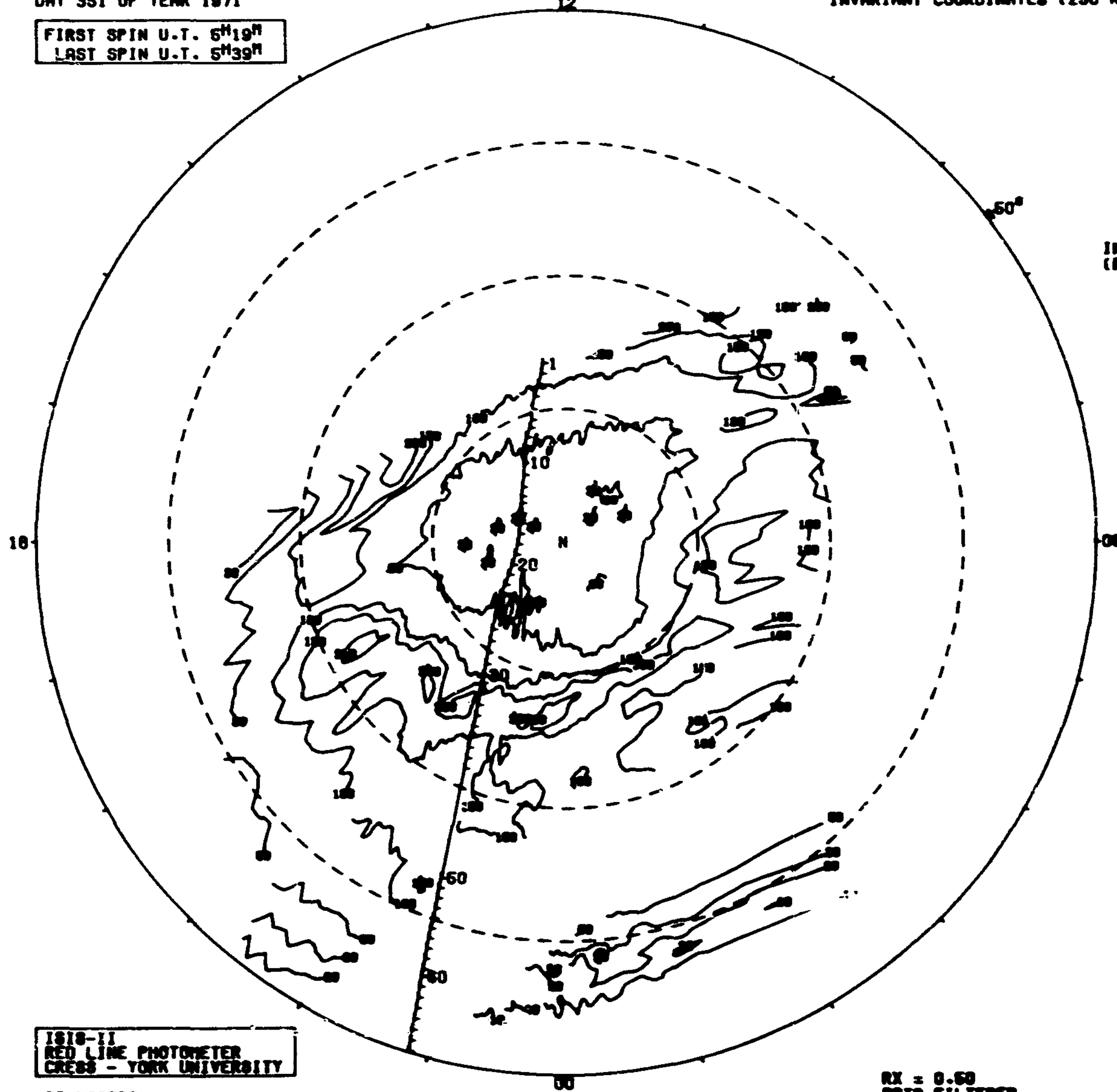

CONTOURS PLOTTED

100
200
300
500
1000
1500
2500
ZENITHAL INTENSITIES (RAYLEIGHS)

SPACECRAFT INFORMATION

SPIN NUMBER	ORBIT TIME (HRMNSC)	INVARIANT LATITUDE (DEGREES)
1	061917	77.2
2	061936	77.8
3	061953	78.7
4	062011	79.4
5	062029	80.0
6	062047	80.7
7	062105	81.5
8	062123	82.3
9	062141	82.9
10	062159	83.4
11	062217	83.8
12	062235	84.0
13	062253	84.2
14	062306	84.3
15	062323	84.3
16	062341	84.3
17	062359	84.3
18	062417	84.3
19	062435	84.3
20	062453	84.3
21	062511	84.2
22	062529	83.8
23	062547	83.4
24	062605	82.9
25	062623	82.3
26	062641	81.7
27	062659	80.9
28	062717	80.1
29	062735	79.4
30	062753	78.7
31	062806	78.2
32	062823	77.6
33	062841	76.7
34	062859	75.9
35	062917	75.2
36	062935	74.4
37	062953	73.6
38	063011	72.8
39	063029	72.0
40	0	0.0
41	0	0.0
42	0	0.0
43	0	0.0
44	0	0.0
45	0	0.0
46	0	0.0
47	0	0.0
48	0	0.0
49	0	0.0
50	063341	63.3
51	063359	62.5
52	063417	61.7
53	063435	60.8
54	063453	60.0
55	063511	59.2
56	063529	58.3
57	063547	57.5
58	063605	56.7
59	063623	55.8
60	063635	55.3
61	063653	54.5
62	063711	53.6
63	063729	52.8
64	063747	52.0
65	063805	51.1
66	063823	50.3
67	063841	49.5
68	063859	48.7
69	063917	47.8

ISIS-II
RED LINE PHOTOMETER
CRESS - YORK UNIVERSITY

MAT Y00278
FILE 10

SPACECRAFT TRACK TRACED DOWN TO 250 KM. (NUMBERS DENOTE SPINS)

RX = 0.60
DATA FILTERED
ZERO SUBTRACTION NOT PERFORMED

SET 1, FORMAT 8

PRECEDING PAGE BLANK NOT FILMED

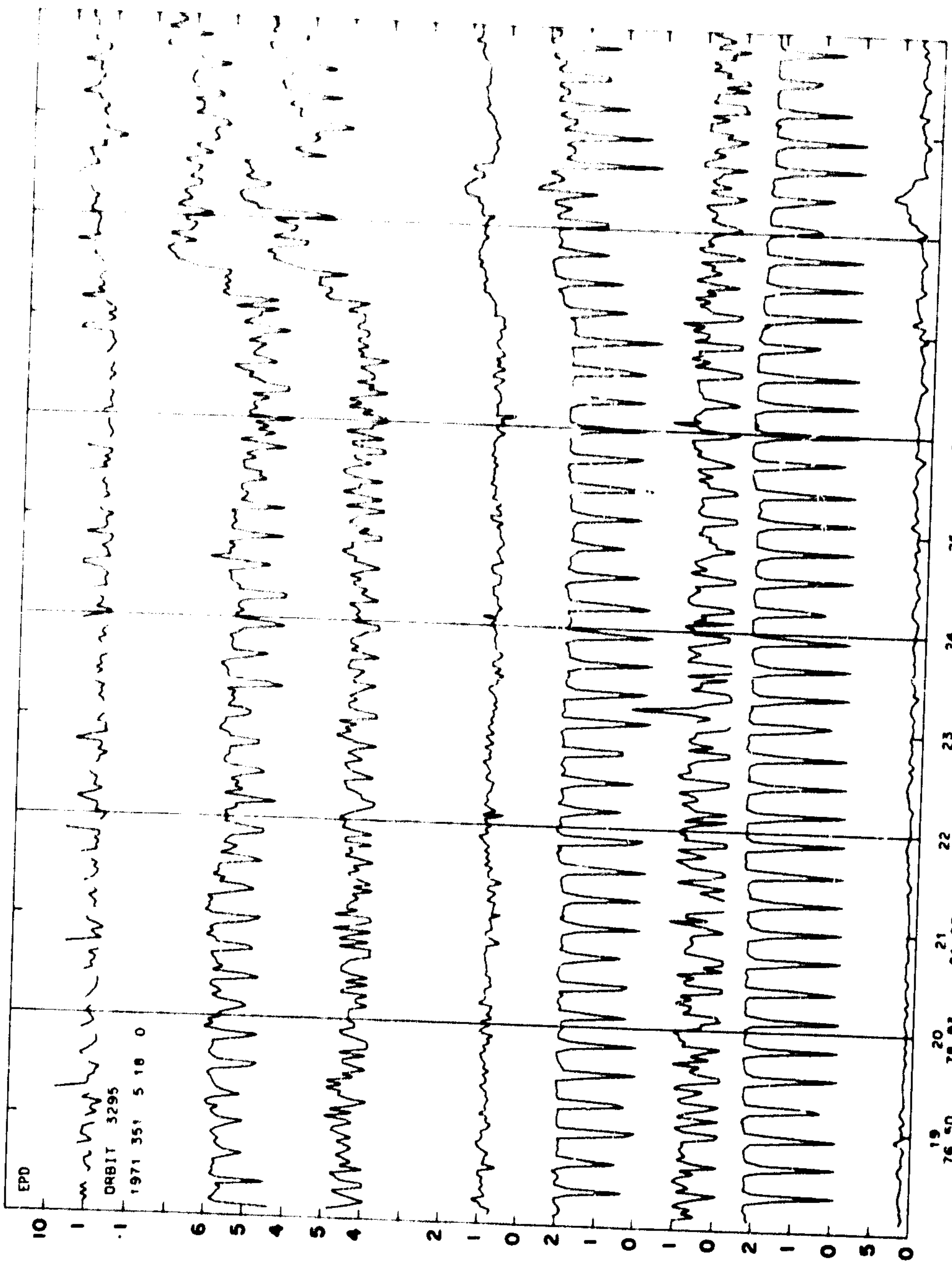

SET 1, FORMAT 3

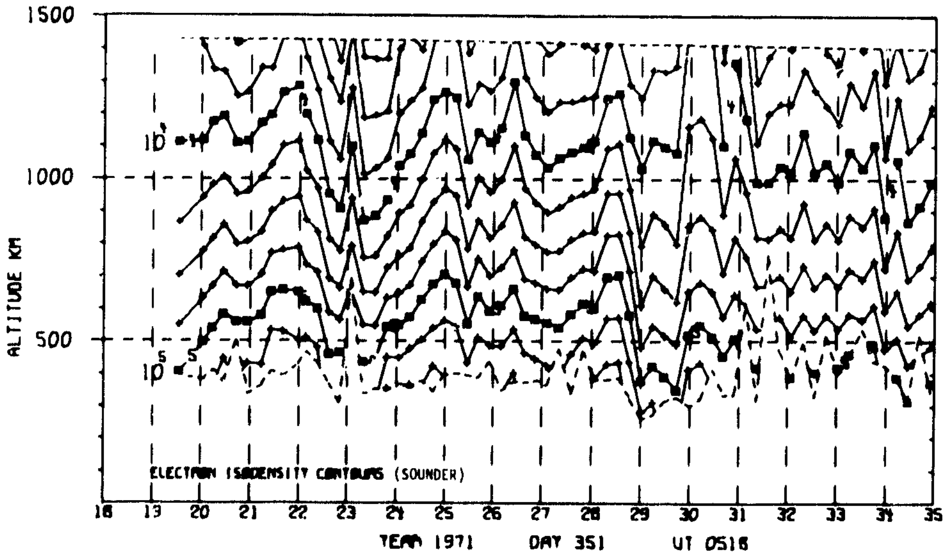

SET 1, FORMAT 10

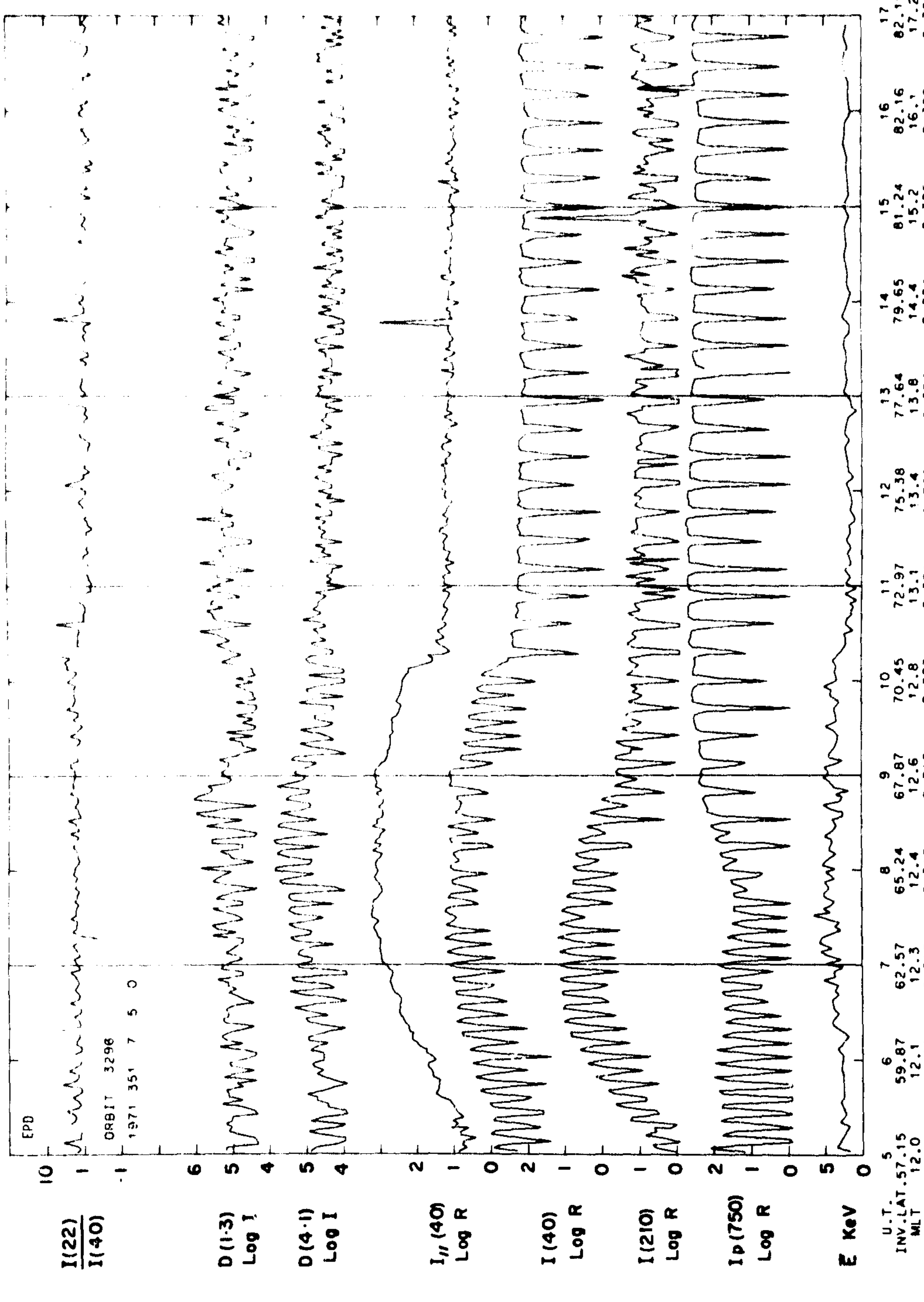

SET 2, FORMAT 3

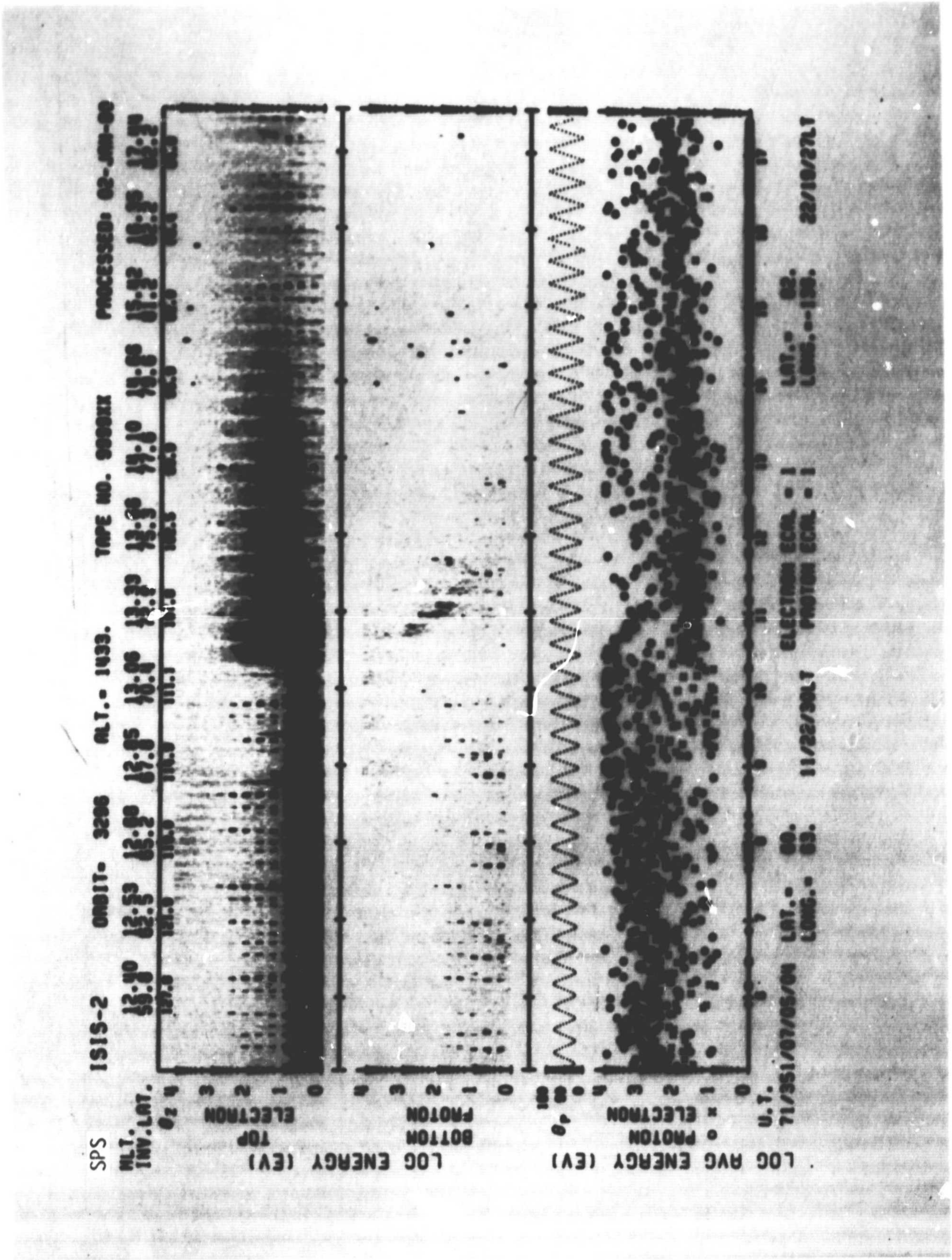

SET 2, FORMAT 6

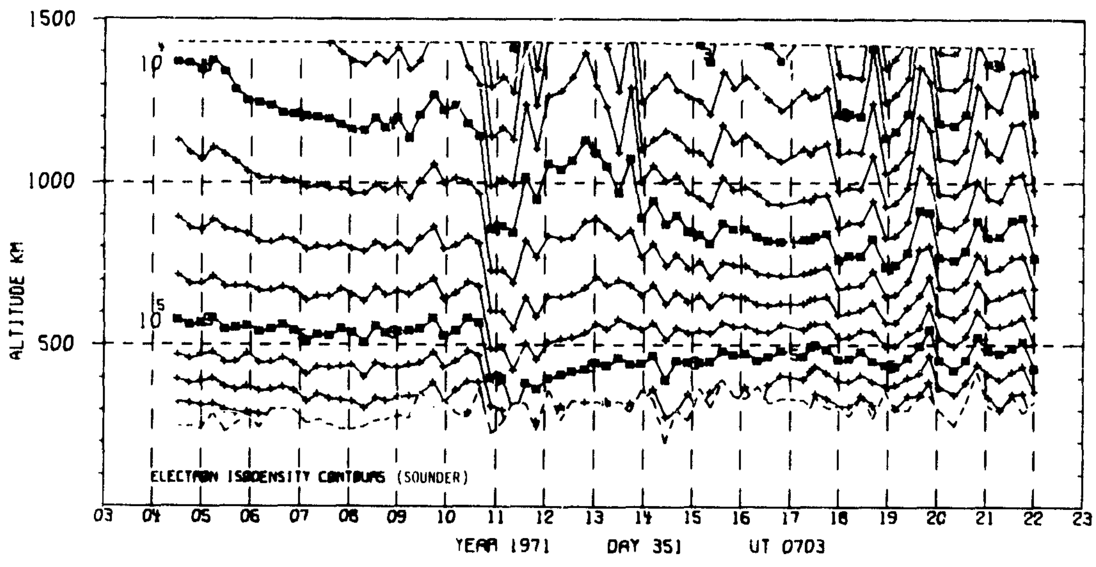

SET 2, FORMAT 10

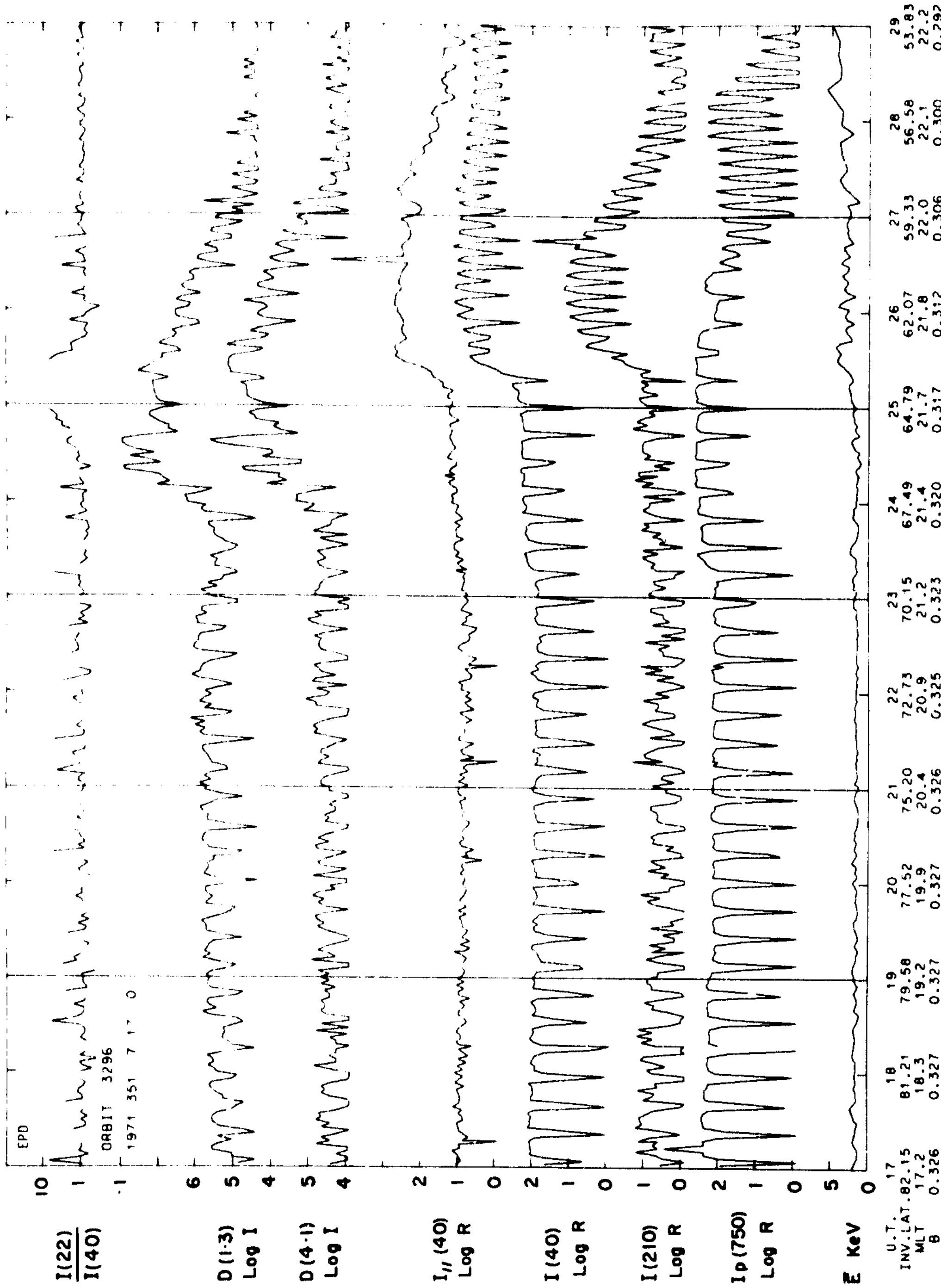

SET 3, FORMAT 3

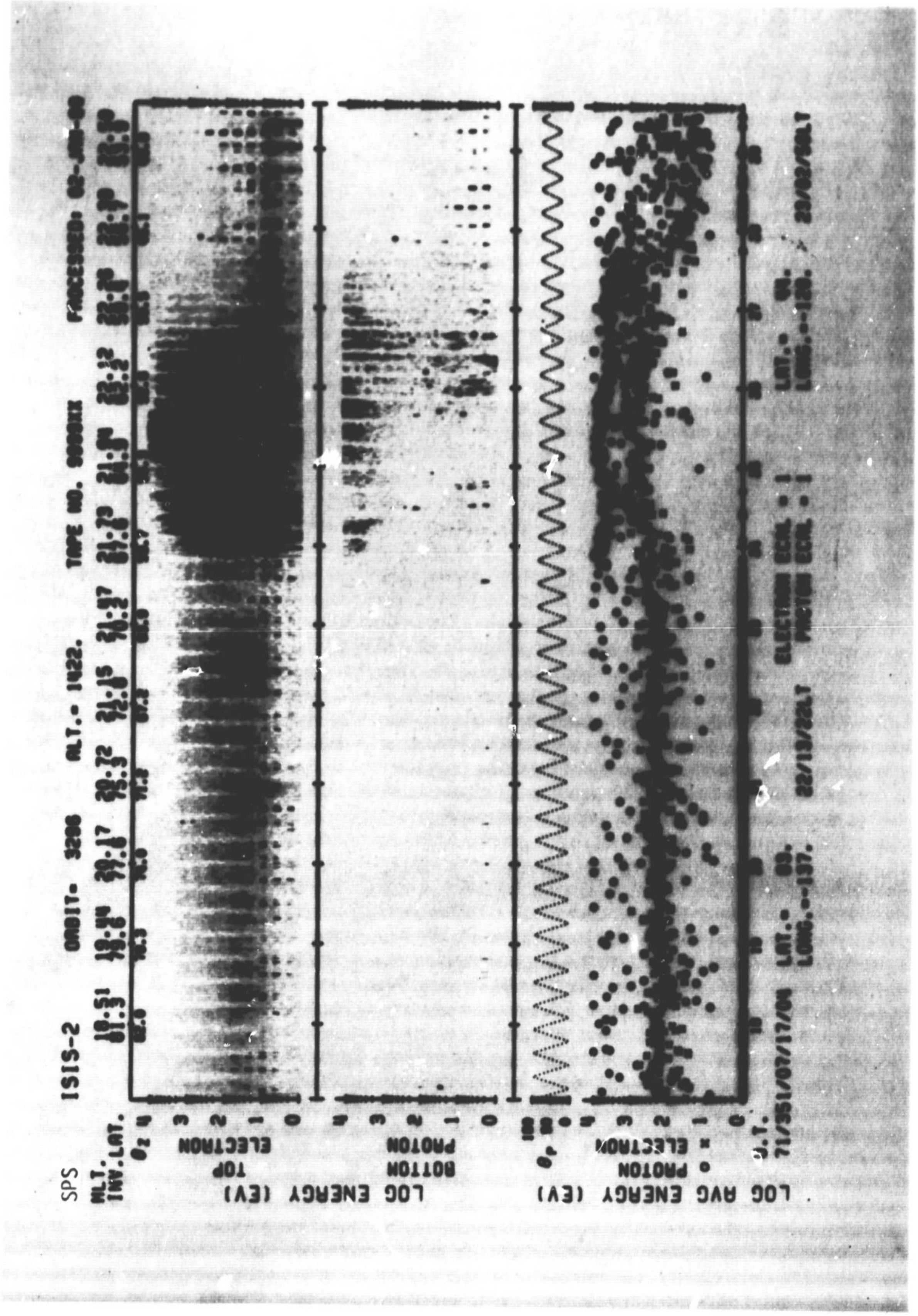

SET 3, FORMAT 6

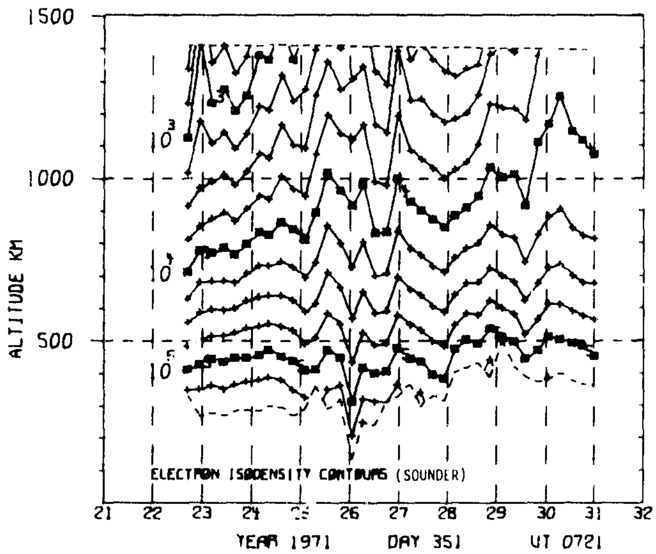

SET 3, FORMAT 10

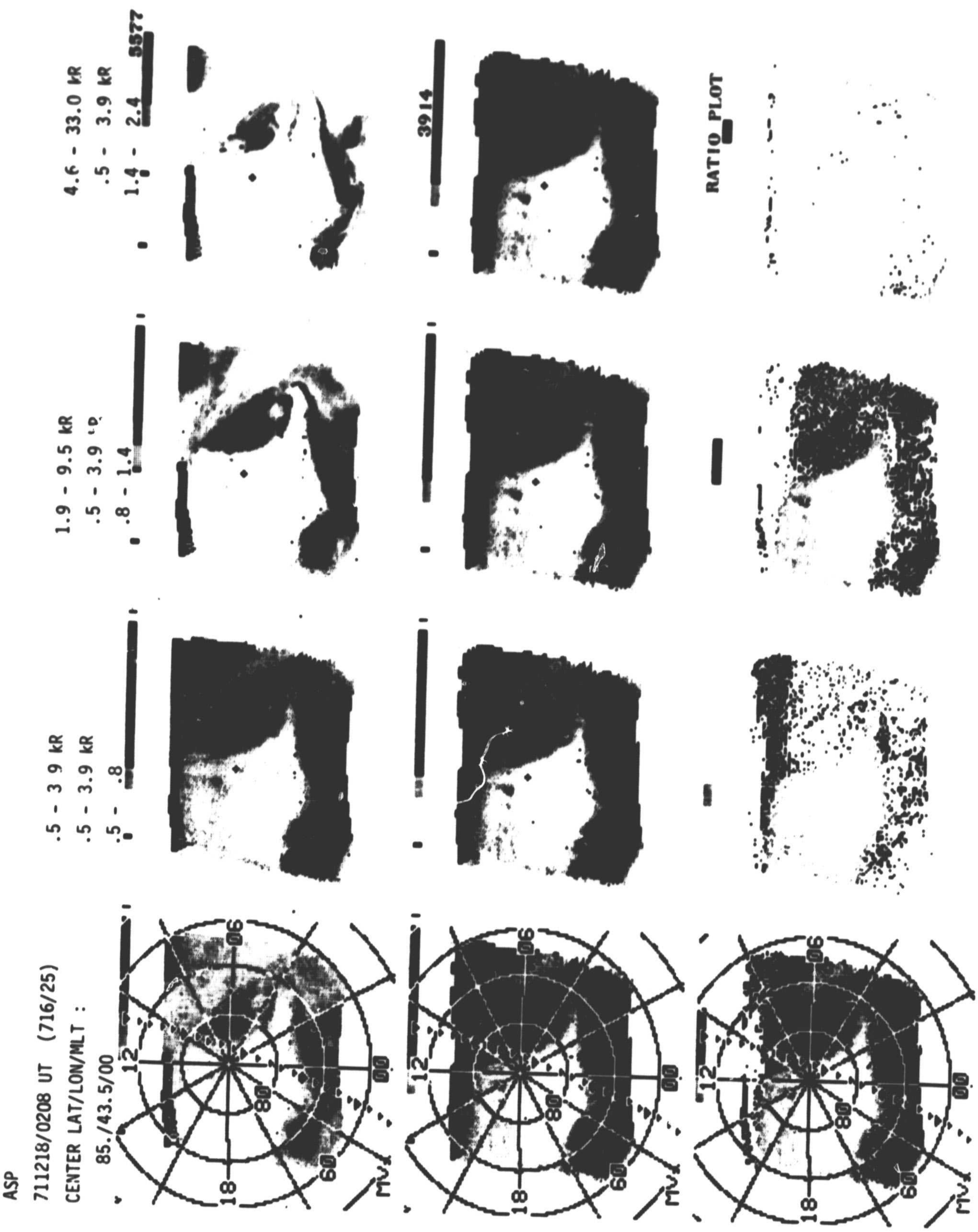

SET 4, FORMAT 7

ORBIT 3306 (71/DEC/18)
DAY 352 OF YEAR 1971

FIRST SPIN U.T. 2^H8^M
LAST SPIN U.T. 2^H19^M

6300 ANGSTROM INTENSITY

DATE PROCESSED: 80/AUG/14
INVARIANT COORDINATES (250 KM.)

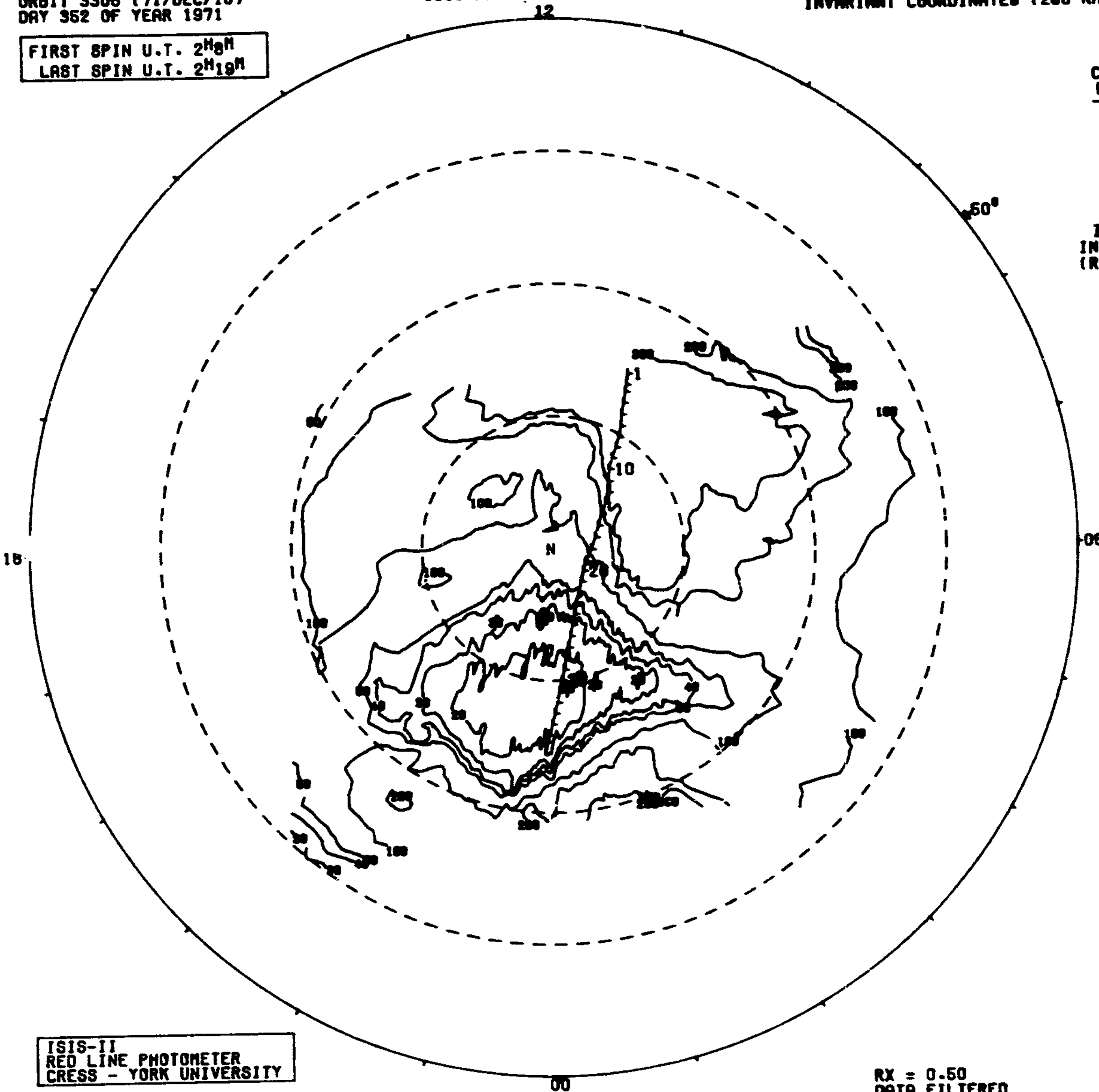

CONTOURS PLOTTED

200
300
400
500
1000
2000
3000
ZENITHAL INTENSITIES (RAYLEIGHS)

SPACECRAFT INFORMATION

SPIN NUMBER	ORBIT TIME (HRMMSC)	INVARIANT LATITUDE (DEGREES)
1	020858	75.9
2	020916	76.8
3	020928	77.3
4	020946	78.1
5	021004	78.9
6	021022	79.6
7	021040	80.4
8	021058	81.3
9	021116	82.3
10	021134	83.2
11	021152	83.8
12	021210	84.1
13	021228	84.2
14	021246	84.2
15	021304	84.3
16	021322	84.3
17	021340	84.3
18	021358	84.3
19	021416	84.3
20	021428	84.3
21	021446	84.3
22	021504	84.3
23	021522	84.2
24	021540	84.1
25	021558	83.9
26	021616	83.4
27	021634	82.7
28	021652	81.7
29	021710	80.7
30	021728	79.9
31	021746	79.3
32	021804	78.5
33	021822	77.7
34	021840	77.0
35	021858	76.1
36	021910	75.6
37	021928	74.8

ISIS-II
RED LINE PHOTOMETER
CRESS - YORK UNIVERSITY

HRT Y00276
FILE 11

SPACECRAFT TRACK TRACED DOWN TO 250 KM. (NUMBERS DENOTE SPINS)

RX = 0.50
DATA FILTERED
ZERO SUBTRACTION NOT PERFORMED

SET 4, FORMAT 8

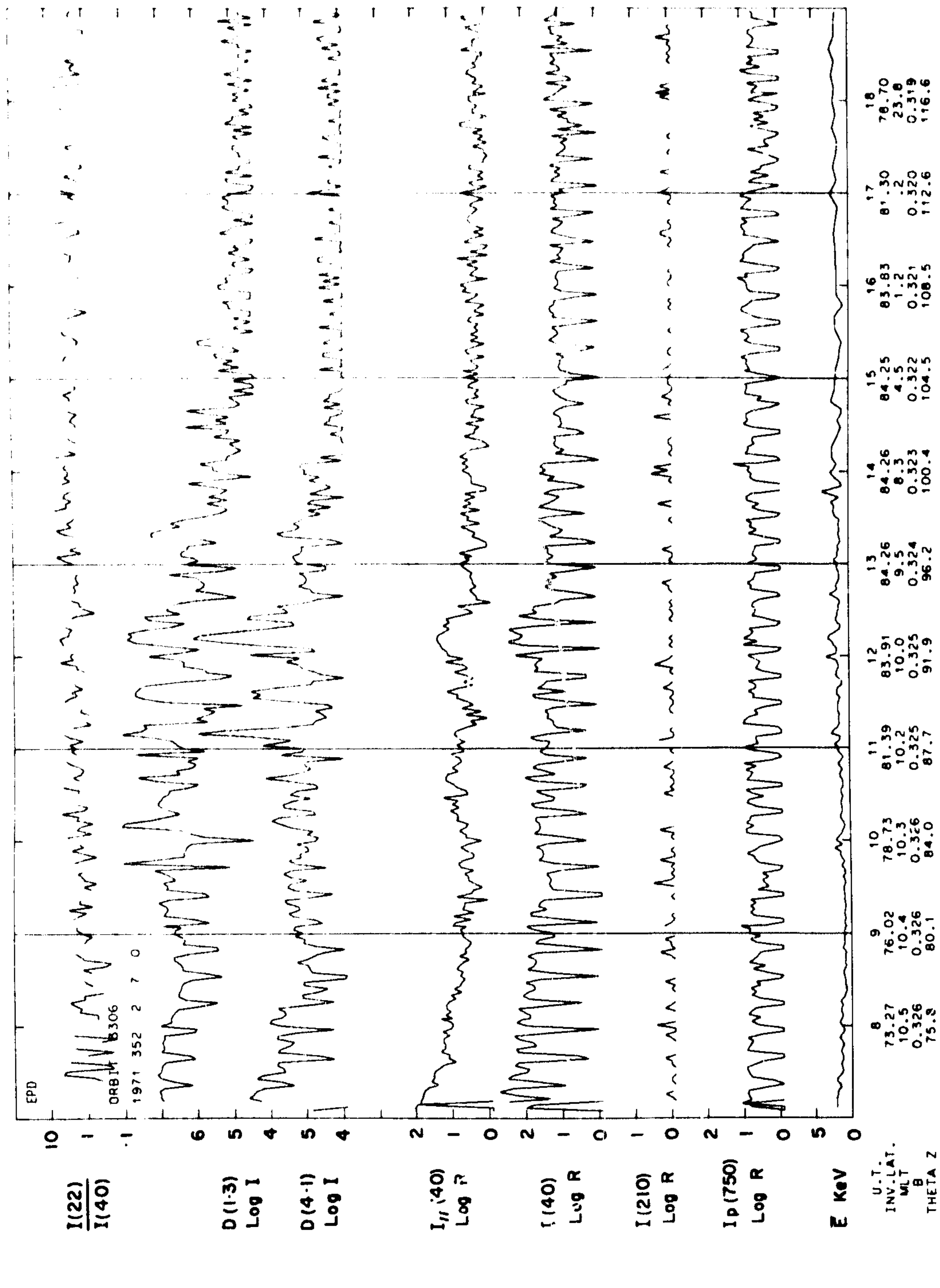

SET 4, FORMAT 3

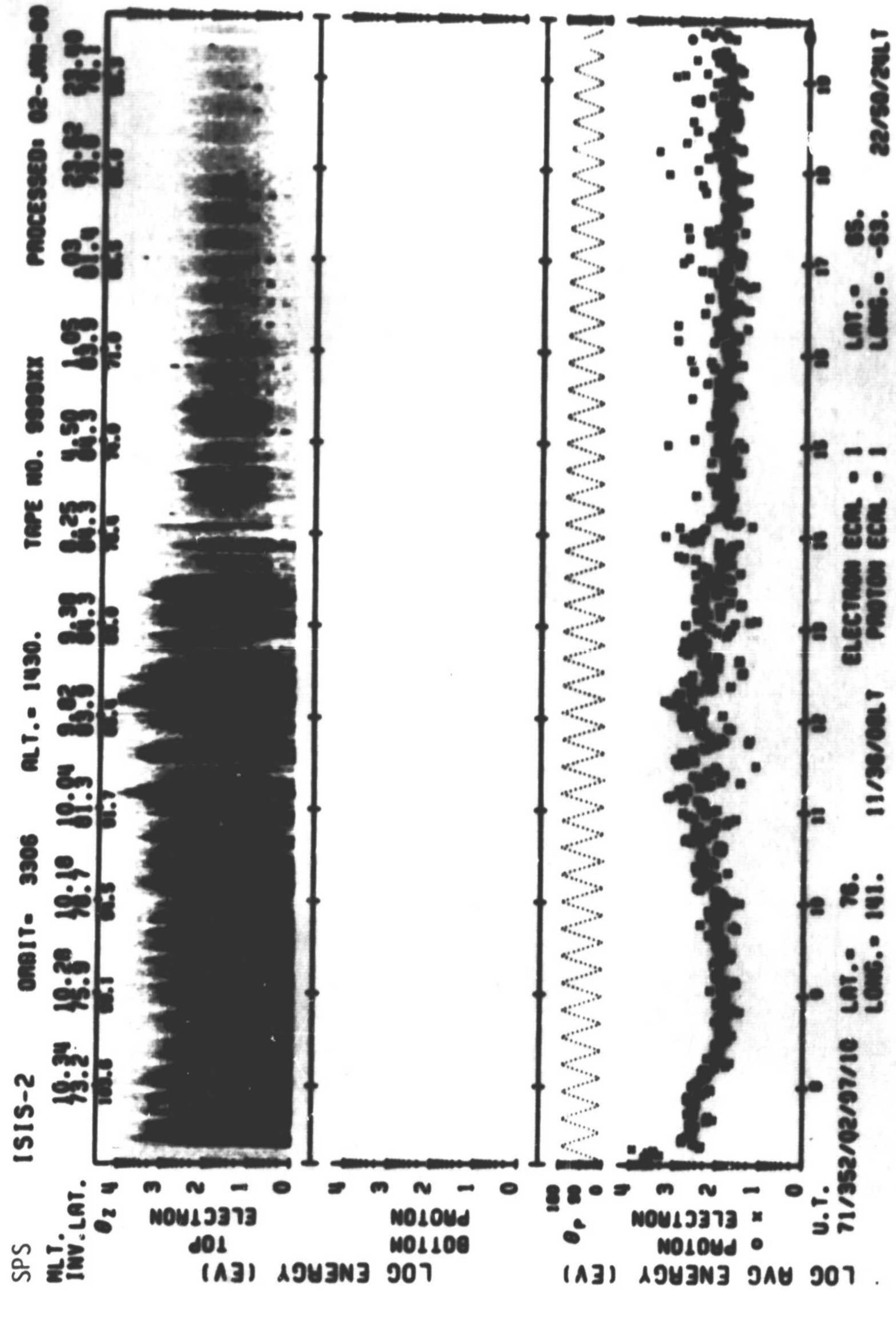

SET 4, FORMAT 6

ORBIT 3306
DATE 71:218
DAY 352

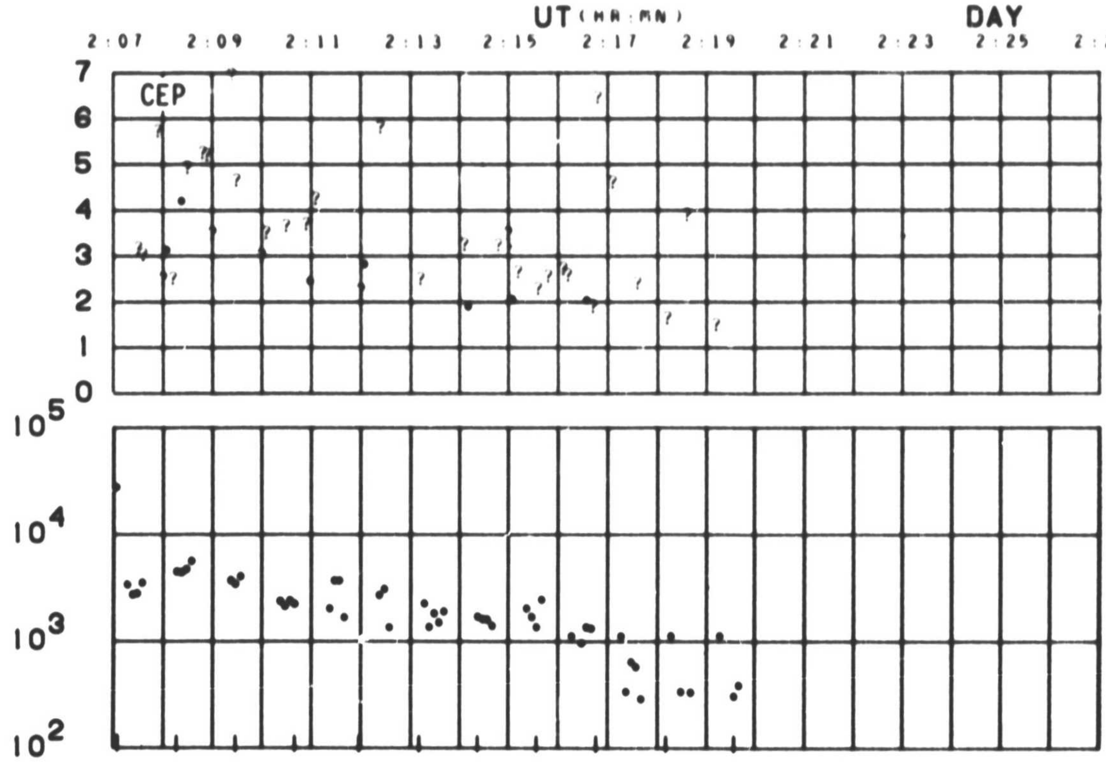

LAT	76	79	83	86	87	84	80	77	73	68	64
LONG	141	143	148	167	-98	-66	-59	-56	-54	-53	-53
LT	11:35	11:46	12:08	13:24	19:42	21:50	22:20	22:34	22:41	22:46	22:50
DIP	85	86	87	88	88	88	88	87	86	85	84
DIPLAT	82	84	85	87	88	88	86	85	84	82	80
L	9.2	13.2	20.7	35.7	88.1	100.3	100.4	96.0	52.4	24.2	14.1
INVLAT	70	74	77	80	83	84	84	84	82	78	74
ZA	99	103	106	110	114	118	121	125	128	133	137

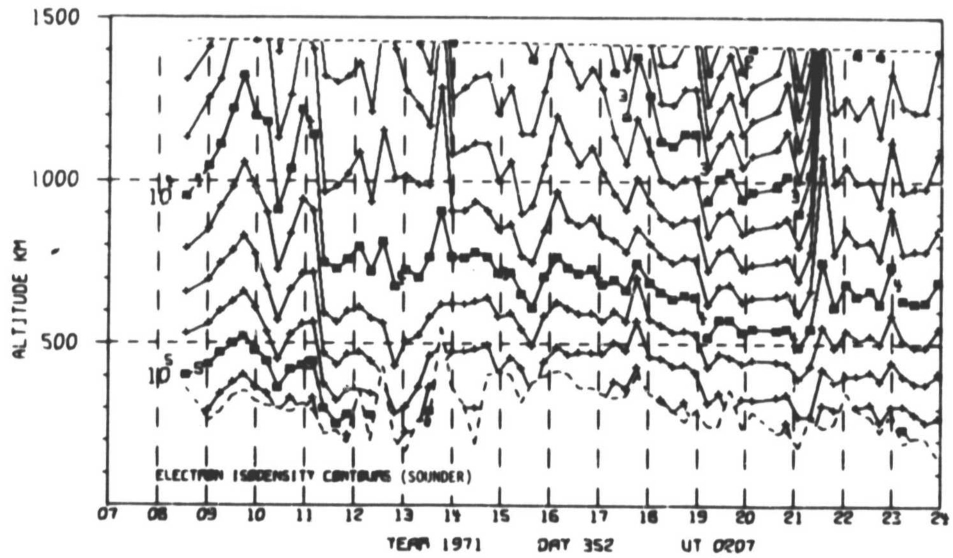

SET 4, FORMAT 10

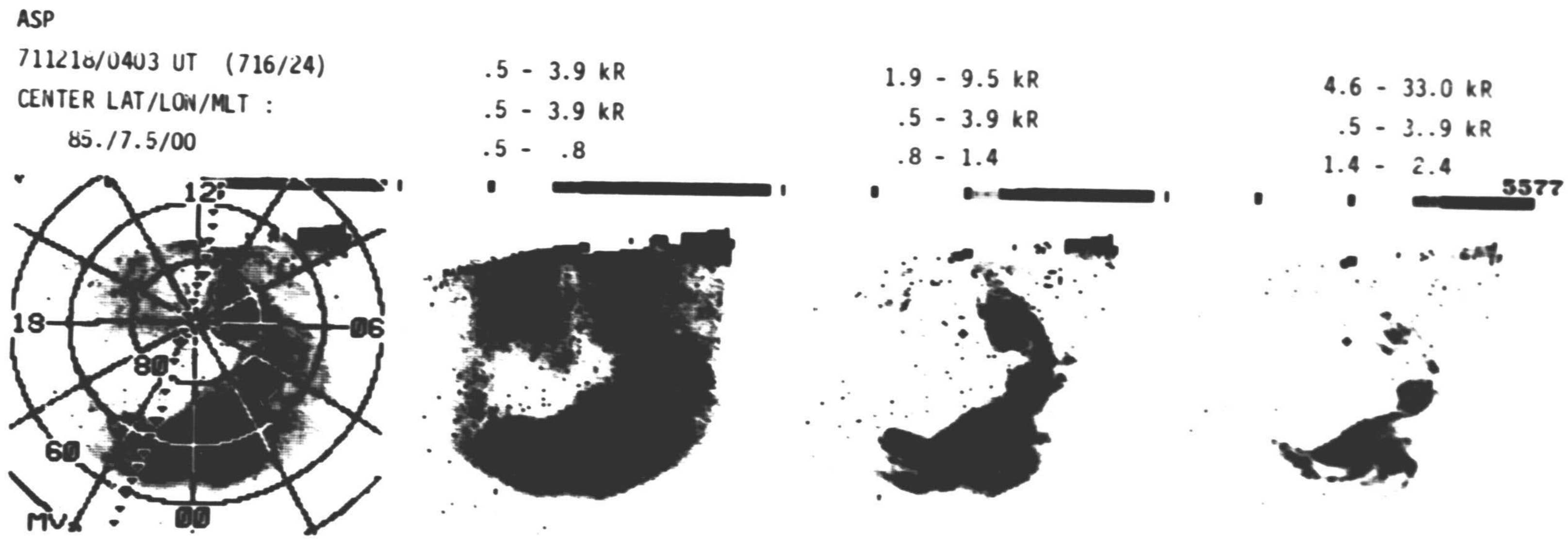

SET 5, FORMAT 7

ORBIT 3307 (71/DEC/18)
DAY 352 OF YEAR 1971

FIRST SPIN U.T. $4^{H}3^{M}$
LAST SPIN U.T. $4^{H}26^{M}$

6300 ANGSTROM INTENSITY

DATE PROCESSED: 80/AUG/14
INVARIANT COORDINATES (250 KM.)

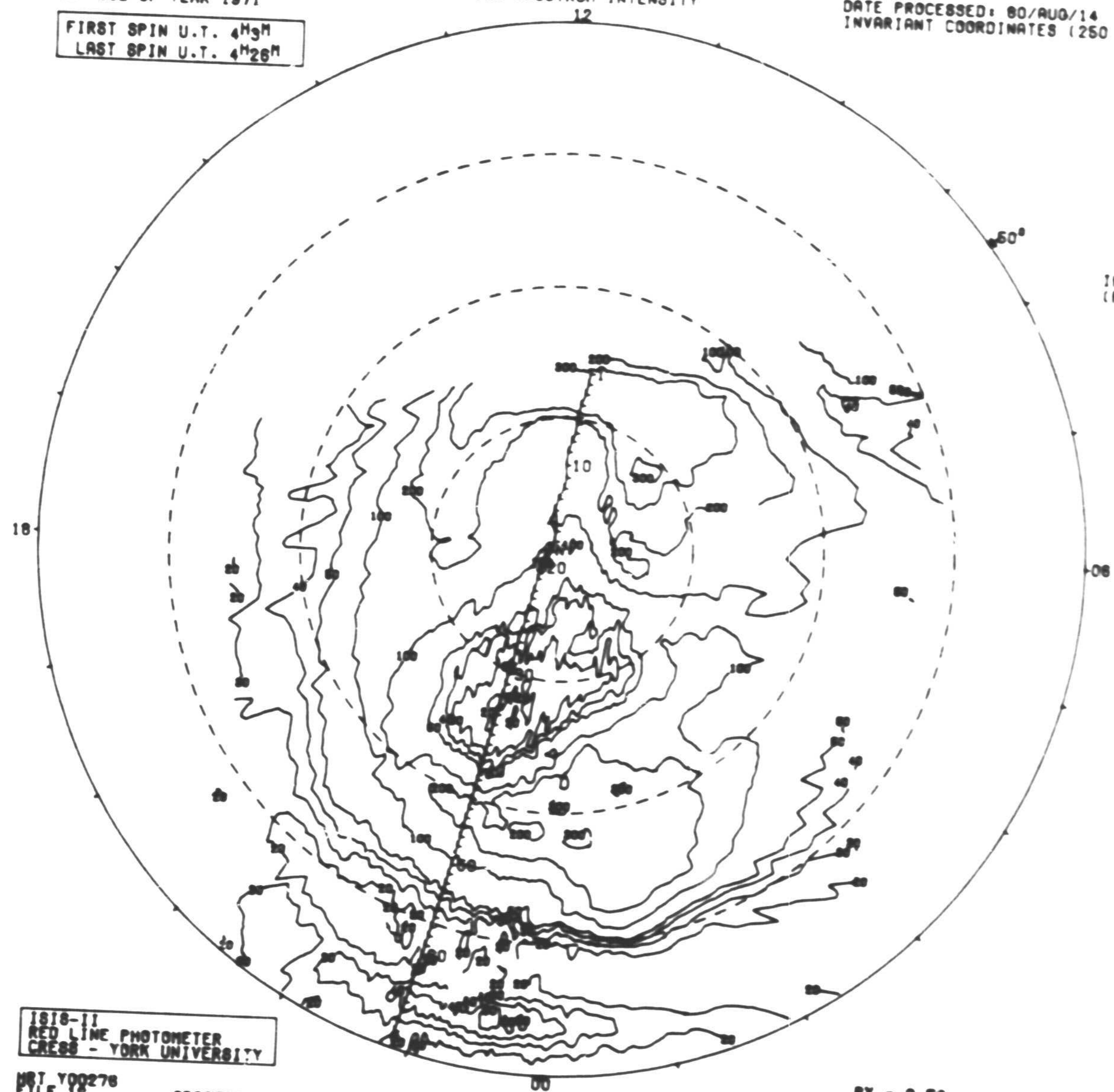

CONTOURS PLOTTED

200
300
400
500
1000
2000
3000
ZENITHAL INTENSITIES (RAYLEIGHS)

SPACECRAFT INFORMATION

SPIN NUMBER	ORBIT TIME (HRMNSC)	INVARIANT LATITUDE (DEGREES)
1	040317	77.1
2	040335	77.8
3	040353	78.8
4	040411	79.4
5	040429	79.8
6	040441	80.5
7	040459	81.4
8	040517	82.5
9	040535	83.3
10	040553	83.8
11	040611	84.2
12	040629	84.2
13	040647	84.2
14	040705	84.3
15	040723	84.3
16	040741	84.3
17	040759	84.3
18	040817	84.2
19	040835	84.2
20	040853	84.3
21	040911	84.3
22	040929	84.3
23	040941	84.3
24	040959	84.3
25	041017	84.0
26	041035	83.6
27	041053	82.8
28	041111	82.2
29	041129	81.6
30	041147	80.7
31	041205	79.8
32	041223	79.0
33	041241	78.2
34	041259	77.5
35	041317	76.7
36	041335	75.8
37	041353	75.1
38	041411	74.3
39	041423	73.8
40	041441	73.0
41	041459	72.2
42	041517	71.4
43	041535	70.6
44	041553	69.8
45	041611	69.0
46	041629	68.2
47	041647	67.4
48	041705	66.6
49	041723	65.8
50	041741	65.0
51	041759	64.2
52	041817	63.4
53	041835	62.6
54	041847	62.[illegible]
55	041905	61.3
56	041923	60.5
57	041941	59.8
58	041959	59.0
59	042017	58.0
60	042035	57.2
61	042053	56.4
62	042111	55.6
63	042129	54.8
64	042147	54.1
65	042205	53.3
66	042223	52.5
67	042241	51.7
68	042259	50.8
69	042311	50.4
70	042329	49.6
71	042347	48.8
72	042405	48.0
73	042423	47.3
74	042441	46.6
75	042459	45.8
76	042517	45.0
77	042535	44.3
78	042553	43.5
79	042611	42.8
80	042629	42.1

ISIS-II
RED LINE PHOTOMETER
CRESS - YORK UNIVERSITY

MRT Y00276
FILE 12

SPACECRAFT TRACK TRACED DOWN TO 250 KM. (NUMBERS DENOTE SPINS)

RX = 0.50
DATA FILTERED
ZERO SUBTRACTION NOT PERFORMED

SET 5, FORMAT 8

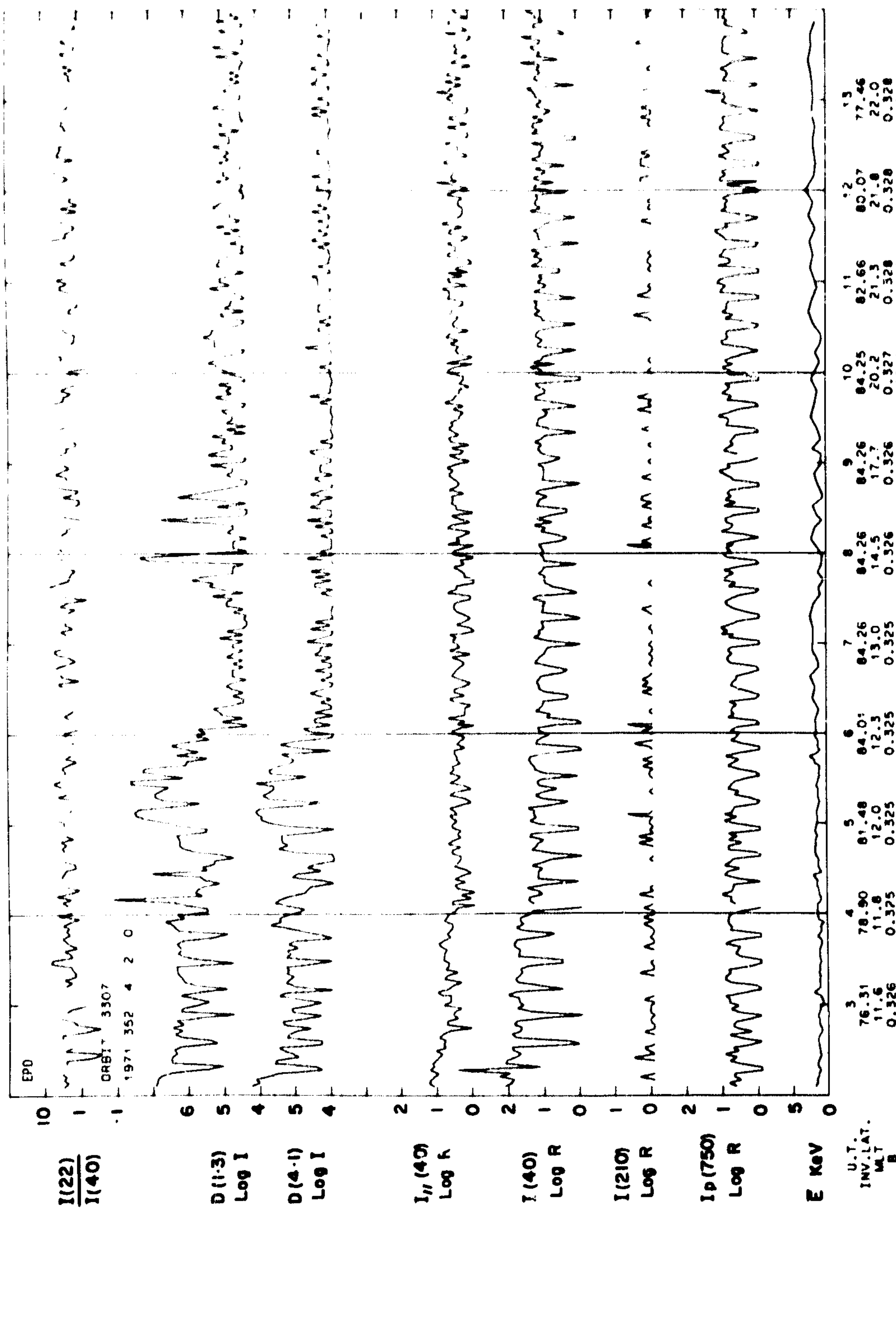

SET 5, FORMAT 3

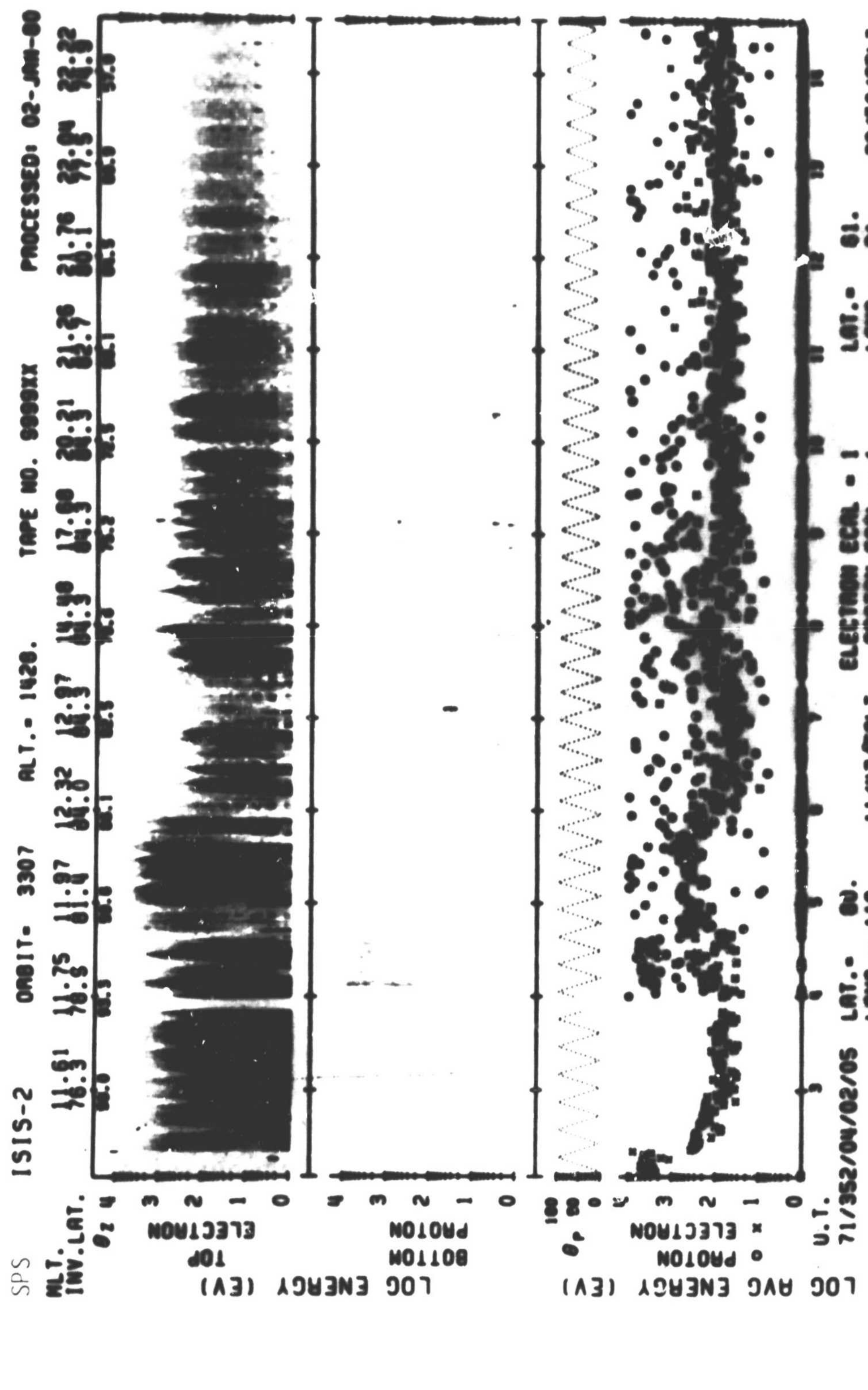

SET 5, FORMAT 6

ORBIT 3307
DATE 711218
DAY 352

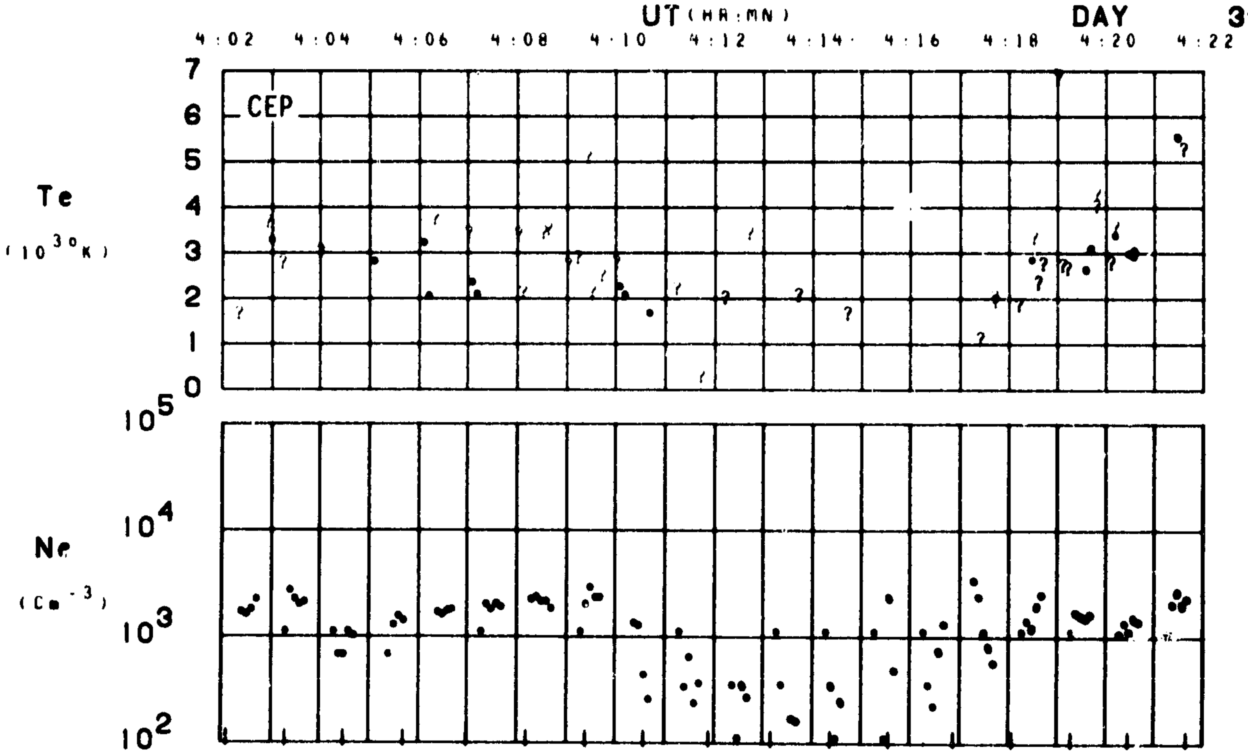

LAT	80	83	87	87	84	80	76	72	68	64	60	57	53	49	45	41	37
LONG	115	120	148	-130	-93	-87	-84	-83	-82	-81	-81	-81	-81	-81	-81	-81	-81
LT	11:47	12:10	14:03	19:27	21:54	22:22	22:34	22:41	22:46	22:50	22:52	22:54	22:55	22:57	22:58	22:59	22:59
DIP	87	87	88	88	89	89	68	88	87	86	85	84	83	82	81	80	78
DIPLAT	84	86	87	88	89	89	88	86	85	83	82	80	78	76	73	71	68
L	13.0	20.0	32.8	78.6	100.0	99.9	102.6	79.3	36.1	19.9	12.9	9.1	6.7	5.2	4.2	3.5	2.9
INVLAT	73	77	79	83	84	84	84	83	80	77	73	70	67	63	60	57	54
ZA	103	107	110	114	118	122	125	129	133	137	140	144	148	151	154	157	160

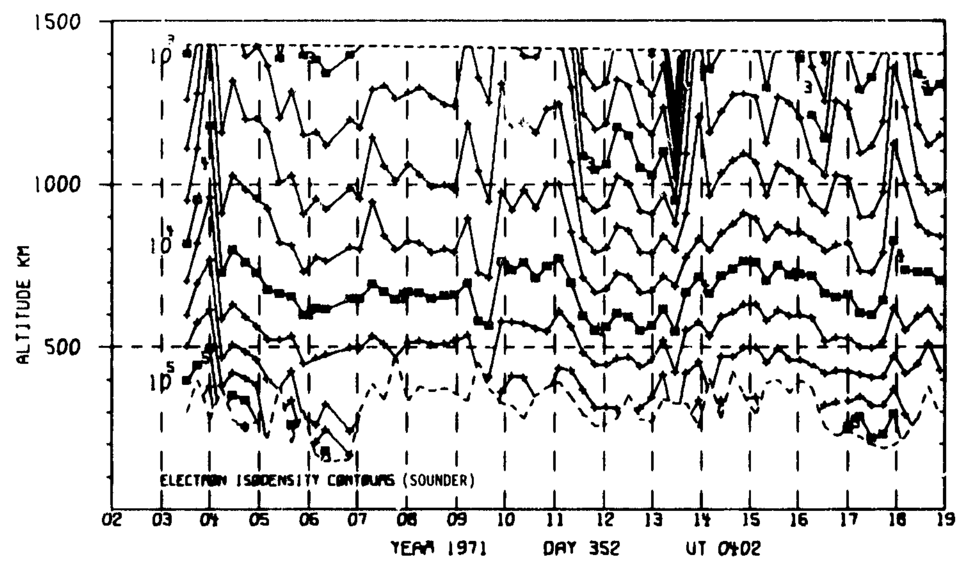

SET 5, FORMAT 10

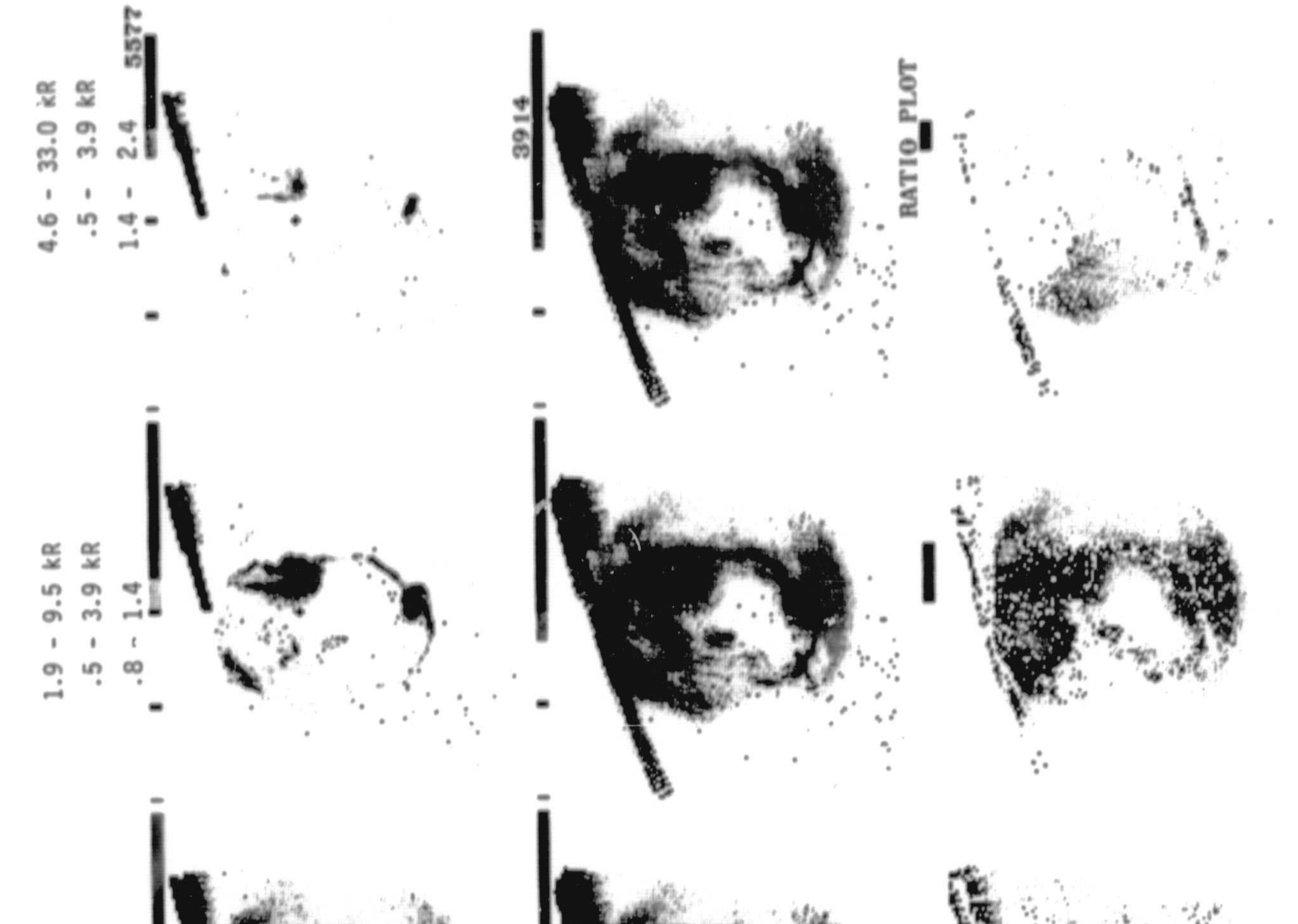

SET 6, FORMAT 7

ORBIT 3308 (71/DEC/18)
DAY 352 OF YEAR 1971

FIRST SPIN U.T. $5^{H}56^{M}$
LAST SPIN U.T. $6^{H}21^{M}$

6300 ANGSTROM INTENSITY

DATE PROCESSED: 80/AUG/14
INVARIANT COORDINATES (250 KM.)

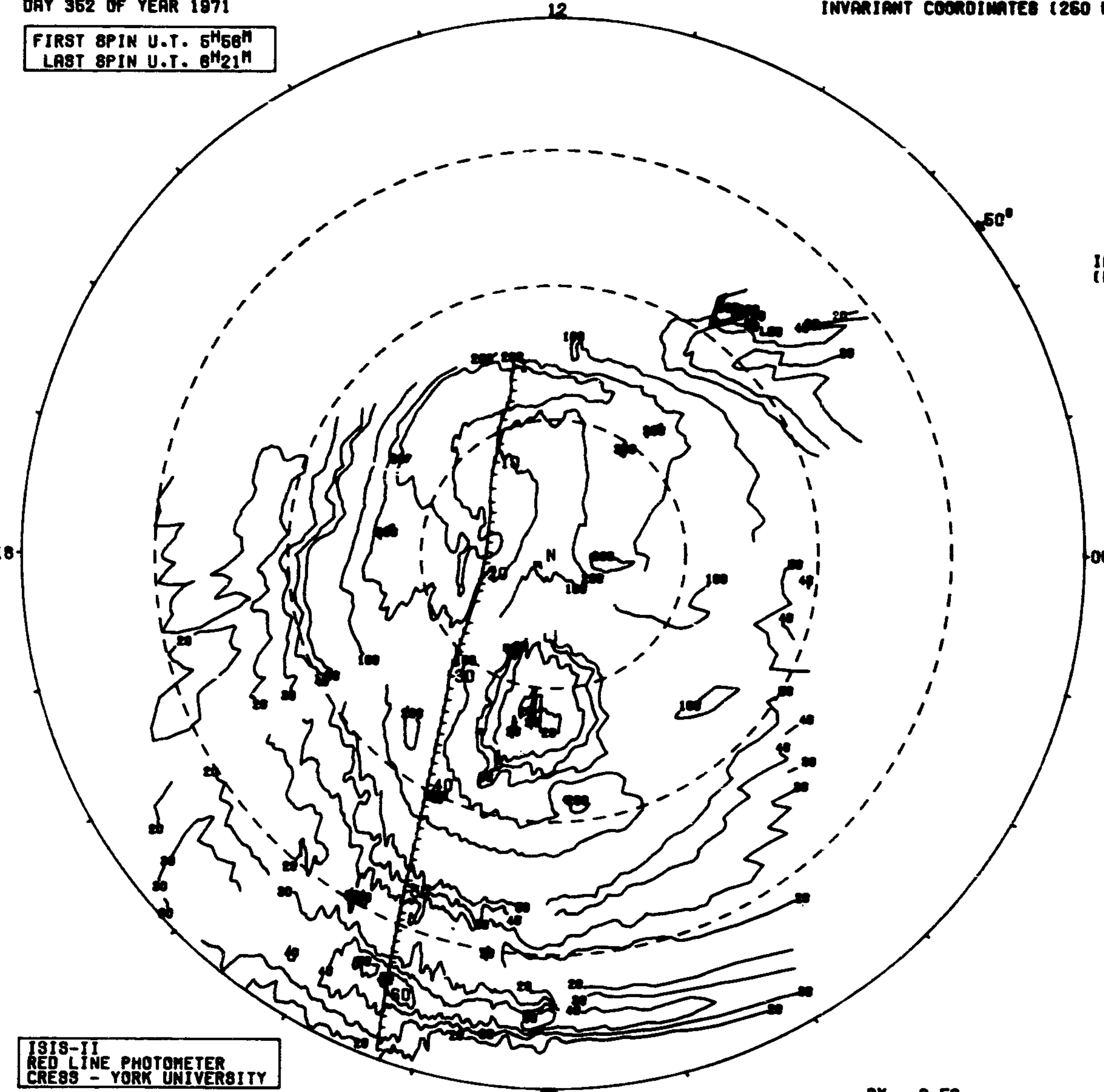

CONTOURS PLOTTED

200
300
400
500
1000
2000
3000
ZENITHAL INTENSITIES (RAYLEIGHS)

SPACECRAFT INFORMATION

SPIN NUMBER	ORBIT TIME (HHMMSEC)	INVARIANT LATITUDE (DEGREES)
1	055630	78.3
2	055703	77.3
3	055721	78.0
4	055739	78.7
5	055751	79.1
6	055809	79.8
7	055827	80.4
8	055845	81.0
9	055903	81.6
10	055921	82.2
11	055939	82.7
12	055957	83.2
13	060015	83.6
14	060033	83.9
15	060051	84.1
16	060109	84.2
17	060127	84.2
18	060145	84.1
19	060203	83.9
20	060221	83.6
21	060239	83.3
22	060251	83.0
23	060309	82.6
24	0	0.0
25	060345	81.4
26	060403	80.7
27	060421	80.1
28	060439	79.4
29	060457	78.7
30	060515	78.0
31	060533	77.3
32	060551	76.6
33	060609	75.9
34	060627	75.1
35	060645	74.3
36	060703	73.5
37	060715	73.0
38	060733	72.2
39	060751	71.4
40	060809	70.6
41	060827	69.8
42	060845	69.0
43	060903	68.2
44	060921	67.4
45	060939	66.6
46	060957	65.8
47	061015	64.9
48	061033	64.1
49	061051	63.3
50	061109	62.5
51	061127	61.8
52	061145	60.9
53	061157	60.2
54	061215	59.4
55	061233	58.6
56	061251	57.7
57	061309	56.9
58	061327	56.1
59	061345	55.2
60	061403	54.4
61	061421	53.6
62	061439	52.7
63	061457	51.9
64	061515	51.1
65	061533	50.2
66	061551	49.4
67	061609	48.6
68	061621	48.0
69	061639	47.2
70	061657	46.4
71	061715	45.6
72	061733	44.8
73	061751	44.0
74	061809	43.2
75	061827	42.4
76	061845	41.6
77	061903	40.9
78	061921	40.1
79	061939	39.3
80	061957	38.6
81	062015	[illegible]
82	062033	37.1
83	062051	36.4
84	062103	35.9
85	062121	35.2
86	062139	34.5

ISIS-II
RED LINE PHOTOMETER
CRESS - YORK UNIVERSITY

MRT Y00276
FILE 13

SPACECRAFT TRACK TRACED DOWN TO 250 KM. (NUMBERS DEN E SPINS)

RX = 0.50
DATA FILTERED
ZERO SUBTRACTION NOT PERFORMED

SET 6, FORMAT 8

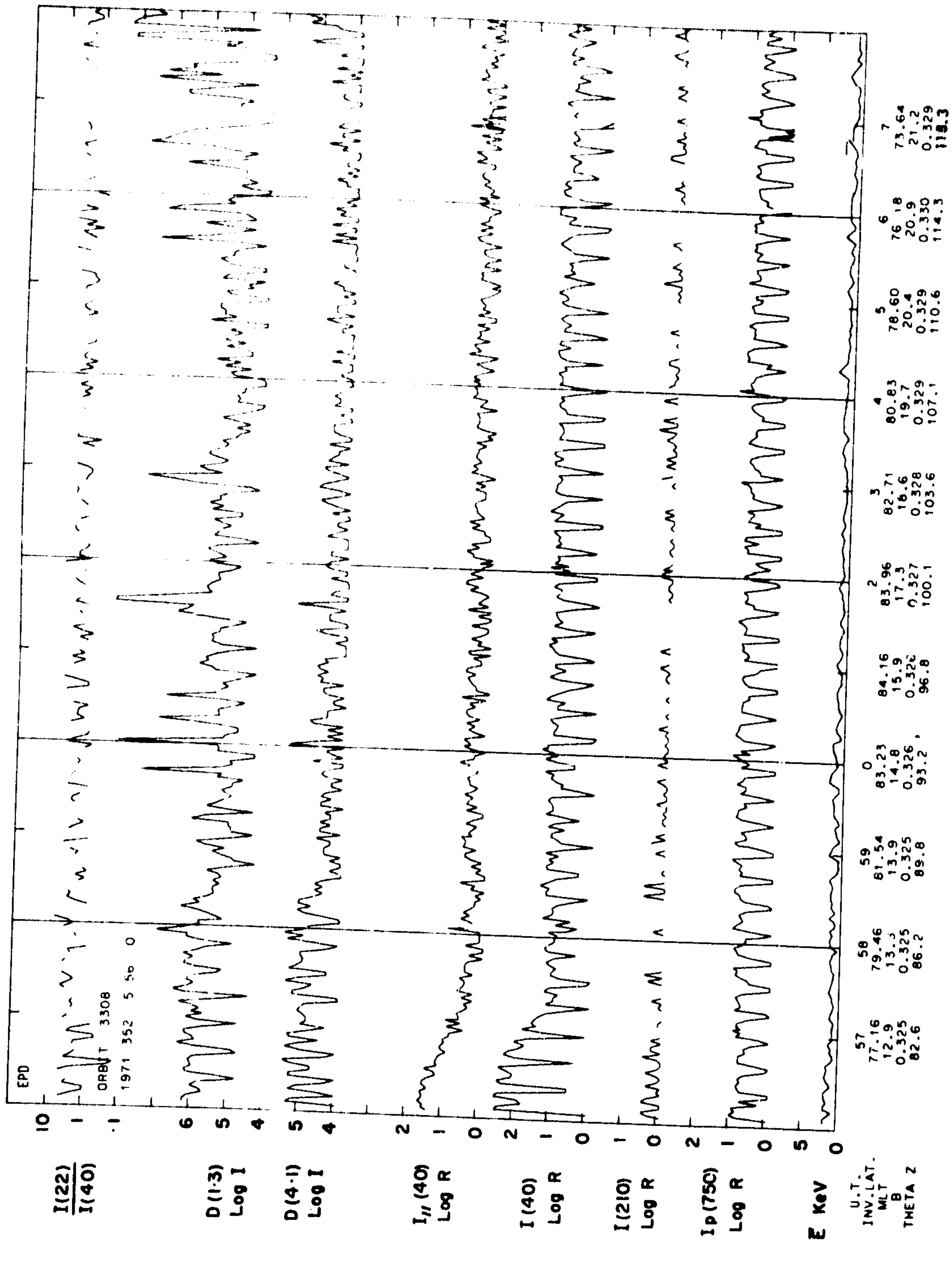

SET 6, FORMAT 3

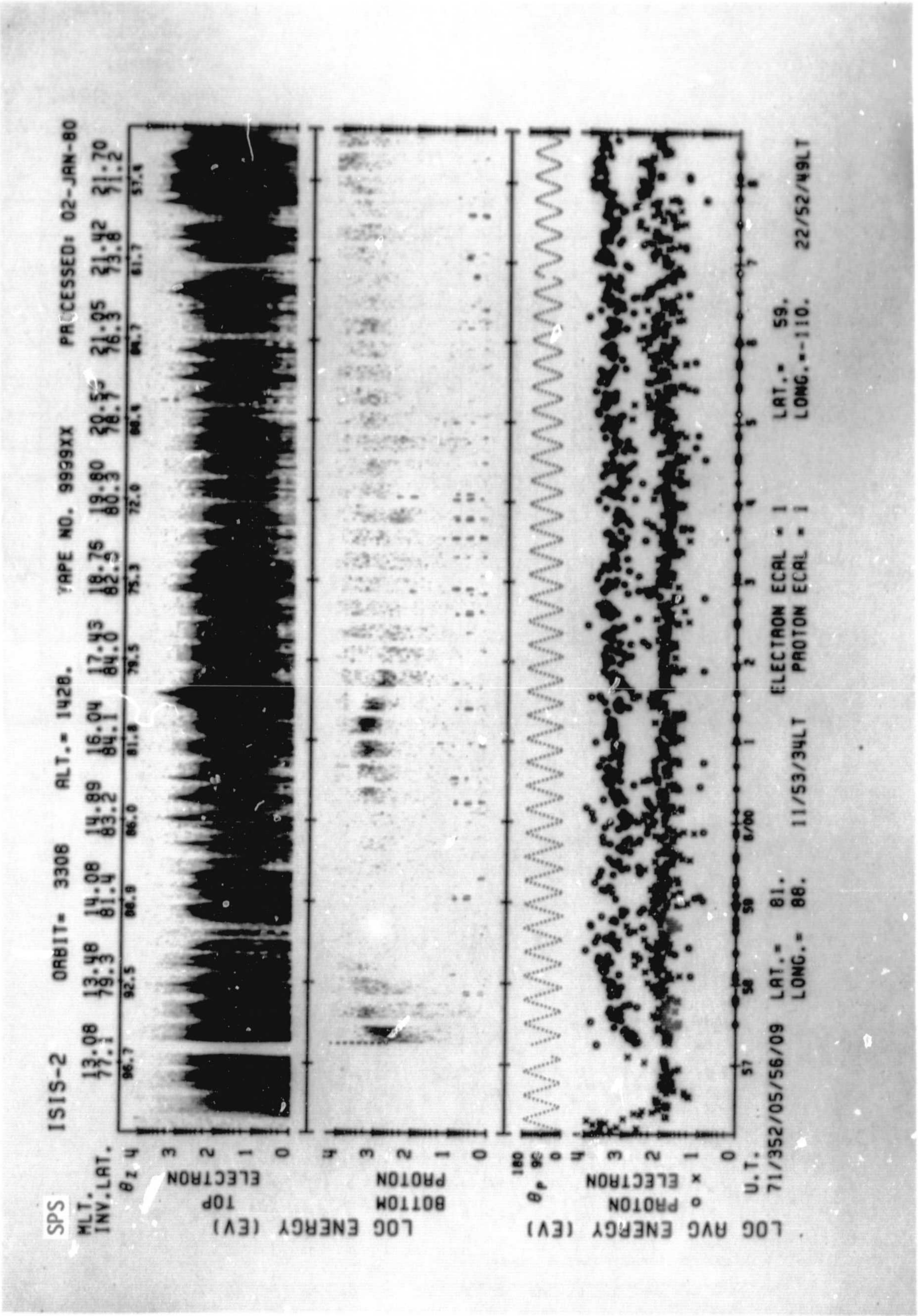

SET 6, FORMAT 6

ORBIT 3308
DATE 711218
DAY 352

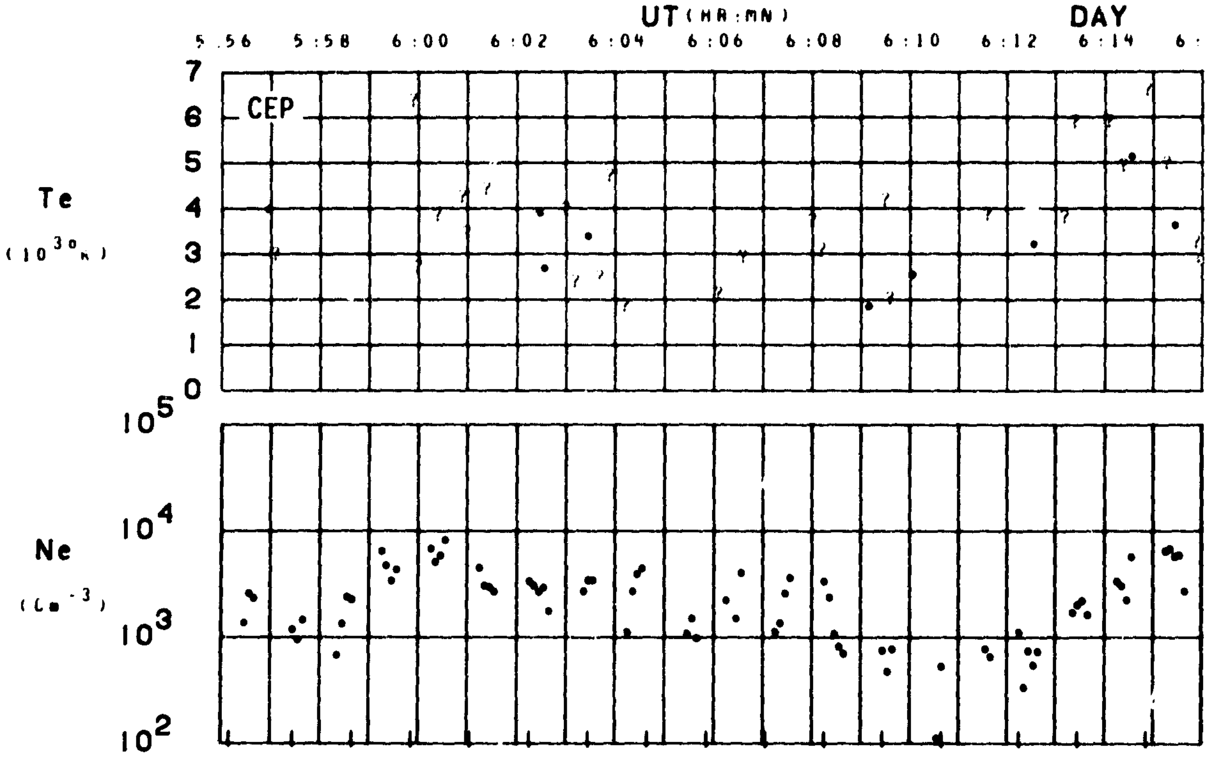

LAT	81	85	87	86	82	79	75	71	67	64	60	56	52	47	43	39
LONG	88	96	154	-135	-119	-114	-112	-111	-110	-110	-109	-109	-109	-109	-109	-109
LT	11:53	12:26	16:20	21:00	22:06	22:2[illegible]	22:37	22:43	22:47	22:50	22:52	22:54	22:55	22:57	22:58	22:59
DIP	87	87	88	89	89	88	88	87	86	85	84	83	82	80	79	77
DIPLAT	85	86	87	89	88	87	86	85	84	82	80	78	75	72	69	66
L	15.2	24.0	39.4	67.8	97.2	84.4	50.8	29.6	18.5	12.4	8.9	6.6	5.1	3.9	3.2	2.7
INVLAT	75	78	80	83	84	83	81	79	76	73	70	67	63	59	56	52
ZA	104	108	112	116	119	123	126	130	134	137	141	144	148	152	156	159

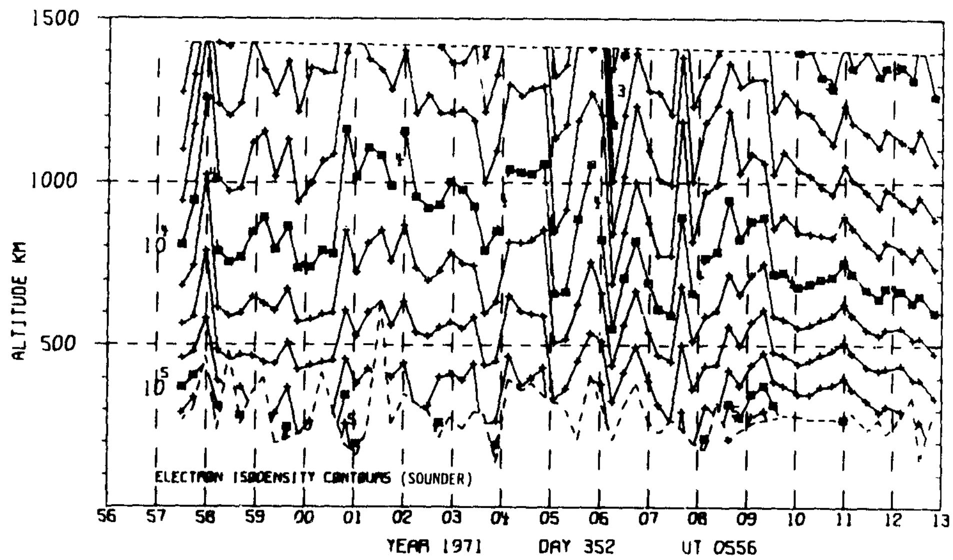

SET 6, FORMAT 10

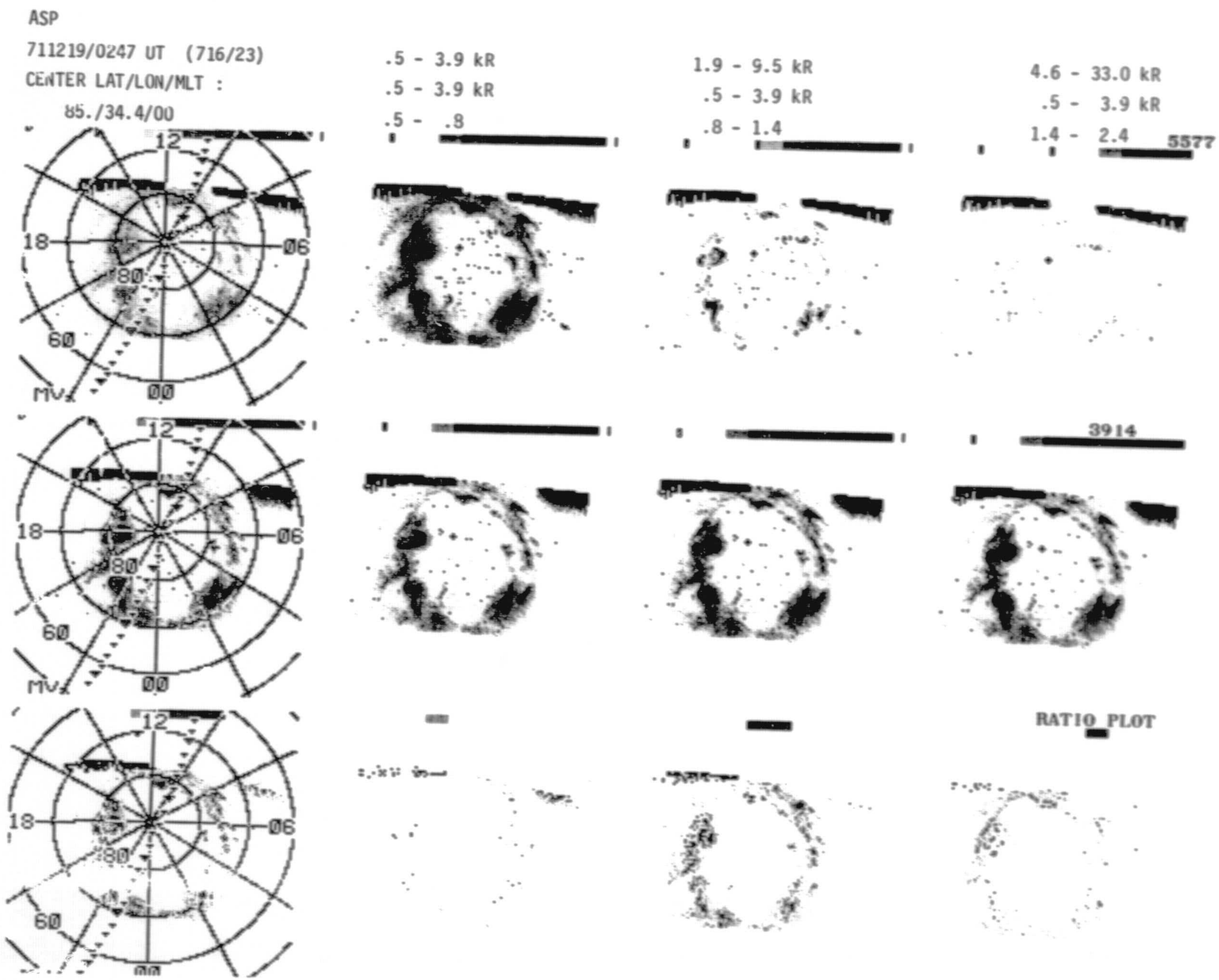

SET 7, FORMAT 7

ORBIT 3319 (71/DEC/19)
DAY 353 OF YEAR 1971

FIRST SPIN U.T. $2^{H}47^{M}$
LAST SPIN U.T. $3^{H}8^{M}$

6300 ANGSTROM INTENSITY

DATE PROCESSED: 80/AUG/14
INVARIANT COORDINATES (250 KM.)

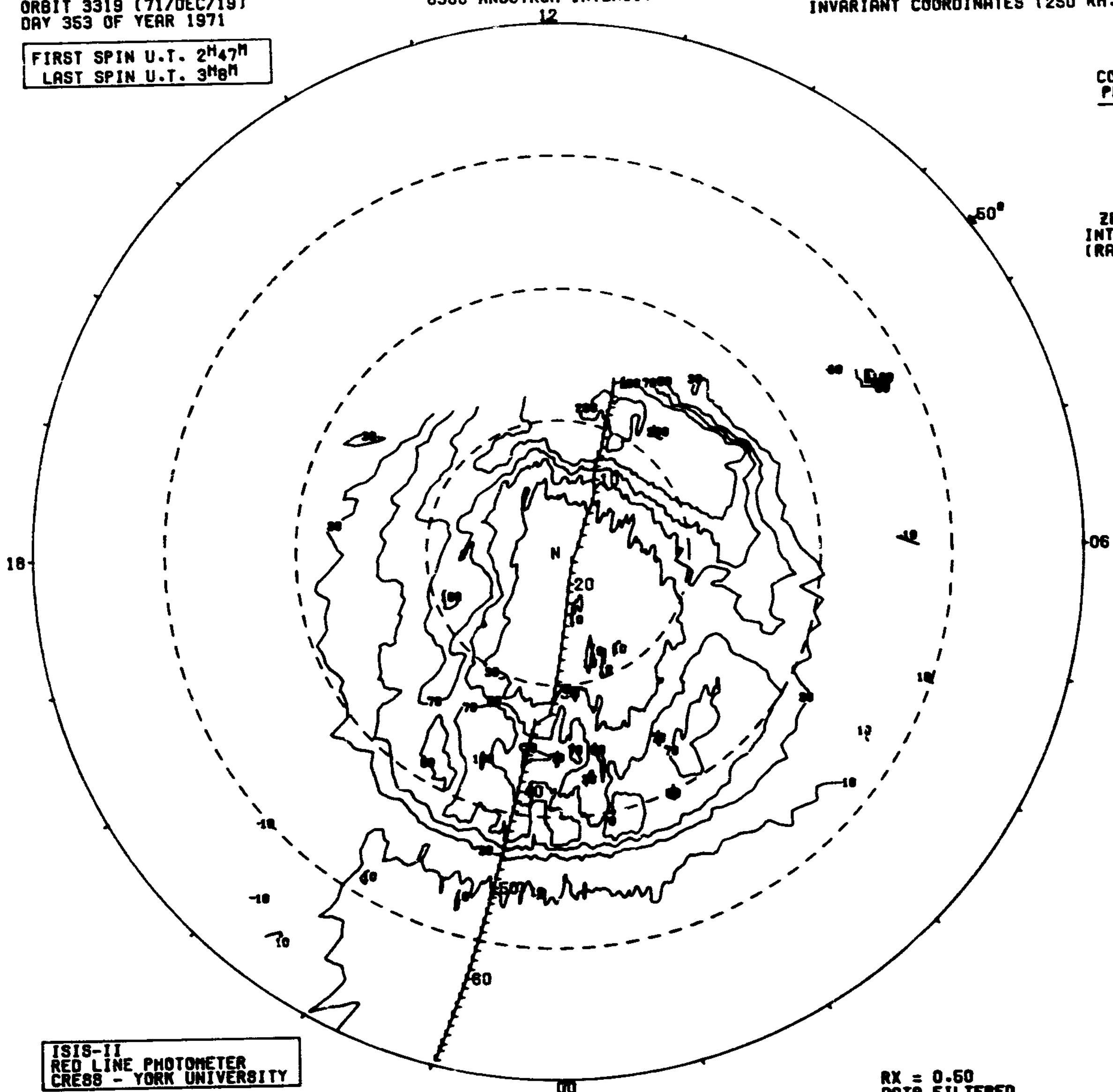

CONTOURS PLOTTED

100
300
500
700
1000
2000
ZENITHAL INTENSITIES (RAYLEIGHS)

SPACECRAFT INFORMATION

SPIN NUMBER	ORBIT TIME (HRMNSC)	INVARIANT LATITUDE (DEGREES)
1	024711	78.9
2	024736	78.0
3	024753	78.8
4	024806	79.3
5	024823	79.9
6	024841	80.7
7	024859	81.7
8	024917	82.8
9	024935	83.6
10	024953	84.2
11	025011	84.4
12	025029	84.4
13	025047	84.3
14	025106	84.3
15	025123	84.2
16	025141	84.2
17	025159	84.3
18	025217	84.2
19	025236	84.2
20	025253	84.2
21	025306	84.3
22	025323	84.4
23	025341	84.4
24	025359	84.3
25	025417	83.9
26	025436	83.3
27	025453	82.4
28	025511	81.5
29	025529	80.7
30	025547	80.0
31	025606	79.2
32	025623	78.4
33	025641	77.6
34	025659	76.8
35	025717	76.0
36	025736	75.3
37	025747	74.7
38	025806	73.9
39	025823	73.1
40	025841	72.3
41	025859	71.5
42	025917	70.7
43	025936	69.9
44	025953	69.1
45	030011	68.4
46	030029	67.6
47	030047	66.8
48	030106	66.0
49	030123	65.2
50	030141	64.4
51	030159	63.8
52	030211	63.1
53	030229	62.3
54	030247	61.5
55	030306	60.7
56	030323	60.0
57	030341	59.2
58	030359	58.4
59	030417	57.6
60	030436	56.9
61	030453	56.1
62	030511	55.3
63	030529	54.6
64	030547	53.8
65	030606	53.1
66	030623	52.3
67	030641	51.6
68	030653	51.1
69	030711	50.4
70	030729	49.6
71	030747	48.9
72	030806	49.2
73	030823	47.5
74	030841	46.8
75	030859	46.1

ISIS-II
RED LINE PHOTOMETER
CRESS - YORK UNIVERSITY

HRT Y00250
FILE 18

SPACECRAFT TRACK TRACED DOWN TO 250 KM. (NUMBERS DENOTE SPINS)

RX = 0.50
DATA FILTERED
ZERO SUBTRACTION NOT PERFORMED

SET 7, FORMAT 8

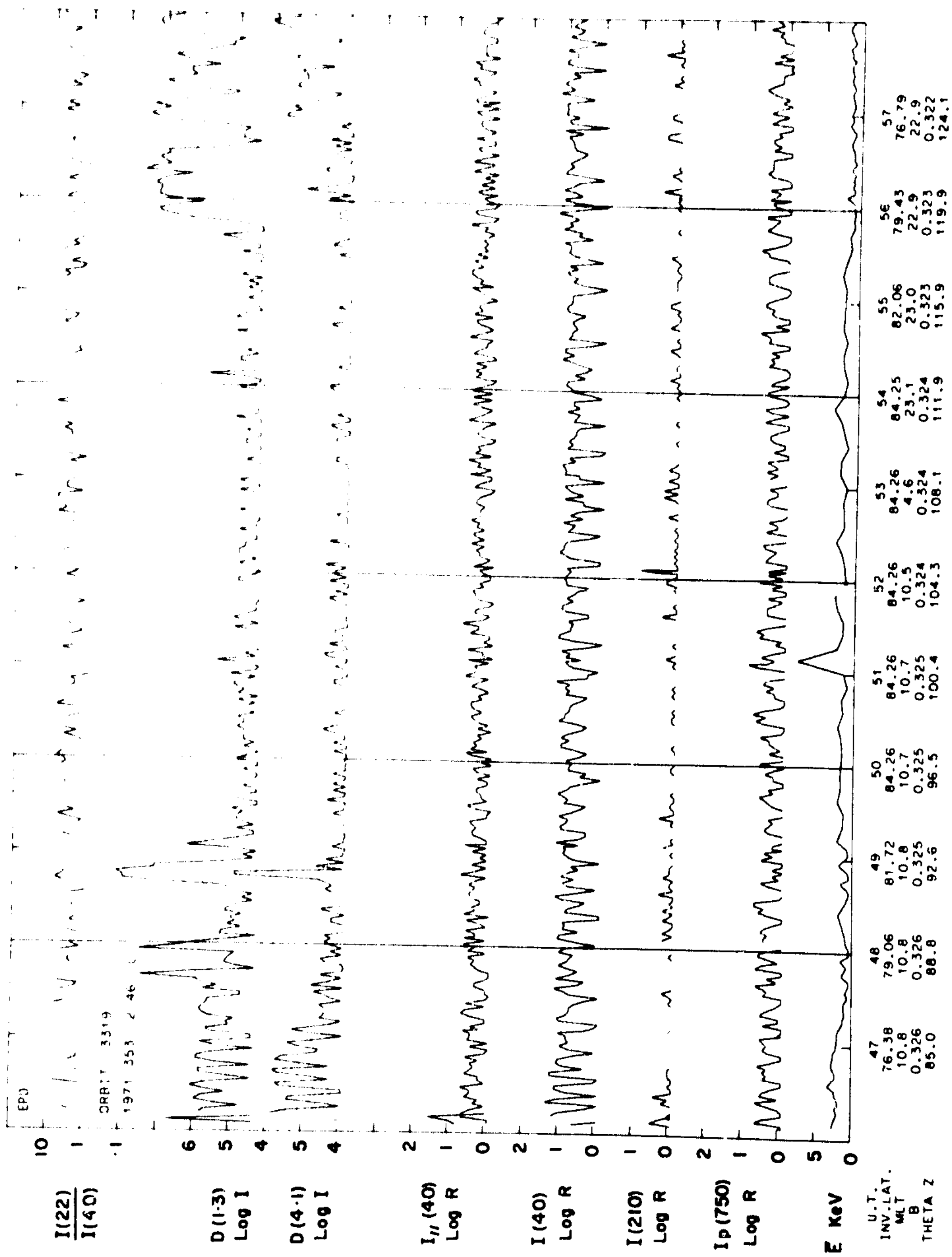

SET 7, FORMAT 3

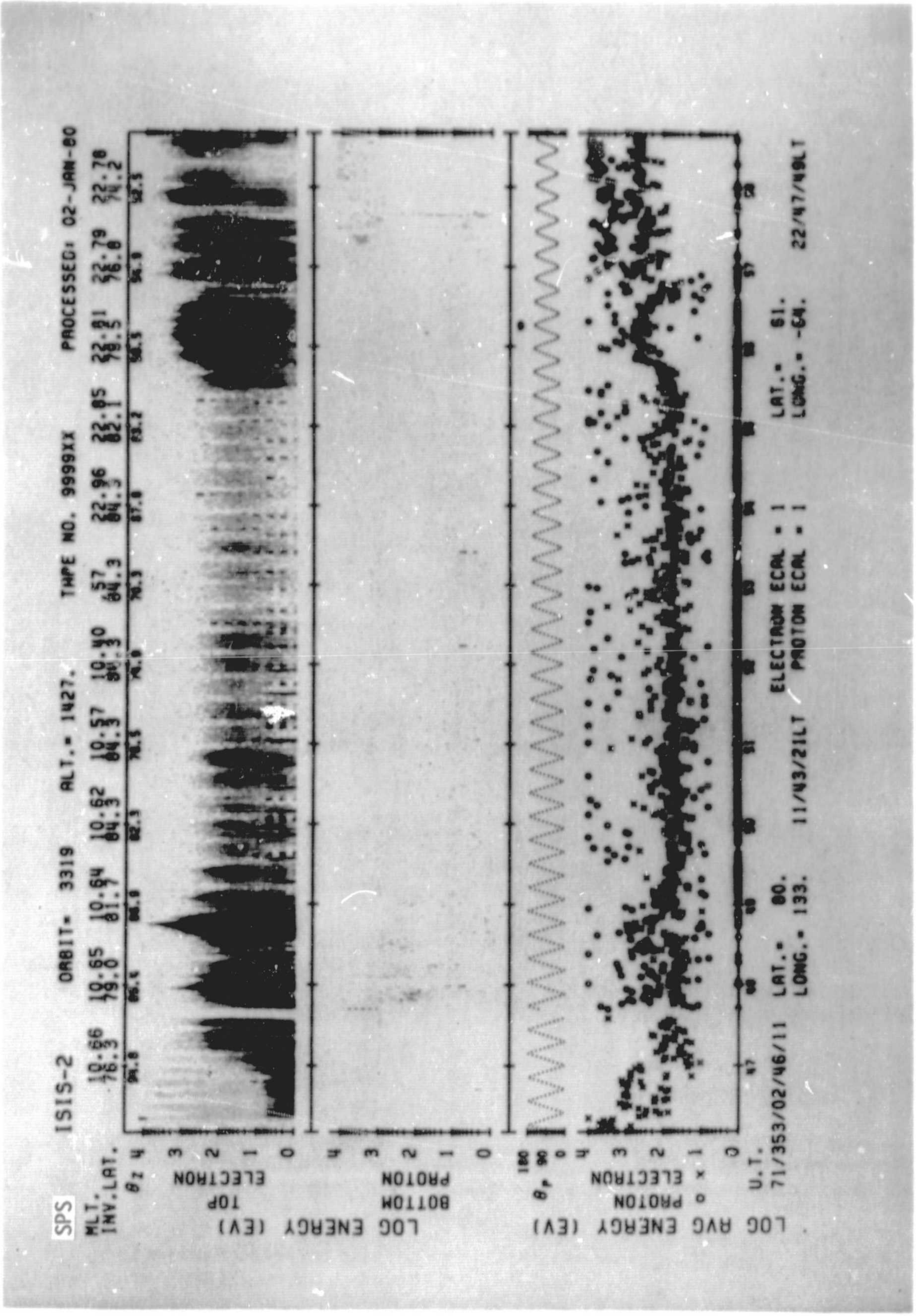

SET 7, FORMAT 6

ORBIT 3319
DATE 711219
DAY 353

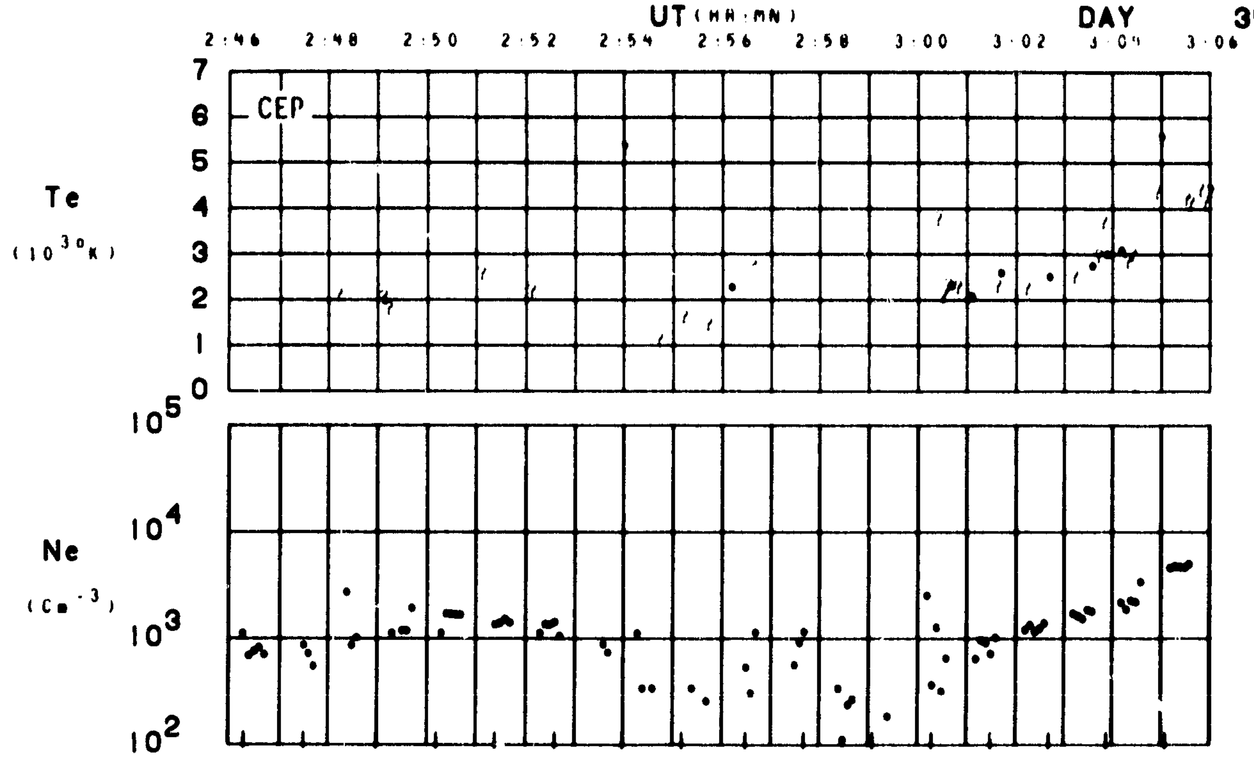

LAT	80	84	87	86	83	79	74	71	67	63	58	55	51	47	43	39
LONG	133	139	-172	-87	-73	-68	-65	-64	-64	-63	-63	-63	-63	-63	-63	-63
LT	11:45	12:09	15:23	21:03	21:59	22:21	22:33	22:39	22:43	22:46	22:48	22:50	22:51	22:52	22:53	22:54
DIP	87	87	88	88	89	88	87	87	86	85	84	83	82	81	79	78
DIPLAT	84	86	87	88	89	87	85	84	82	81	79	77	75	73	70	68
L	13.9	22.0	47.6	104.3	99.4	99.4	100.3	45.7	23.7	14.9	9.7	7.2	5.6	4.5	3.7	3.1
INVLAT	74	77	81	84	84	84	84	81	78	74	71	68	64	61	58	55
ZA	103	107	112	115	119	123	127	130	134	138	142	145	149	152	155	158

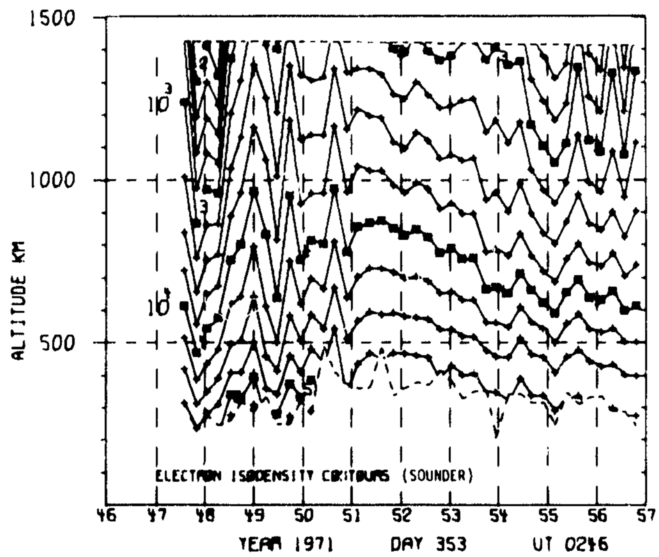

SET 7, FORMAT 10

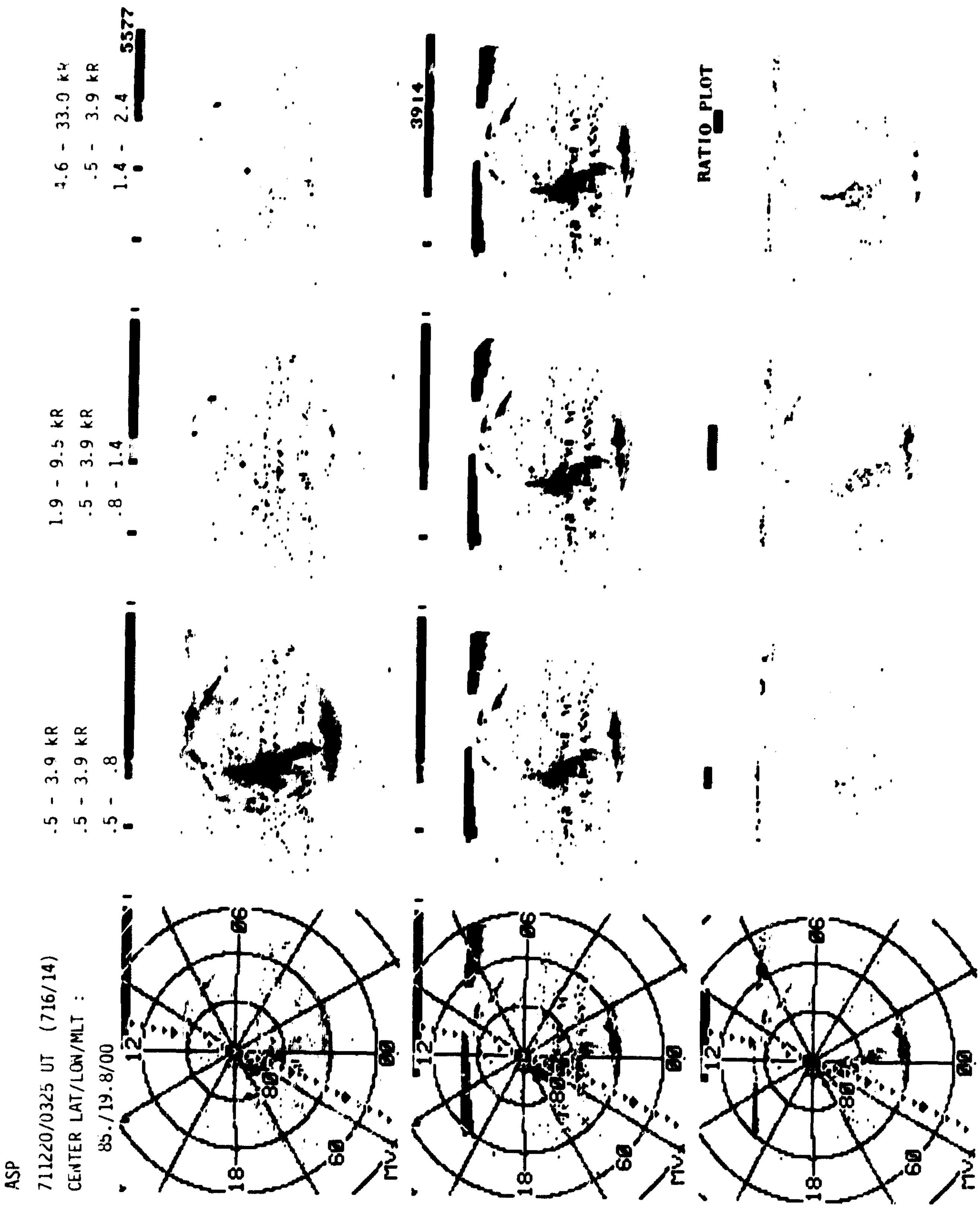

SET 8, FORMAT 7

ORIGINAL PAGE IS OF POOR QUALITY

ORBIT 3392 (71/DEC/20)
DAY 354 OF YEAR 1971

FIRST SPIN U.T. 3^H26^M
LAST SPIN U.T. 3^H48^M

6300 ANGSTROM INTENSITY

DATE PROCESSED: 80/AUG/13
INVARIANT COORDINATES (250 KM.)

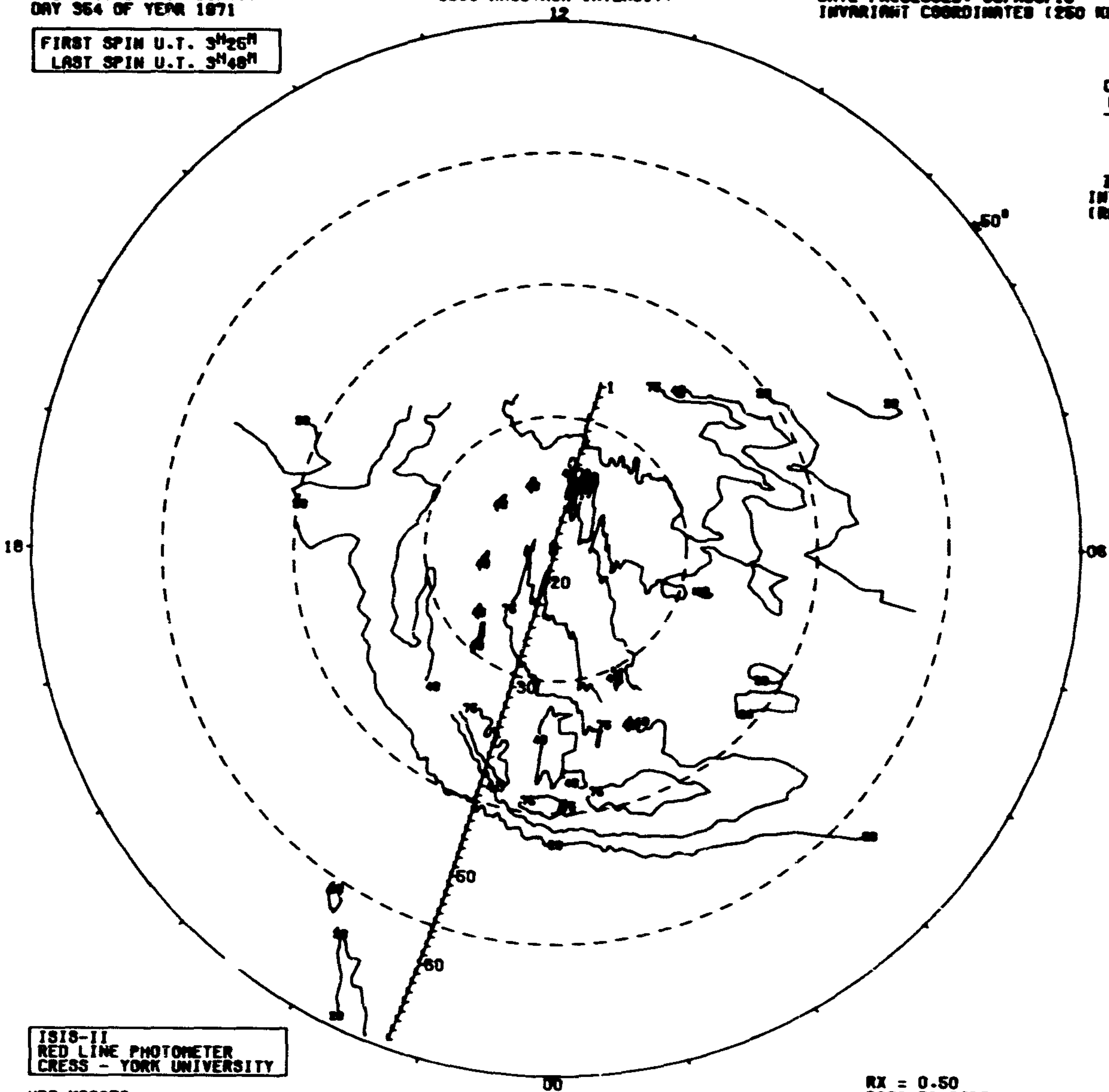

CONTOURS PLOTTED

200
400
750
ZENITHAL INTENSITIES (RAYLEIGHS)

SPACECRAFT INFORMATION

SPIN NUMBER	ORBIT TIME (HHMMSC)	INVARIANT LATITUDE (DEGREES)
1	832522	77.8
2	832540	78.6
3	[illegible]	79.4
4	832616	80.1
5	832634	80.8
6	[illegible]	81.7
7	832710	82.6
8	832722	83.2
9	832740	83.8
10	[illegible]	84.2
11	832816	84.4
12	832834	84.4
13	[illegible]	84.3
14	832910	84.2
15	[illegible]	84.2
16	832946	84.3
17	833004	84.3
18	833022	84.2
19	833040	84.2
20	[illegible]	84.3
21	833116	84.3
22	833134	84.4
23	833152	84.3
24	[illegible]	84.1
25	[illegible]	83.8
26	[illegible]	83.2
27	[illegible]	82.3
28	833316	81.5
29	833334	80.7
[illegible]	833352	79.8
[illegible]	833410	79.1
[illegible]	833428	78.3
[illegible]	833446	77.5
[illegible]	833504	76.8
[illegible]	833522	76.0
36	833540	75.2
37	[illegible]	74.4
38	833616	73.6
39	833634	72.8
40	833652	72.0
41	833710	71.2
42	833722	70.7
43	833740	[illegible]
44	833758	[illegible]
45	833816	[illegible]
46	833834	67.6
47	833852	[illegible]
48	833910	[illegible]
49	833928	[illegible]
50	833946	64.3
51	834004	63.5
52	834022	[illegible]
53	834040	61.8
54	834058	61.1
55	834116	60.3
56	834134	59.5
57	834146	58.8
58	834204	58.2
59	834222	57.4
60	834240	56.7
61	834258	55.9
62	834316	55.1
63	834334	54.3
64	834352	53.5
65	834410	52.8
66	834428	52.0
67	834446	51.2
68	834504	50.5
69	834522	49.7
70	834540	[illegible]
71	834558	48.2
72	834616	47.5
73	834634	46.7
74	834646	[illegible]
75	834704	45.5
76	834722	44.8
77	834740	44.1
78	834758	43.4
79	834816	42.7
80	834834	[illegible]
81	834852	41.3

ISIS-II
RED LINE PHOTOMETER
CRESS - YORK UNIVERSITY

NRT Y00278
FILE 7

SPACECRAFT TRACK TRACED DOWN TO 250 KM. (NUMBERS DENOTE SPINS)

RX = 0.50
DATA FILTERED
ZERO SUBTRACTION NOT PERFORMED

SET 8, FORMAT 8

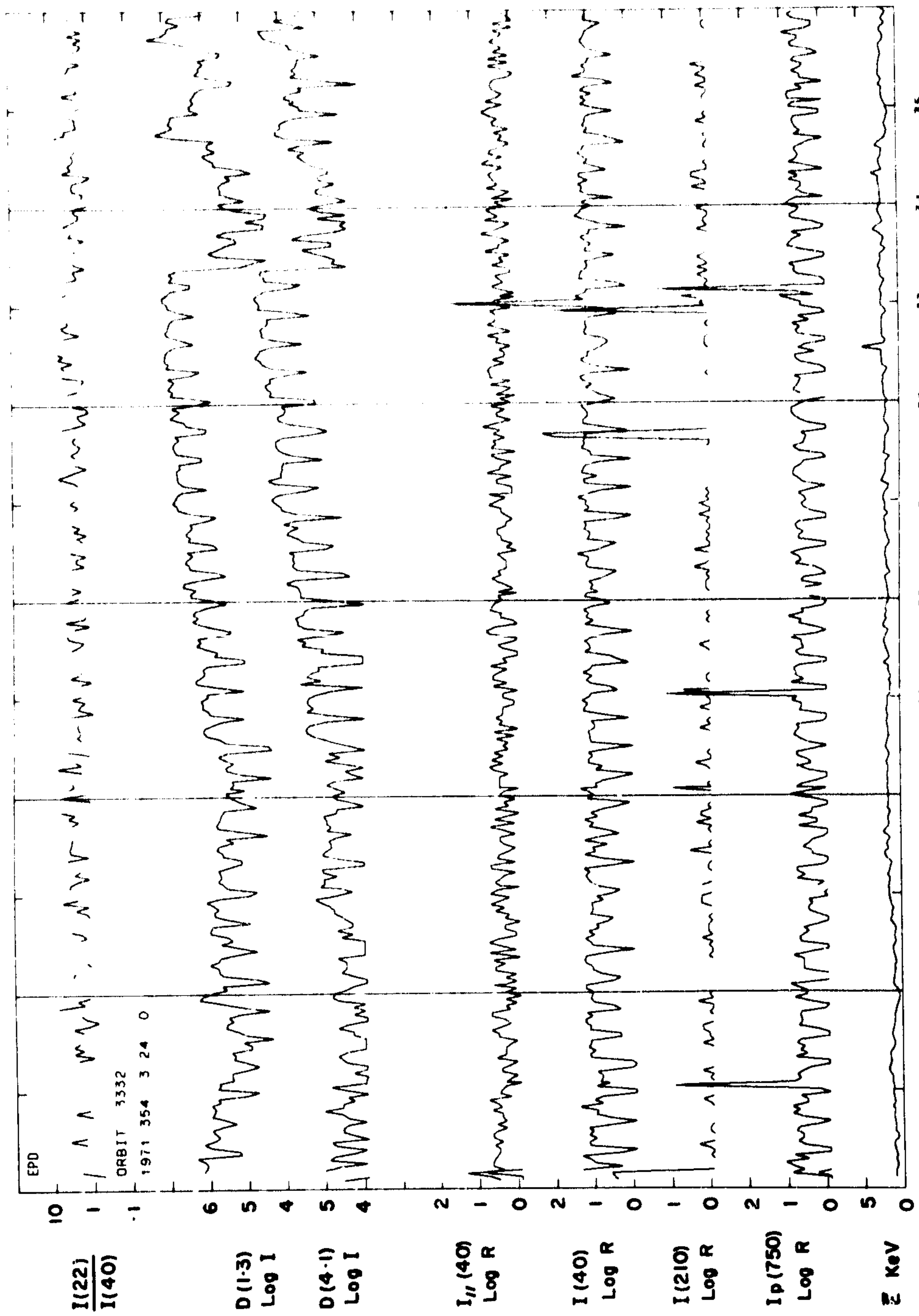

SET 8, FORMAT 3

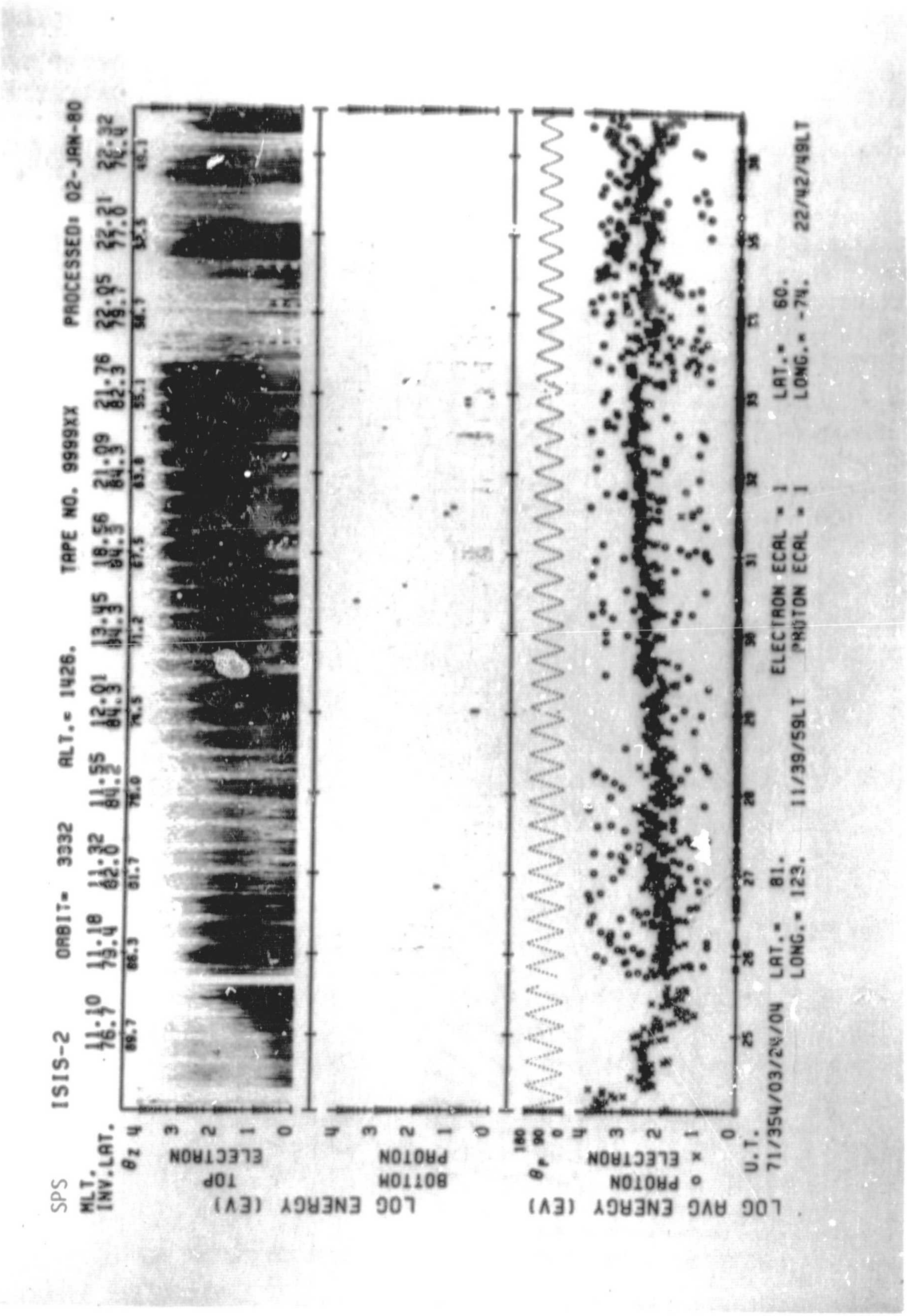

SET 8, FORMAT 6

ORBIT 3332
DATE 711220
DAY 354

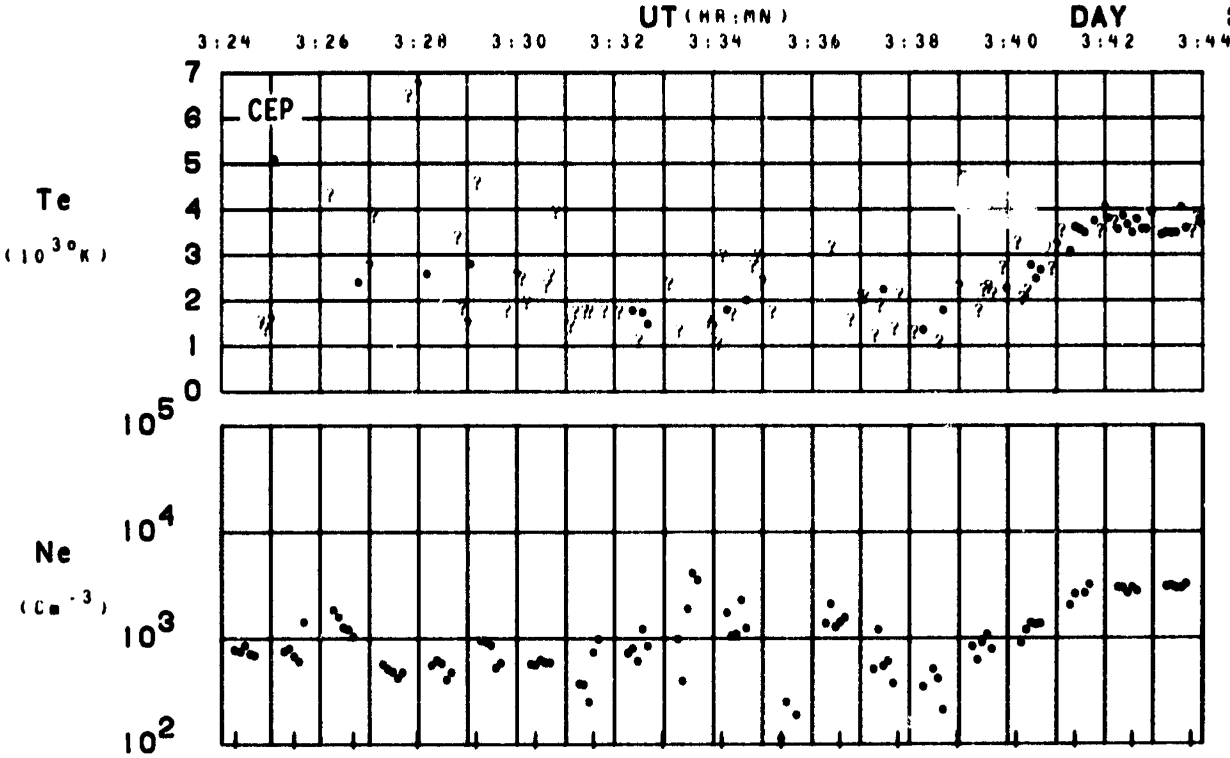

LAT	81	84	87	86	82	79	75	71	67	63	59	56	52	48	44	40	36
LONG	174	130	177	-100	-84	-79	-76	-75	-74	-74	-74	-73	-73	-73	-73	-74	-74
LT	11:43	12:10	15:21	20:49	21:54	22:16	22:27	22:34	22:37	22:40	22:42	22:44	22:46	22:47	22:48	22:49	22:50
DIP	87	88	88	89	89	88	88	87	86	86	85	84	83	82	80	79	77
DIPLAT	85	86	87	88	89	88	87	85	84	82	81	79	77	75	72	70	67
L	14.7	23.3	42.0	99.3	99.4	99.5	103.7	55.6	28.0	17.0	11.4	8.2	6.2	4.9	4.0	3.4	2.9
INVLAT	74	78	81	84	84	84	84	82	79	75	72	69	66	63	60	56	53
ZA	104	108	111	115	119	123	126	130	134	137	141	144	148	151	154	157	159

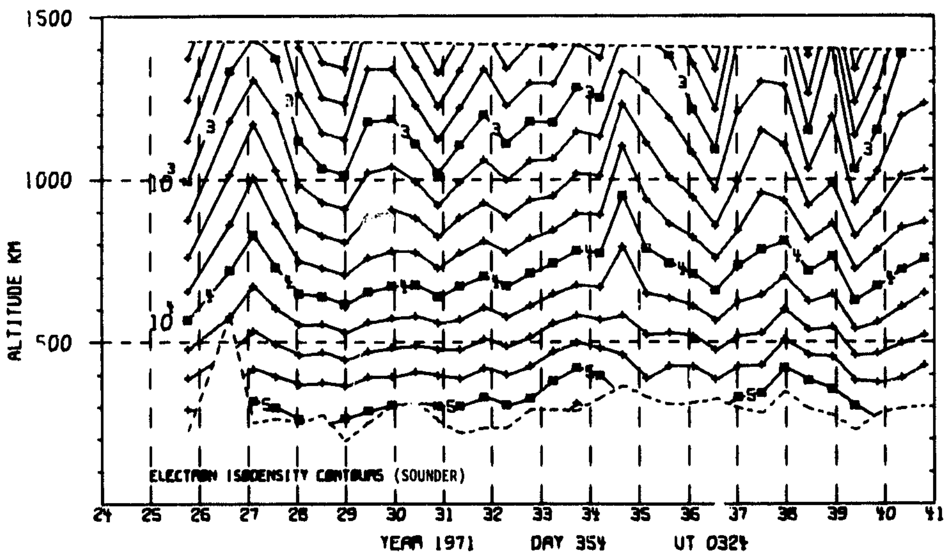

SET 8, FORMAT 10

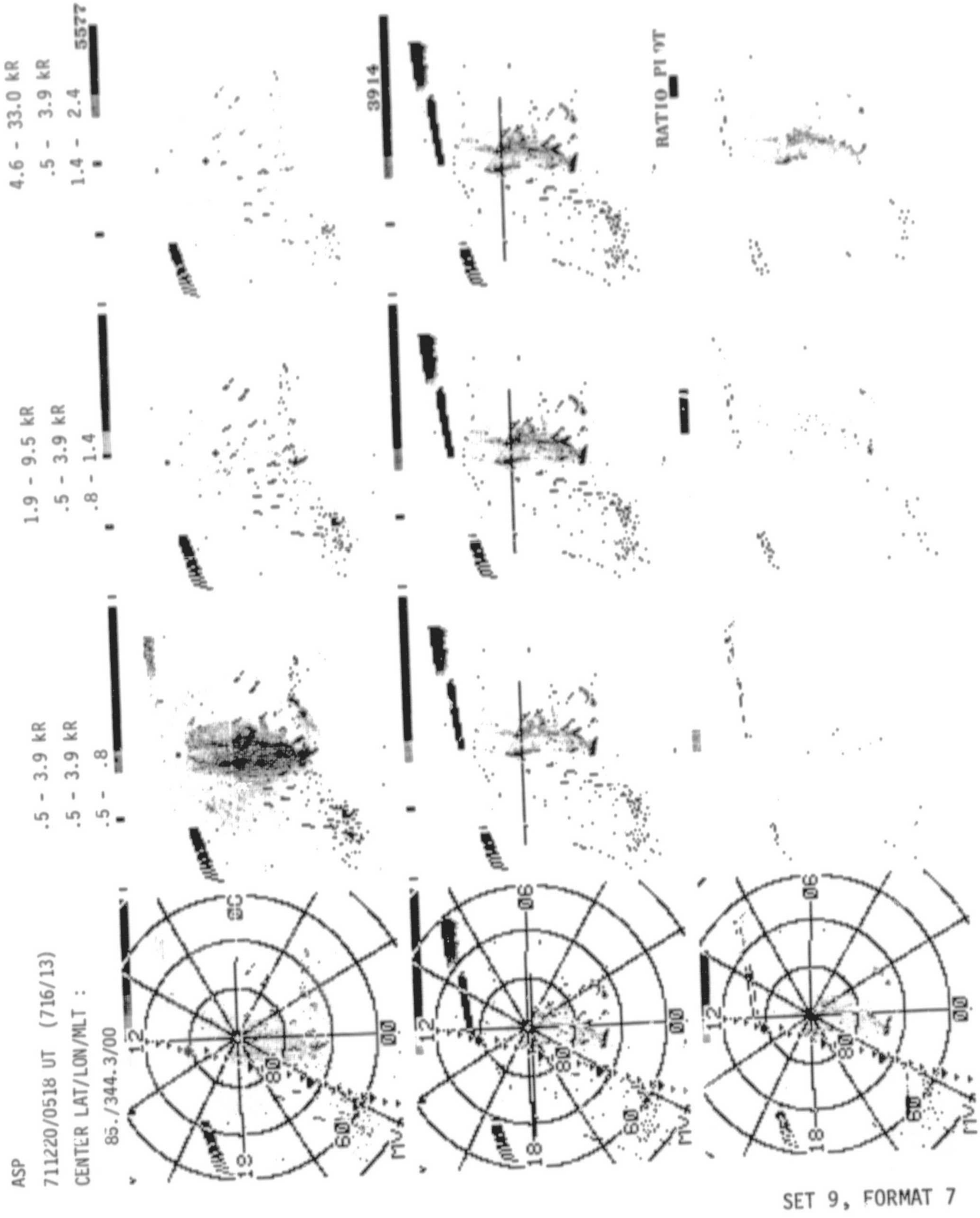

SET 9, FORMAT 7

ORBIT 3333 (71/DEC/20)
DAY 354 OF YEAR 1971

FIRST SPIN U.T. $5^{H}18^{M}$
LAST SPIN U.T. $5^{H}37^{M}$

6300 ANGSTROM INTENSITY

DATE PROCESSED: 80/AUG/13
INVARIANT COORDINATES (250 KM.)

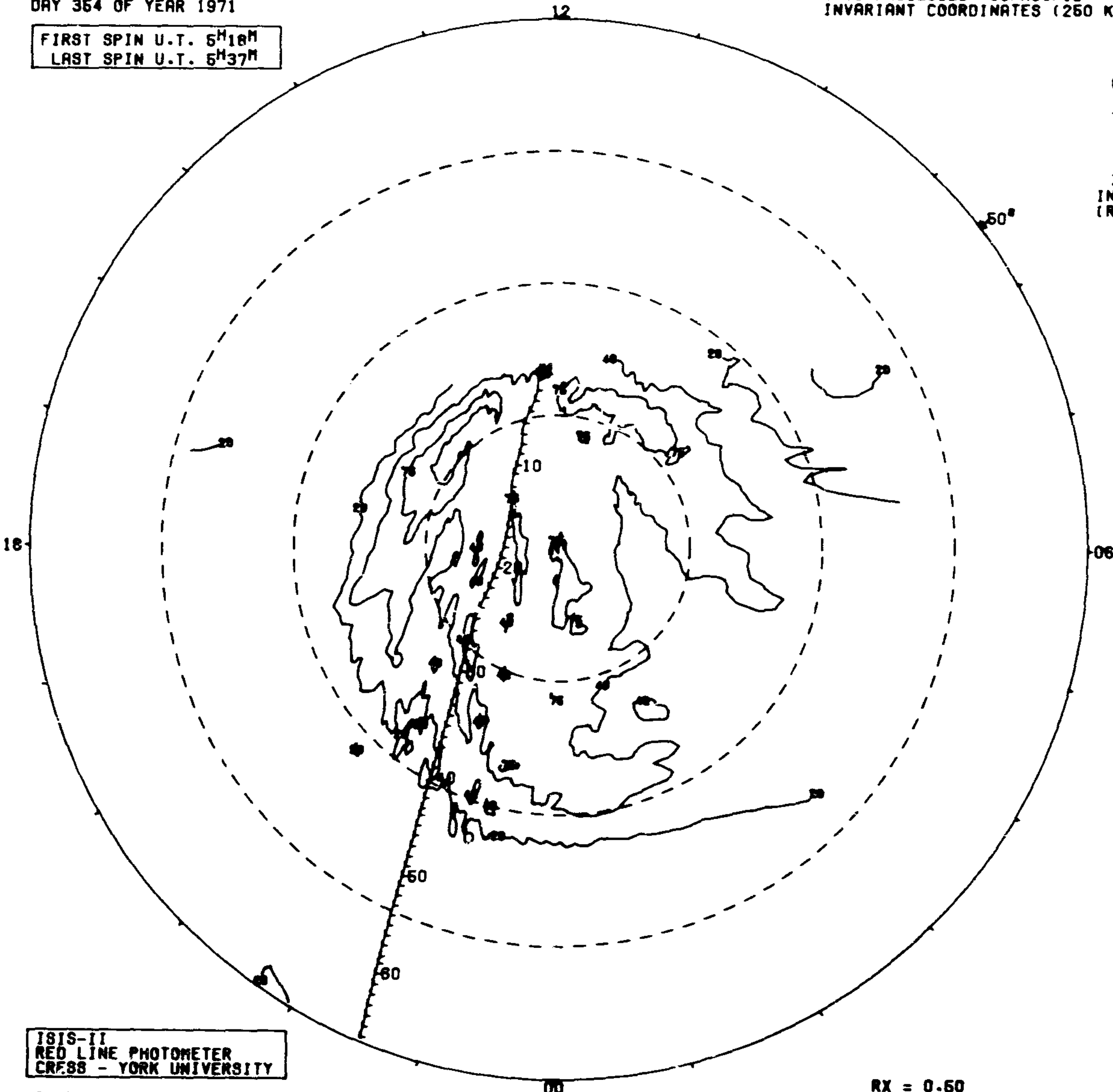

CONTOURS PLOTTED

200
400
750
ZENITHAL INTENSITIES (RAYLEIGHS)

SPACECRAFT INFORMATION

SPIN NUMBER	ORBIT TIME (HRMNSC)	INVARIANT LATITUDE (DEGREES)
1	051852	77.2
2	051910	77.9
3	051928	78.6
4	051946	79.3
5	052004	80.0
6	052022	80.6
7	052040	81.3
8	052058	82.0
9	052116	82.7
10	052134	83.4
11	052146	83.7
12	052204	84.0
13	052222	84.2
14	052240	84.2
15	052258	84.3
16	052316	84.3
17	052334	84.3
18	052352	84.3
19	052410	84.2
20	052428	84.1
21	052446	83.9
22	052504	83.6
23	052522	83.1
24	052540	82.5
25	052558	81.8
26	052616	81.1
27	052634	80.3
28	052646	79.9
29	052704	79.2
30	052722	78.5
31	052740	77.8
32	052758	77.0
33	052816	76.2
34	052834	75.5
35	052852	74.7
36	052910	73.9
37	052928	73.1
38	052946	72.3
39	053004	71.6
40	053022	70.8
41	053040	69.9
42	053058	69.1
43	053116	68.3
44	053128	67.8
45	053146	67.0
46	053204	66.1
47	053222	65.3
48	053240	64.5
49	053258	63.7
50	053316	62.8
51	053334	62.0
52	053352	61.2
53	053410	60.3
54	053428	59.5
55	053446	58.7
56	053504	57.8
57	053522	57.0
58	053540	56.2
59	053552	55.6
60	053610	54.8
61	053628	53.9
62	053646	53.1
63	053704	52.3
64	053722	51.4
65	053740	50.6
66	053758	49.8

ISIS-II
RED LINE PHOTOMETER
CRESS - YORK UNIVERSITY

HRT Y00278
FILE 8

SPACECRAFT TRACK TRACED DOWN TO 250 KM. (NUMBERS DENOTE SPINS)

RX = 0.60
DATA FILTERED
ZERO SUBTRACTION NOT PERFORMED

SET 9, FORMAT 8

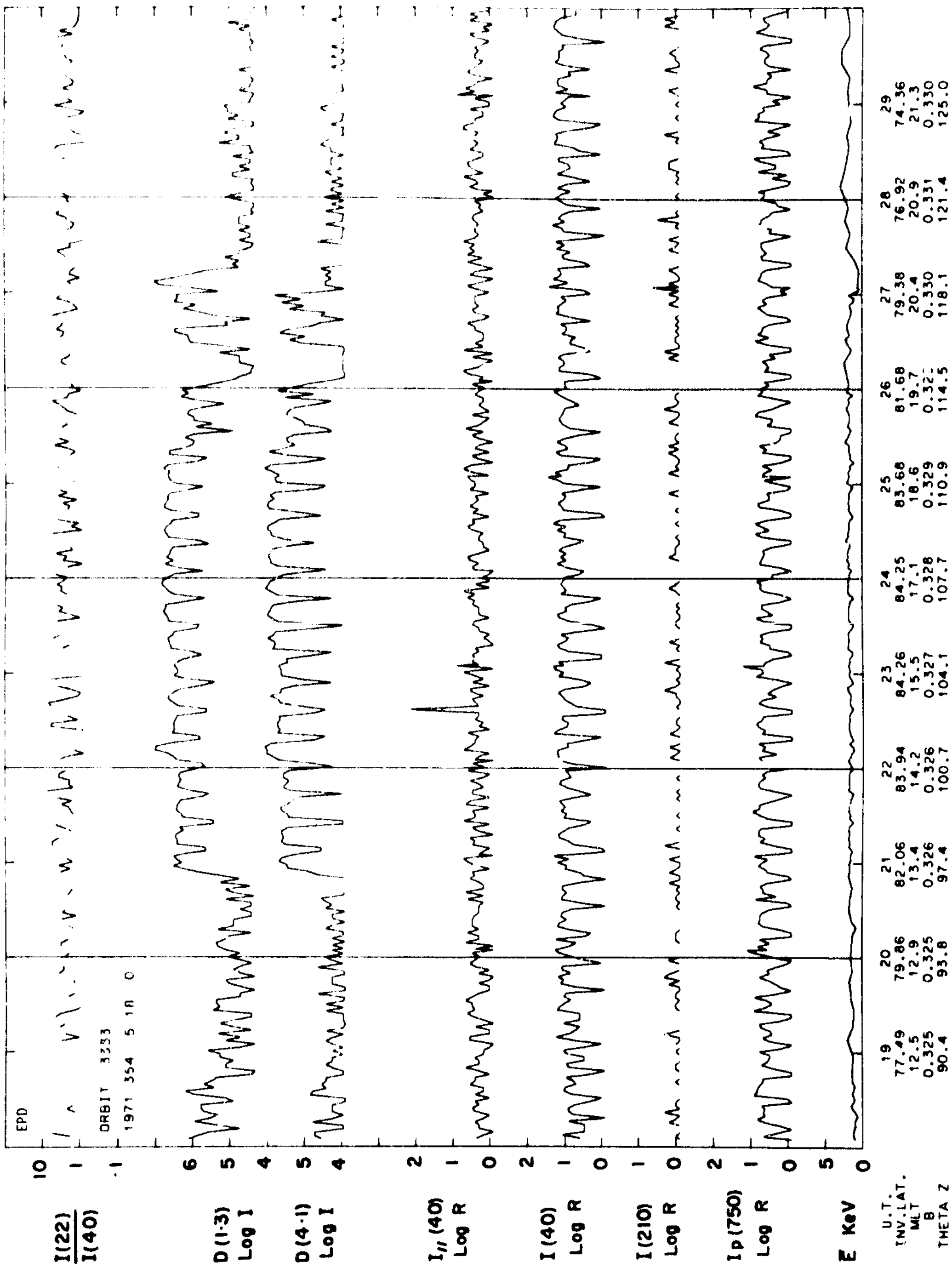

SET 9, FORMAT 3

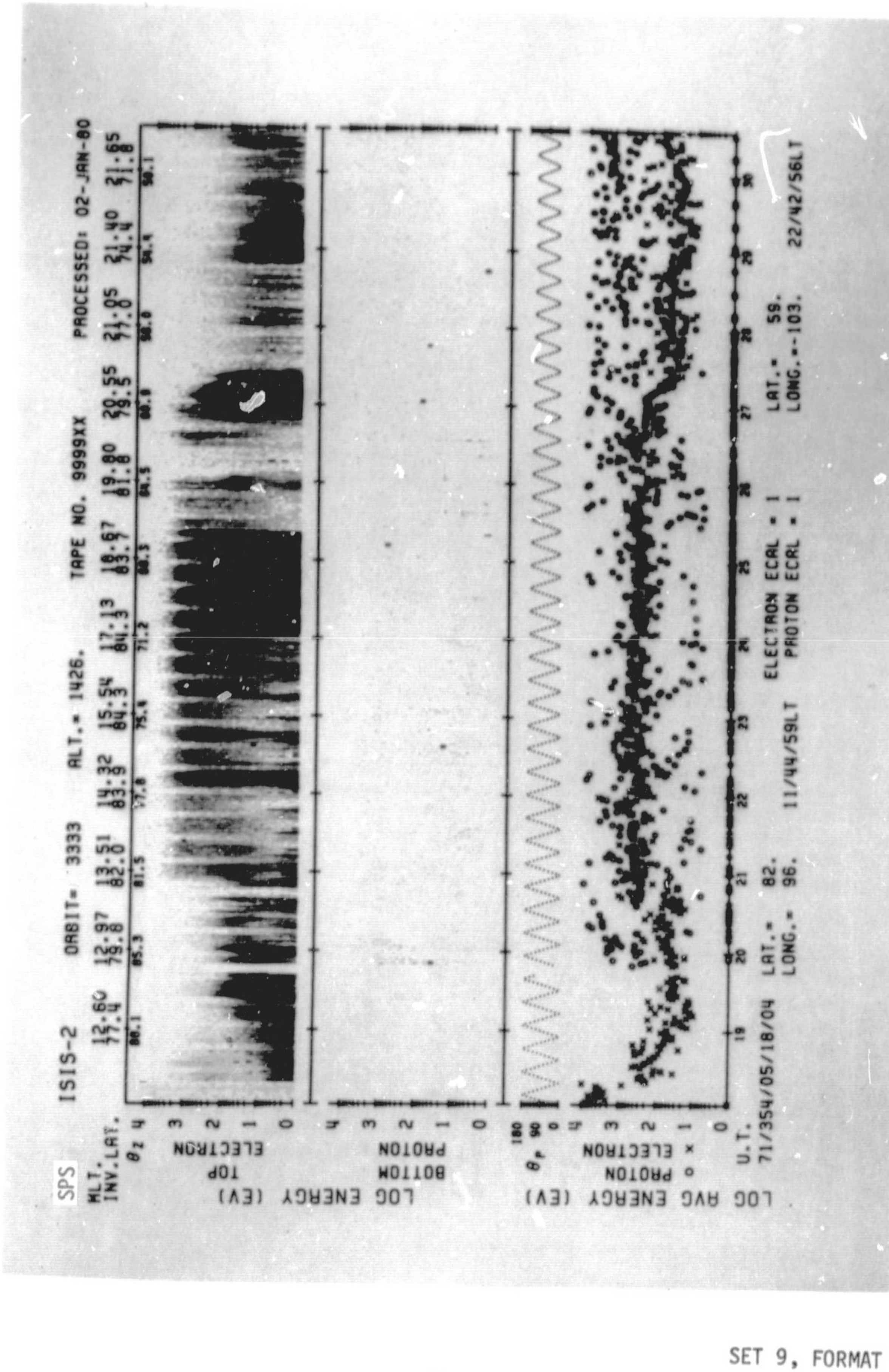

SET 9, FORMAT 6

ORBIT 3333
DATE 711220
DAY 354

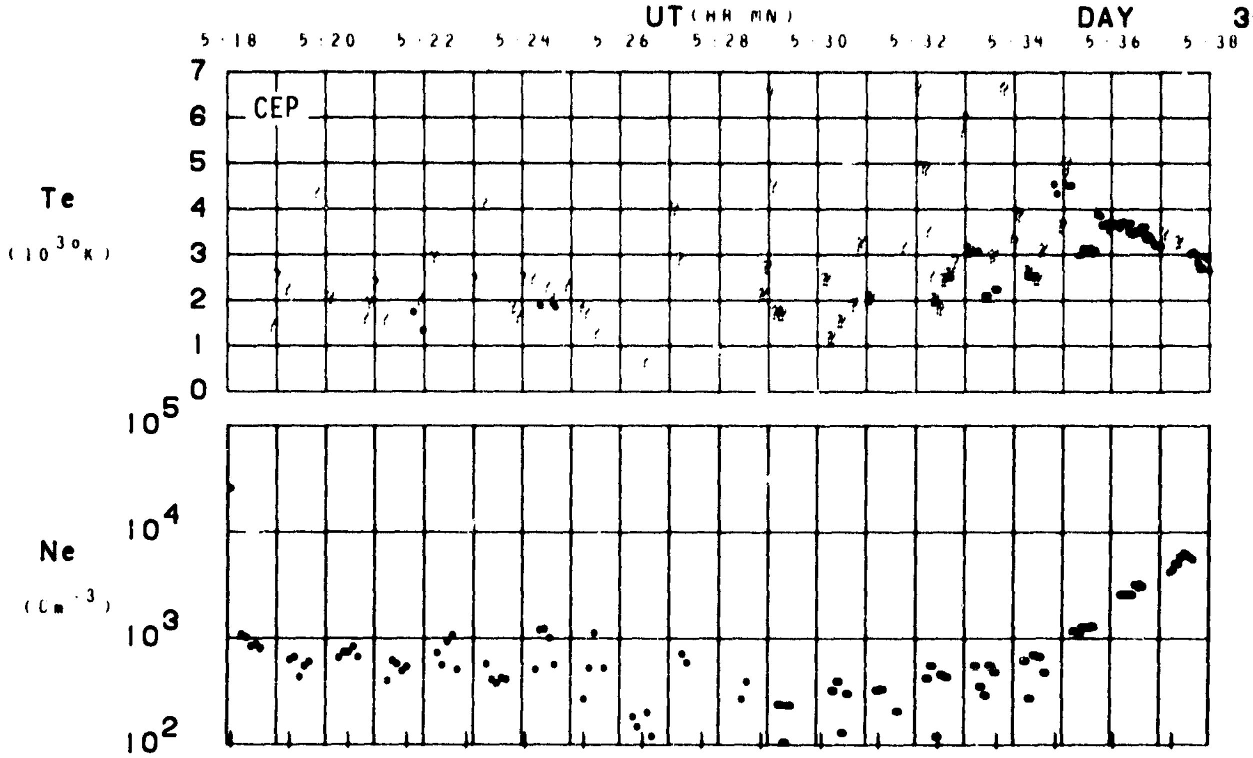

LAT	81	85	87	86	82	79	75	71	67	64	60	56	52	48	45	41	37
LONG	96	104	158	-128	-112	-107	-105	-104	-103	-102	-102	-102	-102	-102	-102	-102	-102
LT	11:44	12:18	15:58	20:49	21:56	22:16	22:26	22:33	22:37	22:40	22:42	22:44	22:45	22:46	22:47	22:48	22:49
DIP	87	88	88	89	89	89	88	87	87	86	85	84	83	81	80	78	77
DIPLAT	85	86	87	88	89	88	87	86	84	83	81	79	77	74	71	68	65
L	15.3	23.6	39.5	78.5	99.4	99.4	73.6	37.3	22.2	14.4	9.9	7.3	5.6	4.5	3.6	3.0	2.6
INVLAT	75	78	80	83	84	84	83	80	77	74	71	68	65	61	58	55	51
ZA	104	108	112	115	119	123	126	130	133	137	140	144	147	150	153	156	159

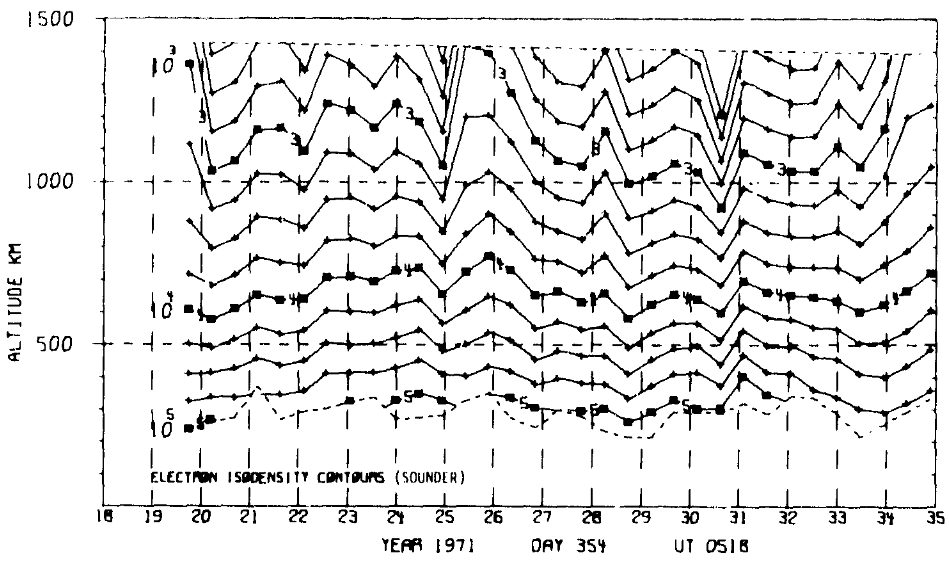

SET 9, FORMAT 10

ASP

711221/0403 UT (714/41)

CENTER LAT/LON/MLT :

85./8.5/00

.5 - 3.9 kR	1.9 - 9.5 kR	4.6 - 33.0 kR
.5 - 3.9 kR	.5 - 3.9 kR	.5 - 3.9 kR
.5 - .8	.8 - 1.4	1.4 - 2.4

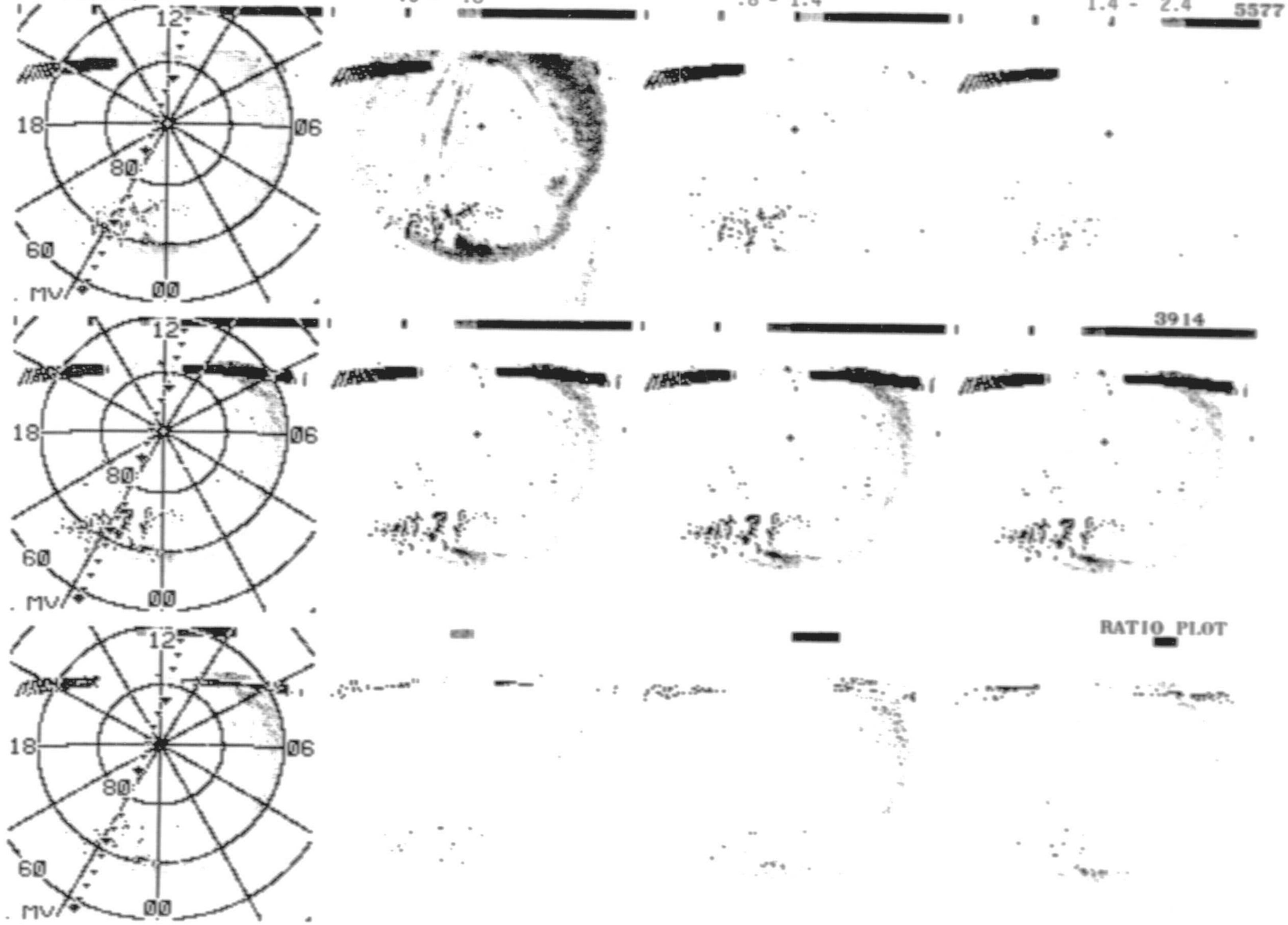

SET 10, FORMAT 7

ORIGINAL PAGE IS OF POOR QUALITY

ORBIT 3345 (71/DEC/21)
DAY 355 OF YEAR 1971

FIRST SPIN U.T. 4^H3^M
LAST SPIN U.T. 4^H25^M

6300 ANGSTROM INTENSITY

DATE PROCESSED: 80/AUG/13
INVARIANT COORDINATES (250 KM.)

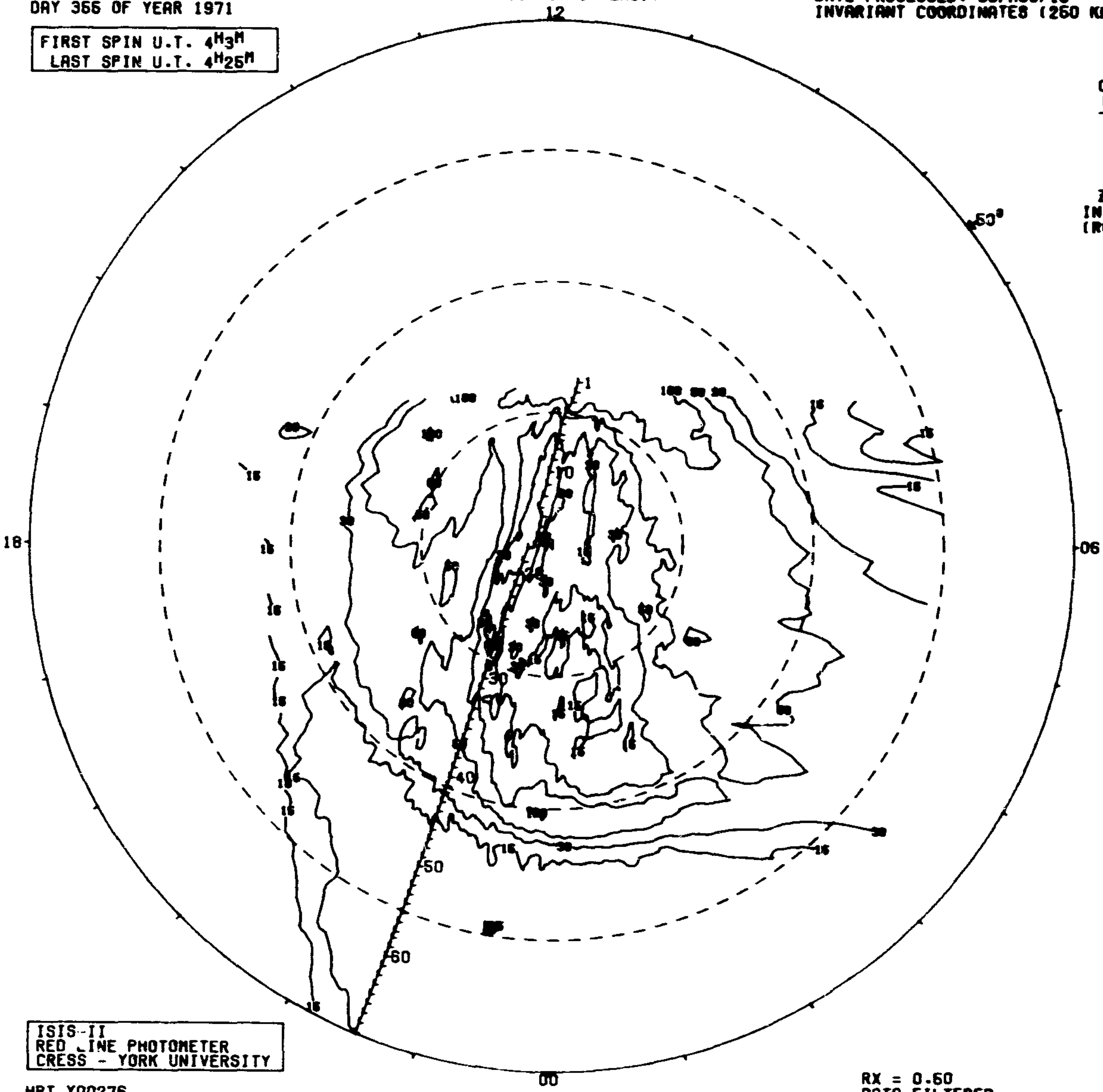

CONTOURS PLOTTED

150
300
500
1000
ZENITHAL INTENSITIES (RAYLEIGHS)

SPACECRAFT INFORMATION

SPIN NUMBER	ORBIT TIME (HHMMSC)	INVARIANT LATITUDE (DEGREES)
1	040316	78.0
2	040334	78.7
3	040352	79.6
4	040410	80.3
5	040428	81.0
6	040446	81.8
7	040458	82.3
8	040516	83.1
9	040534	83.7
10	040552	84.2
11	040610	84.4
12	040628	84.4
13	040646	84.3
14	040704	84.3
15	040722	84.2
16	040740	84.2
17	040758	84.3
18	040816	84.3
19	040834	84.3
20	040852	84.3
21	040910	84.3
22	040928	84.3
23	040946	84.2
24	041004	83.8
25	041016	83.6
26	041034	82.8
27	041052	81.8
28	041110	80.8
29	041128	80.1
30	041146	79.6
31	041204	78.7
32	041222	78.0
33	041240	77.2
34	041258	76.4
35	041316	75.6
36	041334	74.8
37	041352	74.0
38	041410	73.2
39	041428	72.4
40	041446	71.6
41	041504	70.8
42	041516	70.3
43	041534	69.5
44	041552	68.7
45	041610	67.8
46	041628	67.0
47	041646	66.2
48	041704	65.4
49	041722	64.6
50	041740	63.8
51	041758	63.0
52	041816	62.2
53	041834	61.4
54	041852	60.6
55	041910	59.8
56	041928	58.9
57	041946	58.1
58	041958	57.6
59	042016	56.8
60	042034	56.0
61	042052	55.2
62	042110	54.4
63	042128	53.6
64	042146	52.8
65	042204	52.0
66	042222	51.2
67	042240	50.4
68	042258	49.6
69	042316	48.8
70	042334	48.0
71	042352	47.2
72	042410	46.4
73	042428	45.7
74	042446	44.9
75	042510	43.9

ISIS-II
RED LINE PHOTOMETER
CRESS - YORK UNIVERSITY

HRT Y00276
FILE 10

SPACECRAFT TRACK TRACED DOWN TO 250 KM. (NUMBERS DENOTE SPINS)

RX = 0.60
DATA FILTERED
ZERO SUBTRACTION NOT PERFORMED

SET 10, FORMAT 8

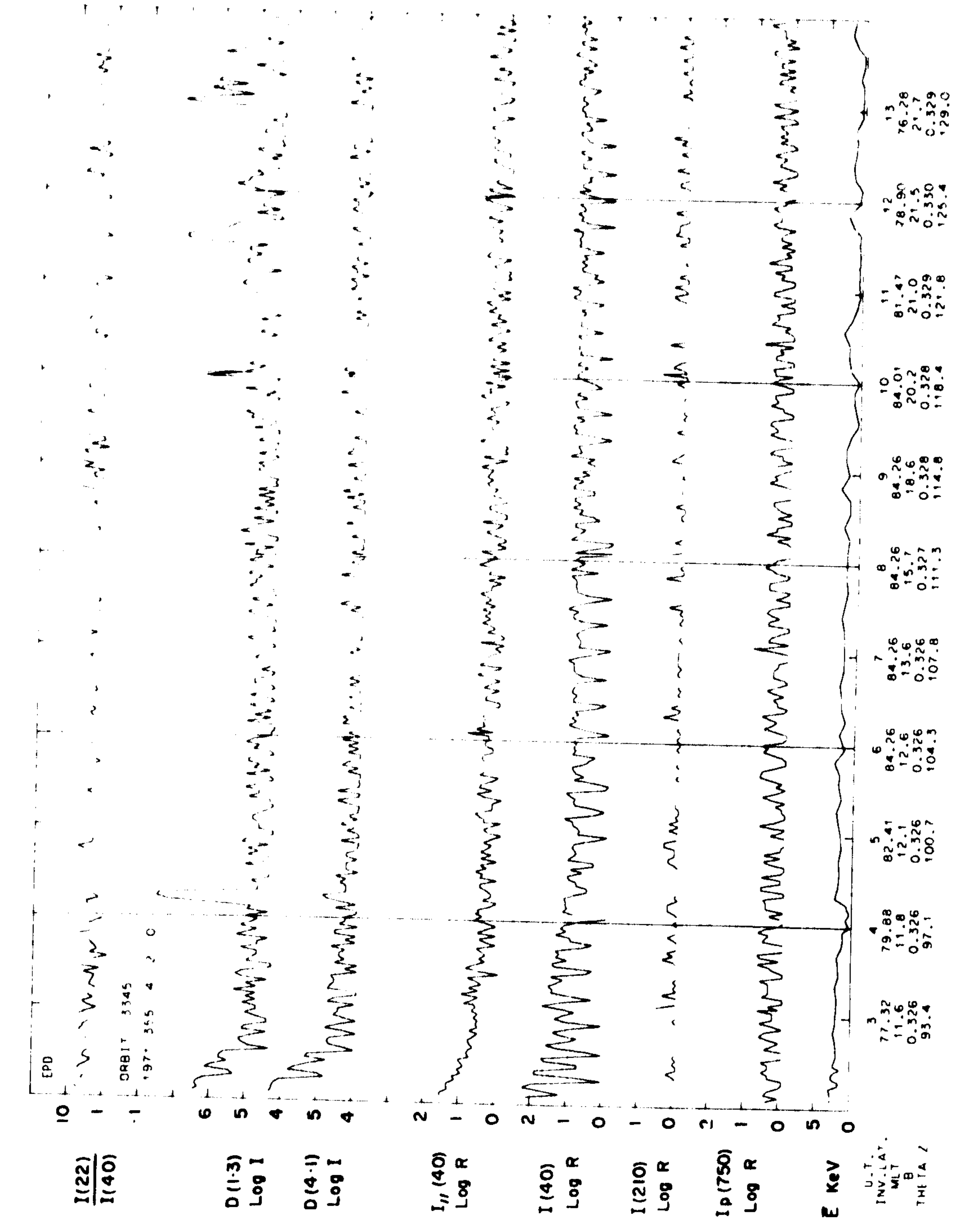

SET 10, FORMAT 3

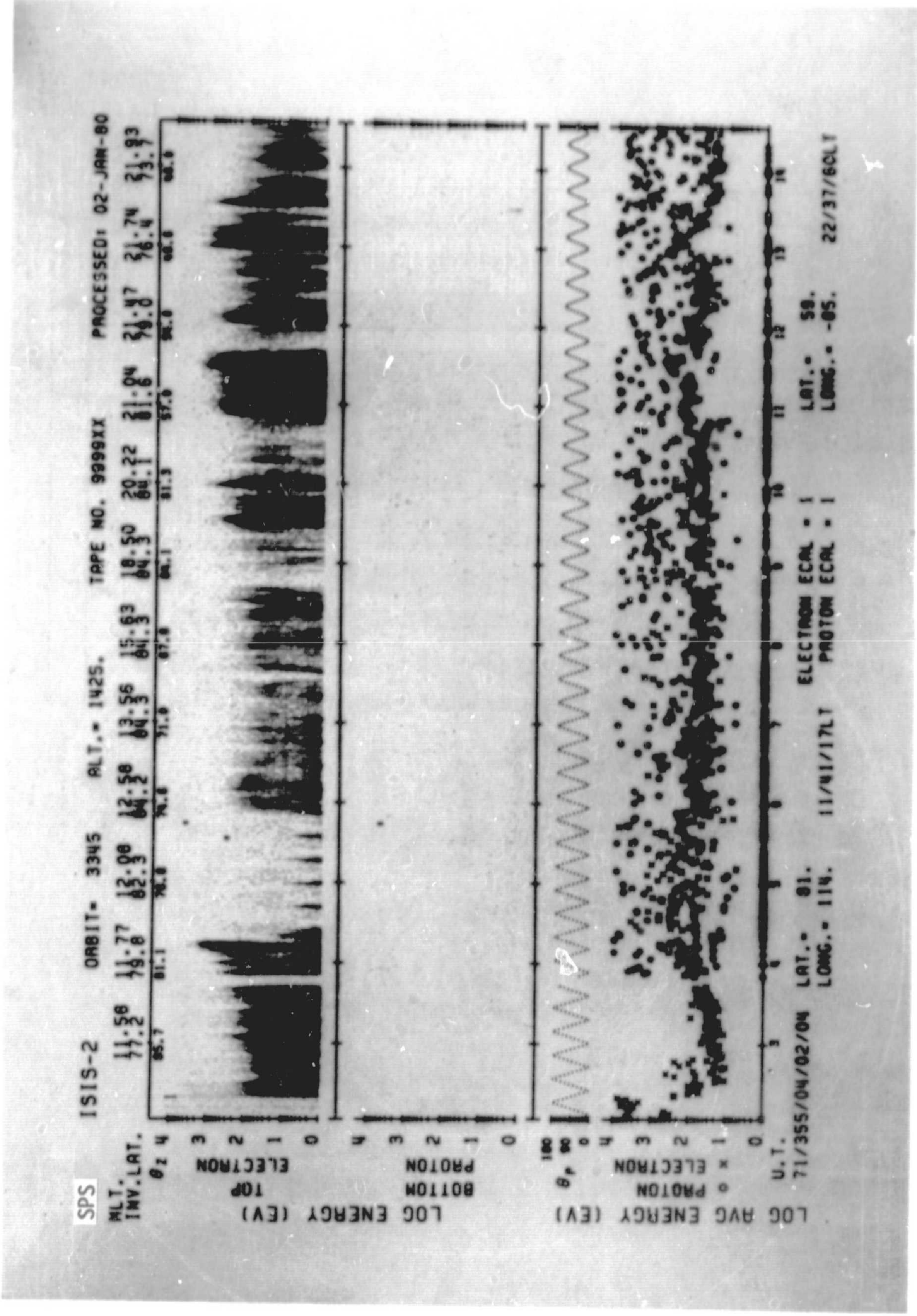

SET 10, FORMAT 6

ORBIT 3345
DATE 711221
DAY 355

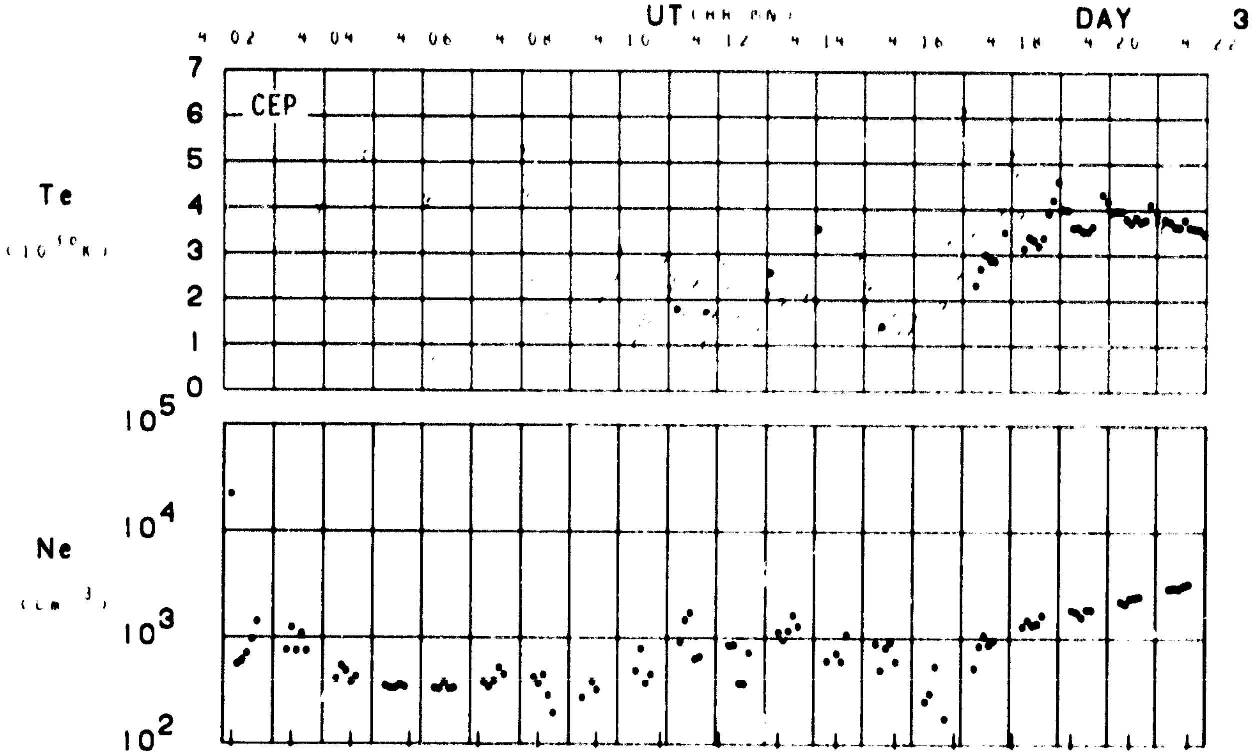

LAT	81	85	87	86	82	78	74	70	66	63	59	55	51	47	44	40	36
LONG	115	121	179	-111	-93	-89	-87	-85	-85	-84	-84	-84	-84	-84	-84	-84	-84
LT	11:45	12:12	16:03	20:43	21:55	22:14	22:23	22:29	22:33	22:35	22:37	22:39	22:41	22:42	22:43	22:44	22:44
DIP	87	88	88	89	-89	89	88	87	87	86	85	84	83	82	80	79	77
DIPLAT	85	86	87	88	89	88	87	86	85	83	81	79	77	75	72	69	67
L	15.2	24.0	43.8	93.5	99.5	100.1	99.4	50.7	26.2	16.2	10.0	7.9	6.0	4.8	3.9	3.2	2.8
INVLAT	75	78	81	84	84	84	84	81	78	75	72	69	65	62	59	56	53
ZA	105	108	112	115	120	123	127	131	134	137	141	144	148	151	154	156	159

SET 10, FORMAT 10

VI-B. GEOPHYSICAL DATA SET: AIRGLOW AND RELATED MEASUREMENTS

DATA SET DESCRIPTION

Although the Auroral Scanning Photometer (ASP) and the Red Line Photometer (RLP) were designed and used primarily for auroral studies, they have also been used to make measurements of the OI 5577Å and 6300Å airglow emissions. Airglow limb observations provide slant emission rates free from atmospheric scattering and albedo effects. The ISIS 2 instruments, however, do not permit the transformation into real height profiles of the volume emission rate due to the relatively large fields of view. Nevertheless, the equivalent vertical column emission rate can be deduced from each limb observation; this is the geophysical quantity that an upward-viewing photometer would record from below the layer. The airglow latitude profiles presented here (Format 9) give the vertical column emission rate in rayleighs.

This data set has been selected to provide representative observations of airglow emission rates at different latitudes and times of the year. All data are from night-time passes at American longitudes. Because the E- and F-region components of the 5577Å airglow are separable at the limb, they are both plotted. The upper limit for detection of the F-region component varies from 5 to 10R depending on the level of background noise present. Gaps in the corresponding red line plots are due principally to the presence of high background signal when the satellite was in the Atlantic anomaly region.

The data set includes measurements from other satellite instruments. Of most relevance to the F-region emissions is the electron density obtained from the Topside Sounder (Format 2). Electron density and temperature are also available at 1400 km from the Cylindrical Electrostatic Probe (Format 4). Ion concentrations at 1400 km are obtained with the Ion Mass Spectrometer (Format 4) and the Retarding Potential Analyzer (Format 5). Measurements of energetic electrons and protons were made with two instruments, the Soft Particle Spectrometer (Format 6) and the Energetic Particle Detector (Format 3). It should be noted that the airglow latitudes of Format 9 refer to the locations of the limb, not the positions of the satellite. In cartwheel mode, the limb is observed either before or after the satellite reaches that position or passes through the magnetic field line joining the F-region limb and the satellite.

The pass on 711017 was chosen to demonstrate the large variation with latitude of the E-region 5577Å airglow that occurs in October. There are two prominent midlatitude enhancements with the larger one in the Northern (winter) Hemisphere. There is no evidence for similar behavior in the F-region airglow for this pass.

Slant emission profiles of 5577Å airglow (Format 12) are shown for 711122. Variations in the slant intensity are evident, with the minimum near the equator. The E-region limb at 5577Å is prominent in the polar cap, and it is obviously due to airglow rather than aurora because the corresponding 3914Å limb (shown) is weak. On the following day, 711123, there was an F-region airglow enhancement related to the equatorial ionospheric anomaly. This is very pronounced in the data, particularly at 6300Å.

Two passes were selected to illustrate the April maximum in the E-region green line. The large winter hemisphere enhancement at -40° latitude is a persistent feature, although it was unusually large on 720420 and 720421. The equatorial minimum and secondary maximum in the summer hemisphere are also characteristic features of this period of the year. The F-region emissions are more variable as an examination of these two passes demonstrates. On both days the 6300Å intensity was enhanced at high latitudes due to the effects of twilight and/or particle precipitation. The equatorial anomaly was well developed on 720420 for 5577Å as can be seen from the double-humped shape of the latitude profile.

In this data set the following instruments are used:

1. Auroral Scanning Photometer, Format 9, 12

2. Red Line Photometer, Format 9

3. Topside Sounder, Format 2

4. Cylindrical Electrostatic Probe, Format 4

5. Ion Mass Spectrometer, Format 4

6. Retarding Potential Analyzer, Format 5

7. Soft Particle Spectrometer, Format 6

8. Energetic Particle Detector, Format 3

9. VLF, Format 11

Table 2 Data Set Pass List

Date	UT	Format									Page	Data Set
		9(5577)	9(6300)	12	2	4	5	6	3	11		
711117	0850	yes	no	yes	yes	yes	yes	yes	no	no	81	11
711122	0648	no	no	yes	yes	yes	yes	yes	yes	yes	87	12
711123	0538	yes	yes	yes	no	yes	yes	yes	no	no	96	13
720420	0730	yes	yes	yes	yes	yes	no	yes	no	no	102	14
720421	0610	yes	yes	yes	yes	yes	yes	yes	no	no	108	15

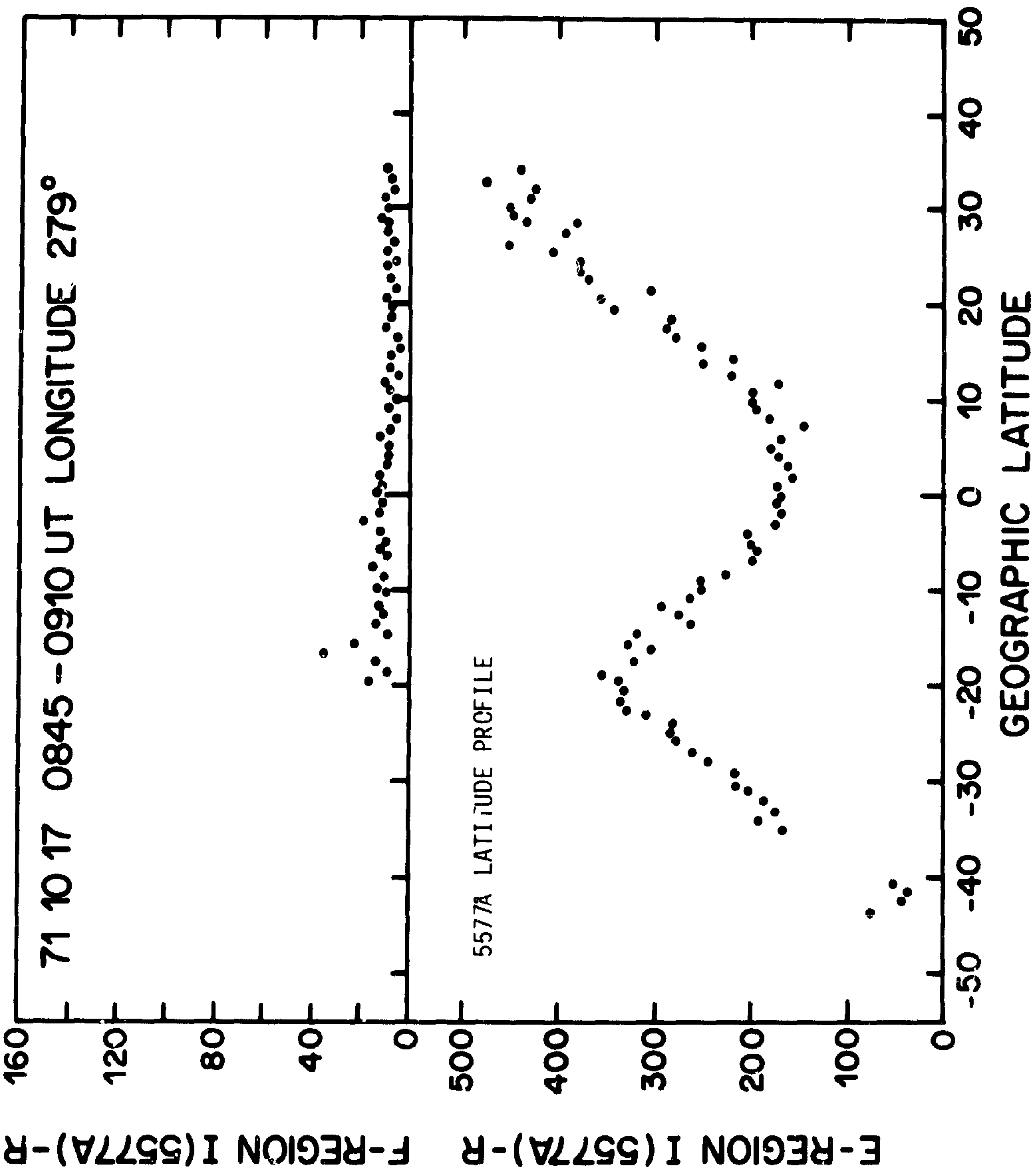

SET 11, FORMAT 9

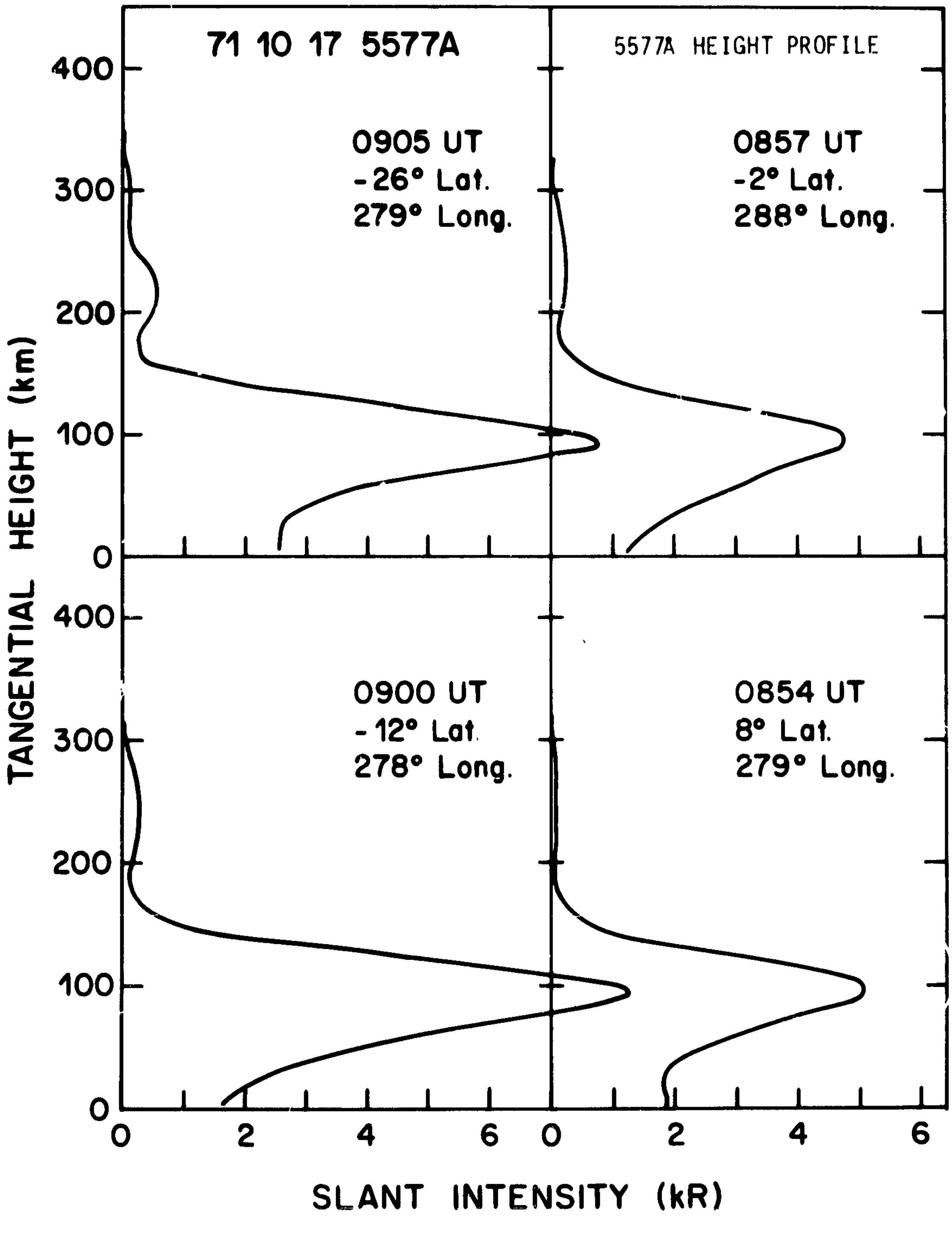

SET 11, FORMAT 12

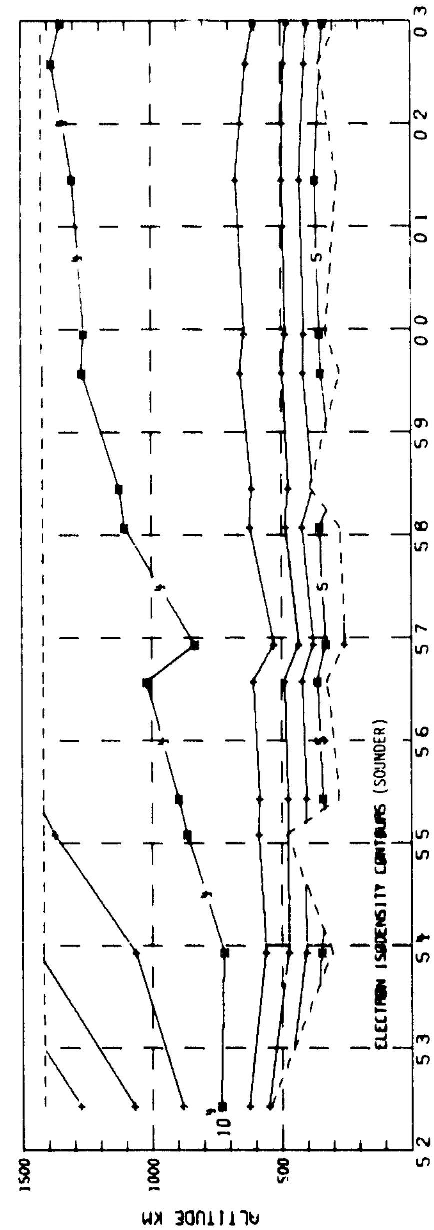

SET 11, FORMAT 2

RPA

711017

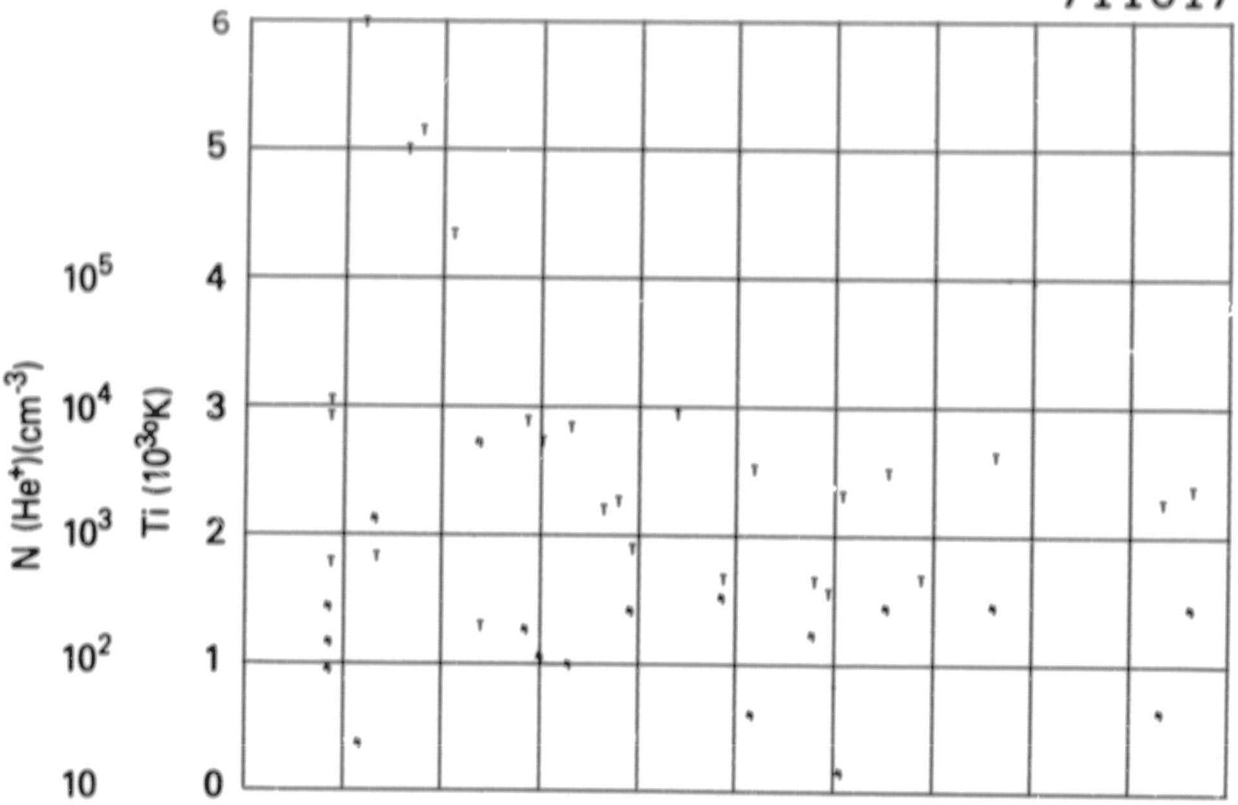

UT	08:52	08:54	08:56	08:58	09:00	09:02	09:04	09:06	09:08
LAST									
MLT									
DLAT									
INVL	63	58	53	48	43	38	34	31	29
GLAT	48	41	35	29	22	16	9	2	-5
GLNG	-78	-79	-79	-79	-80	-80	-80	-80	-8[illegible]
SZEN									
ALT	1417	1419	1421	1422	1424	1425	1426	1428	1430

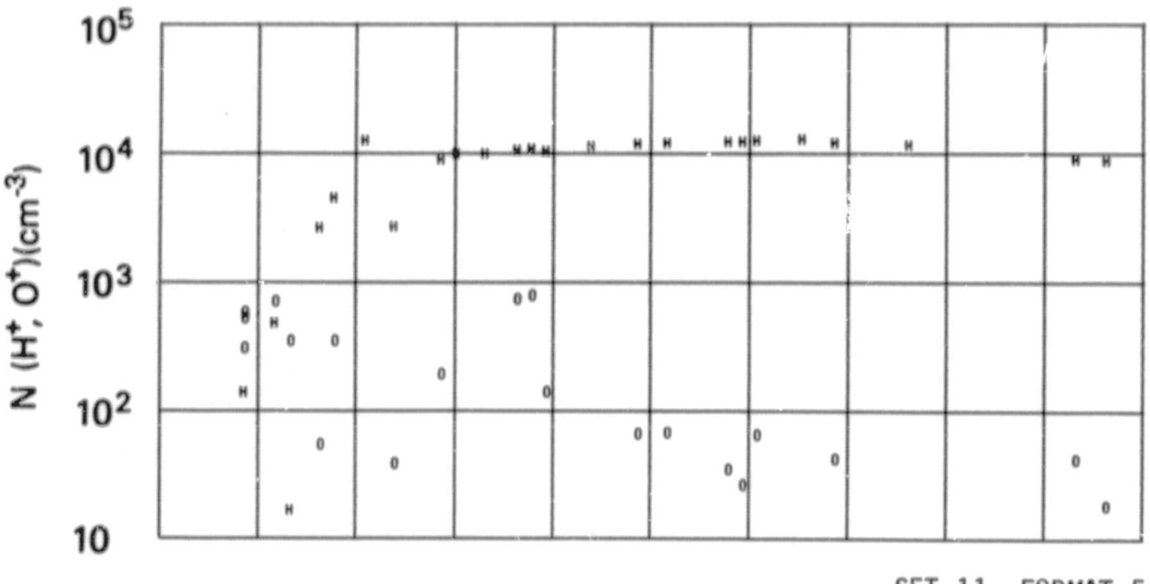

SET 11, FORMAT 5

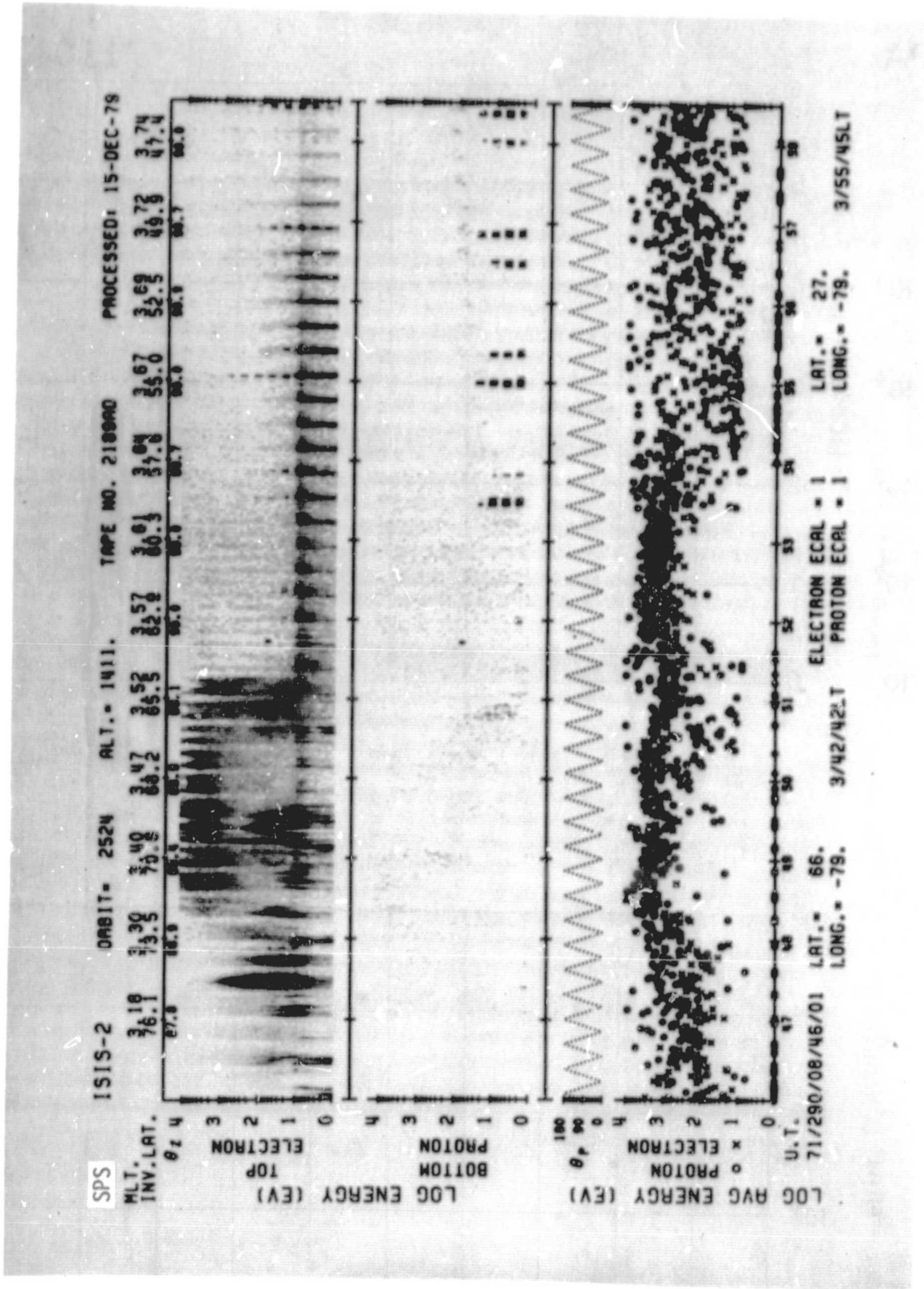

SET 11, FORMAT 6

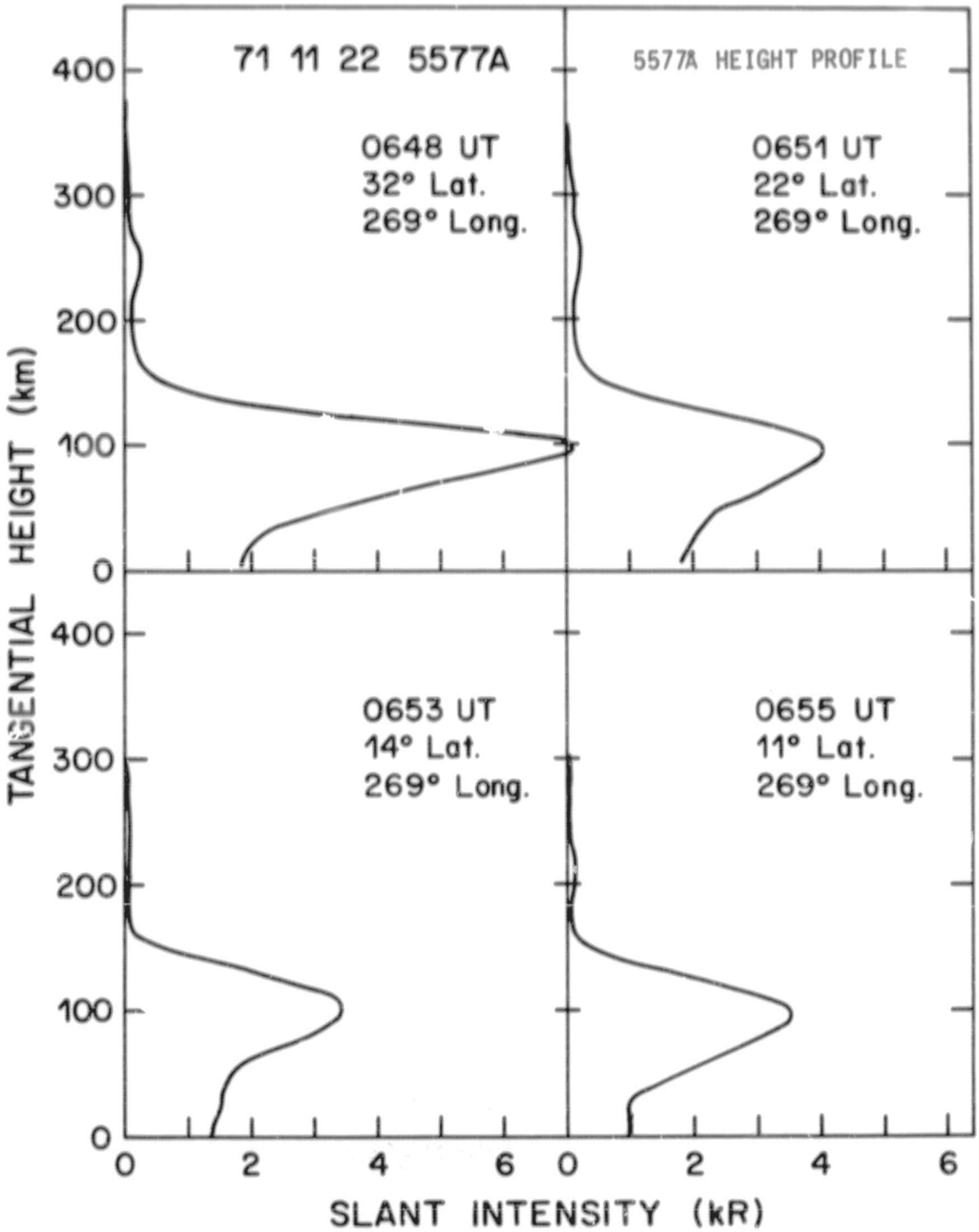

SET 12, FORMAT 12

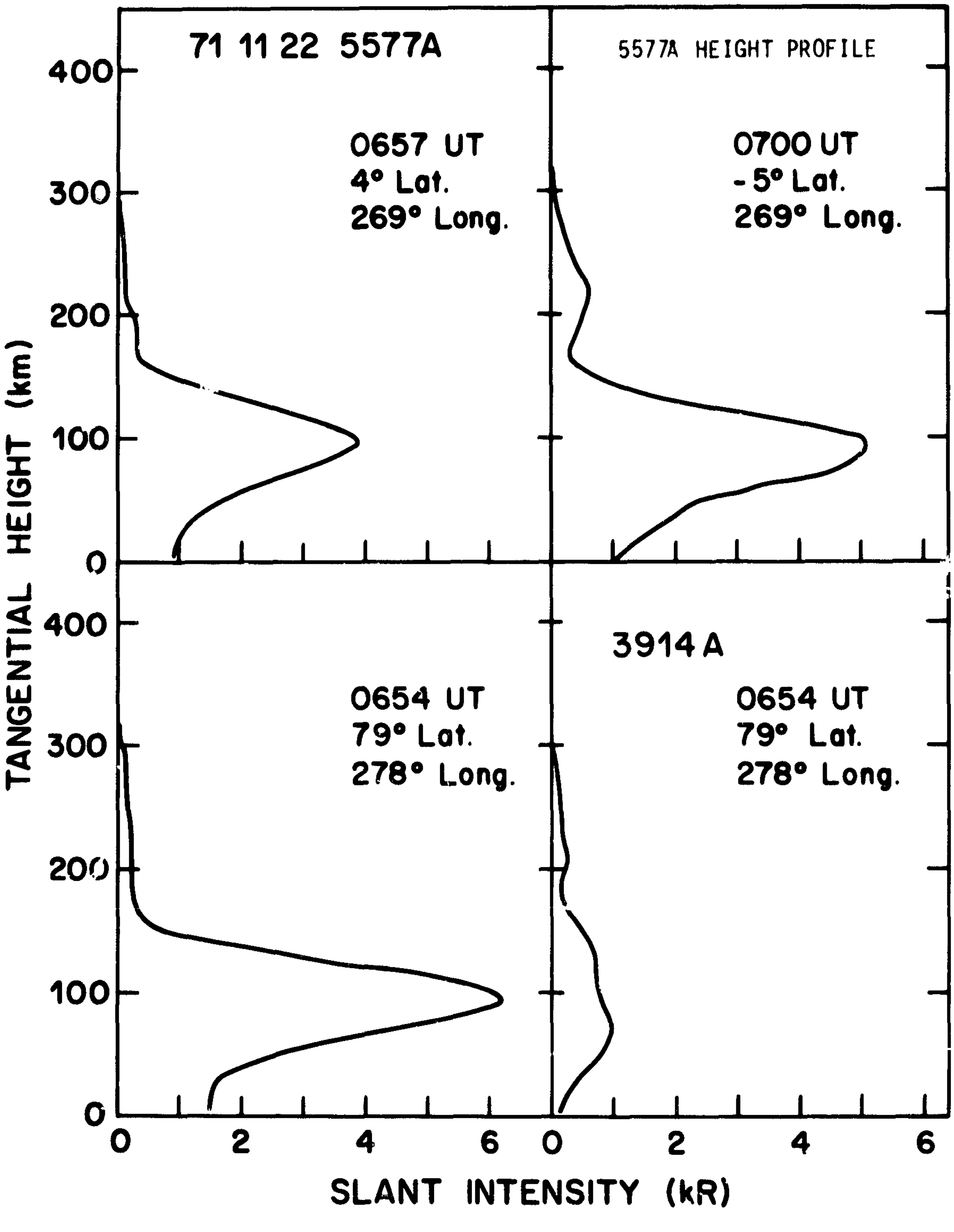

SET 12, FORMAT 12

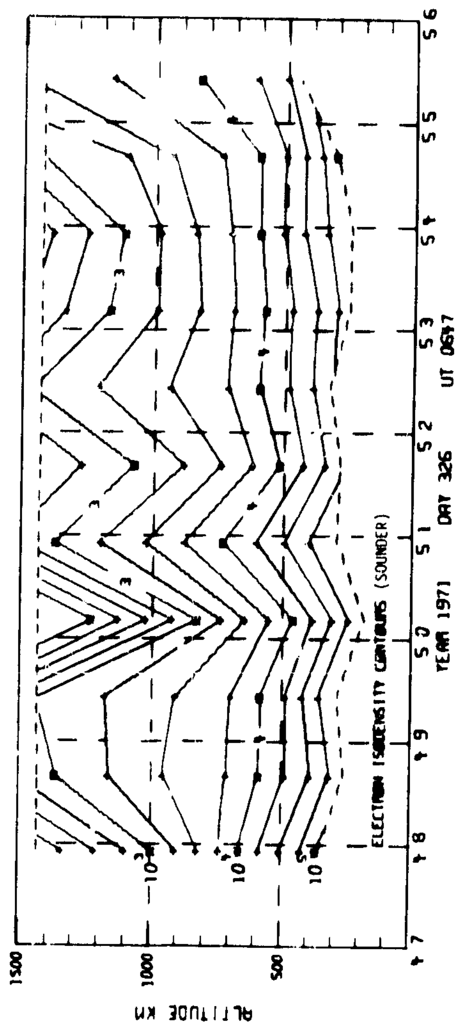

SET 12, FORMAT 2

ORBIT 2979
DATE 711122
DAY 326

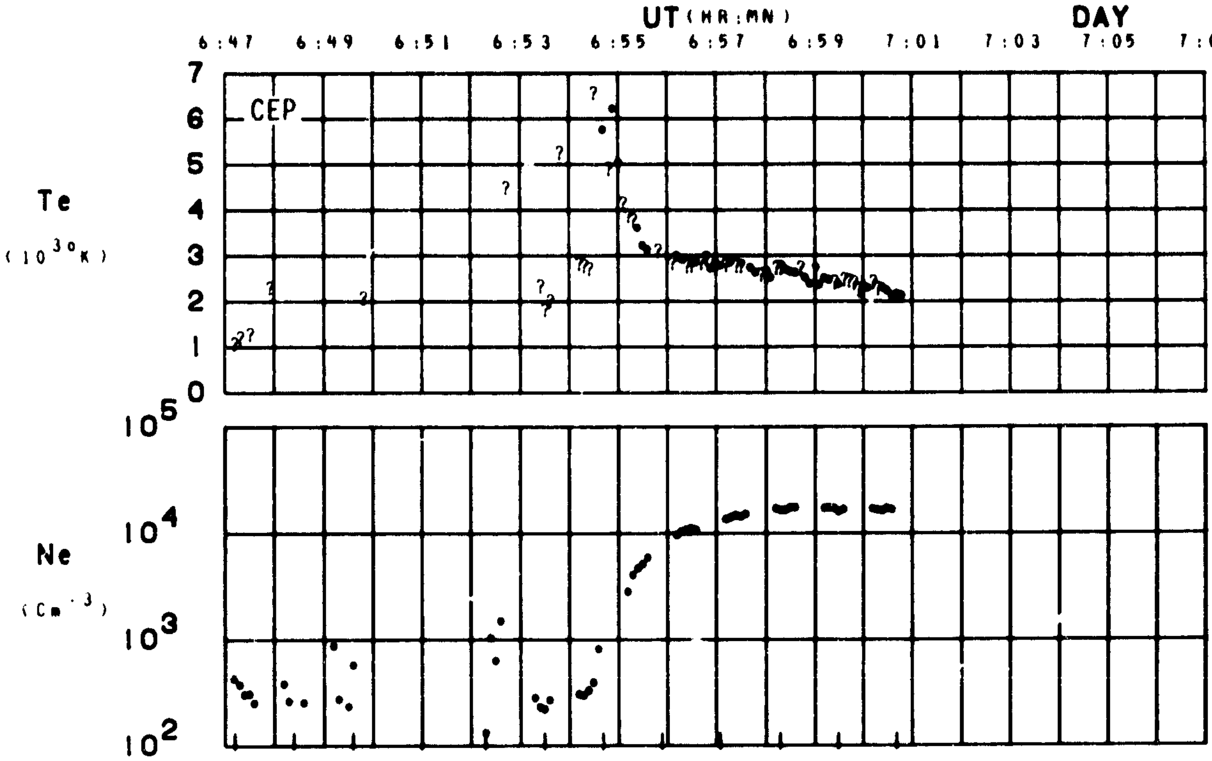

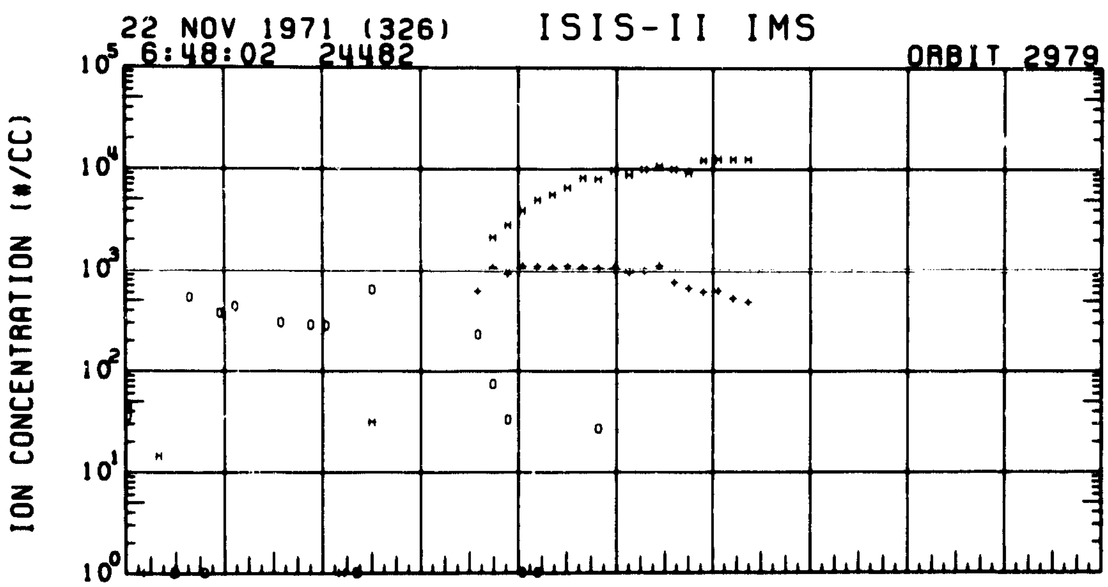

1 - H	UT	6:50	6:52	6:56	6:58	7:00
4 +	LAST	1:02	1:05	1:08	1:10	1:11
8 - △	MLT	0:17	0:32	0:48	0:54	0:58
14 N	DLAT	73	67	53	46	39
16 - O	INVL	72	67	56	50	45
	GLAT	59	53	40	34	28
	GLNG	-89	-89	-89	-90	-90
	SZEN	139	145	155	158	162
	ALT	1433	1430	1423	1419	1415

SET 12, FORMAT 4

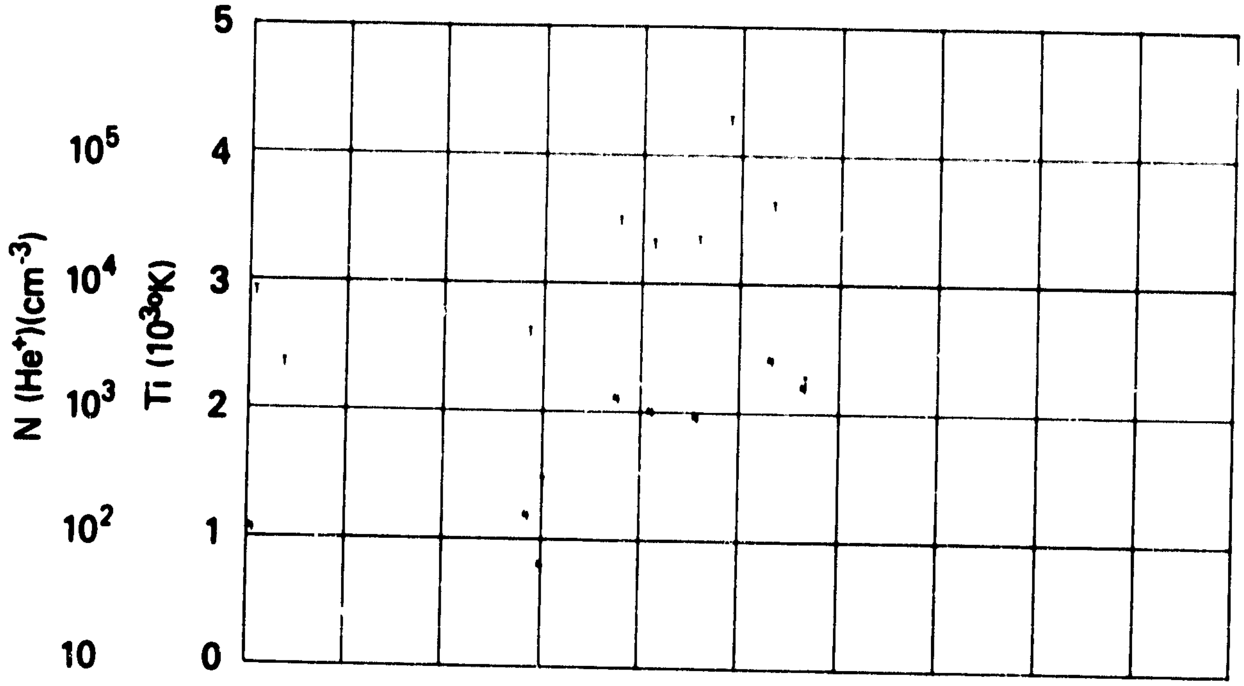

UT	6:50	6:52	6:56	6:58	7:00
LAST	1:02	1:05	1:08	1:10	1:11
MLT	0:17	0:32	0:48	0:54	0:58
DLAT	73	67	53	46	38
INVL	72	67	56	50	45
GLAT	59	53	40	34	28
GLNG	-88	-88	-89	-90	-80
SZEN	138	145	155	158	162
ALT	1433	1430	1423	1418	1415

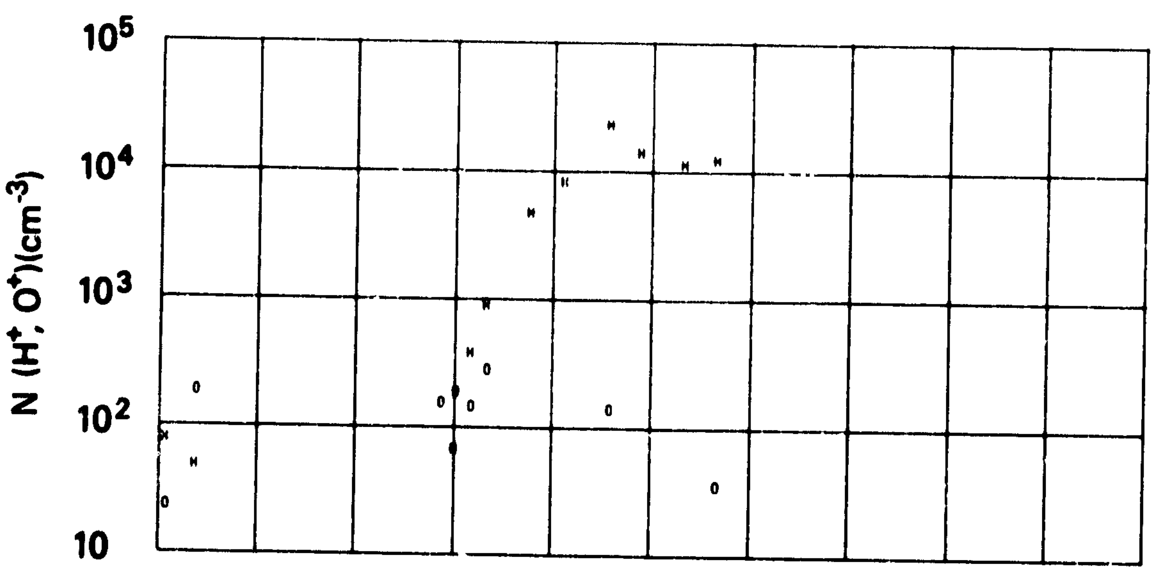

SET 12, FORMAT 5

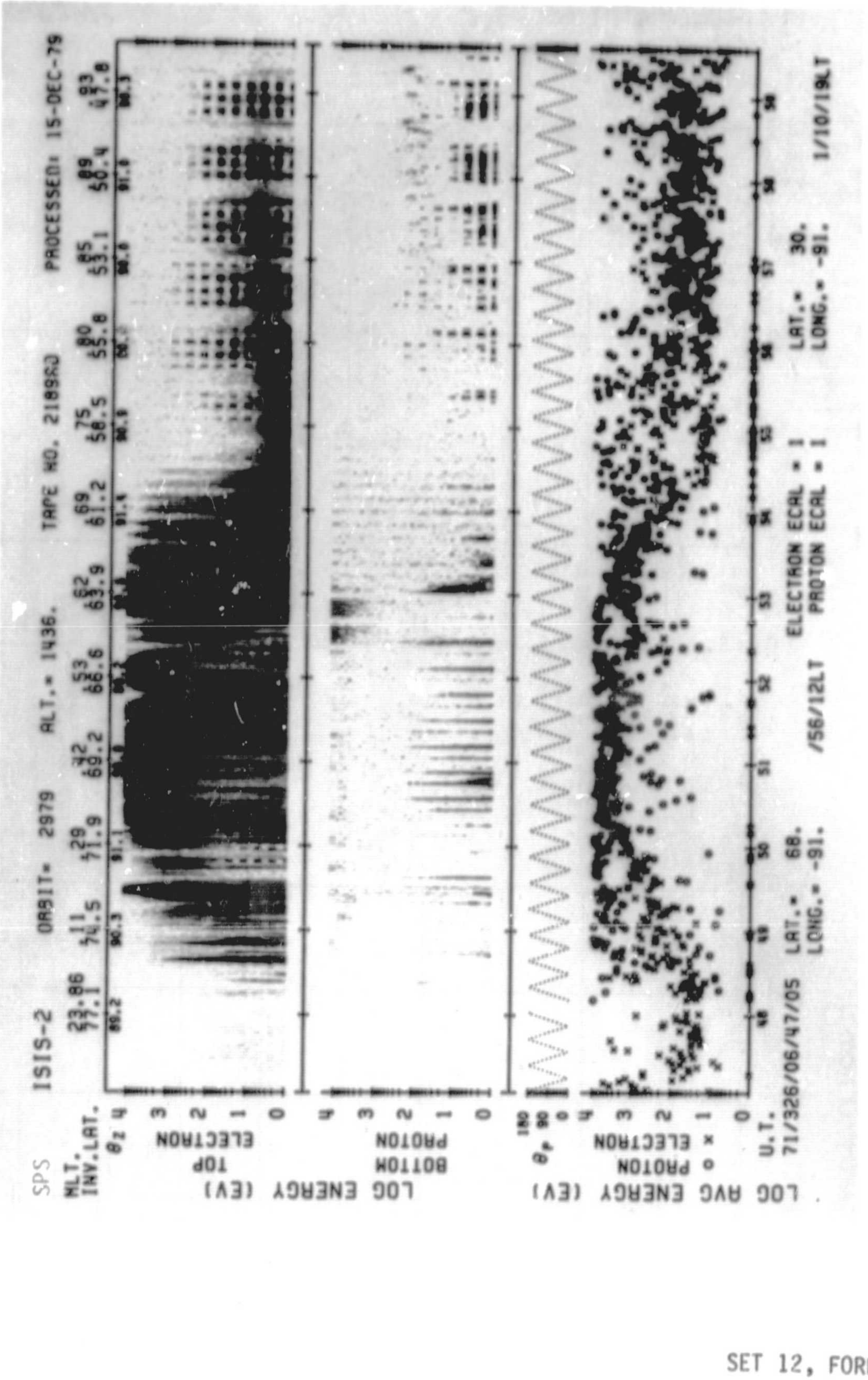

SET 12, FORMAT 6

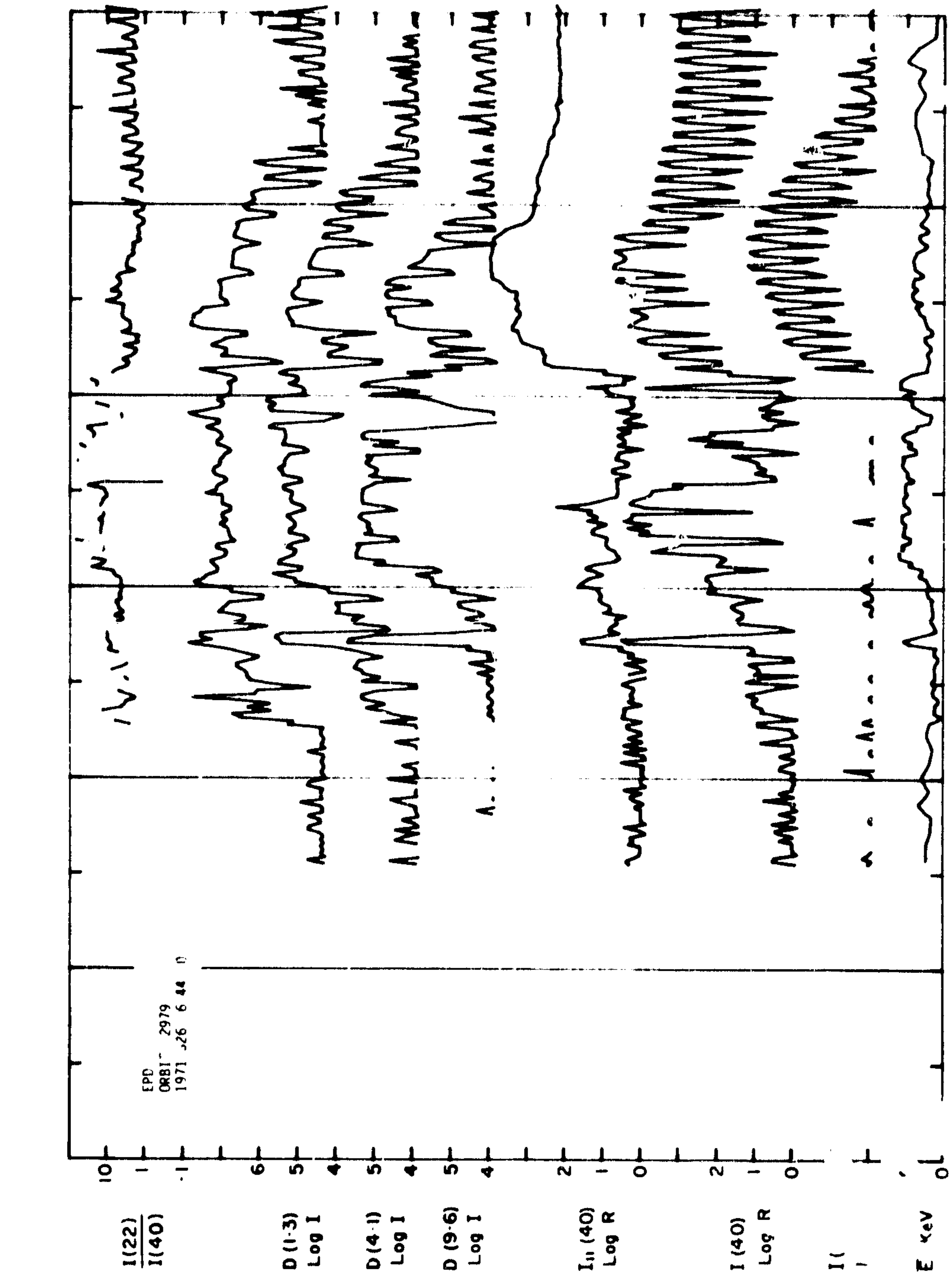

SET 12, FORMAT 3

71/326/0644

Excerpts of VLF Spectral film for the period 0647 - 0656

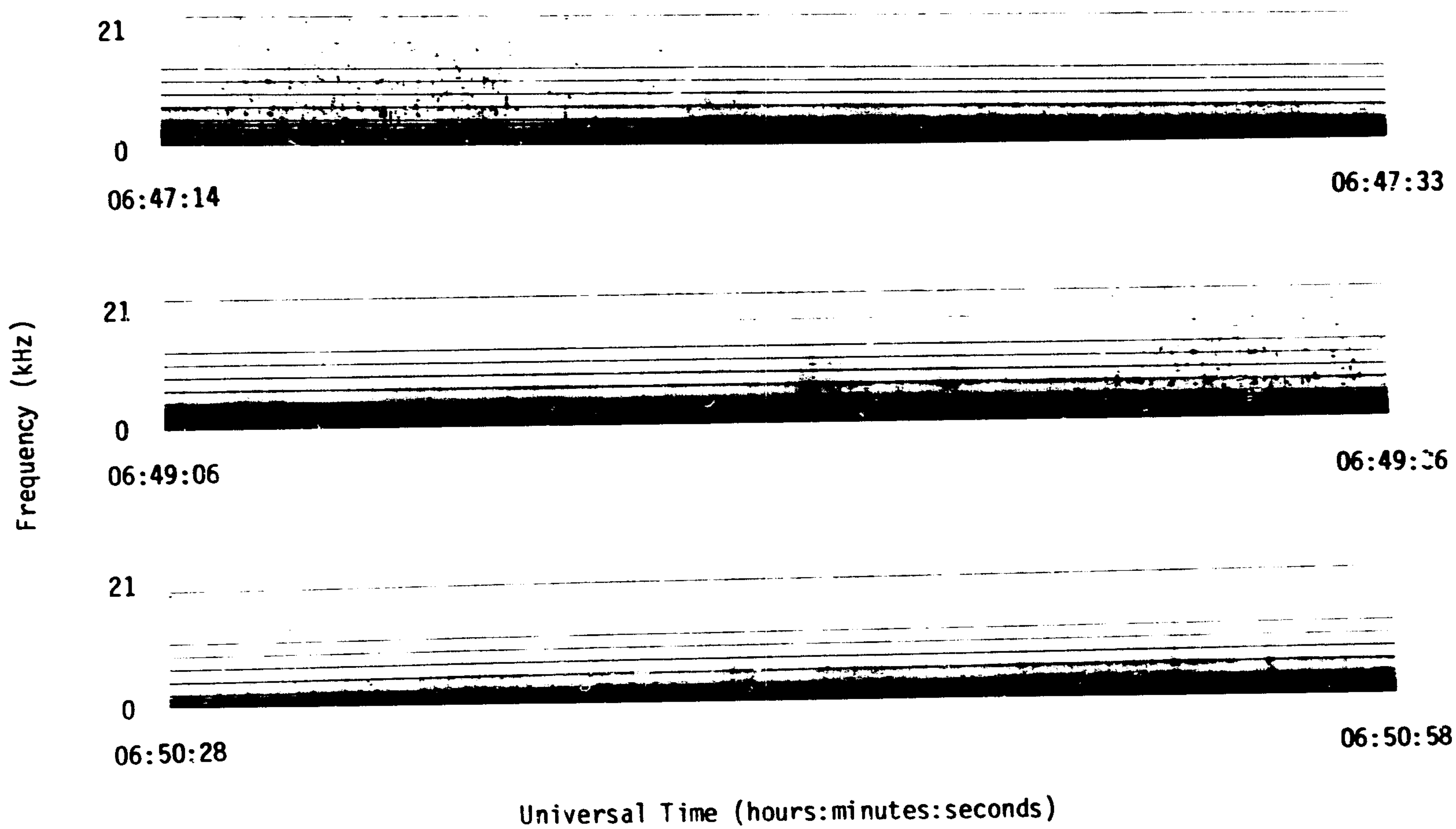

SET 12, FORMAT 11

C 2

71/326/0644

Excerpts of VLF Spectral film for the period 0647 - 0656

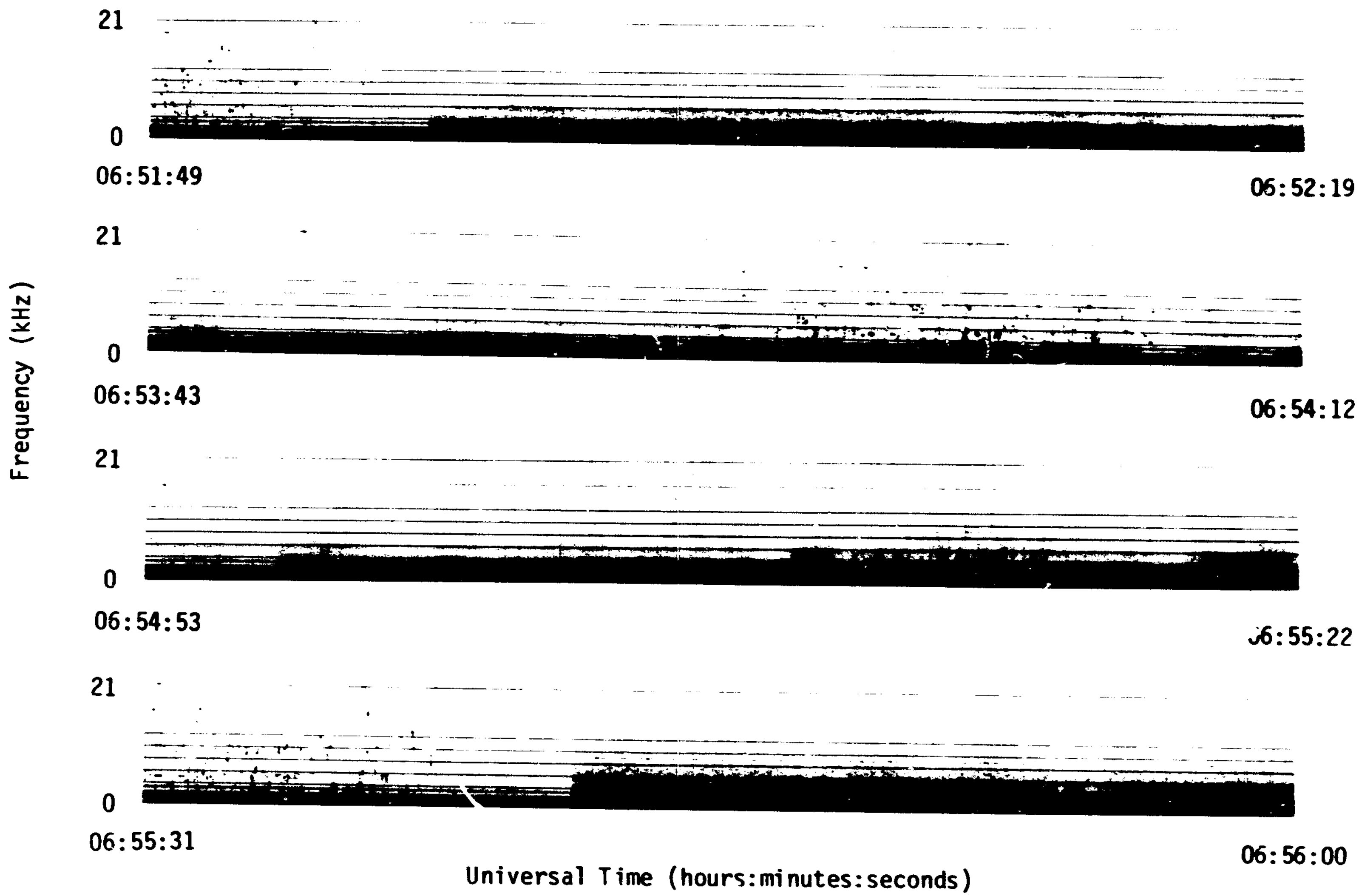

SET 12, FORMAT 11

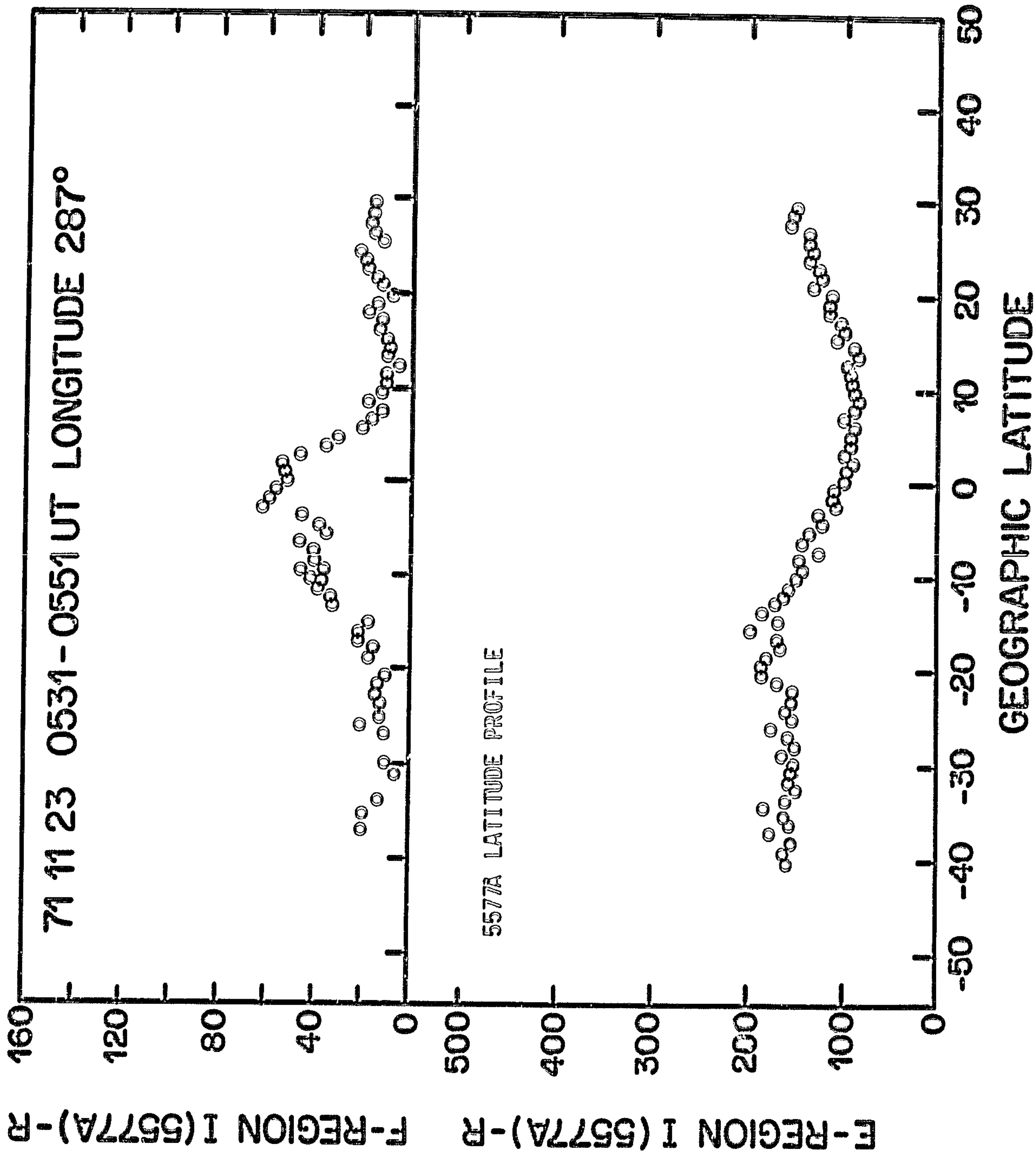

SET 13, FORMAT 9

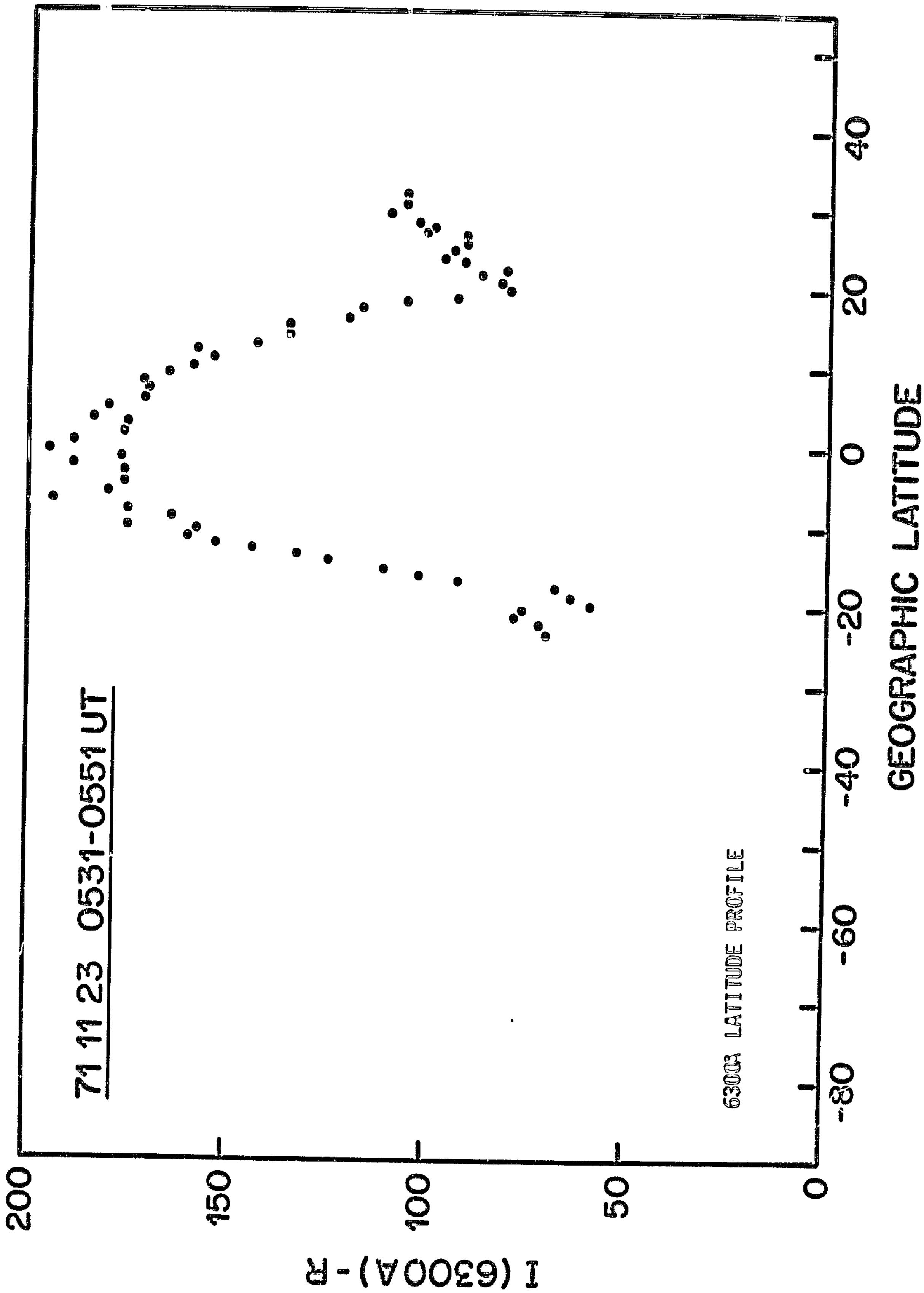

SET 13, FORMAT 9

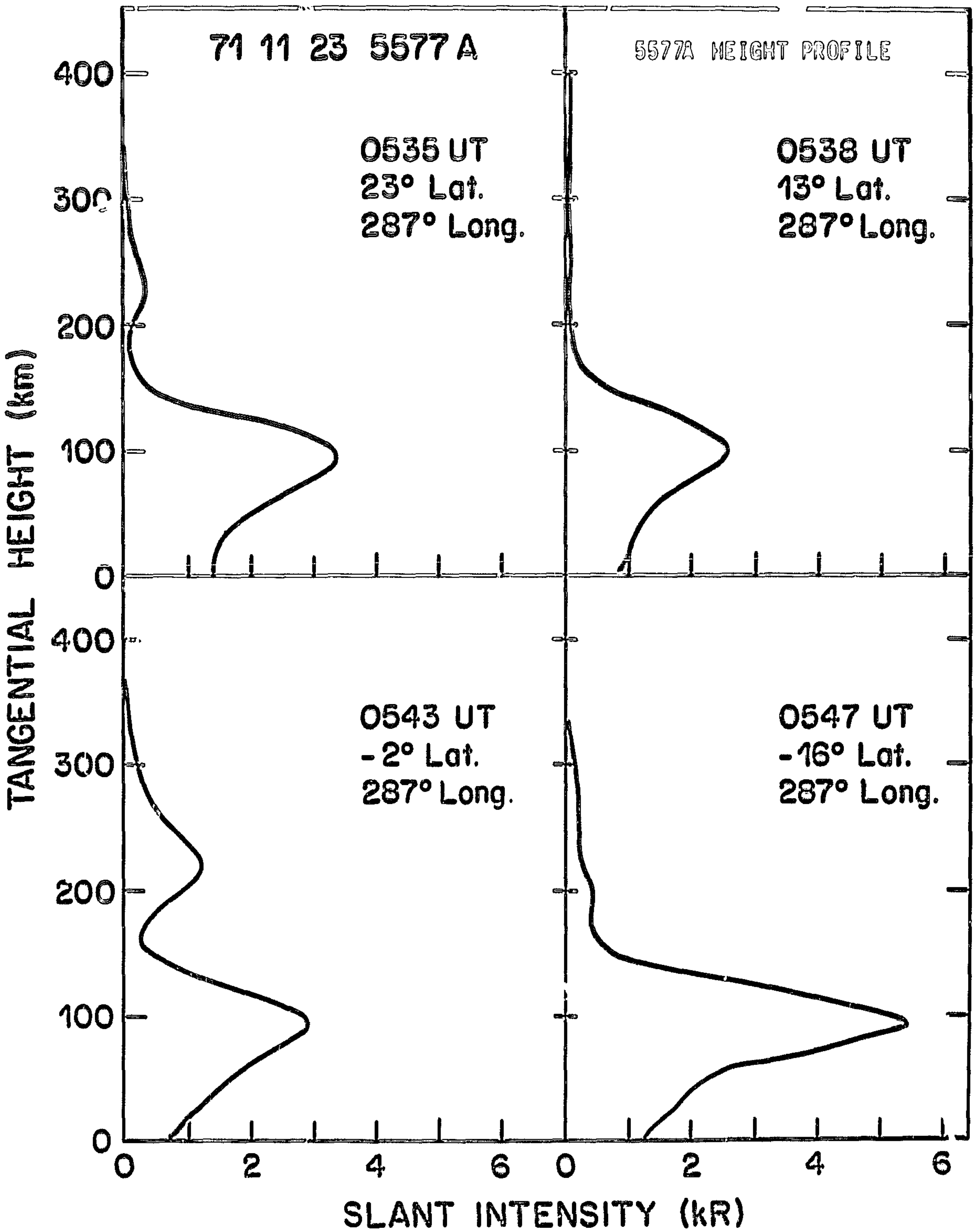

SET 13, FORMAT 12

ORBIT 2991
DATE 711123
DAY 327

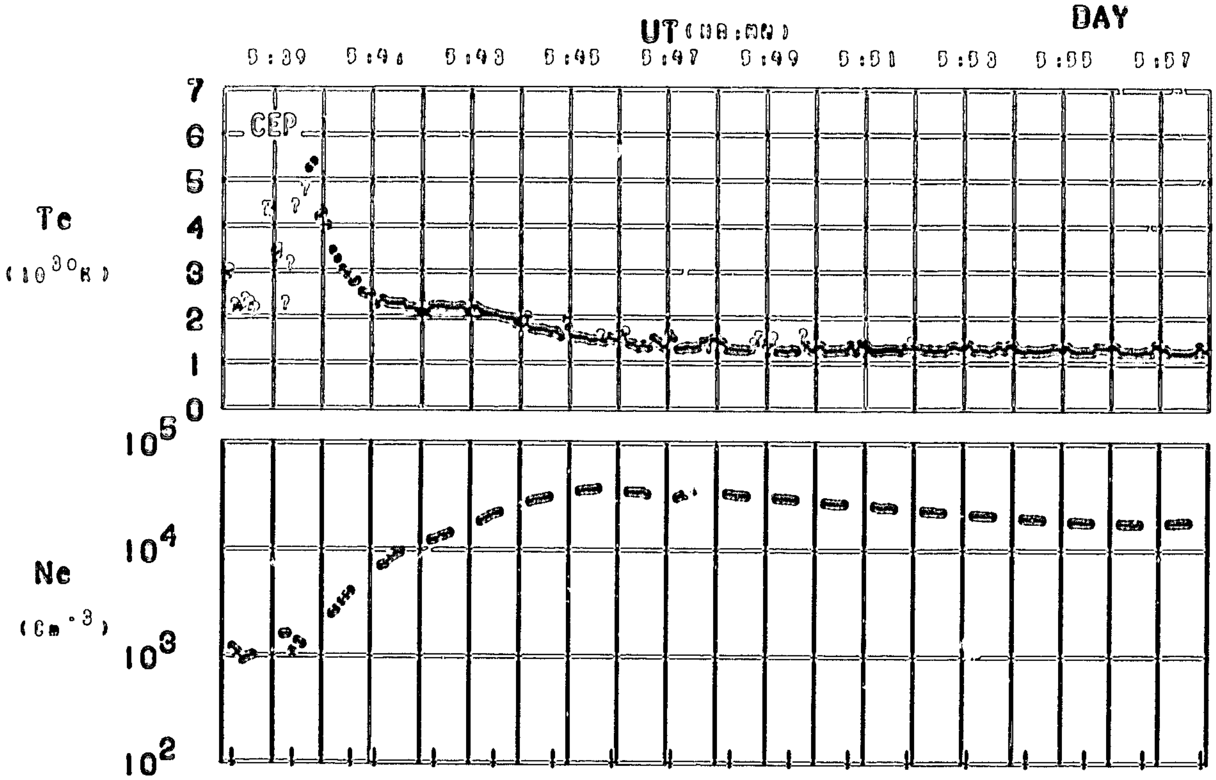

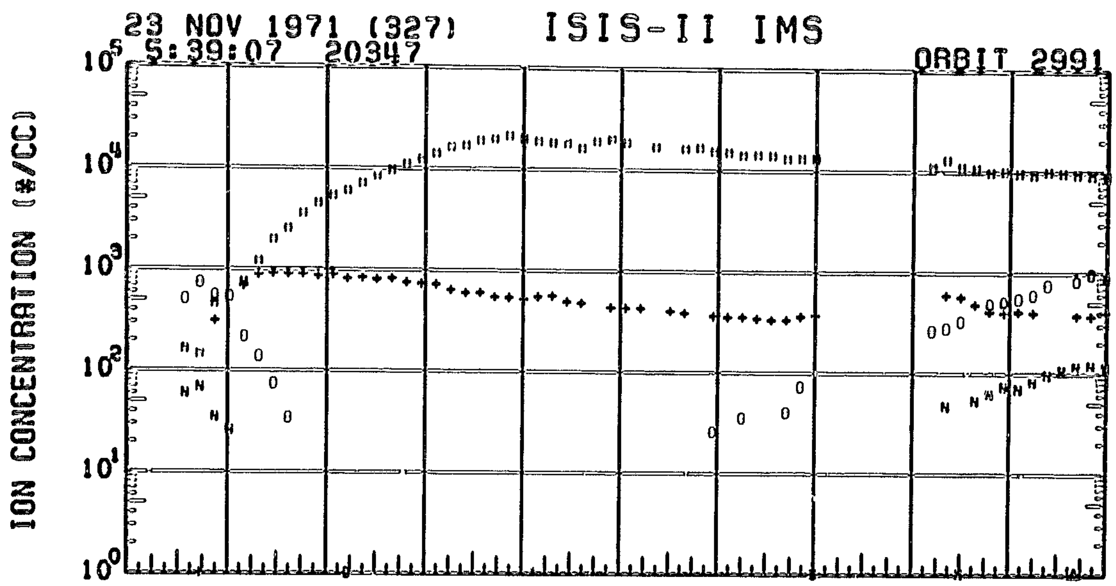

1 - H
4 - +
8 - △
14 - N
16 - O

UT	5:40	5:42	5:44	5:46	5:48	5:50	5:54	5:56
LAST	1:04	1:05	1:06	1:07	1:08	1:09	1:10	1:11
MLT	0:53	0:55	0:57	0:58	0:60	1:01	1:04	1:06
DLAT	54	47	40	34	27	21	8	3
INVL	57	52	47	42	38	34	29	27
GLAT	40	34	28	22	16	9	-3	-9
GLNG	-72	-72	-72	-72	-72	-73	-73	-74
SZEN	156	160	163	164	163	160	150	145
ALT	1422	1418	1415	1411	1407	1404	1398	1395

SET 13, FORMAT 4

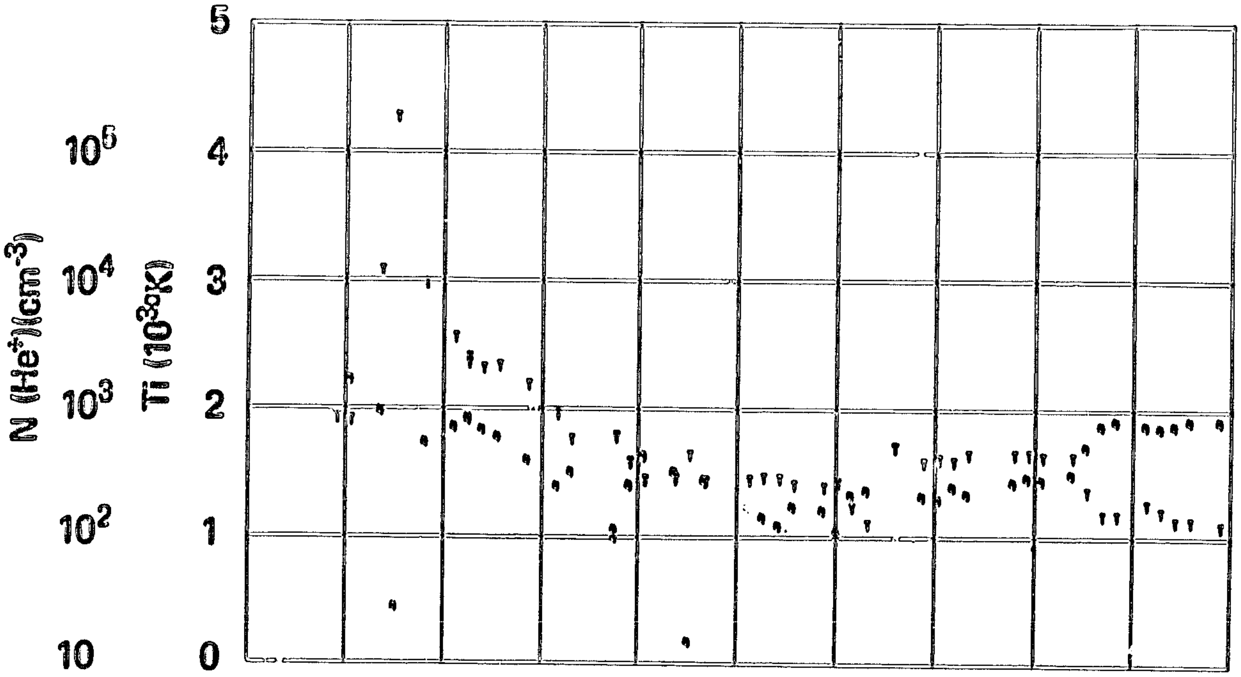

UT	0:40	0:42	0:44	0:40	0:48	0:50	0:54	0:56
LAST	1:04	1:00	1:00	1:07	1:08	1:09	1:10	1:11
MLT	0:53	0:55	0:57	0:58	0:60	1:01	1:04	1:06
DLAT	54	47	40	34	27	21	8	3
INVL	57	52	47	42	38	34	20	27
GLAT	40	34	28	22	15	9	-3	-9
GLNG	-72	-72	-72	-72	-72	-73	-73	-74
SZEN	100	100	103	104	103	100	100	140
ALT	1422	1418	1415	1411	1407	1404	1398	1393

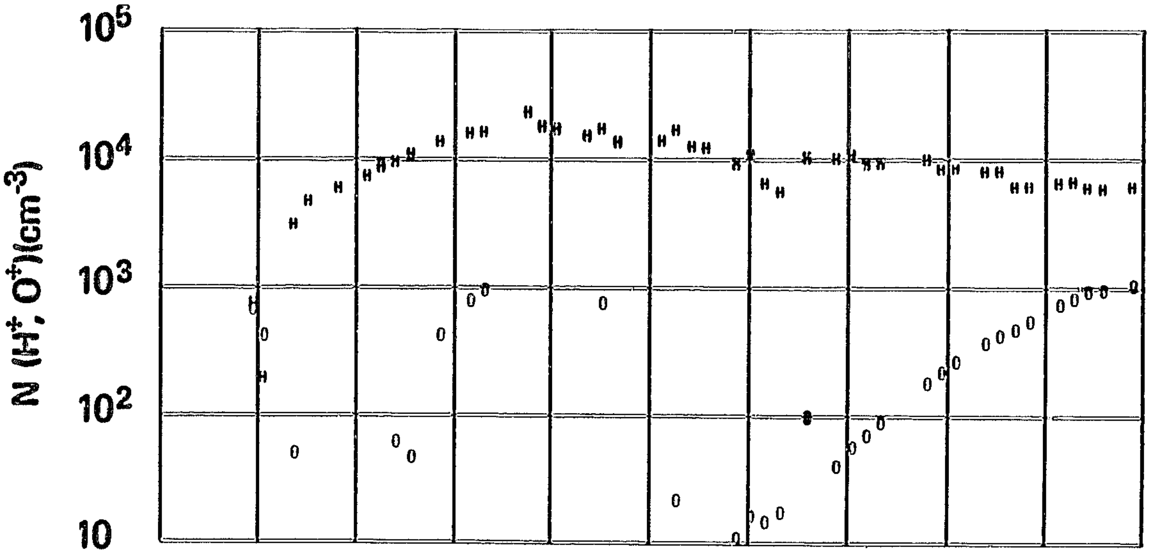

SET 13, FORMAT 5

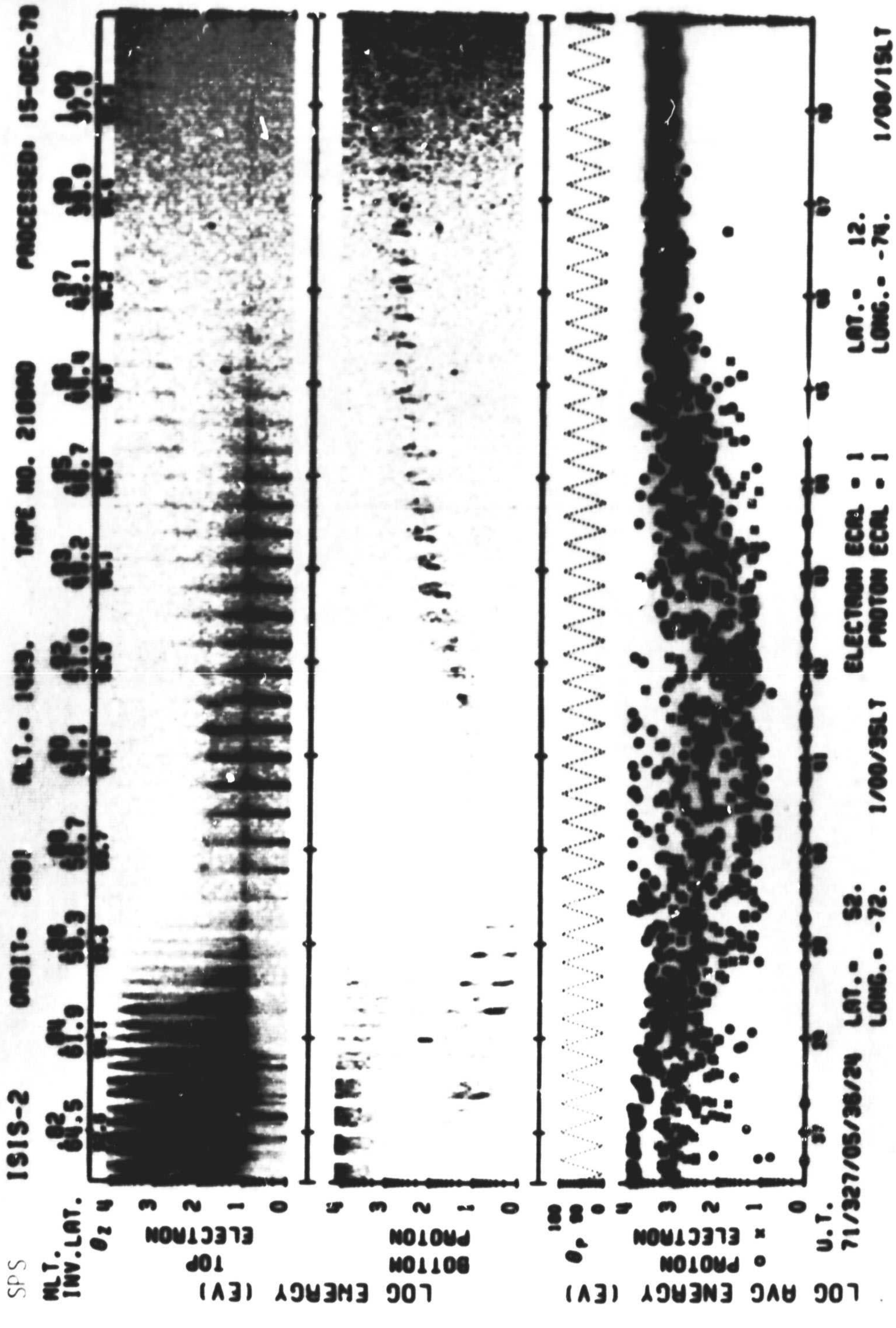

SET 13, FORMAT 6

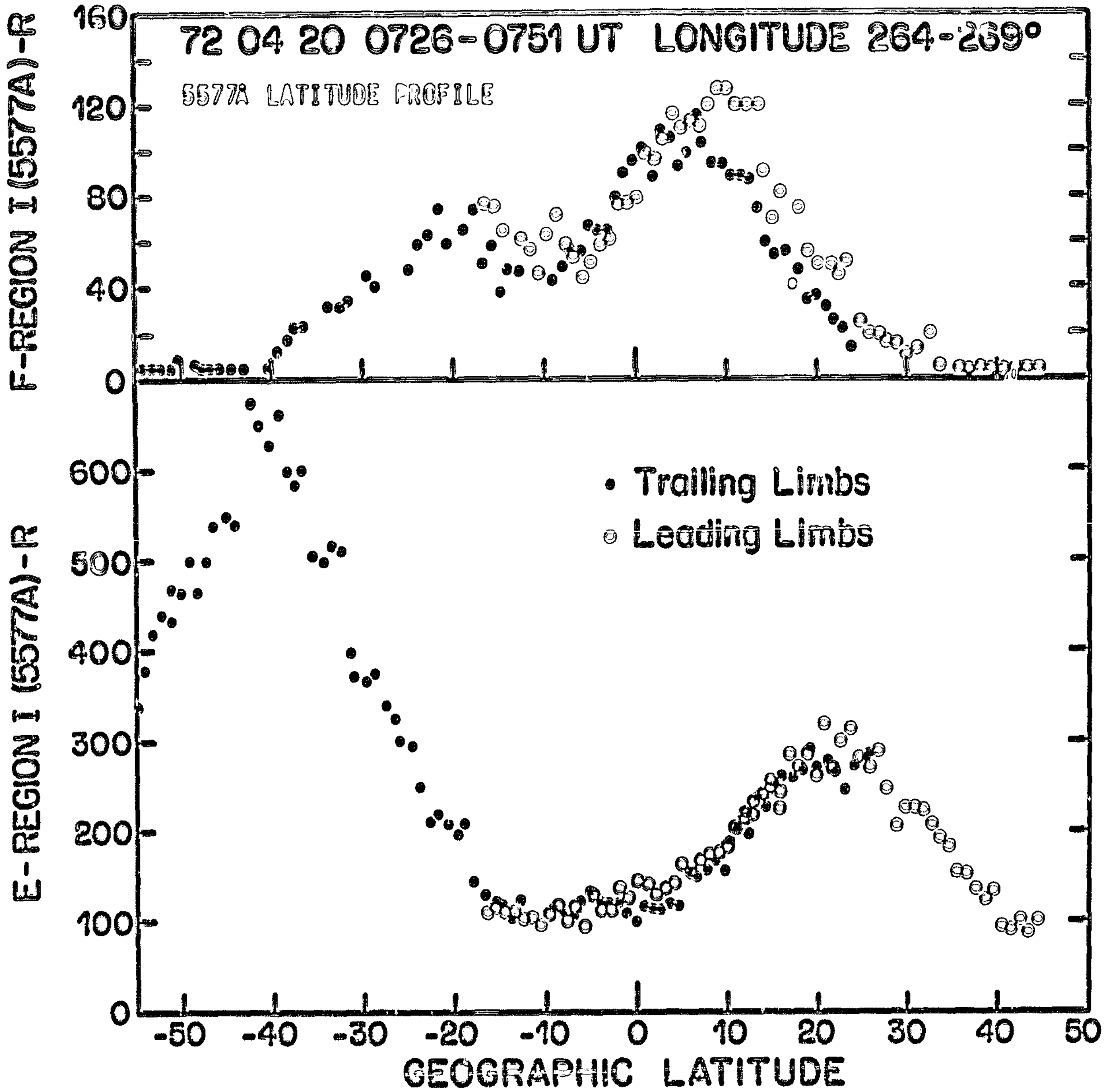

SET 14, FORMAT 9

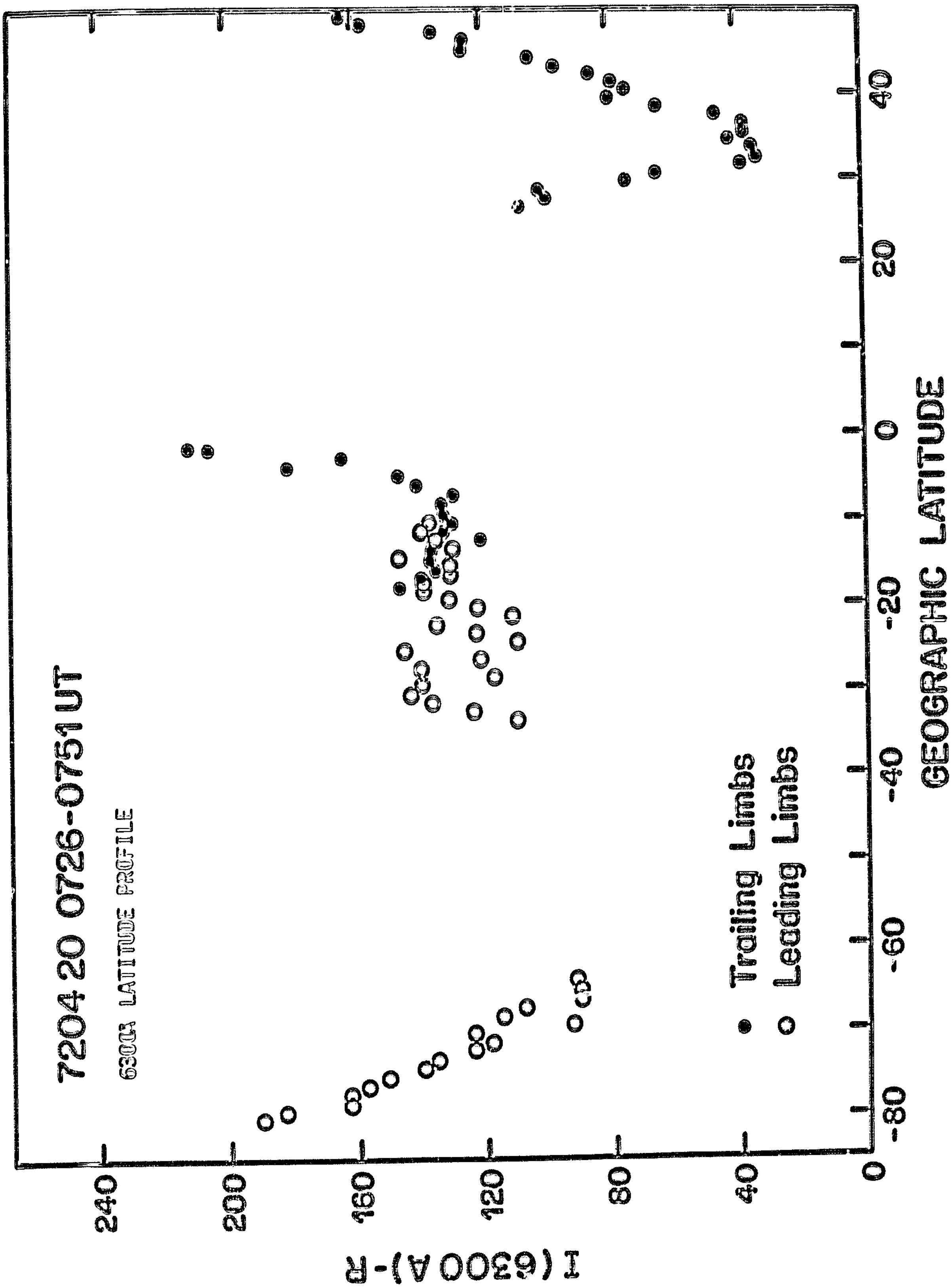

SET 14, FORMAT 9

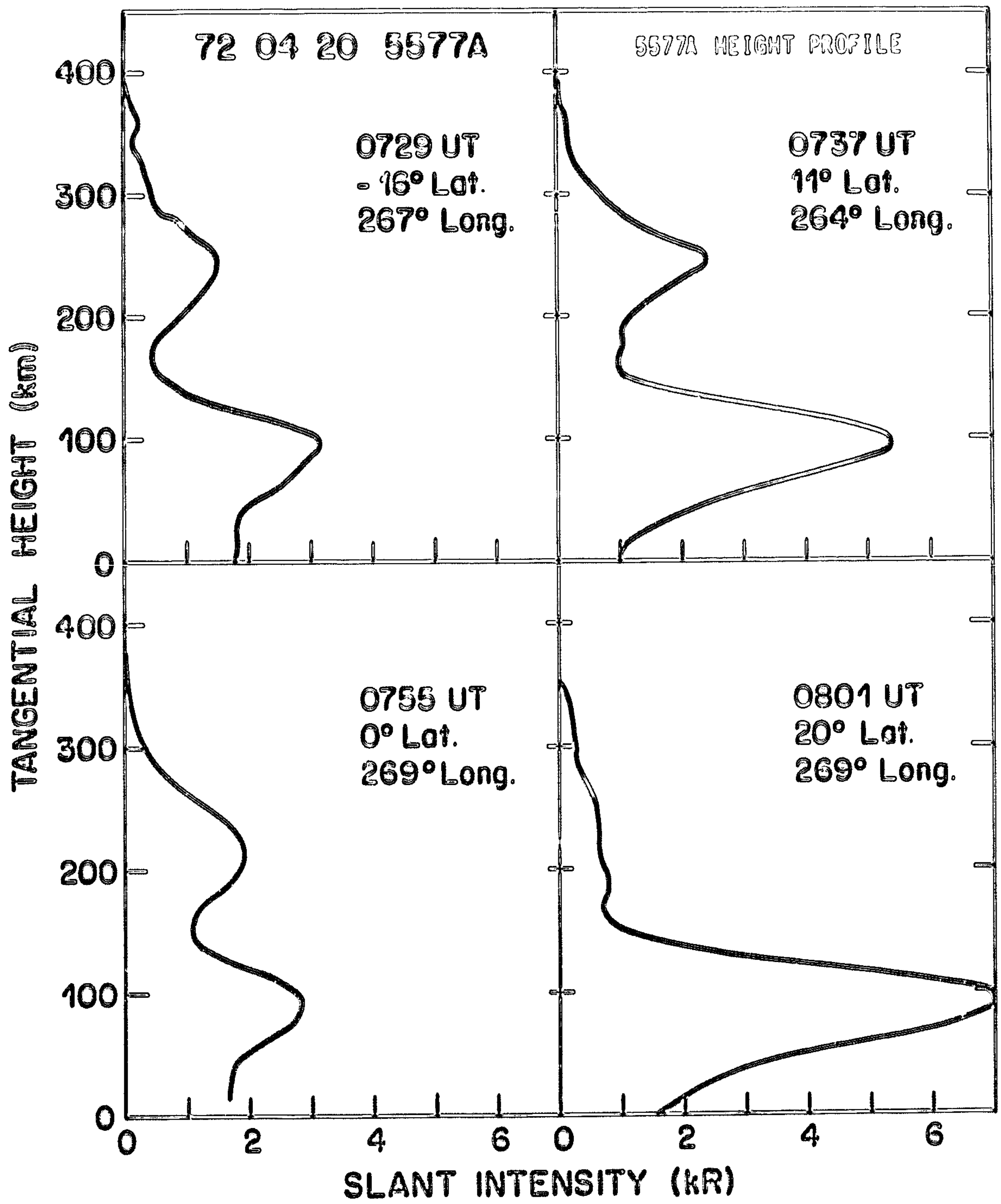

SET 14, FORMAT 12

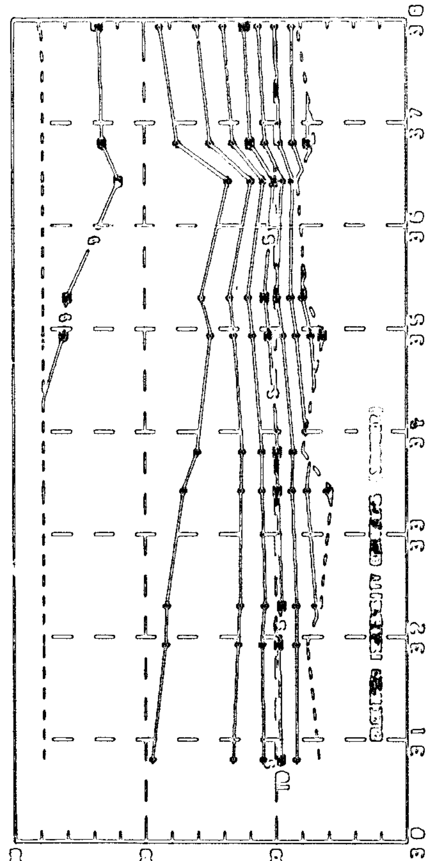

SET 14, FORMAT 2

ORBIT 4870
DATE 720420
DAY 111

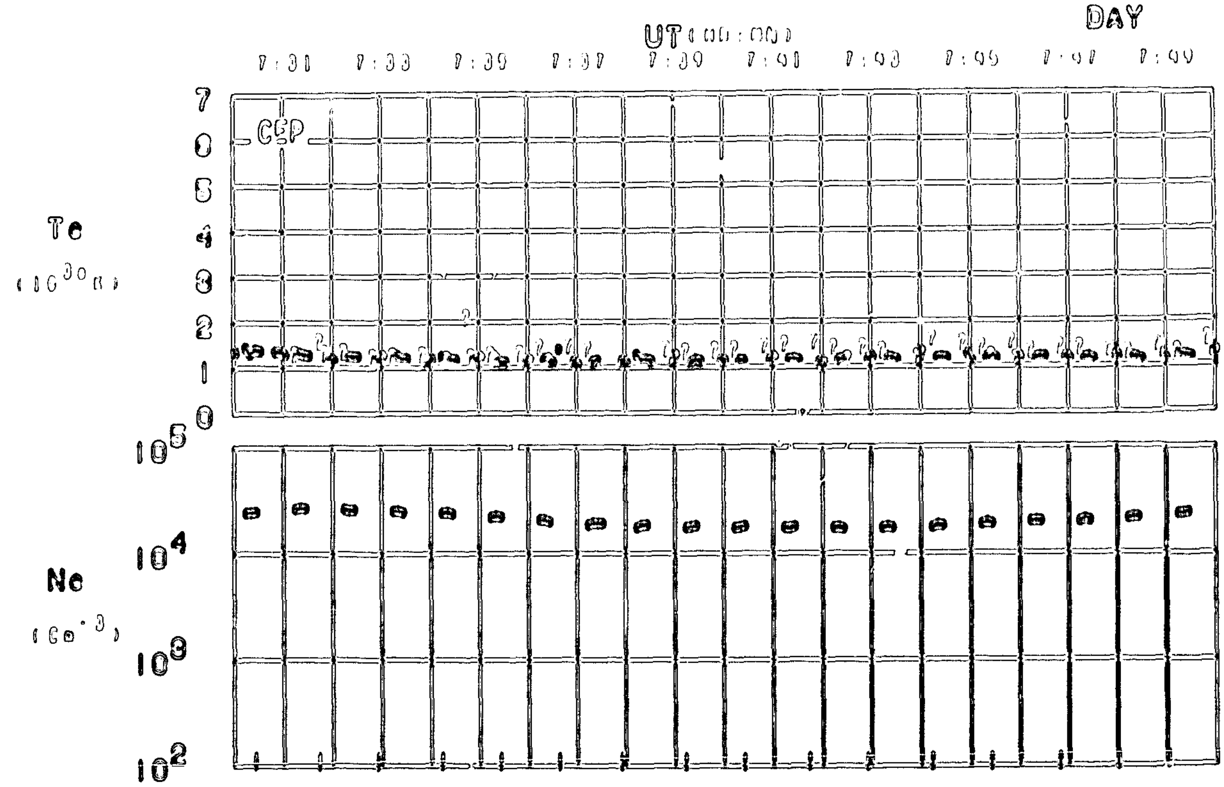

LAT	-49	-40	-35	-32	-30	-24	-20	-16	-12	-8	-4	0	3	7	11	14
LONG	-91	-91	-91	-91	-91	-91	-91	-92	-92	-92	-92	-92	-93	-93	-93	-93
LT	1:25	1:27	1:28	1:29	1:29	1:29	1:31	1:31	1:32	1:32	1:33	1:33	1:34	1:35	1:35	1:35
DIP	-43	-40	-41	-35	-31	-25	-10	-11	-4	3	10	10	20	27	33	42
DIPLAT	-25	-27	-24	-20	-17	-13	-9	-6	-2	1	5	9	13	17	21	24
L	1.7	1.6	1.5	1.4	1.4	1.3	1.3	1.3	1.2	1.2	1.2	1.3	1.3	1.4	1.4	1.6
INVLAT	40	37	35	32	31	29	27	25	25	25	25	27	25	25	33	35
ZA	142	145	143	150	153	154	155	157	157	155	155	154	152	149	145	144

SET 14, FORMAT 4

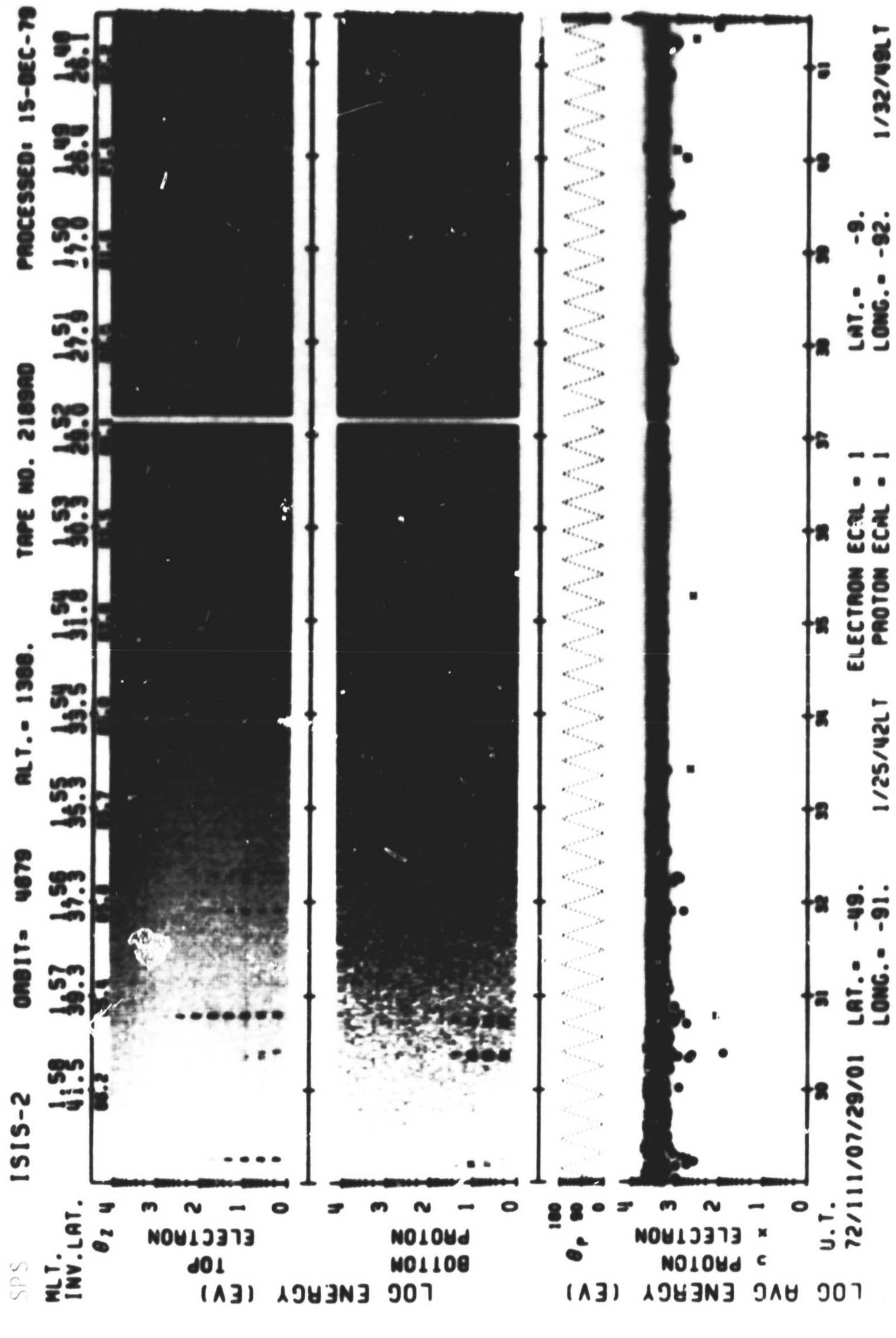

SET 14, FORMAT 6

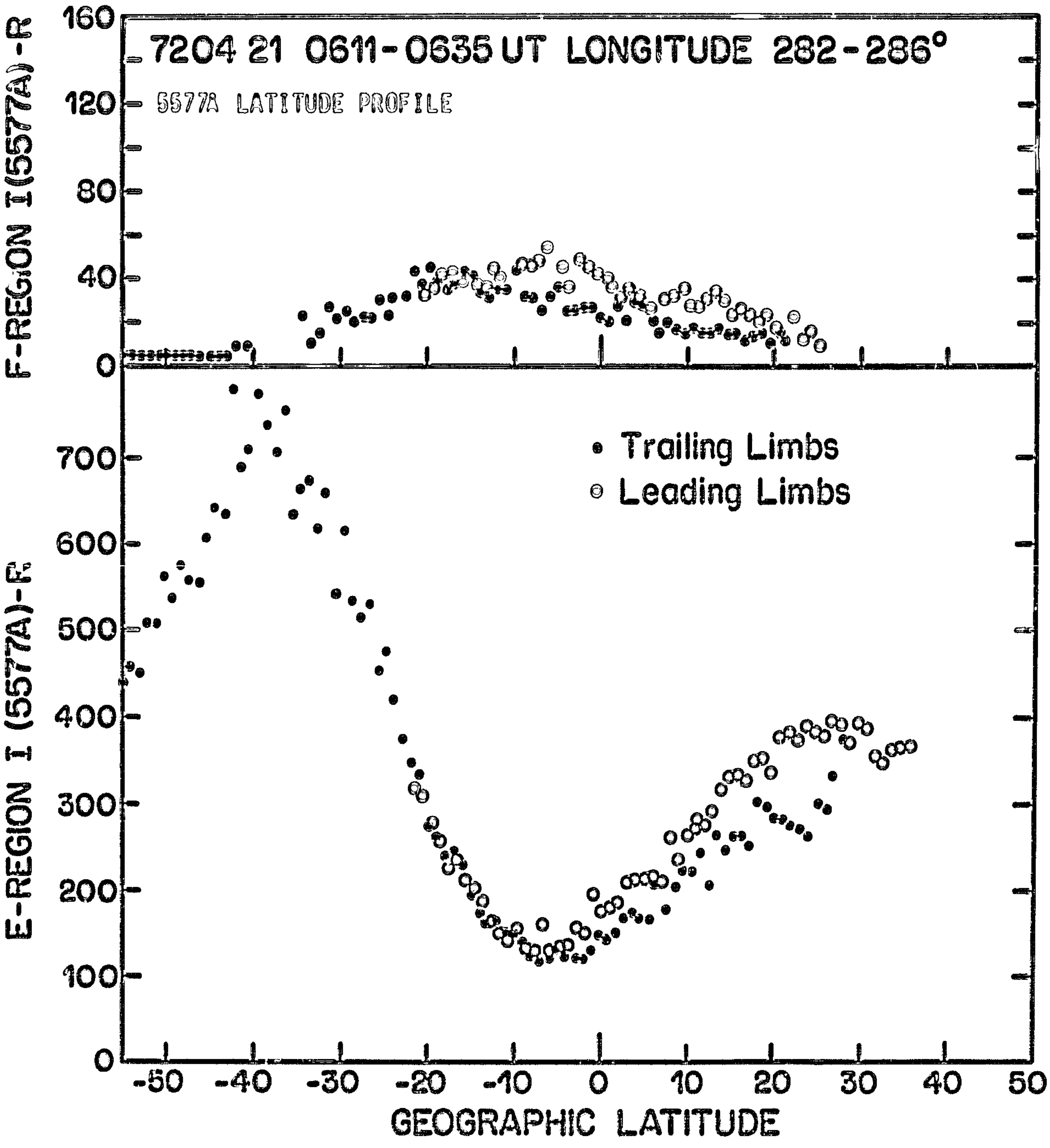

SET 15, FORMAT 9

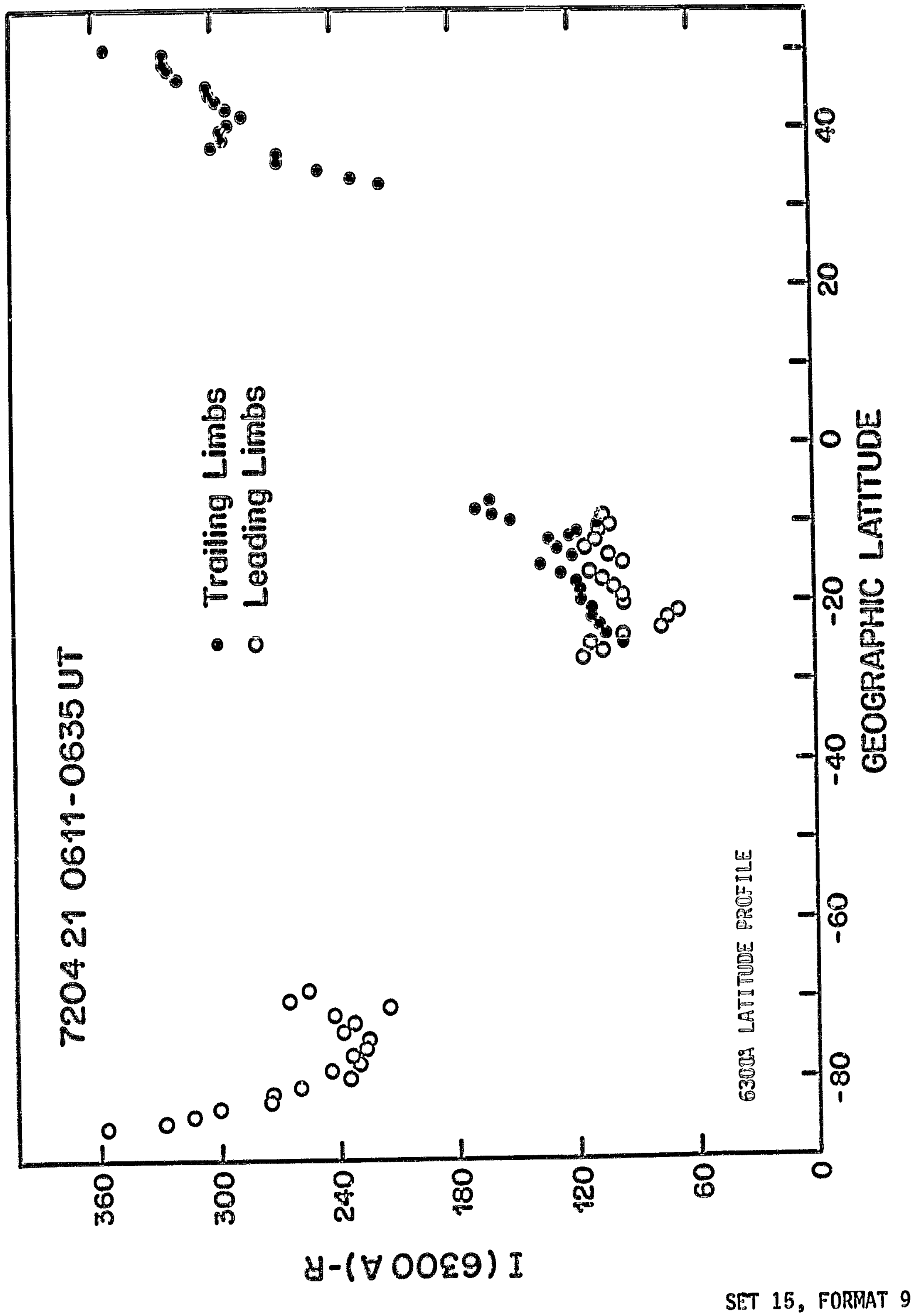

SET 15, FORMAT 9

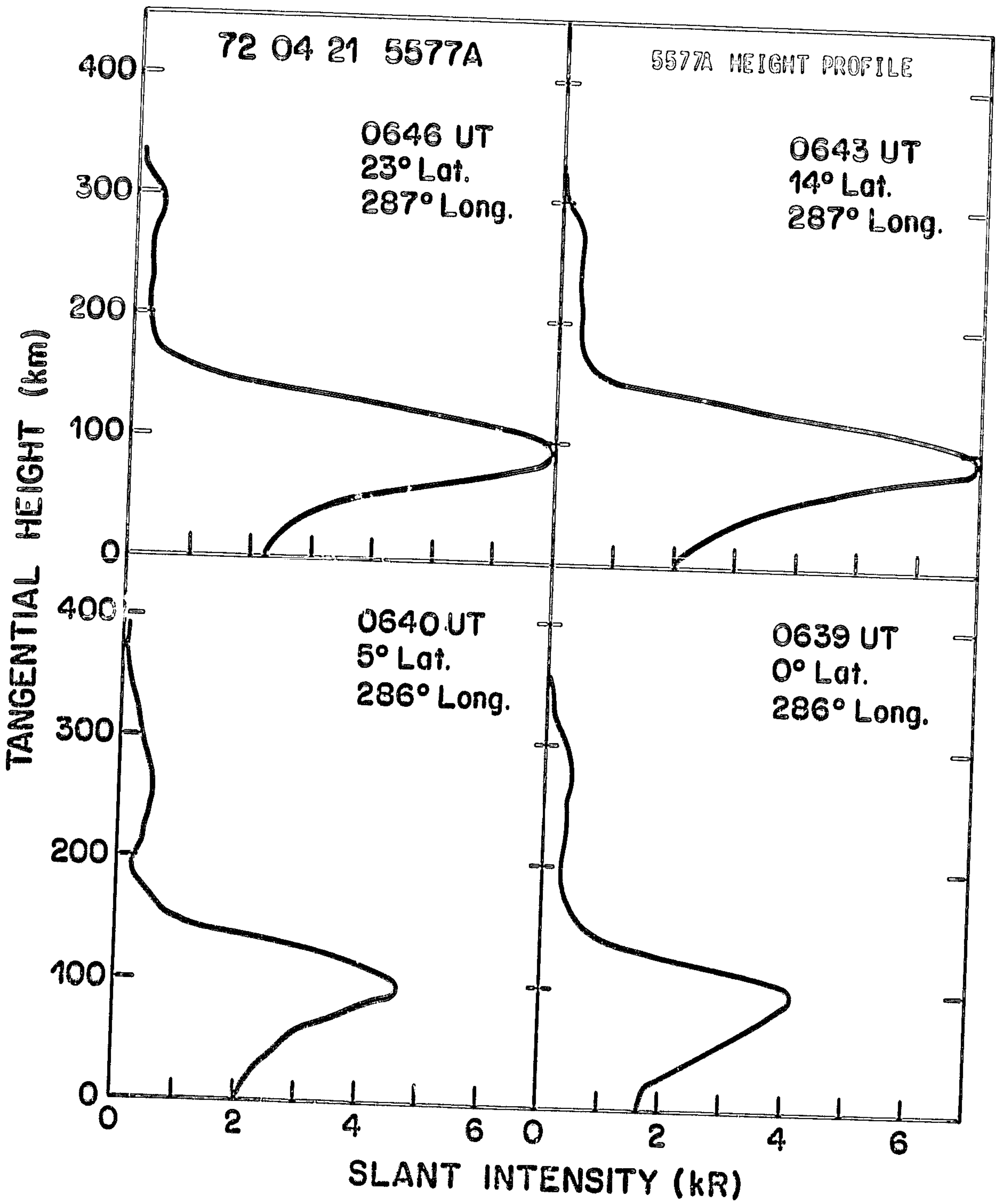

SET 15, FORMAT 12

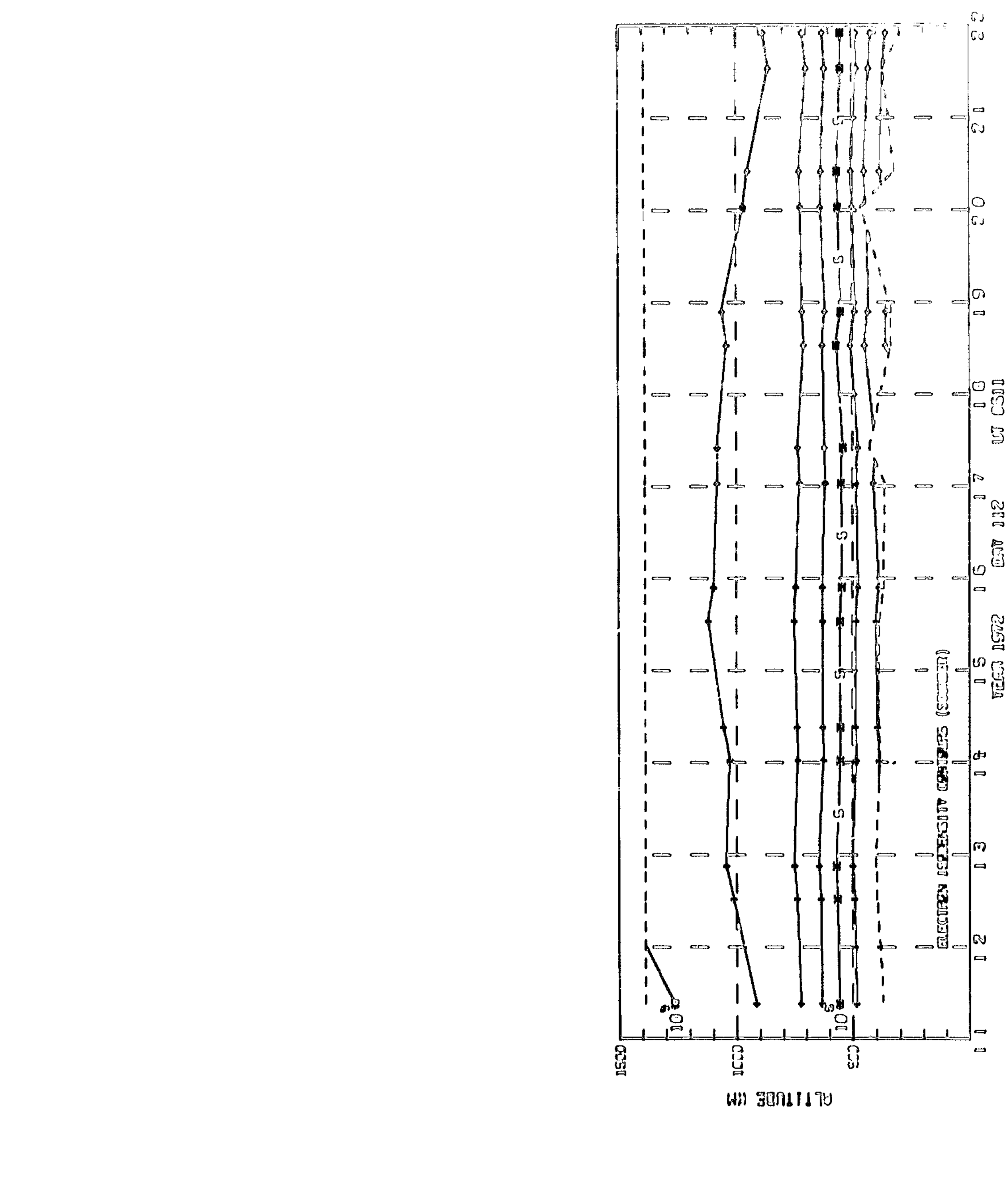

SET 15, FORMAT 2

ORBIT 4891
DATE 720421
DAY 112

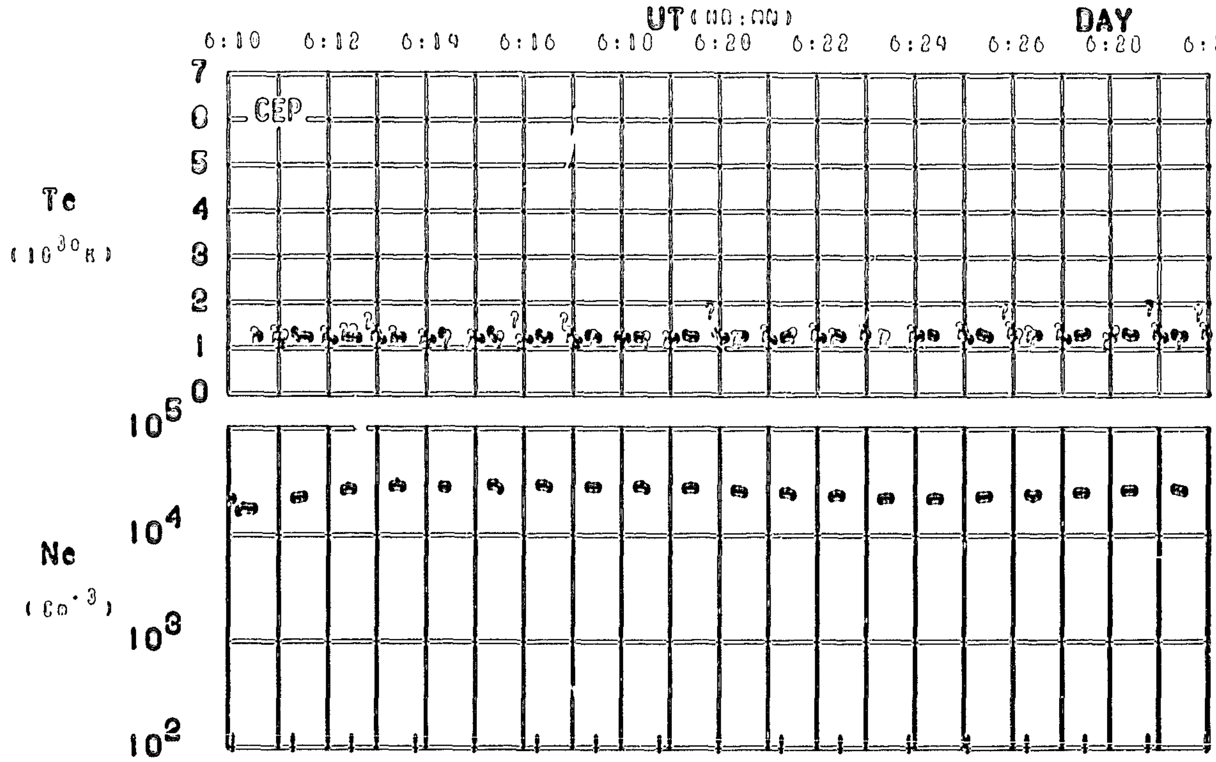

LAT	-53	-54	-50	-46	-42	-38	-34	-30	-26	-22	-19	-14	-10	-6	-3	1	4
LONG	-73	-73	-73	-73	-73	-73	-73	-73	-73	-73	-74	-74	-74	-74	-74	-75	-75
LT	1:18	1:19	1:20	1:22	1:23	1:24	1:24	1:25	1:26	1:26	1:27	1:27	1:28	1:28	1:29	1:30	1:30
DIP	-57	-55	-51	-48	-44	-40	-36	-30	-24	-18	-11	-3	4	10	18	26	31
DIPLAT	-38	-35	-32	-29	-26	-22	-19	-16	-12	-9	-6	-1	2	5	9	13	16
L	2.4	2.1	1.9	1.8	1.6	1.5	1.5	1.4	1.3	1.3	1.3	1.3	1.3	1.3	1.3	1.3	1.4
INVLAT	49	46	43	40	38	35	33	31	30	28	27	27	27	27	28	30	31
ZA	131	134	137	141	144	147	150	152	154	155	157	158	158	157	156	154	151

SET 15, FORMAT 4

RPA 720421

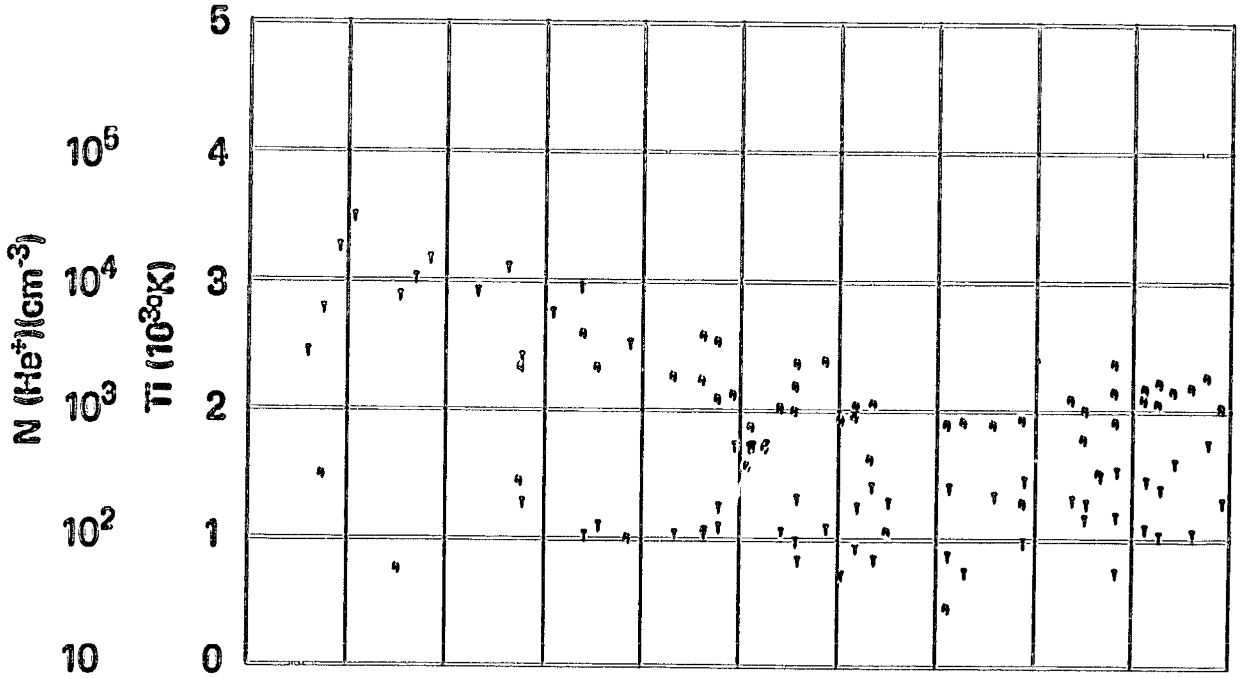

UT	00:12	00:14	00:16	00:18	00:20	00:22	00:24	00:26	00:28
LAST	01:20	01:22	01:24	01:25	01:26	01:27	01:28	01:29	01:30
MLT									
DLAT									
INVL	45	40	36	33	30	28	27	27	20
GLAT	-52	-46	-40	-33	-27	-21	-14	-8	-2
GLNG	-73	-73	-73	-74	-74	-74	-74	-75	-75
SZEN	136	141	146	151	154	157	163	157	155
ALT	1388	1388	1389	1389	1390	1391	1393	1395	1397

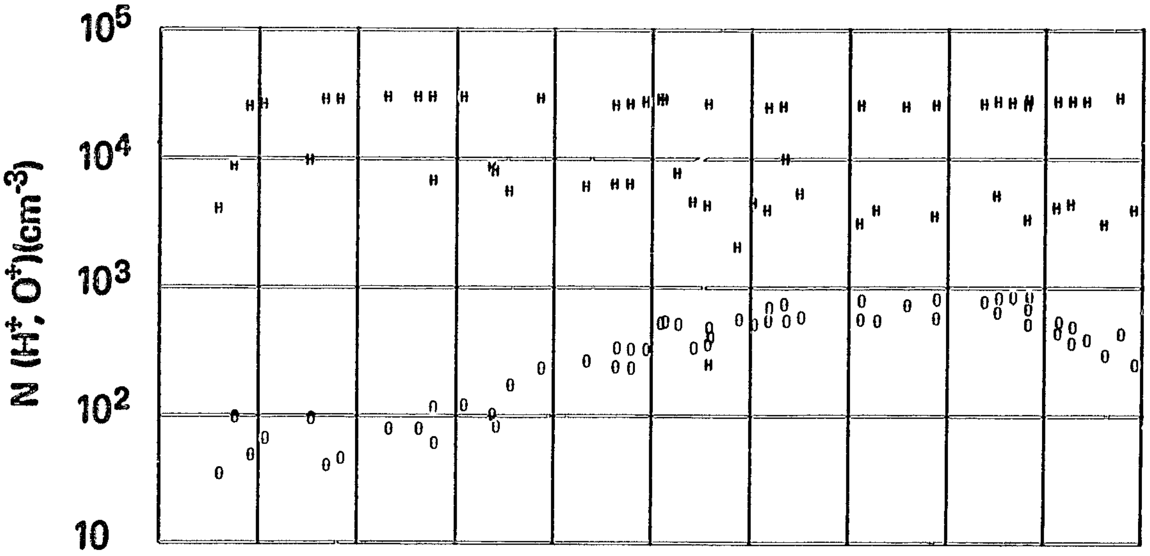

SET 15, FORMAT 5

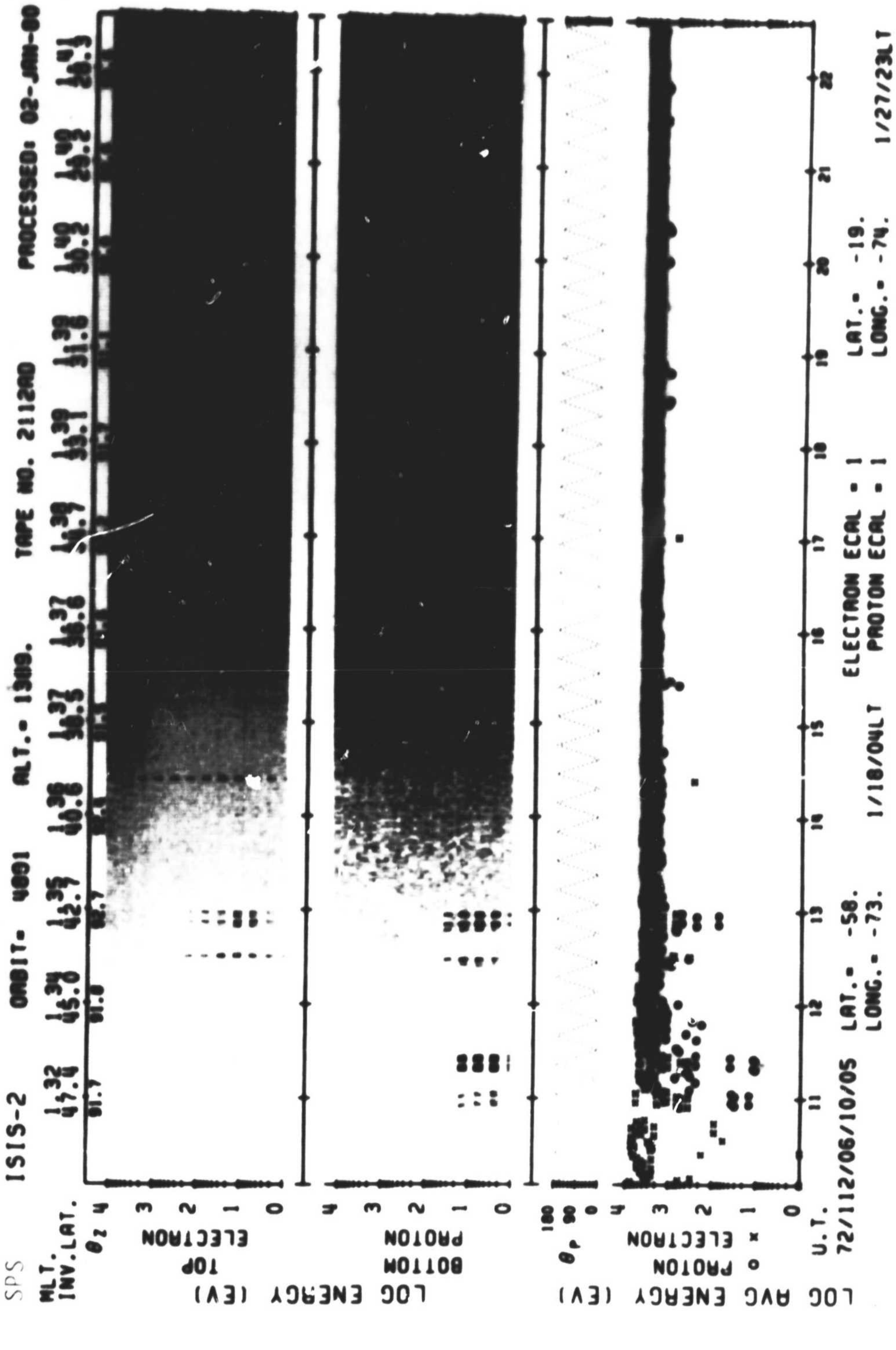

SET 15, FORMAT 6

VI-C. GEOPHYSICAL DATA SET: VLF OBSERVATIONS

DATA SET DESCRIPTION

The VLF film has been selected from a rather limited set of processed VLF data to show some of the variety of phenomena typically recorded. Most of the ISIS 2 VLF data films correspond to mid- and high-latitude passes (i.e., most are Ottawa or Resolute Bay passes). The data set pass list (Table 3) contains the times of the selected data, as well as some descriptive information. The passes are ordered within the list as follows: equatorial (no. 16); midlatitude (17); midlatitude auroral (18-21); and auroral-polar (22-24). In the "Phenomena" column, the panel in which a given phenomenon occurs is identified by a number after the phenomenon name (the numbers are shown at the top of each panel). The spacecraft was either in the cartwheel (CW) or the orbit-aligned (OA) mode, as indicated in the column labeled "Spacecraft Mode." In either case, data from instruments operational in that mode are presented. The standard formats presented, and instruments used, for data obtained during operation in cartwheel orientation are:

1. Very Low Frequency Receiver, Format 11
2. Topside Sounder, Format 2

   Magnetometer, Format 2
3. Energetic Particle Detector, Format 3
4. Cylindrical Electrostatic Probe, Format 4

   Ion Mass Spectrometer, Format 4
5. Retarding Potential Analyzer, Format 5
6. Soft Particle Spectrometer, Format 6

The standard formats presented, and instruments used, for data obtained during orbit-aligned orientation are:

1. Very Low Frequency Receiver, Format 11
2. Energetic Particle Detector, Format 3
3. Soft Particle Spectrometer, Format 6
4. Auroral Scanning Photometer, Format 7
5. Red Line Photometer, Format 8
6. Cylindrical Electrostatic Probe, Format 10

   Topside Sounder, Format 10

Table 3 Data Set Pass List

Date	UT	K_p	MLT	Phenomena	Page	Data Set	Spacecraft Mode
710515	0905	3	0330	sferics (1-4) whistlers (3,4)	117	16	CW
730704	0833	1+	0330	sferics (1-4) LHR noise (1-3) (nose) whistlers (3-4)	121	17	CW
710702	0329	3	0030	sferics (1-3) whistlers (1) LHR noise (1-2) risers (2-3) VLF hiss (4)	127	18	OA
730618	0951	4+	0500	VLF hiss (1) chorus (2-3) sferics, whistlers (4)	132	19	CW
711127	0414	2+	0040	VLF hiss (1,2) saucers (2) LHR noise, risers (3) ELF hiss (3-4) sferics, whistlers (4)	138	20	CW
711224	0415	2+	2200	VLF hiss (1) sferics, whistlers (2)	144	21	OA
711224	0403	2+	1300- 2200	VLF hiss (1-4) saucers (4)	150	22	OA
720108	0551	1+	1100- 2200	(V-shaped) VLF hiss (1,2) saucers (3) nose whistlers (4)	157	23	OA
710814	0409	1	2000- 1000	(V-shaped) VLF hiss	164	24	OA

71/135/0905

Excerpts of VLF Spectral film for the period 0906 - 0917

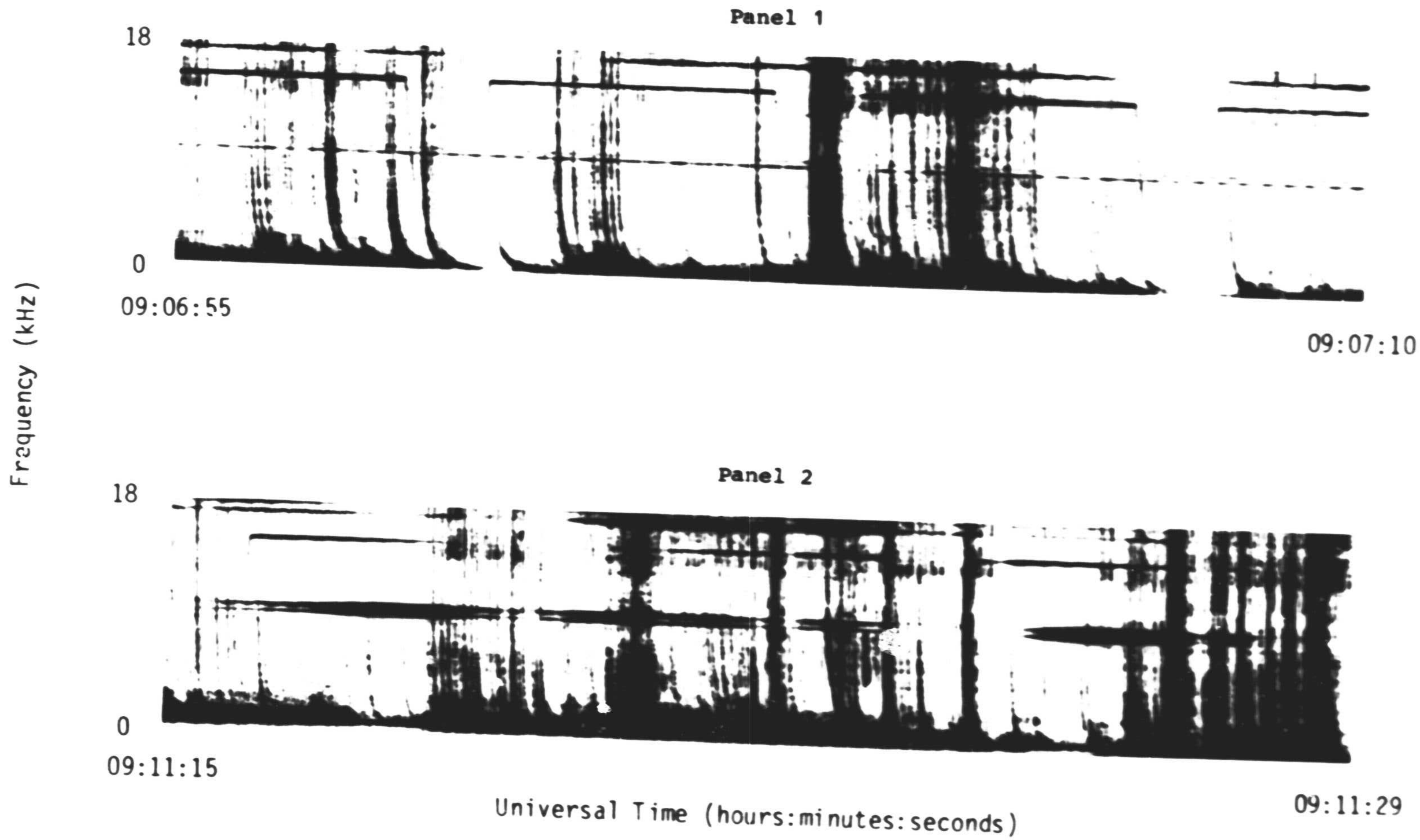

SET 16, FORMAT 11

71/135/0905

Excerpts of VLF Spectral film for the period 0906 - 0917

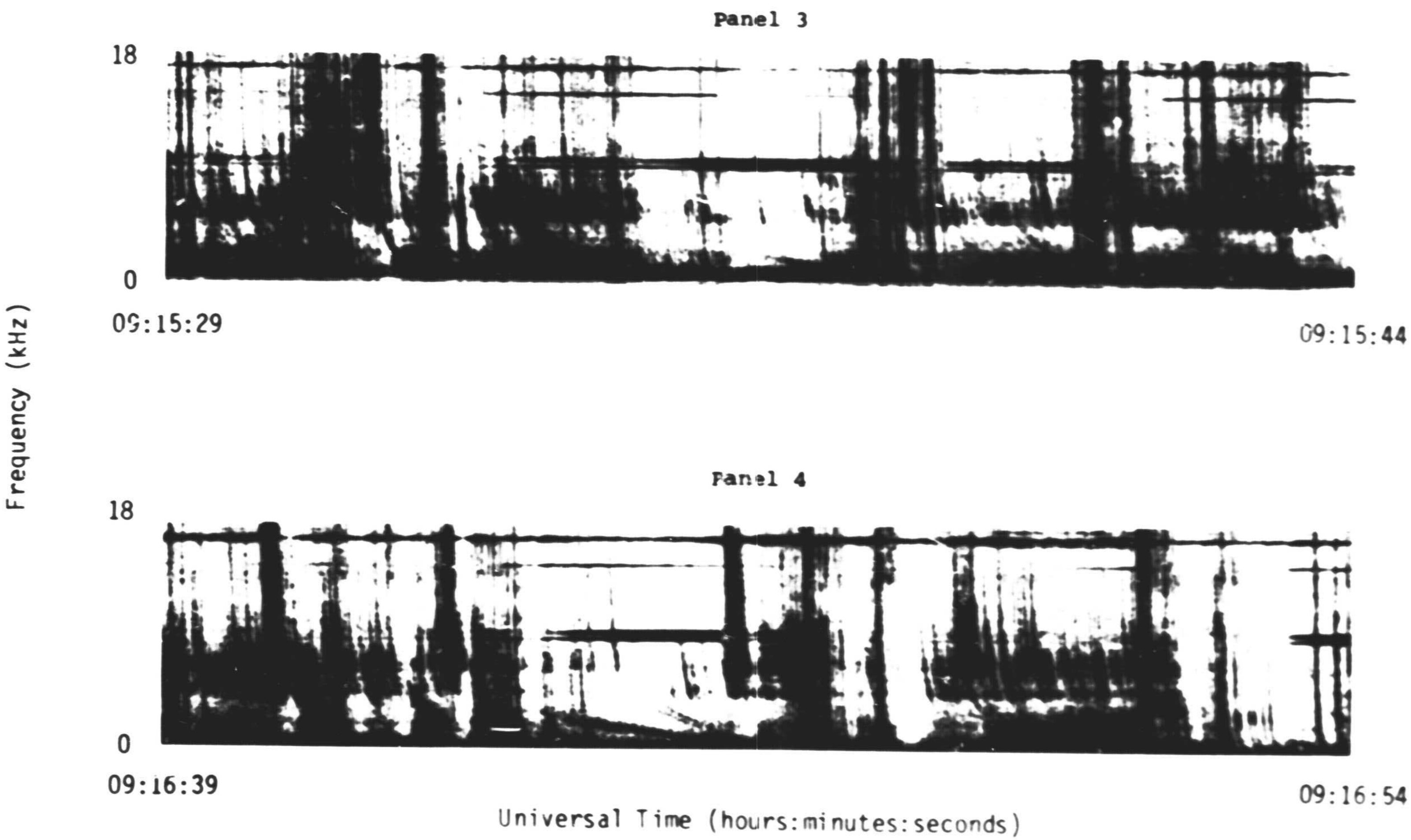

ORBIT 558
DATE 710515
DAY 135

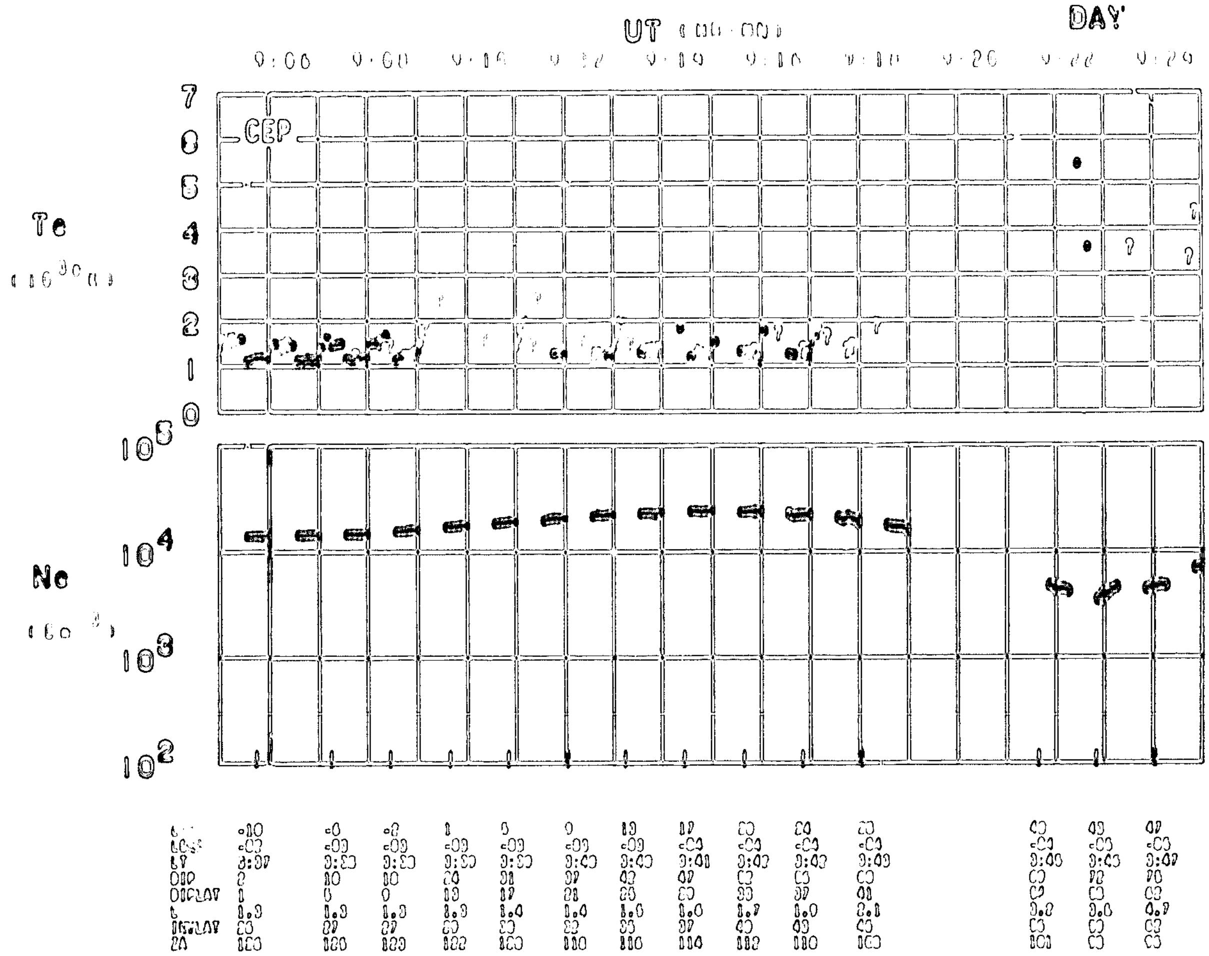

SET 16, FORMAT 4

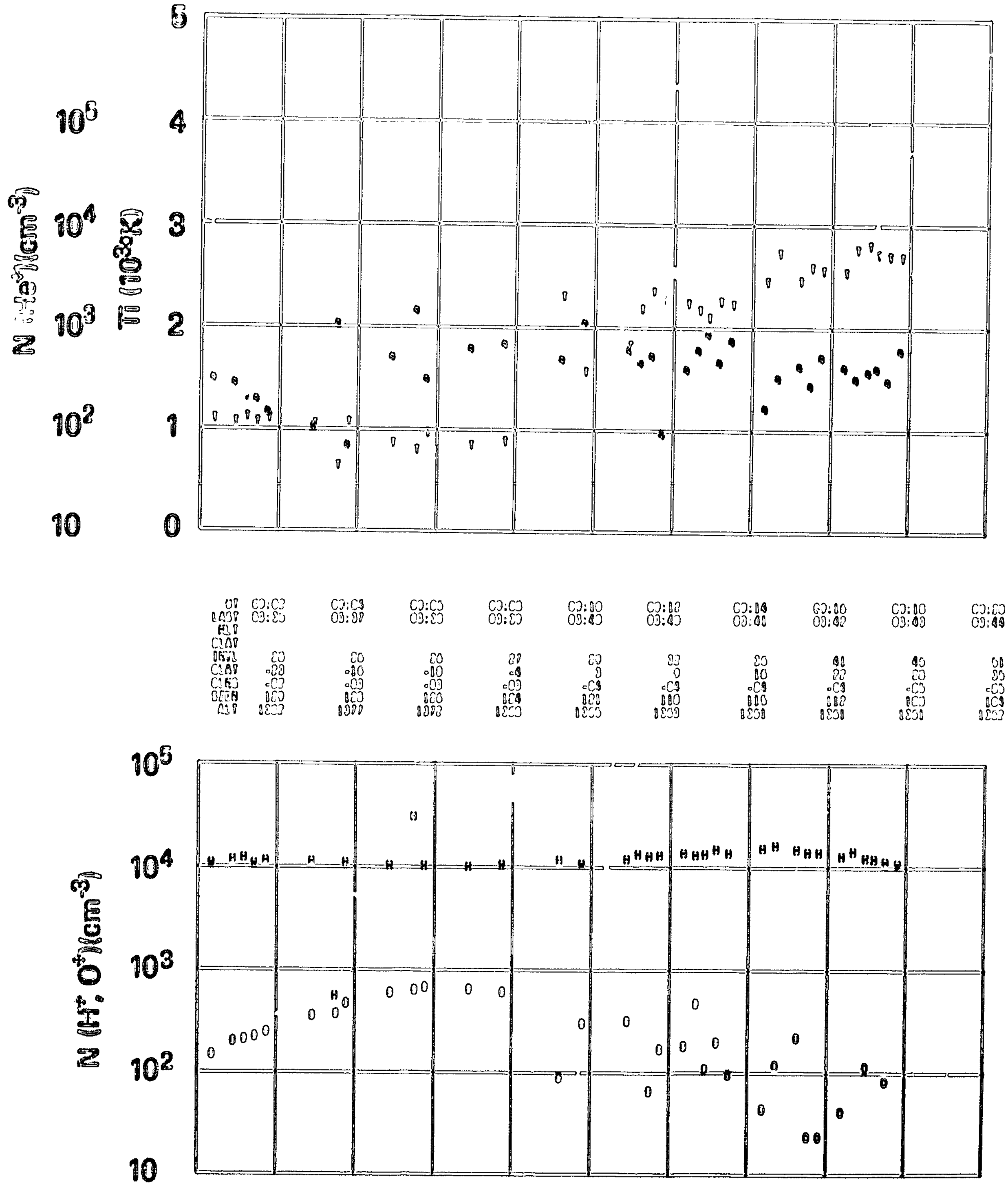

SET 16, FORMAT 5

73/185/0833

Excerpts of VLF Spectral film for the period 0838 - 0844

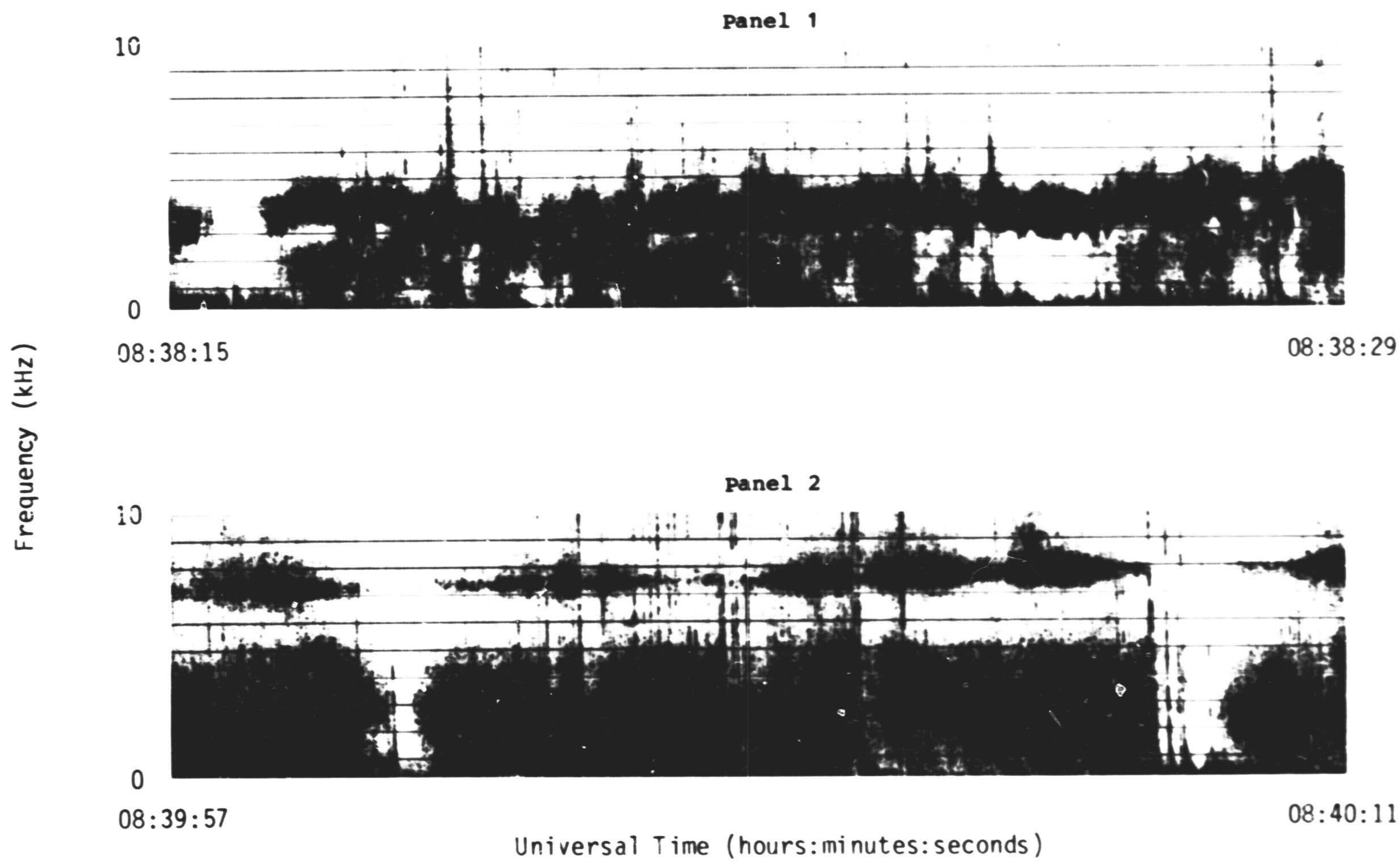

SET 17, FORMAT 11

73/185/0833

Excerpts of VLF Spectral film for the period 0838 - 0844

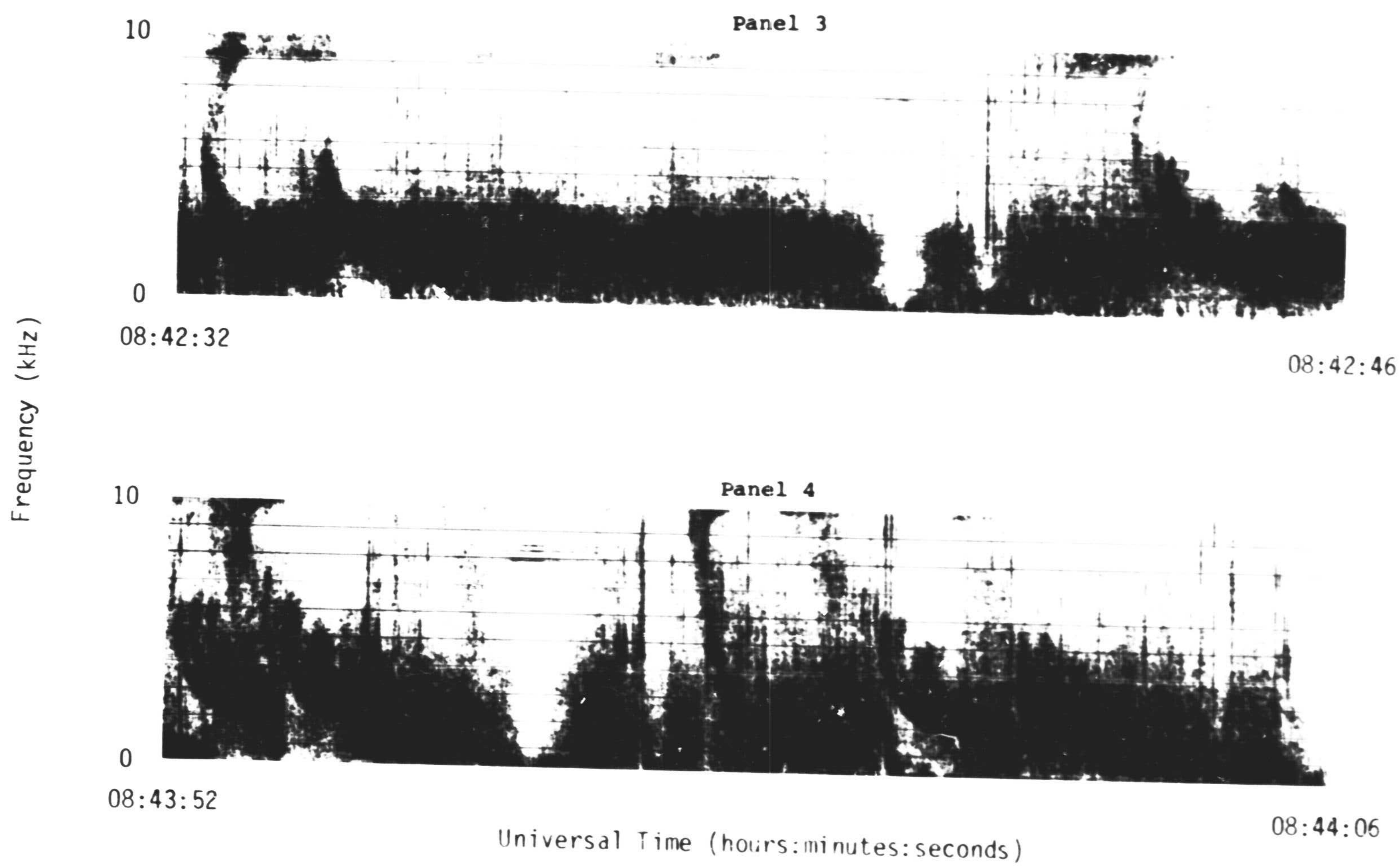

SET 17, FORMAT 11

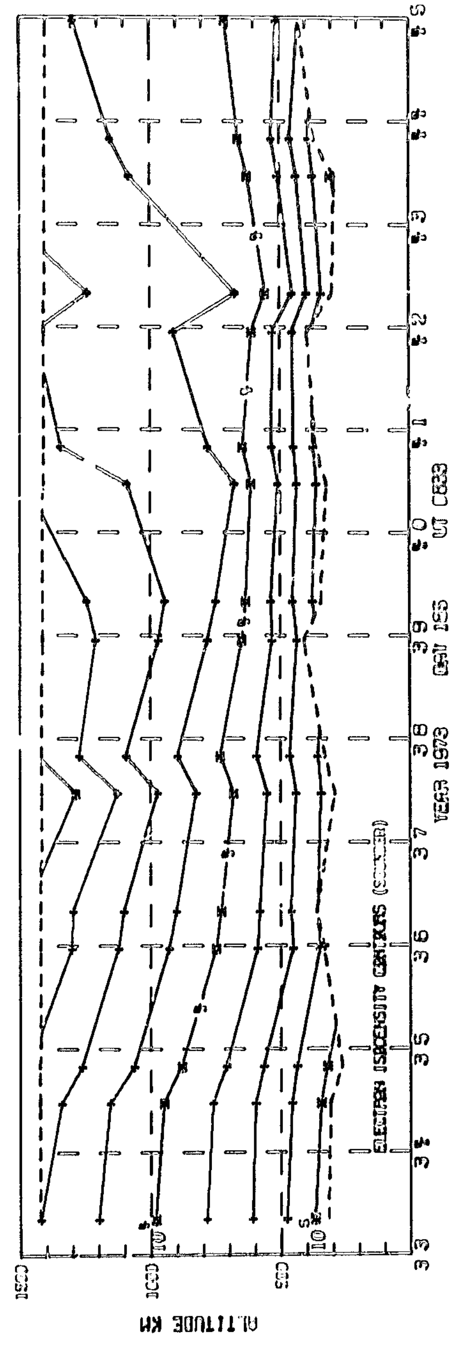

SET 17, FORMAT 2

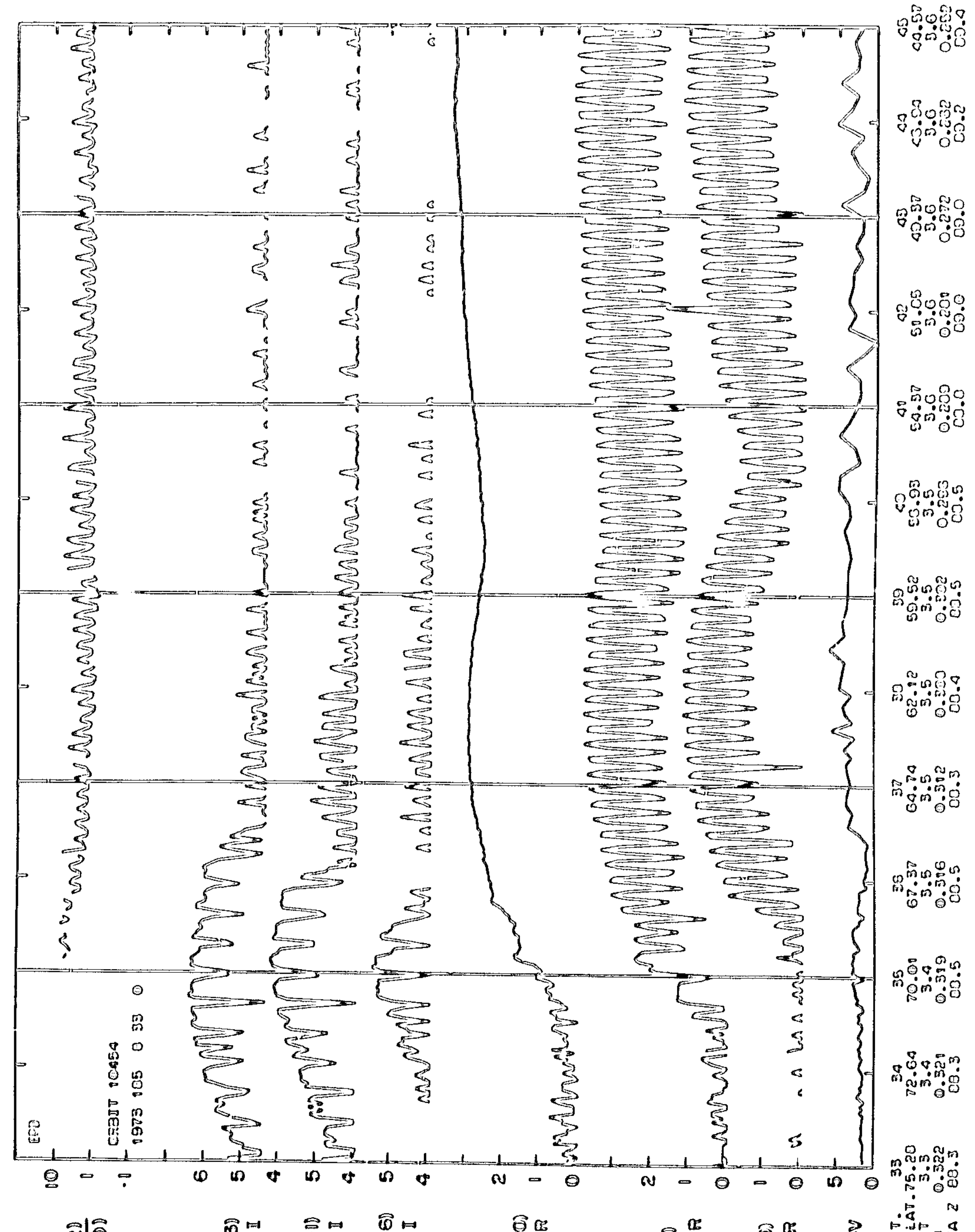

SET 17, FORMAT 3

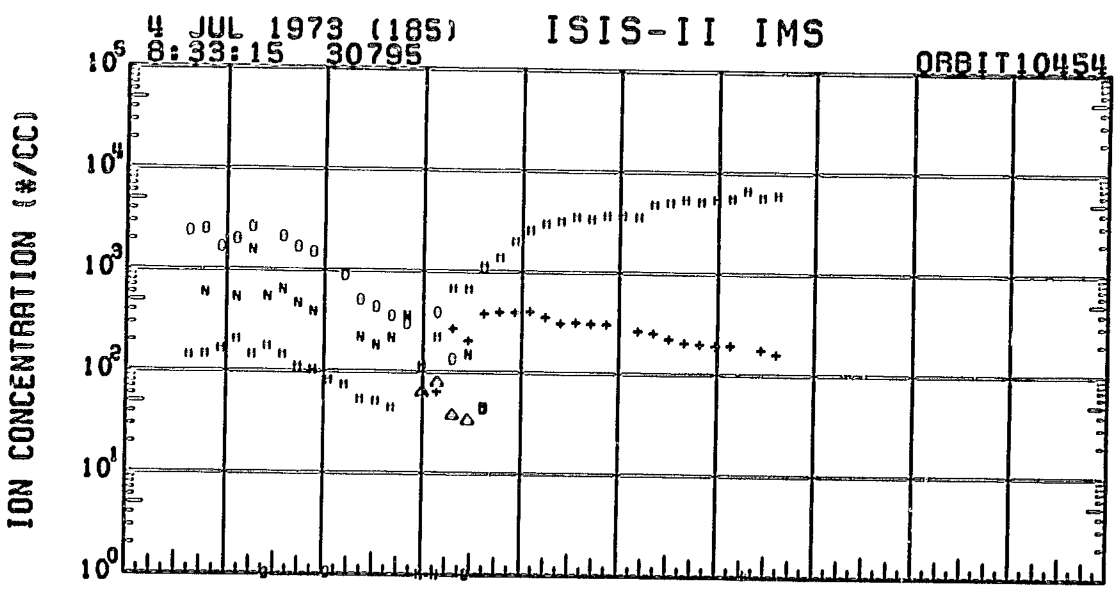

1 - H	UT	8:34	8:36	8:38	8:40	8:42	8:44
4 - +	LAST	3:42	3:45	3:47	3:48	3:49	3:51
8 - △	MLT	3:28	3:30	3:33	3:35	3:37	3:38
14 - N	DLAT	72	66	60	54	47	41
16 - O	INVL	73	67	62	57	52	47
	GLAT	60	54	47	41	35	28
	GLNG	-71	-71	-71	-71	-71	-71
	SZEN	86	90	93	97	101	105
	ALT	1425	1421	1417	1412	1407	1403

SET 17, FORMAT 4

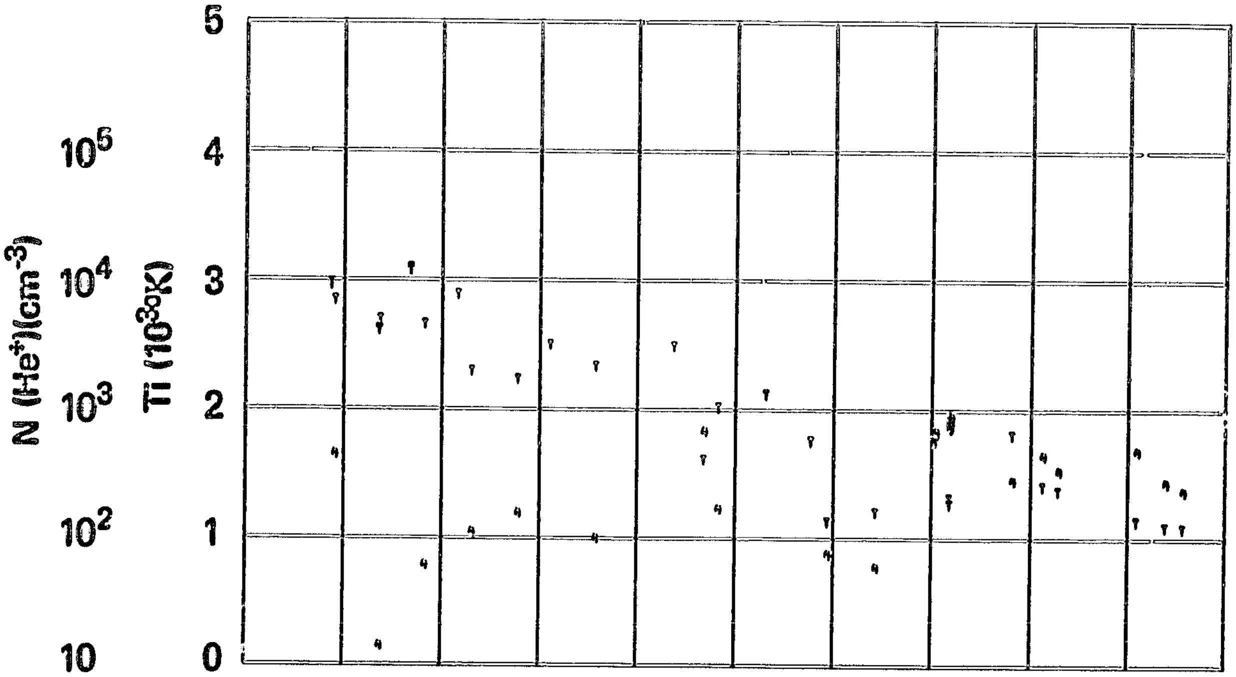

UT	0:26	0:28	0:30	0:32	0:34	0:36	0:38	0:40	0:42	0:44
LAST	2:28	3:17	3:33		3:42	3:45	3:47	3:48	3:49	3:51
MLT					3:26	3:30	3:33	3:35	3:37	3:39
DLAT					72	66	69	64	47	41
INVL	84	84	83		73	67	62	67	62	47
GLAT	86	80	74		60	54	47	41	33	28
GLNG	-80	-77	-74		-71	-71	-71	-71	-71	-71
SZEN					86	90	93	97	101	105
ALT					1426	1421	1417	1412	1407	1403

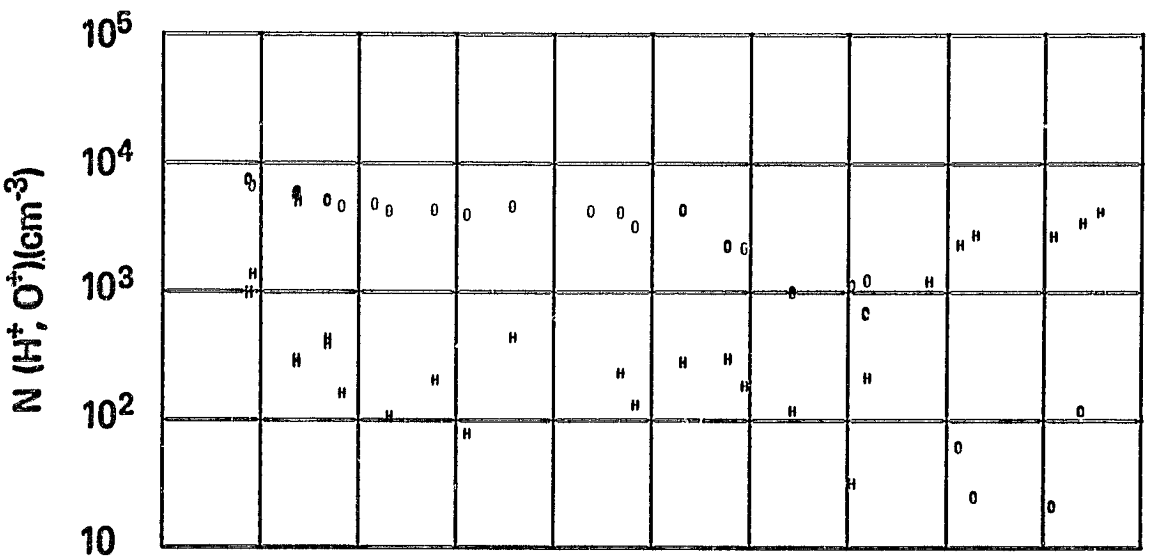

SET 17, FORMAT 5

71/183/0329

Excerpts of VLF Spectral film for the period 0333 - 0343

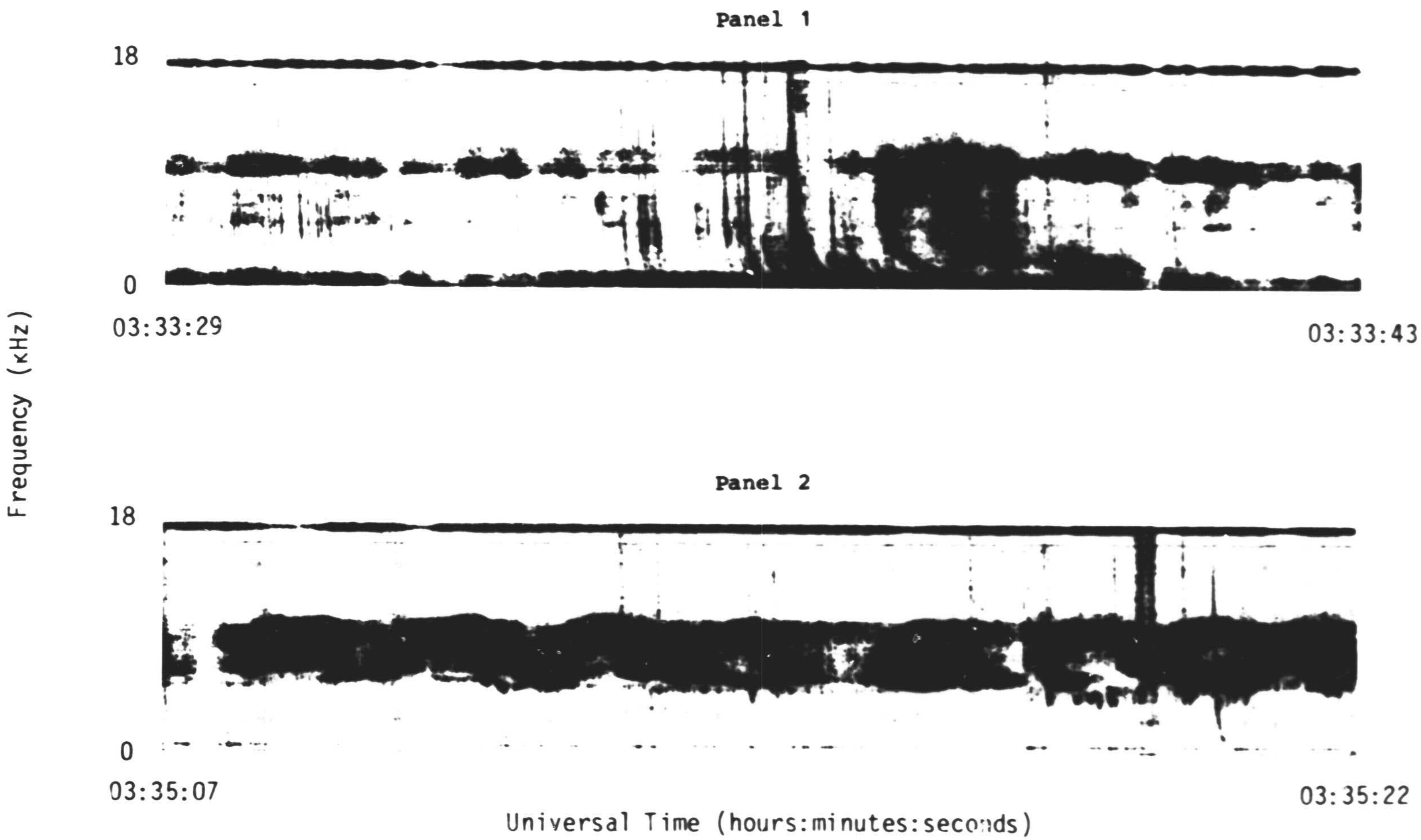

71/183/0329

Excerpts of VLF Spectral film for the period 0333 - 0343

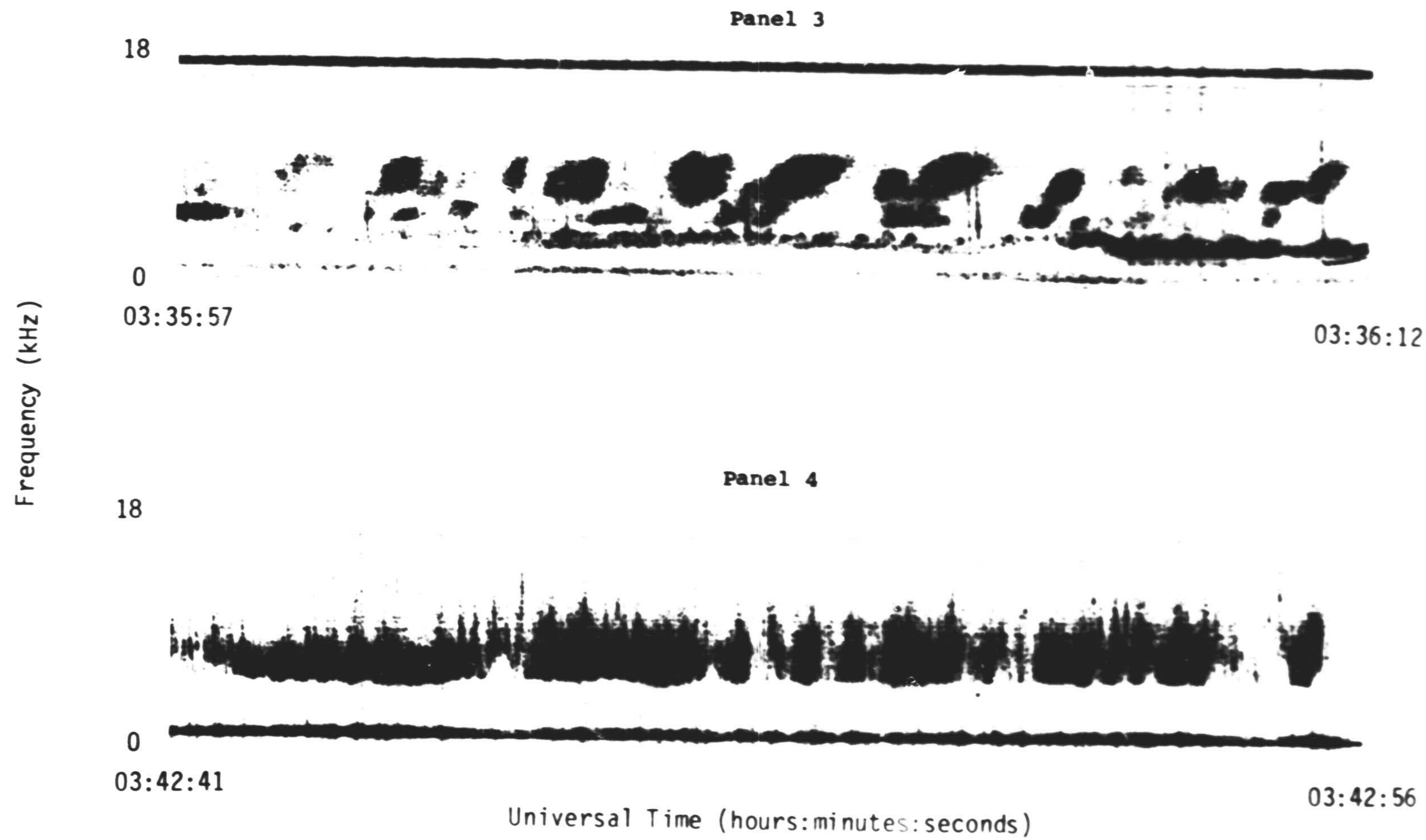

SET 18, FORMAT 11

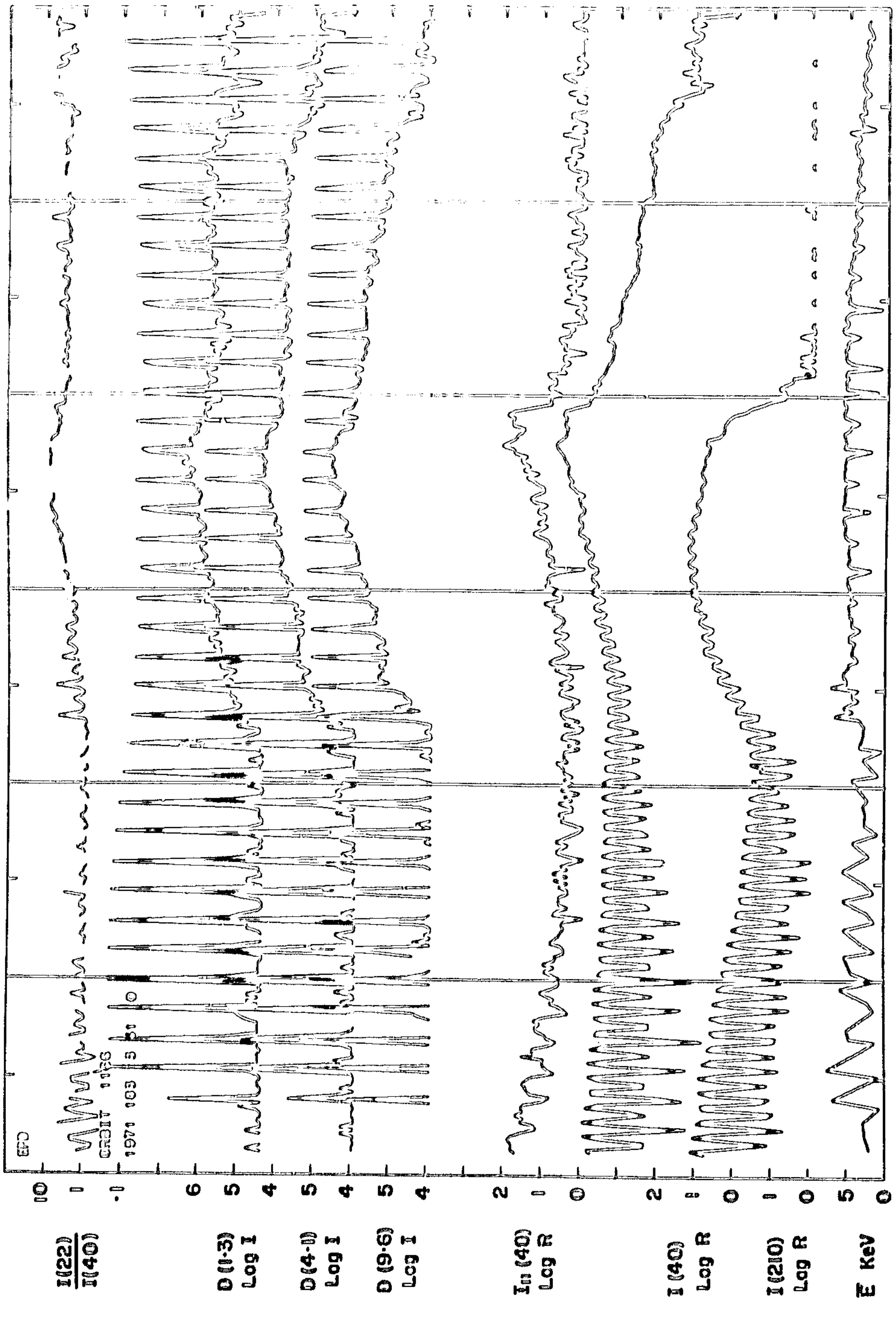

SET 18, FORMAT 3

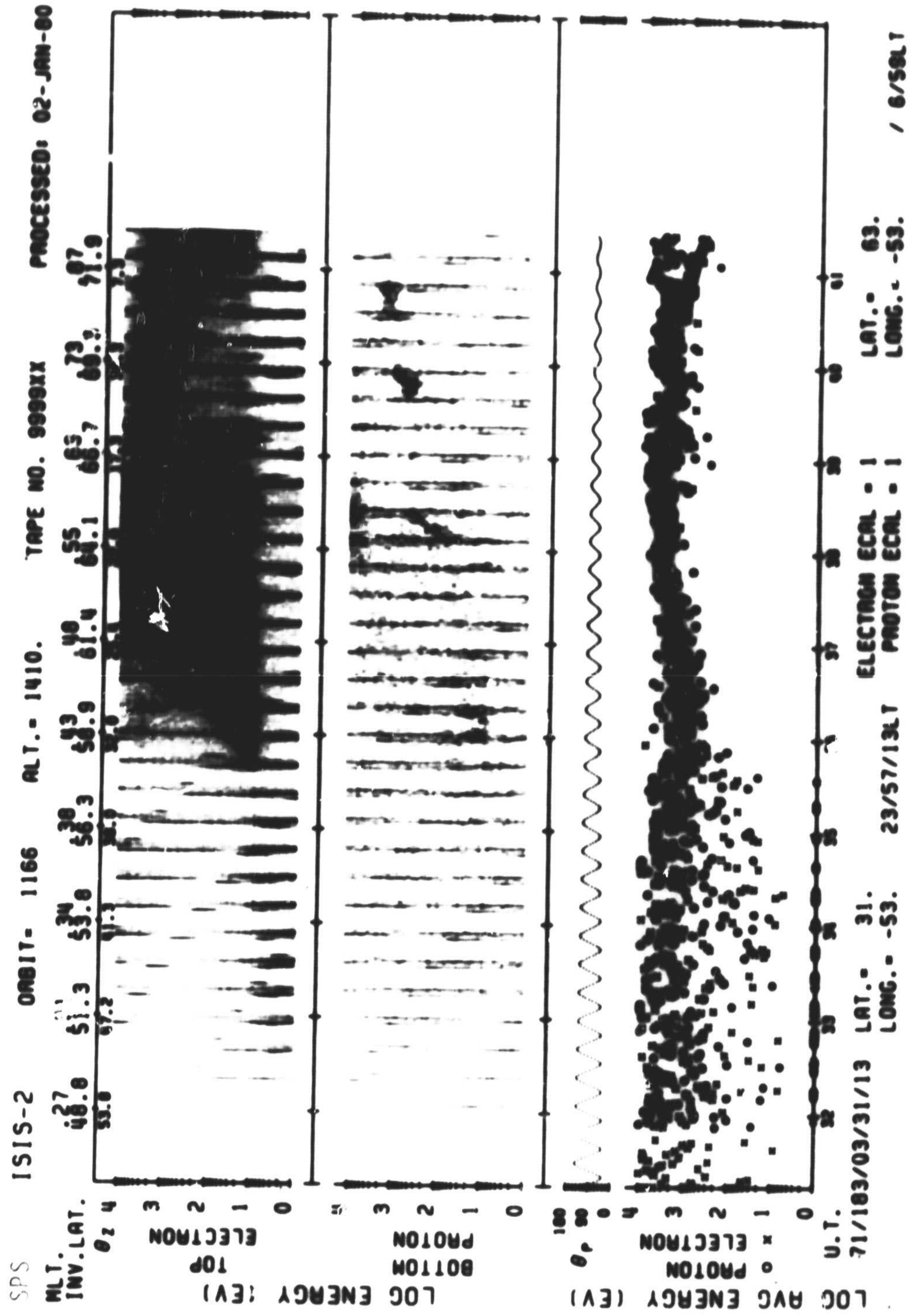

SET 18, FORMAT 6

ORBIT 1166
DATE 710702
DAY 183

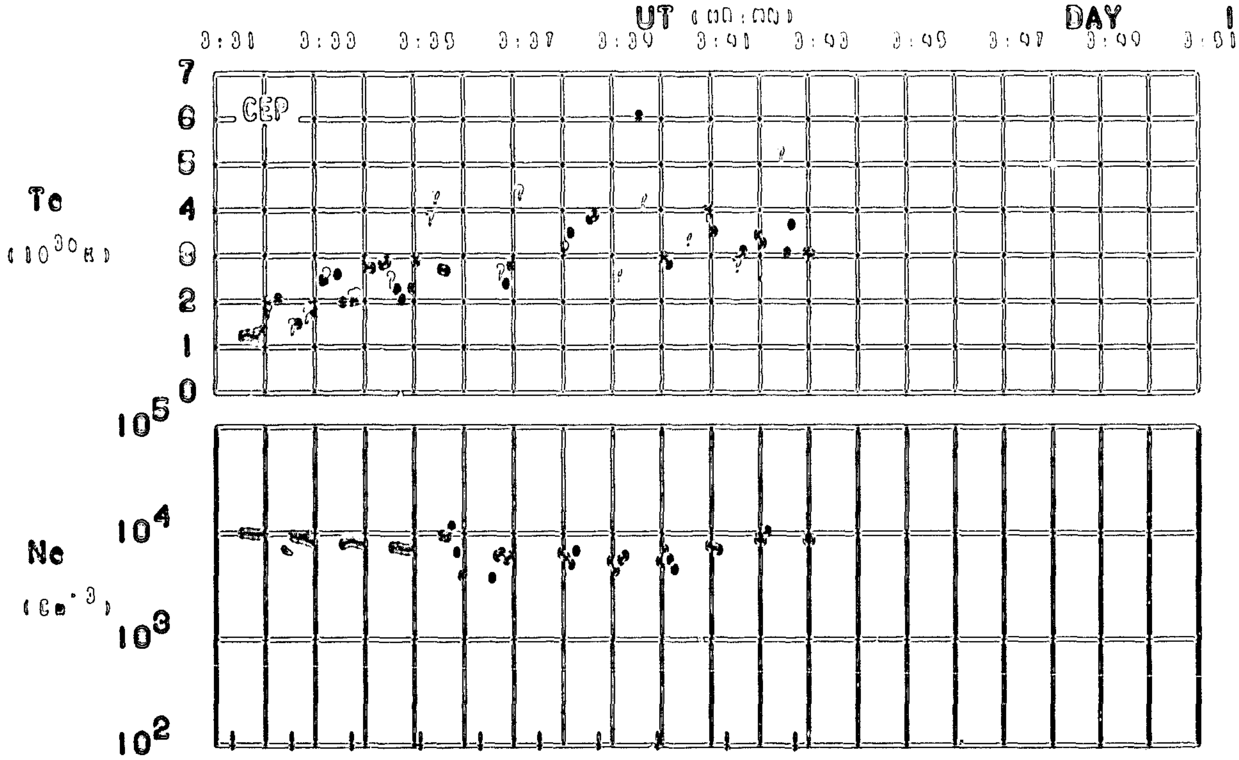

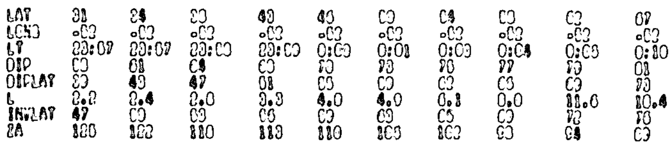

SET 18, FORMAT 10

73/169/0951

Excerpts of VLF Spectral film for the period 0952 - 1003

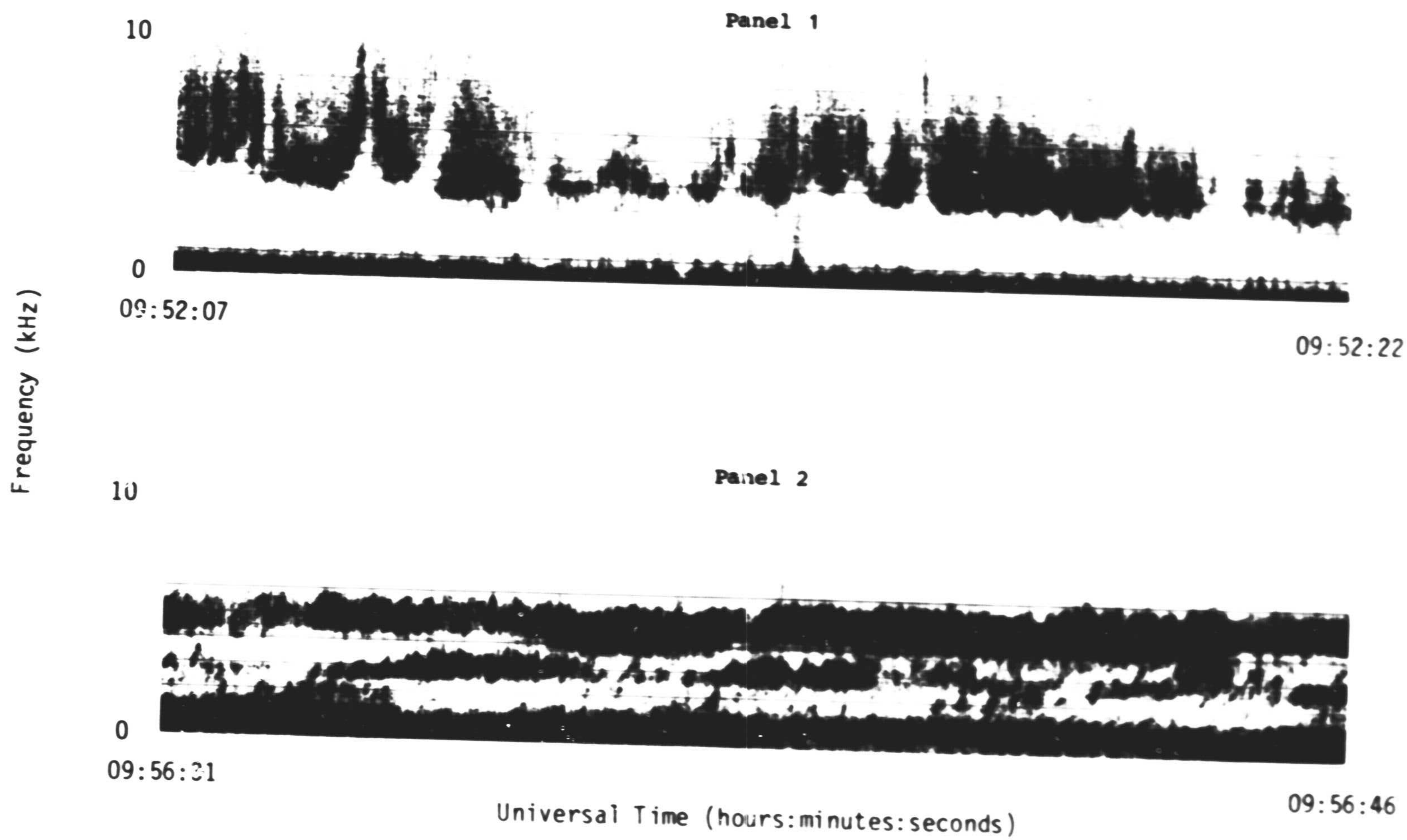

SET 19, FORMAT 11

73/169/0951

Excerpts of VLF Spectral film for the period 0952 - 1003

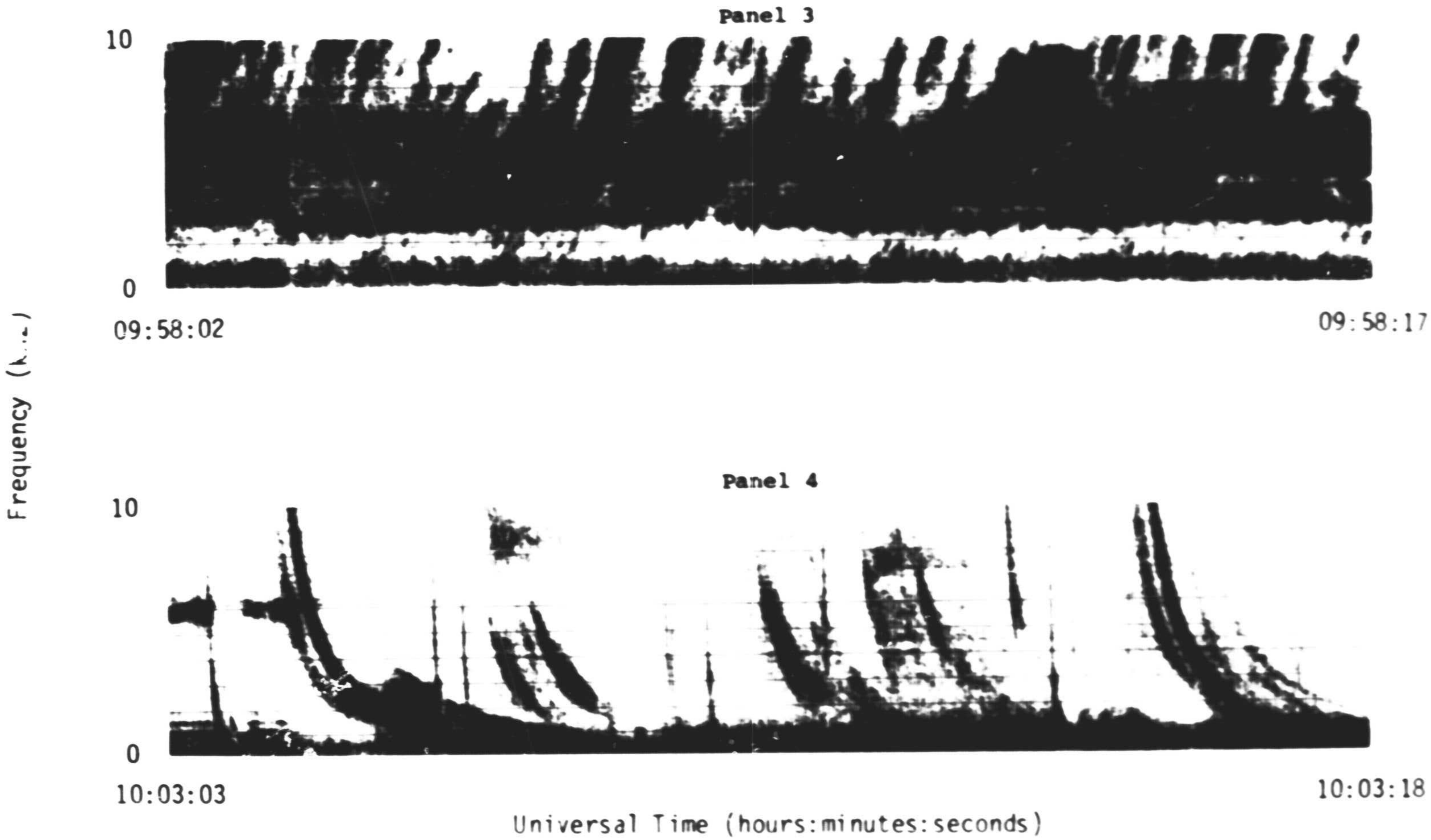

SET 19, FORMAT 11

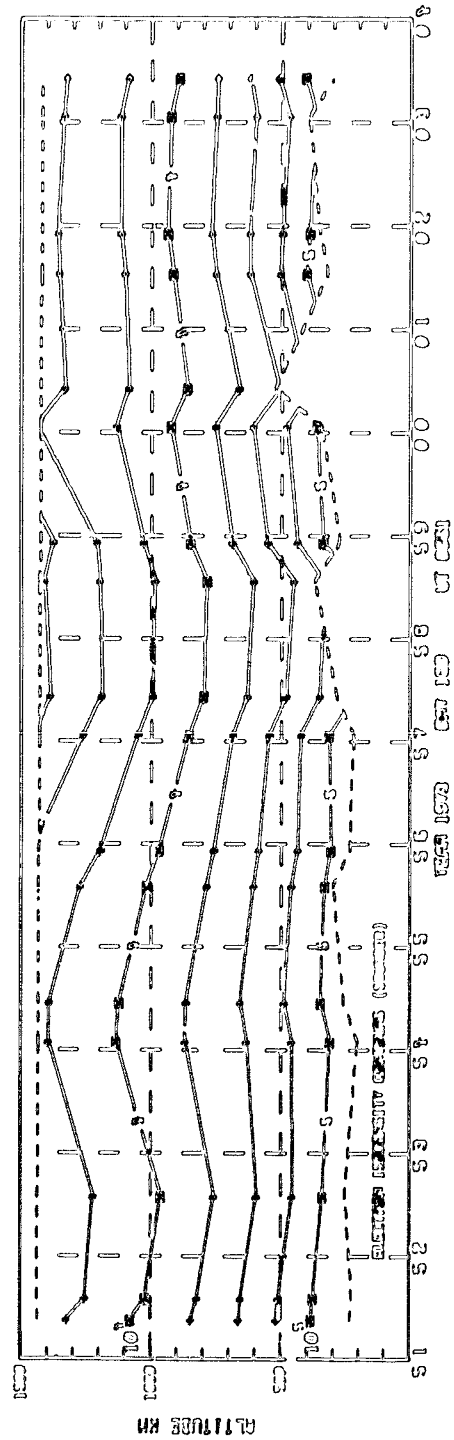

SET 19, FORMAT 2

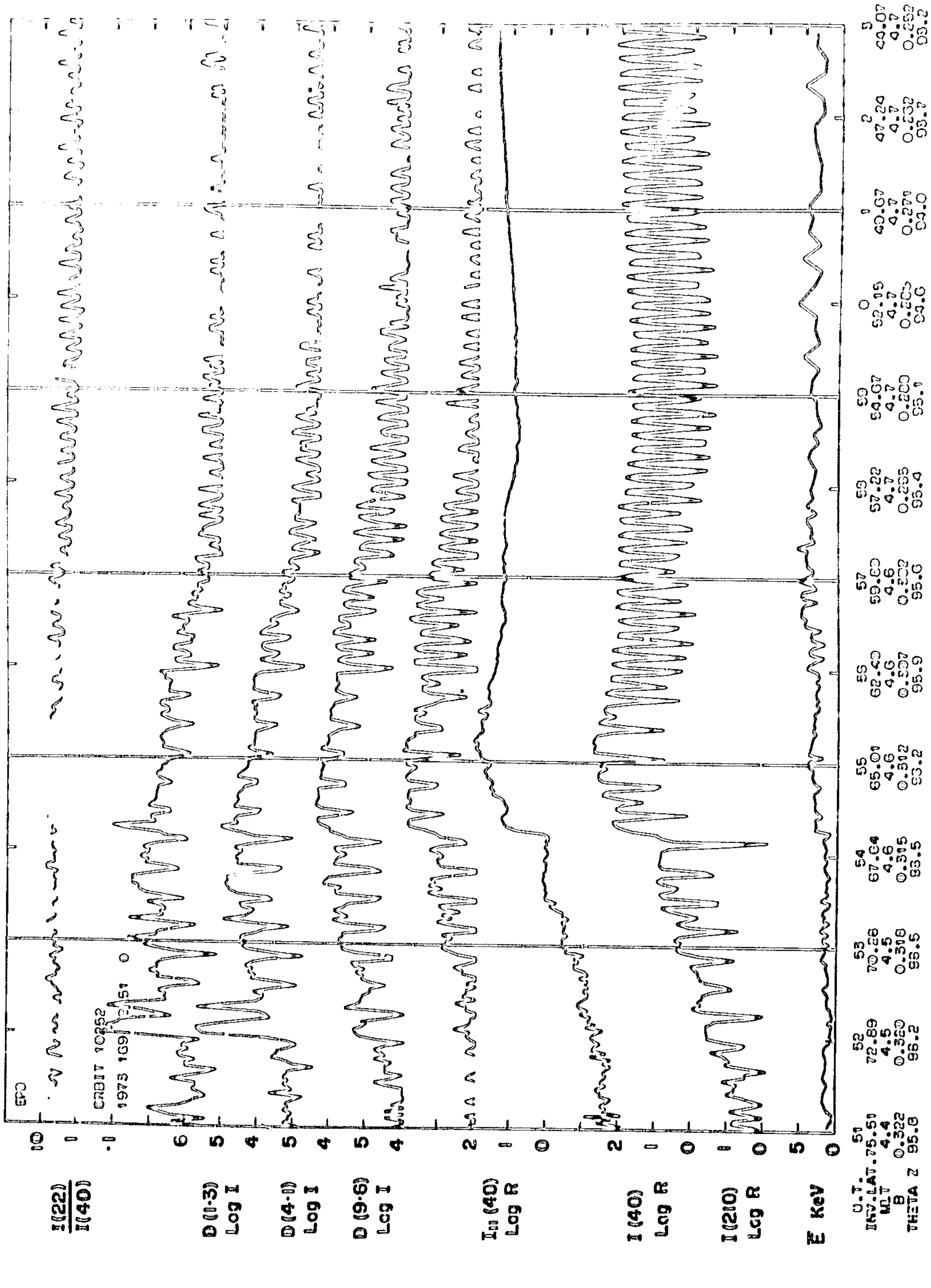

SET 19, FORMAT 3

ORBIT10252
DATE 730618
DAY 169

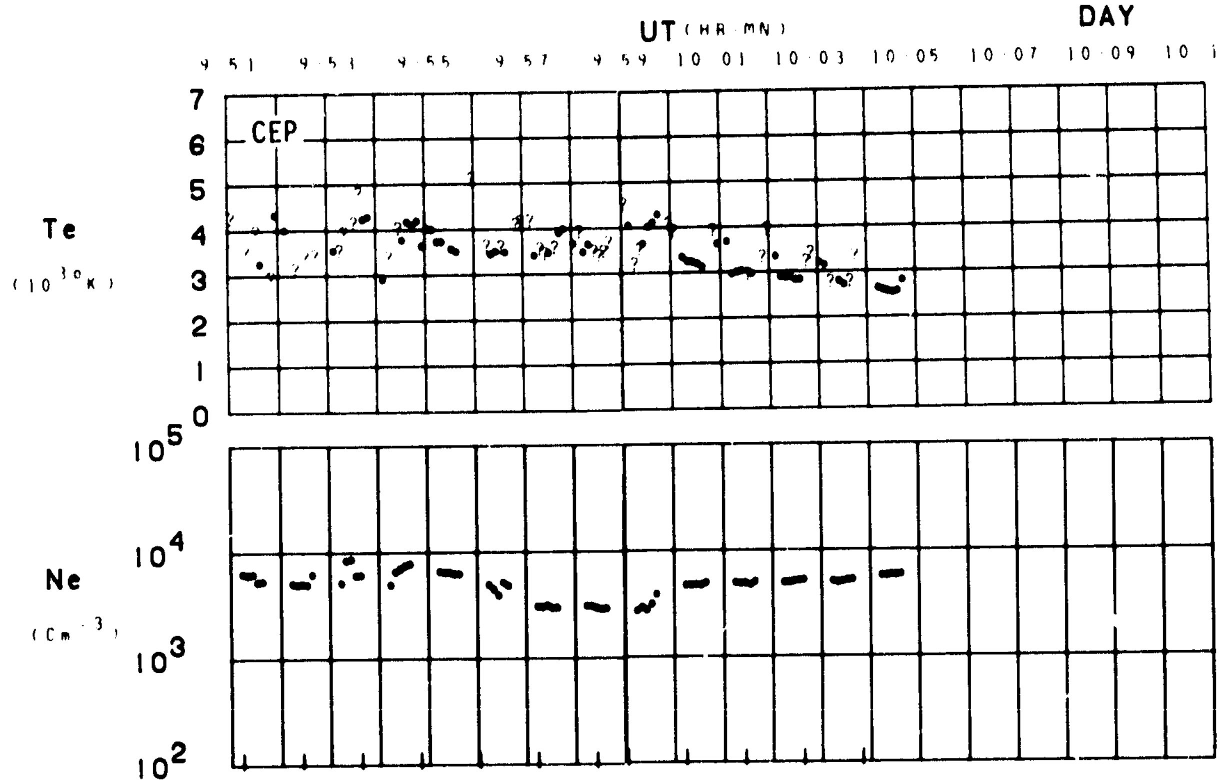

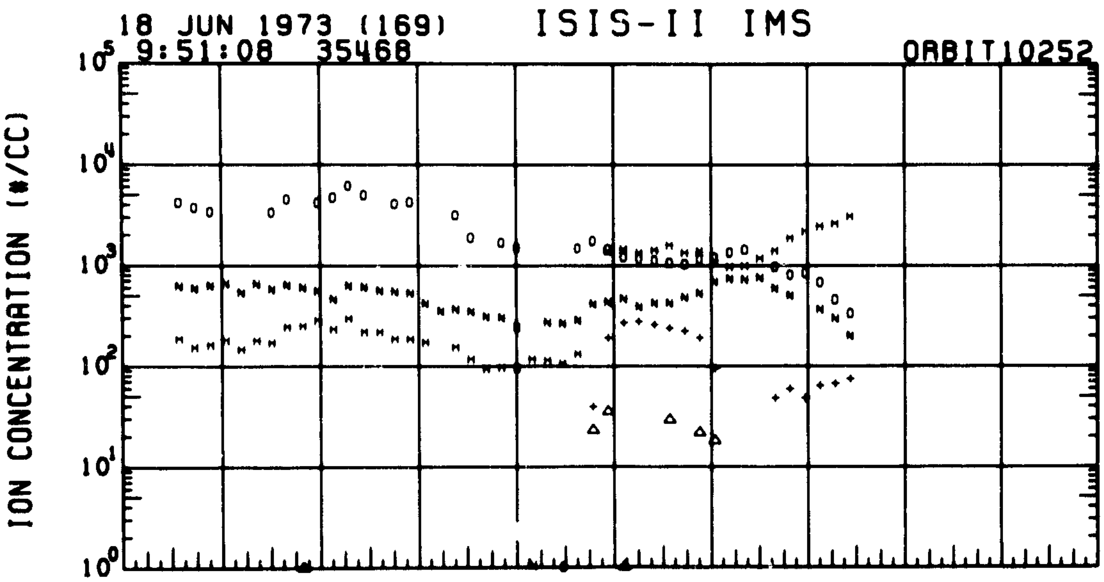

1 - H	UT	9:52	9:54	9:56	9:58	10:00	10:02	10:04
4 - +	LAST	4:58	5:01	5:03	5:04	5:06	5:07	5:08
8 - △	MLT	4:31	4:37	4:40	4:43	4:45	4:46	4:48
14 - N	DLAT	73	67	61	54	48	41	34
16 - O	INVL	73	68	62	57	52	47	43
	GLAT	60	54	48	41	35	29	22
	GLNG	-72	-72	-72	-72	-72	-73	-73
	SZEN	77	80	82	85	87	90	92
	ALT	1435	1433	1431	1428	1425	1422	1419

SET 19, FORMAT 4

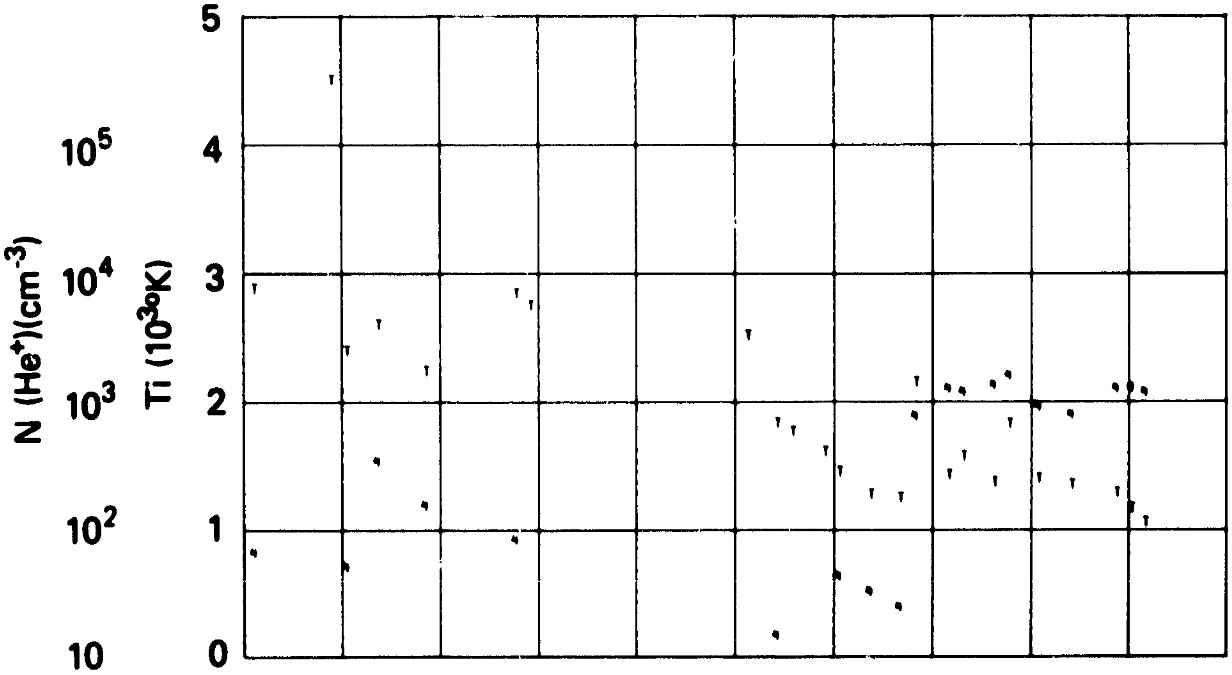

UT	9:48	9:50	9:52	9:54	9:56	9:58	10:00	10:02	10:04
LAST	4:48	4:54	4:58	5:01	5:03	5:04	5:06	5:07	5:08
MLT			4:31	4:37	4:40	4:43	4:45	4:46	4:48
DLAT			73	67	61	54	48	41	34
INVL	83	78	73	68	[illegible]	57	52	47	43
GLAT	73	66	60	54	48	41	35	29	22
GLNG	-75	-74	-72	-72	-72	-72	-72	-73	-73
SZEN	73	75	77	80	82	85	87	90	92
ALT	1437	1436	1435	1433	1431	1428	1425	1422	1419

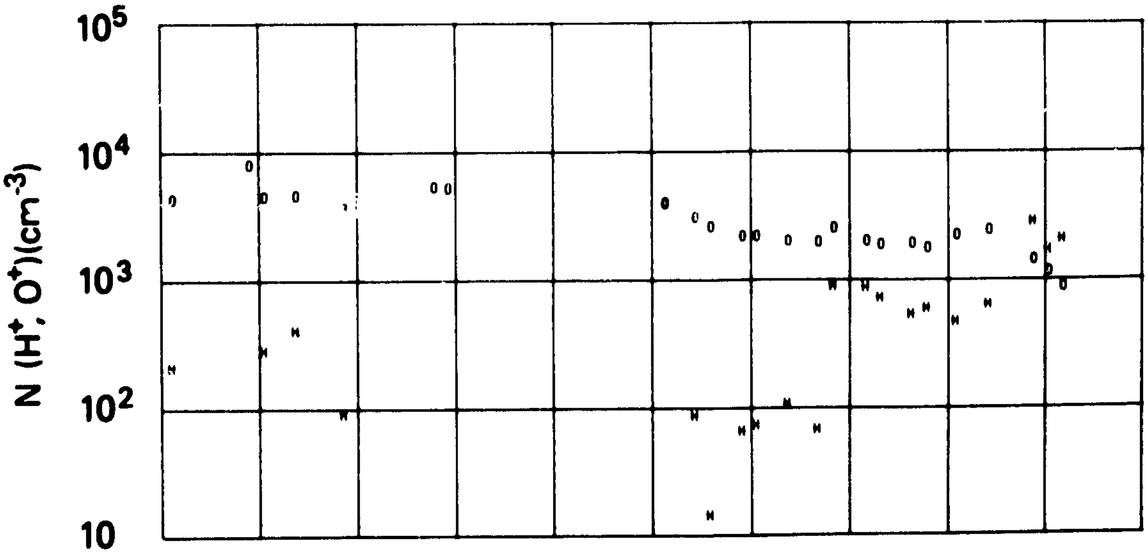

SET 19, FORMAT 5

71/331/0414

Excerpts of VLF Spectral film for the period 0415 - 0429

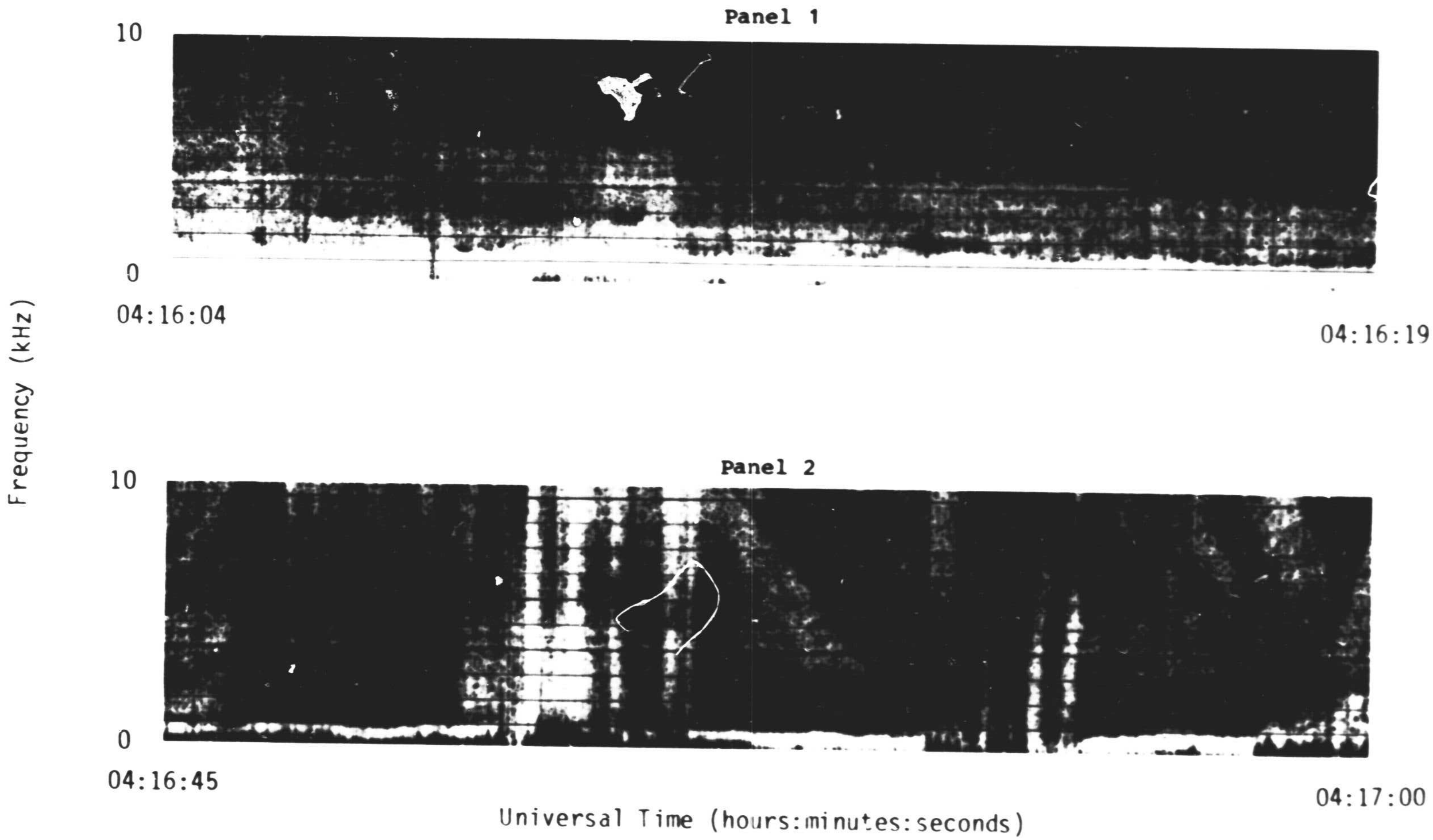

71/331/0414

Excerpts of VLF Spectral film for the period 0415 - 0429

Panel 3

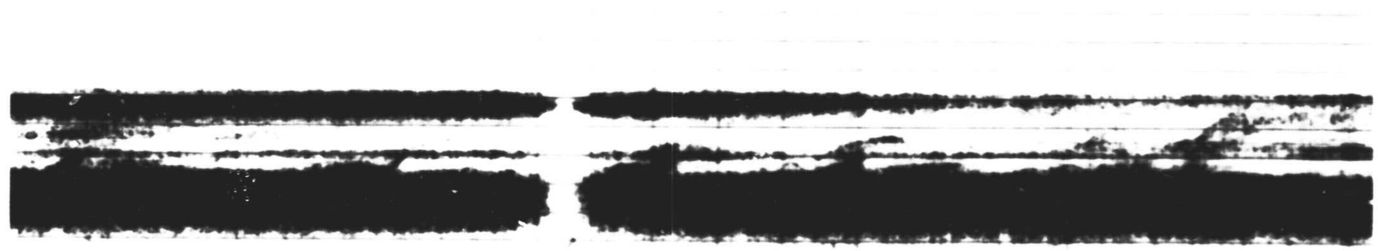

Panel 4

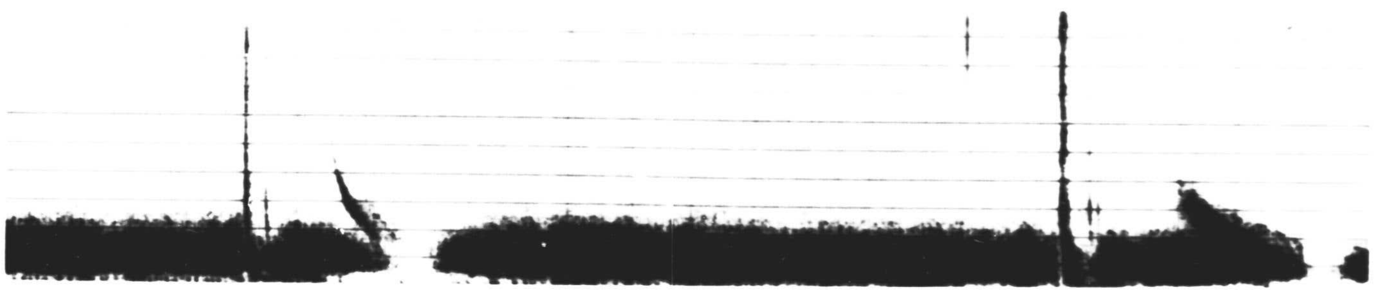

Frequency (kHz)

Universal Time (hours:minutes:seconds)

SET 20, FORMAT 11

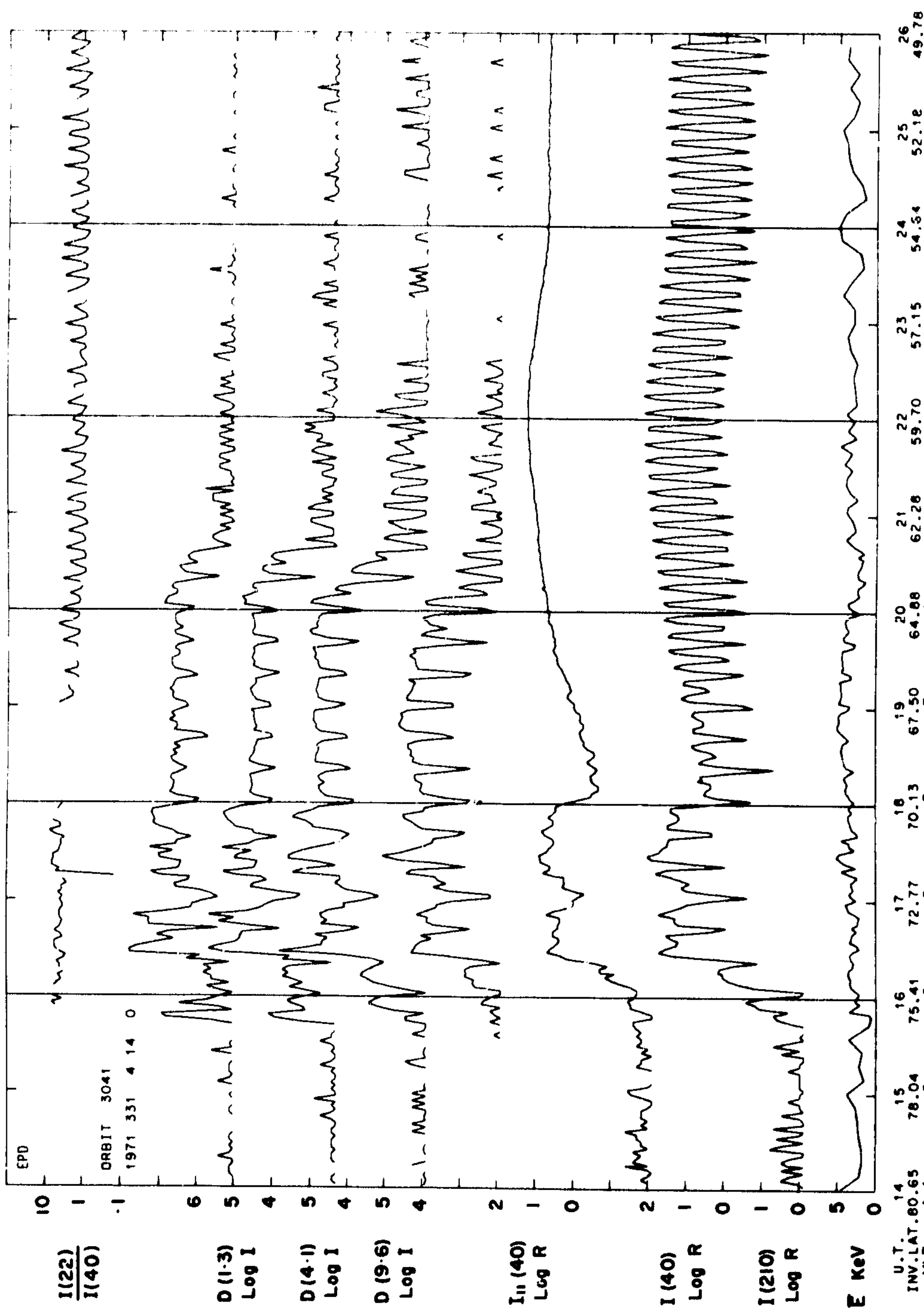

SET 20, FORMAT 3

ORBIT 3041
DATE 711127
DAY 331

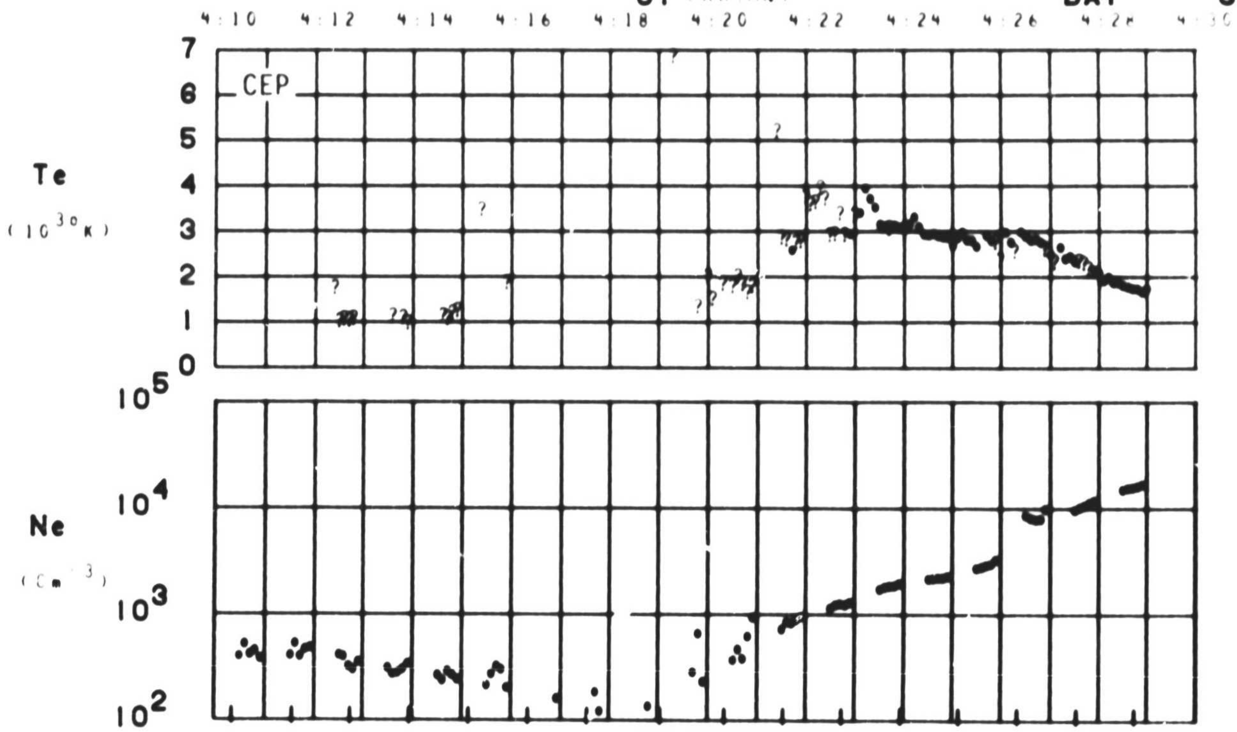

LAT	82	78	74	71	67	63	59	55	51	47	43	39	35	32	28	24
LONG	-66	-62	-60	-59	-58	-58	-58	-57	-57	-57	-57	-58	-58	-58	-58	-58
LT	23:55	0:14	0:23	0:29	0:33	0:35	0:38	0:40	0:41	0:42	0:43	0:44	0:45	0:46	0:46	0:47
DIP	87	86	85	83	82	80	78	76	74	71	69	66	63	60	57	54
DIPLAT	85	83	80	78	75	72	69	64	60	57	53	49	46	42	38	35
L	99.3	102.0	81.4	39.6	22.0	14.1	9.8	6.8	5.2	4.2	3.5	3.0	2.6	2.3	2.1	1.9
INVLAT	84	84	83	80	77	74	71	67	64	60	57	54	51	48	46	43
ZA	118	122	126	129	133	137	140	145	149	152	155	159	162	164	167	168

SET 20, FORMAT 4

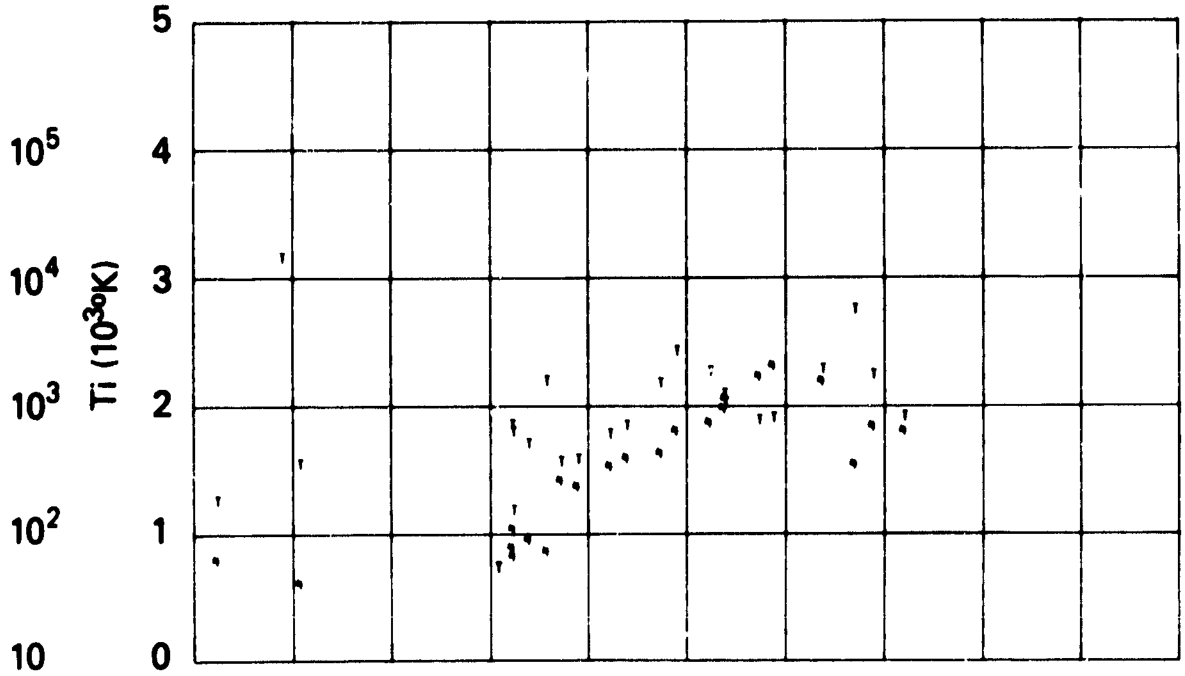

UT	04:16	04:18	04:20	04:22	04:24	04:26	04:28	04:30	04:32
LAST	00:35	00:39	00:41	00:43	00:45	00:46	00:47		
MLT									
DLAT									
INVL	75	70	64	59	54	49	45		
GLAT	65	58	52	46	39	33	27		
GLNG	-58	-58	-58	-58	-58	-58	-58		
SZEN	136	142	148	153	159	164	167		
ALT	1432	1428	1425	1421	1416	1412	1408		

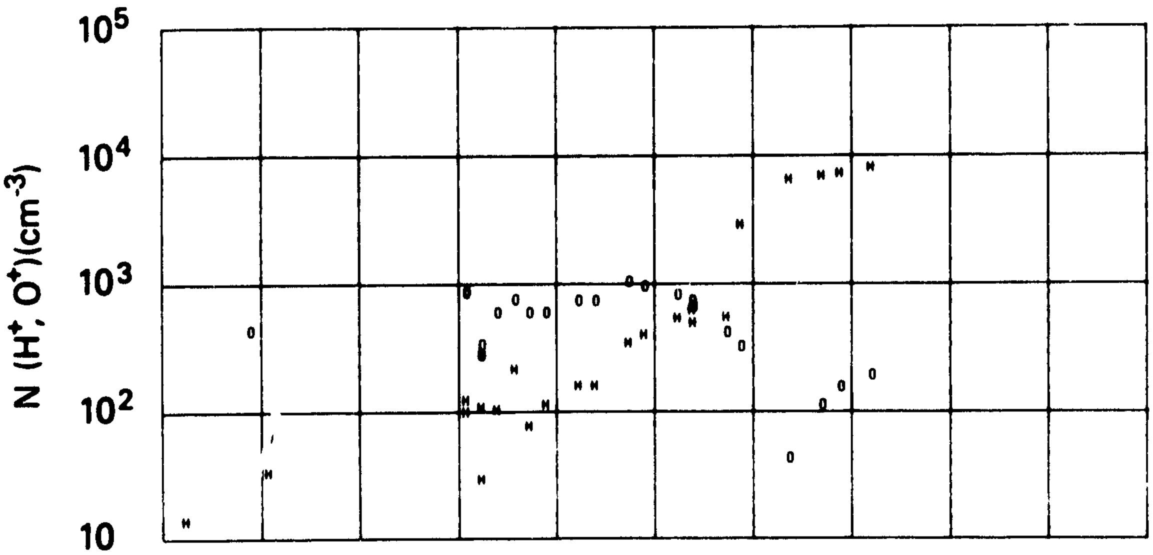

SET 20, FORMAT 5

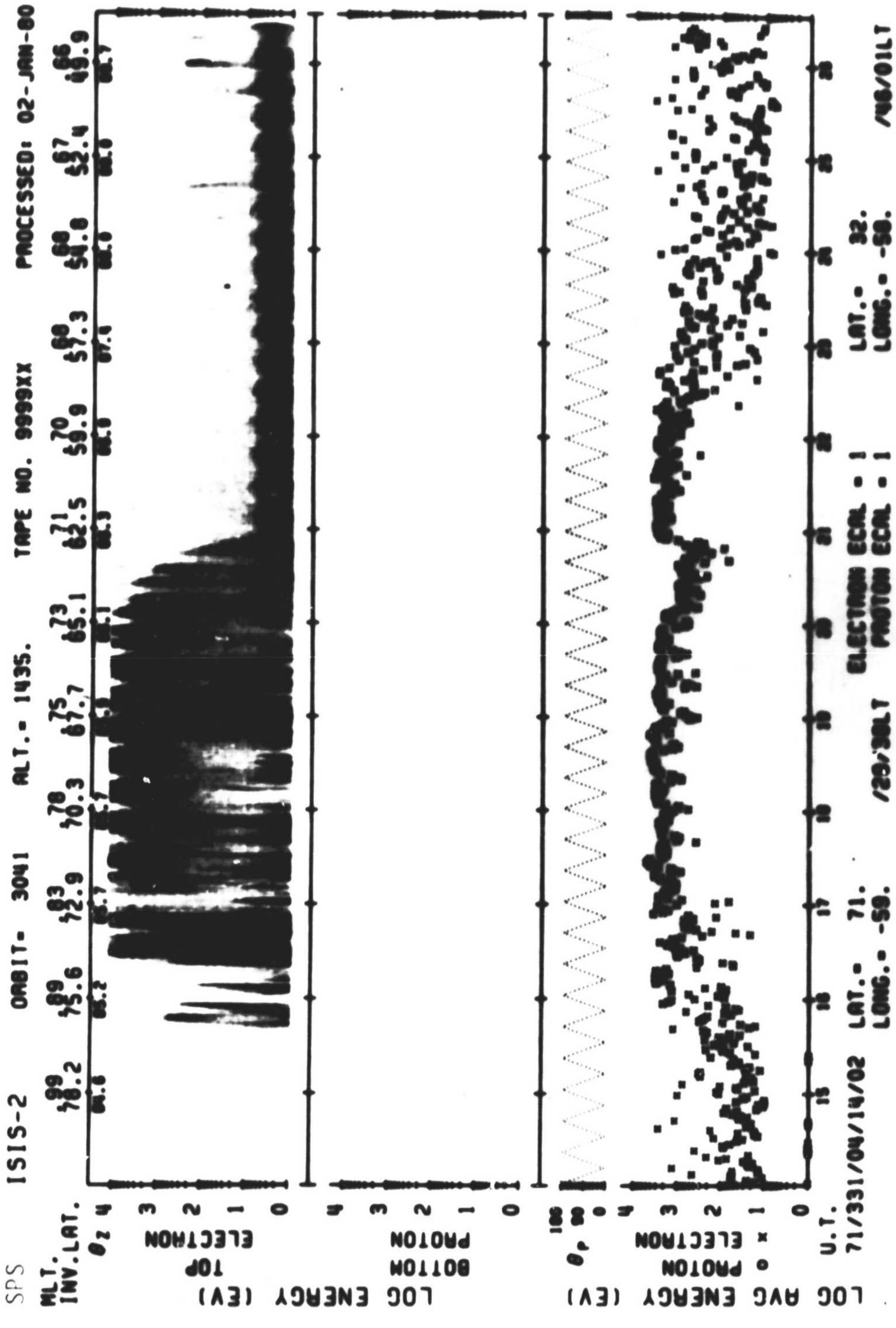

SET 20, FORMAT 6

71/358/0415

Excerpts of VLF Spectral film for the period 0415 - 0425

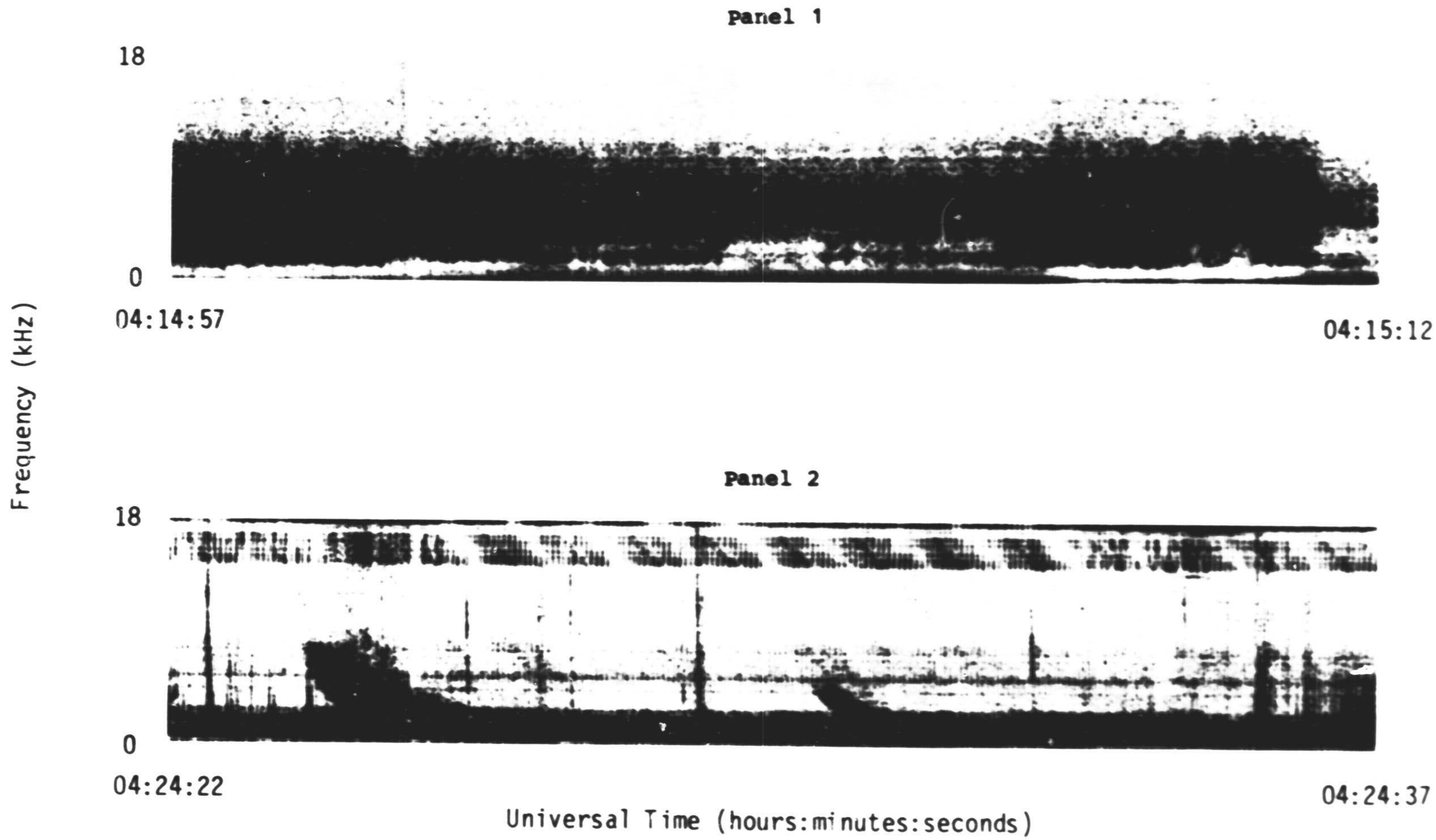

SET 21, FORMAT 11

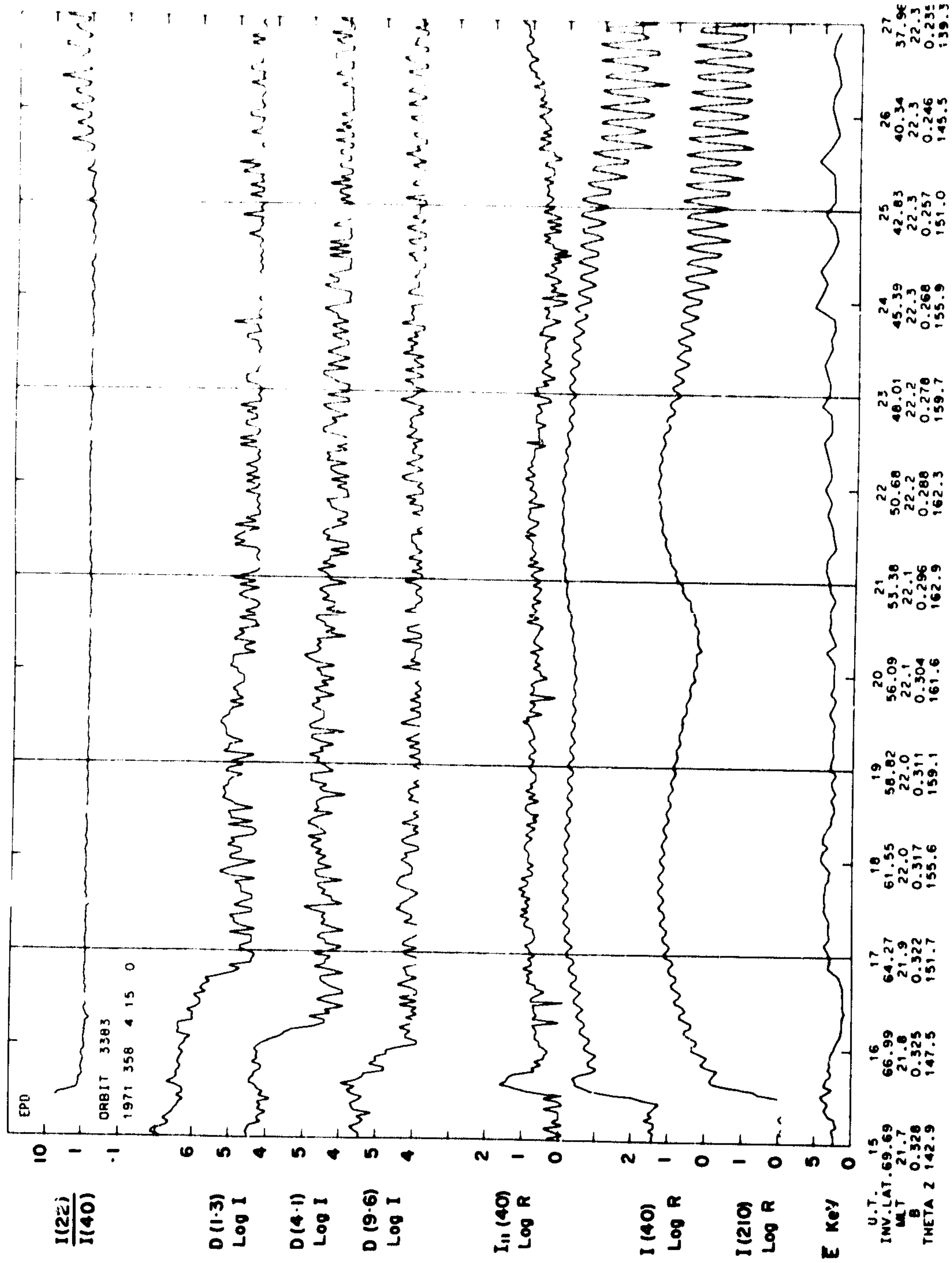

SET 21, FORMAT 3

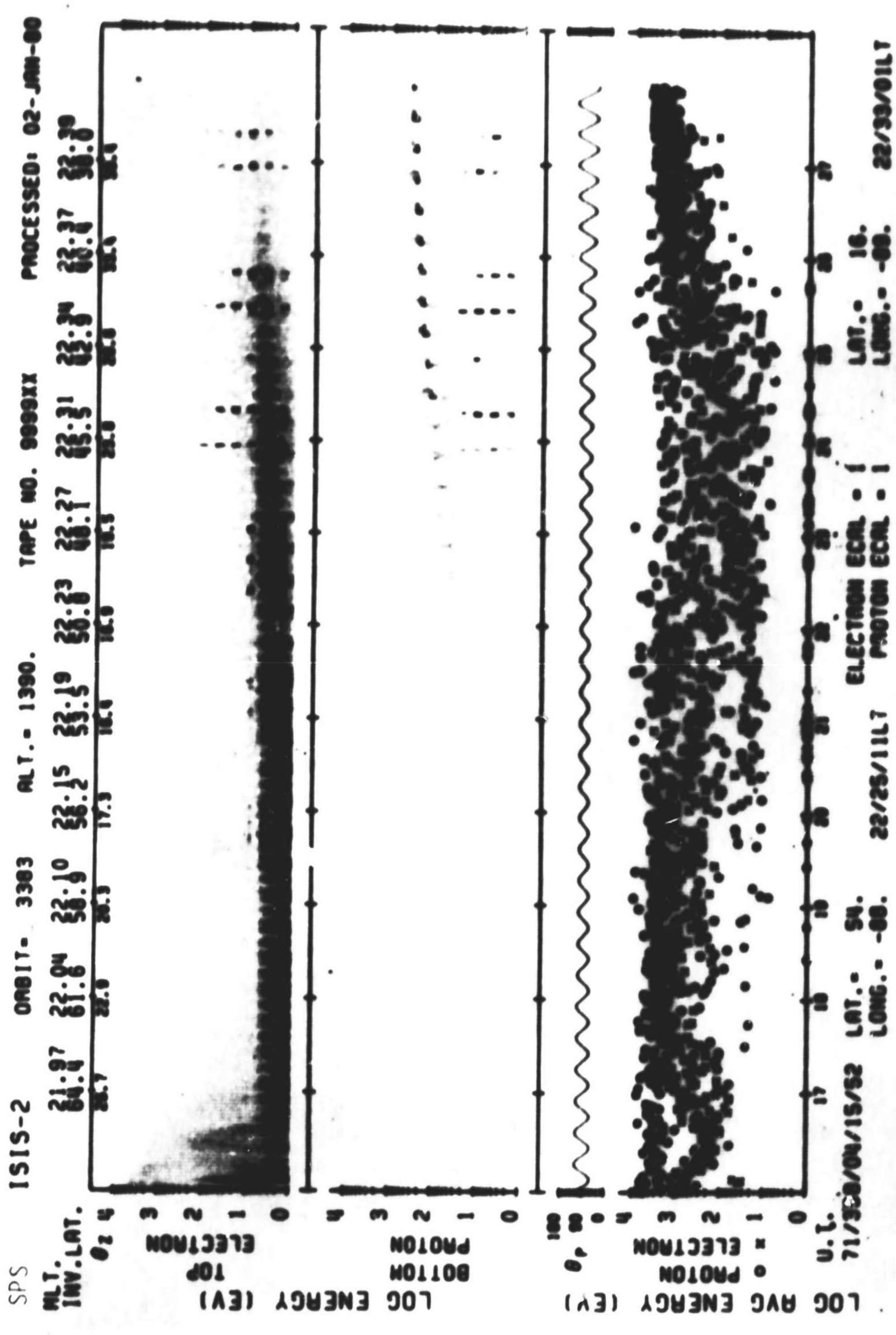

SET 21, FORMAT 6

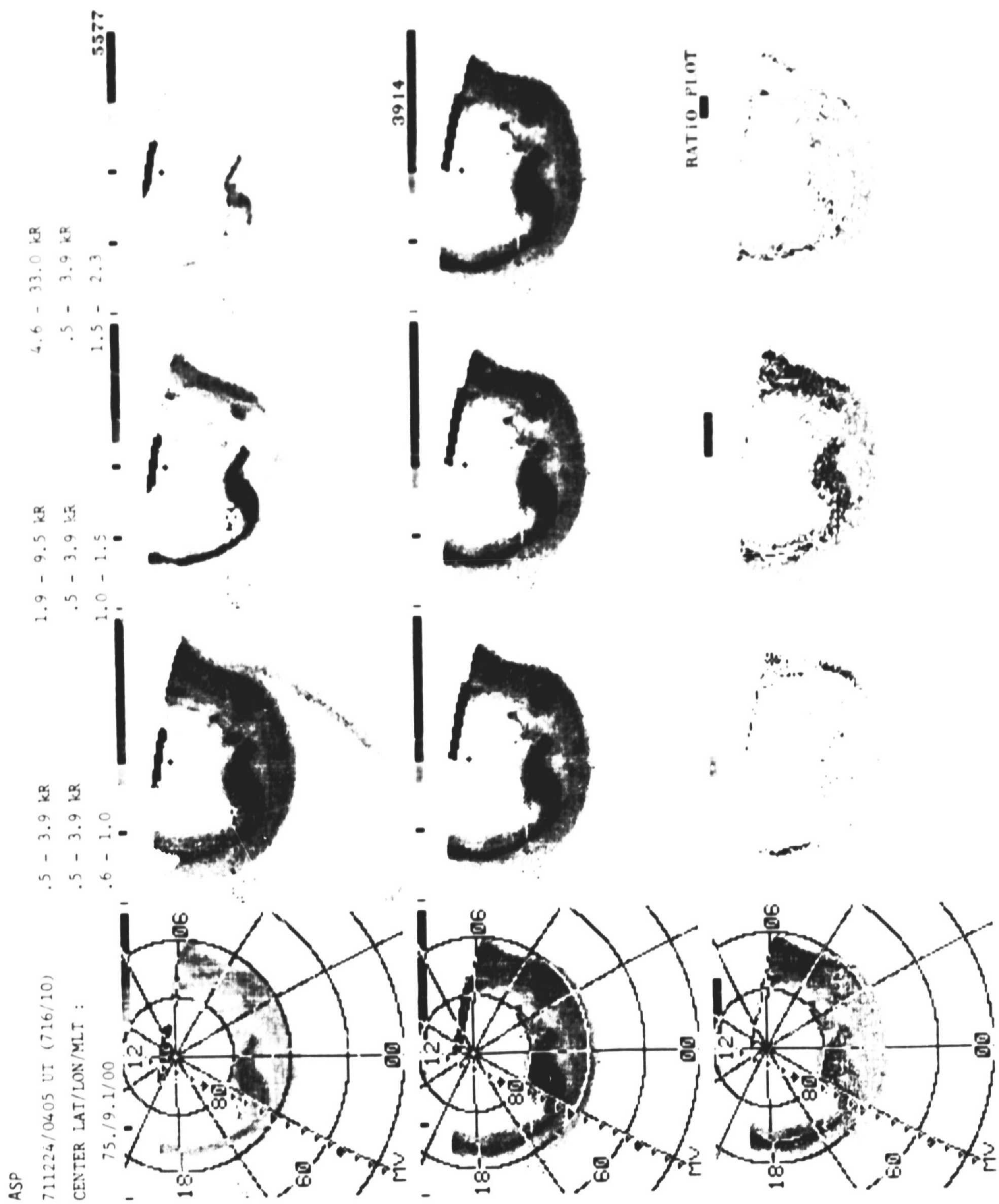

SET 21, FORMAT 7

ORIGINAL PAGE IS
OF POOR QUALITY

ORBIT 3383 (71/DEC/24)
DAY 358 OF YEAR 1971

FIRST SPIN U.T. 4H6M
LAST SPIN U.T. 4H37M

6300 ANGSTROM INTENSITY

DATE PROCESSED: 80/SEP/09
INVARIANT COORDINATES (250 KM.)

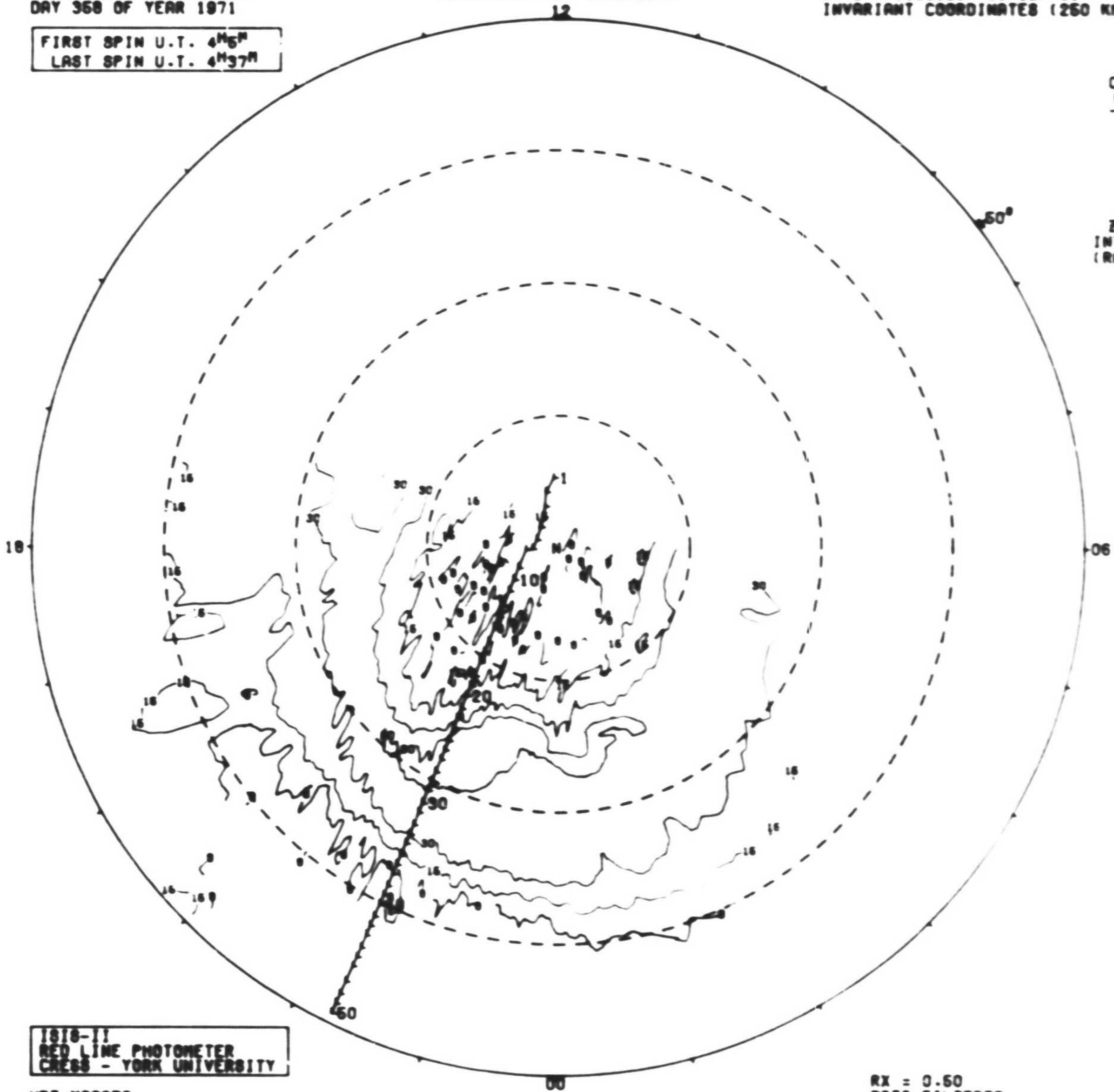

CONTOURS PLOTTED

80
150
300
600
1200
2400
ZENITHAL INTENSITIES (RAYLEIGHS)

SPACECRAFT INFORMATION

SPIN NUMBER	ORBIT TIME (HRMNSC)	INVARIANT LATITUDE (DEGREES)
1	040534	84.0
2	040558	94.3
3	040622	84.3
4	040640	84.3
5	040658	84.3
6	040722	84.2
7	040740	84.2
8	040758	84.3
9	040822	84.3
10	040840	84.3
11	040858	84.3
12	040922	83.9
13	040940	83.4
14	040958	82.8
15	041022	81.9
16	041040	81.2
17	041058	80.3
18	041122	79.2
19	041140	78.5
20	041158	77.7
21	041222	76.7
22	041240	75.9
23	041258	75.1
24	041322	74.1
25	041340	73.3
26	041358	72.5
27	041422	71.4
28	041440	70.6
29	041458	69.8
30	041522	68.7
31	041540	67.9
32	041604	66.8
33	041622	66.0
34	041640	65.2
35	041704	64.1
36	041722	63.3
37	041740	62.5
38	041804	61.4
39	041822	60.6
40	041840	59.7
41	041904	58.6
42	041922	57.8
43	041940	57.0
44	042004	55.9
45	042022	55.1
46	042040	54.3
47	042110	52.9
48	042134	51.8
49	042152	51.0
50	042210	50.2
51	042234	49.2
52	042252	48.4
53	042310	47.6
54	042334	46.5
55	042352	45.7
56	042410	45.0
57	042434	43.9
58	042452	43.2
59	042510	42.4
60	042534	41.4

ISIS-II
RED LINE PHOTOMETER
CRESS - YORK UNIVERSITY

MRT Y00270
FILE 16

SPACECRAFT TRACK TRACED DOWN TO 250 KM. (NUMBERS DENOTE SPINS)

RX = 0.50
DATA FILTERED
ZERO SUBTRACTION NOT PERFORMED

SET 21, FORMAT 8

ORBIT 3383
DATE 711224
DAY 358

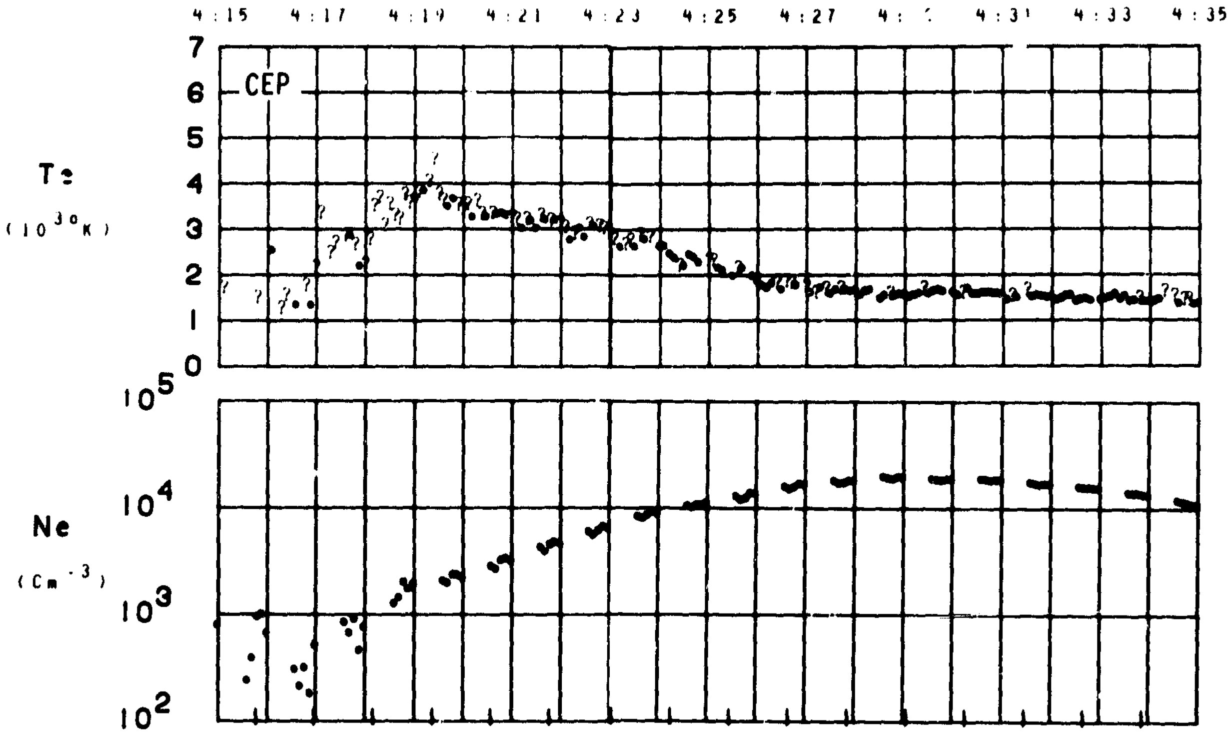

LAT	53	50	46	42	38	34	30	26	23	19	15	11	7	3	0	-3
LONG	-87	-87	-87	-87	-88	-88	-88	-88	-88	-88	-88	-89	-89	-89	-89	-89
LT	22:25	22:26	22:27	22:28	22:29	22:29	22:30	22:31	22:31	22:32	22:33	22:33	22:34	22:34	22:35	22:35
DIP	84	82	81	80	78	76	74	72	69	66	62	58	52	45	36	24
DIPLAT	78	76	74	71	68	65	61	57	53	49	44	39	33	26	20	12
L	6.9	5.3	4.3	3.5	3.0	2.6	2.2	2.0	1.8	1.6	1.5	1.4	1.4	1.3	1.3	1.3
INVLAT	67	64	61	57	54	51	47	44	41	38	36	33	31	29	27	26
ZA	144	147	150	153	155	157	158	159	159	159	157	156	154	151	148	145

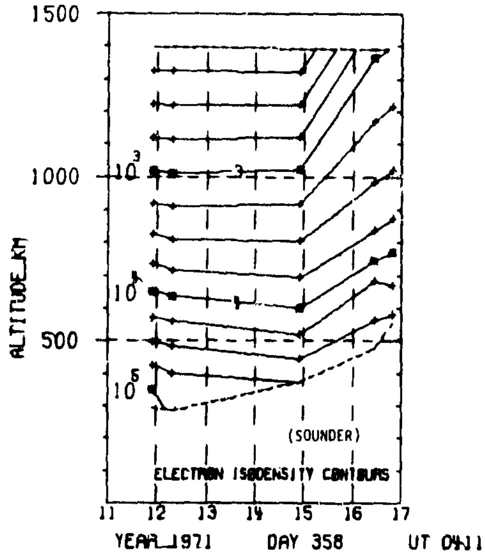

SET 21, FORMAT 10

71/358/0403

Excerpts of VLF Spectral film for the period 0406 - 0414

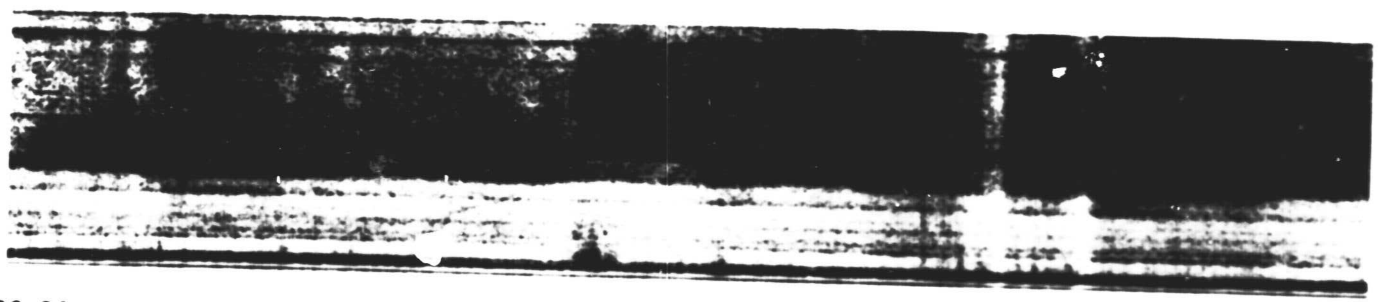

Panel 2

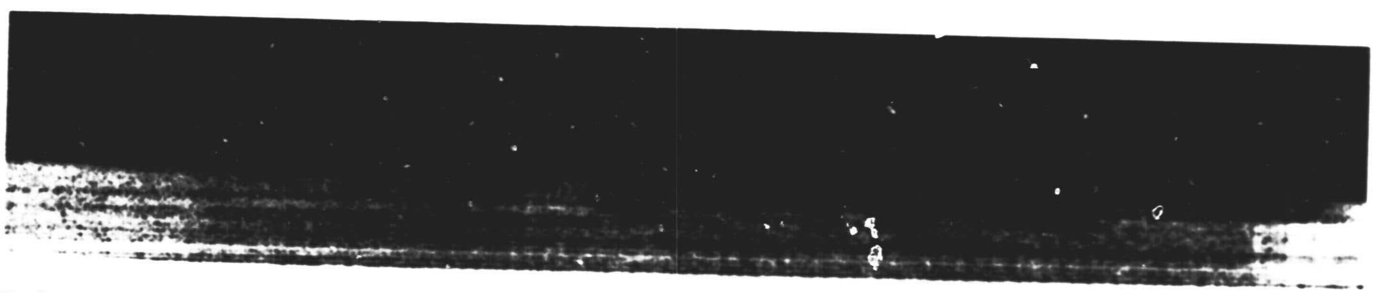

SET 22, FORMAT 11

71/135/0403

Excerpts of VLF Spectral film for the period 0406 - 0414

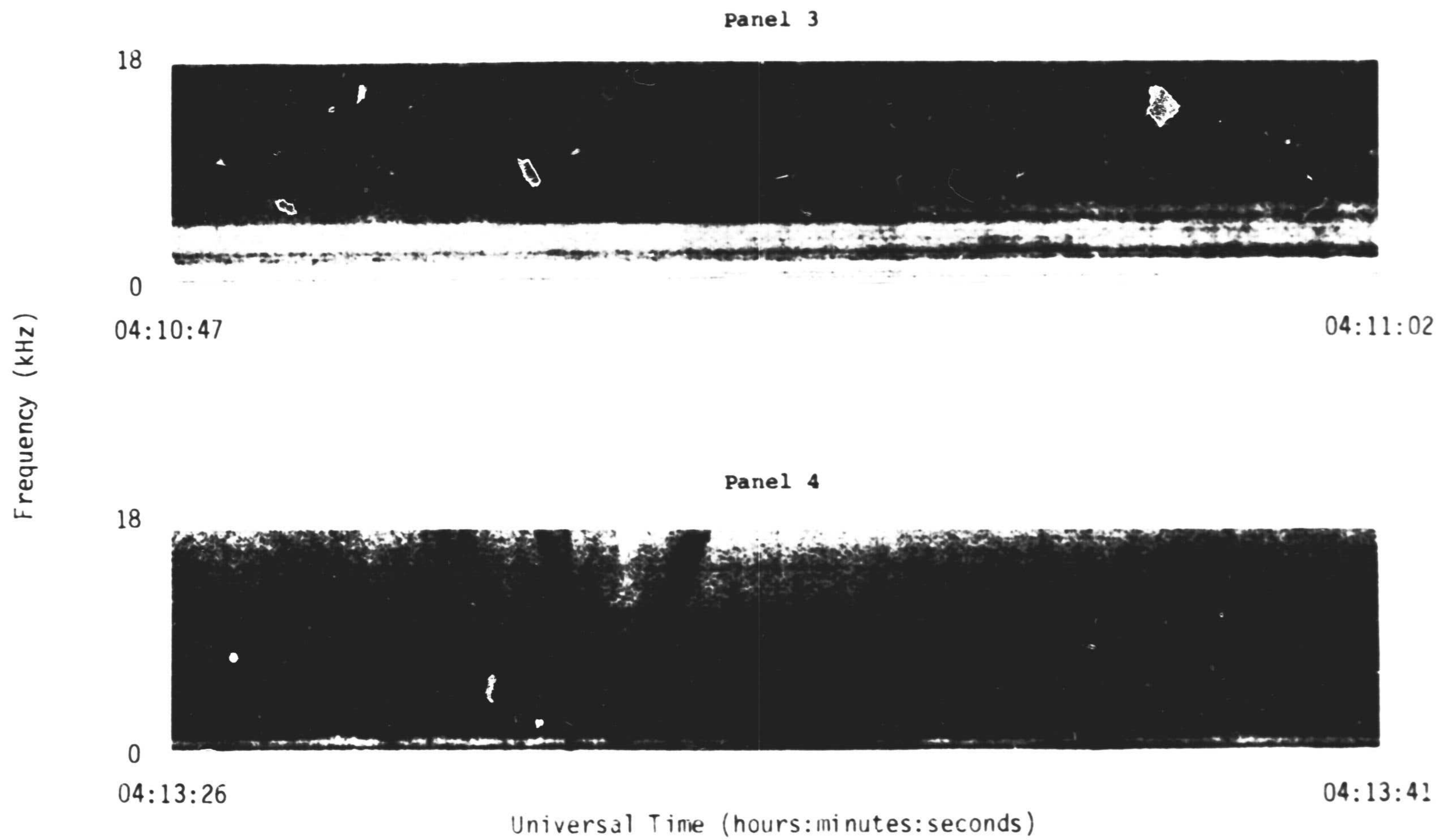

SET 22, FORMAT 11

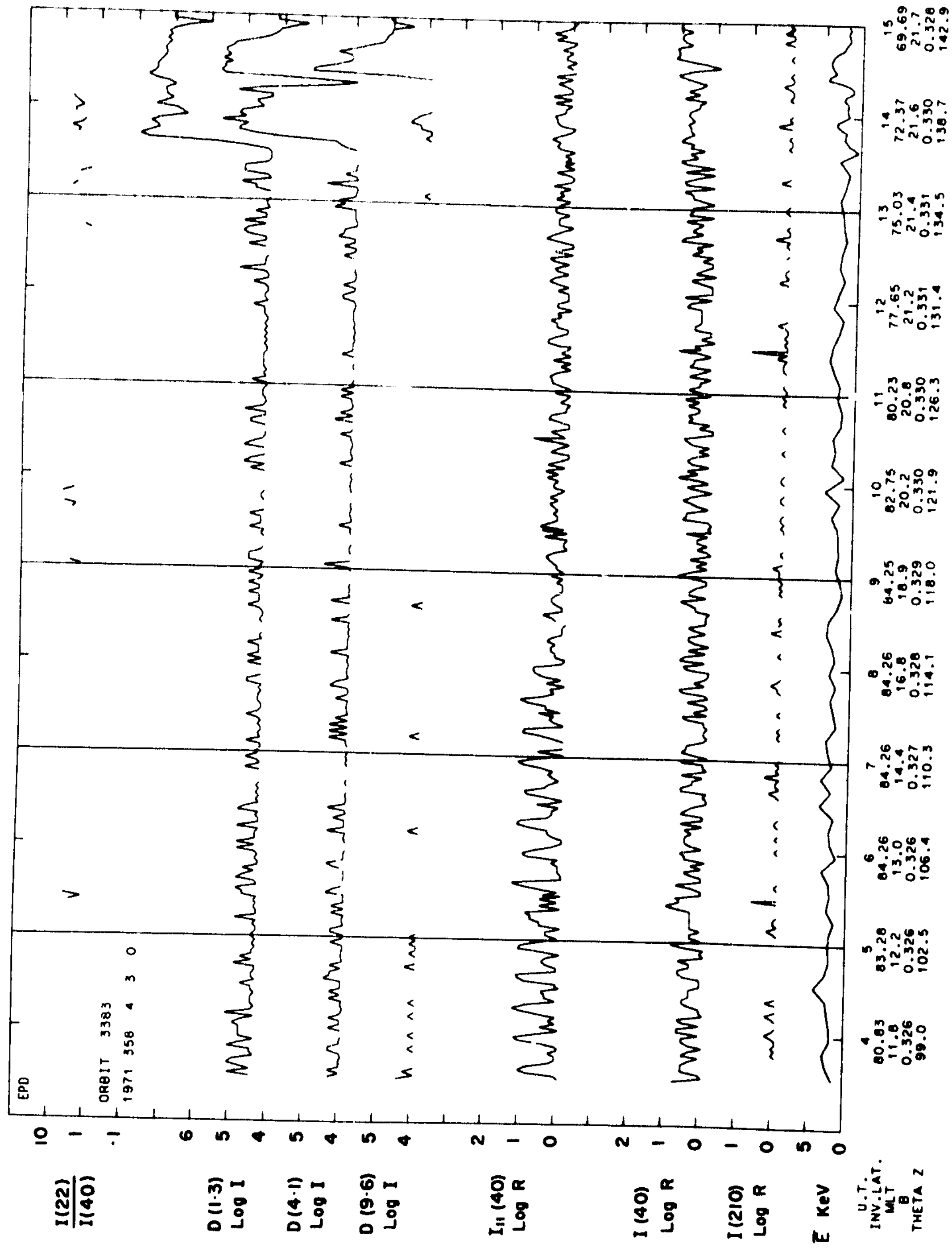

SET 22, FORMAT 3

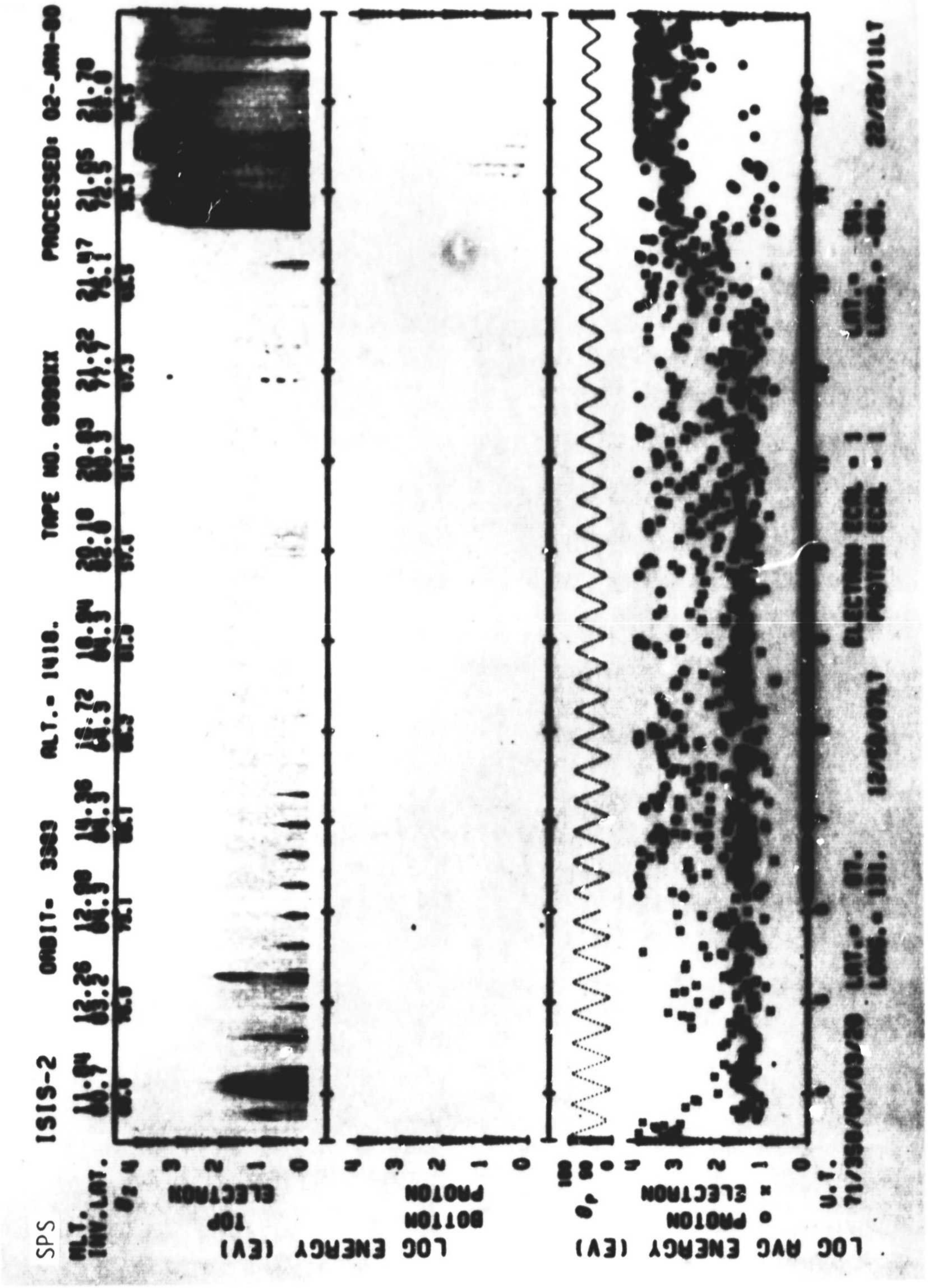

SET 22, FORMAT 6

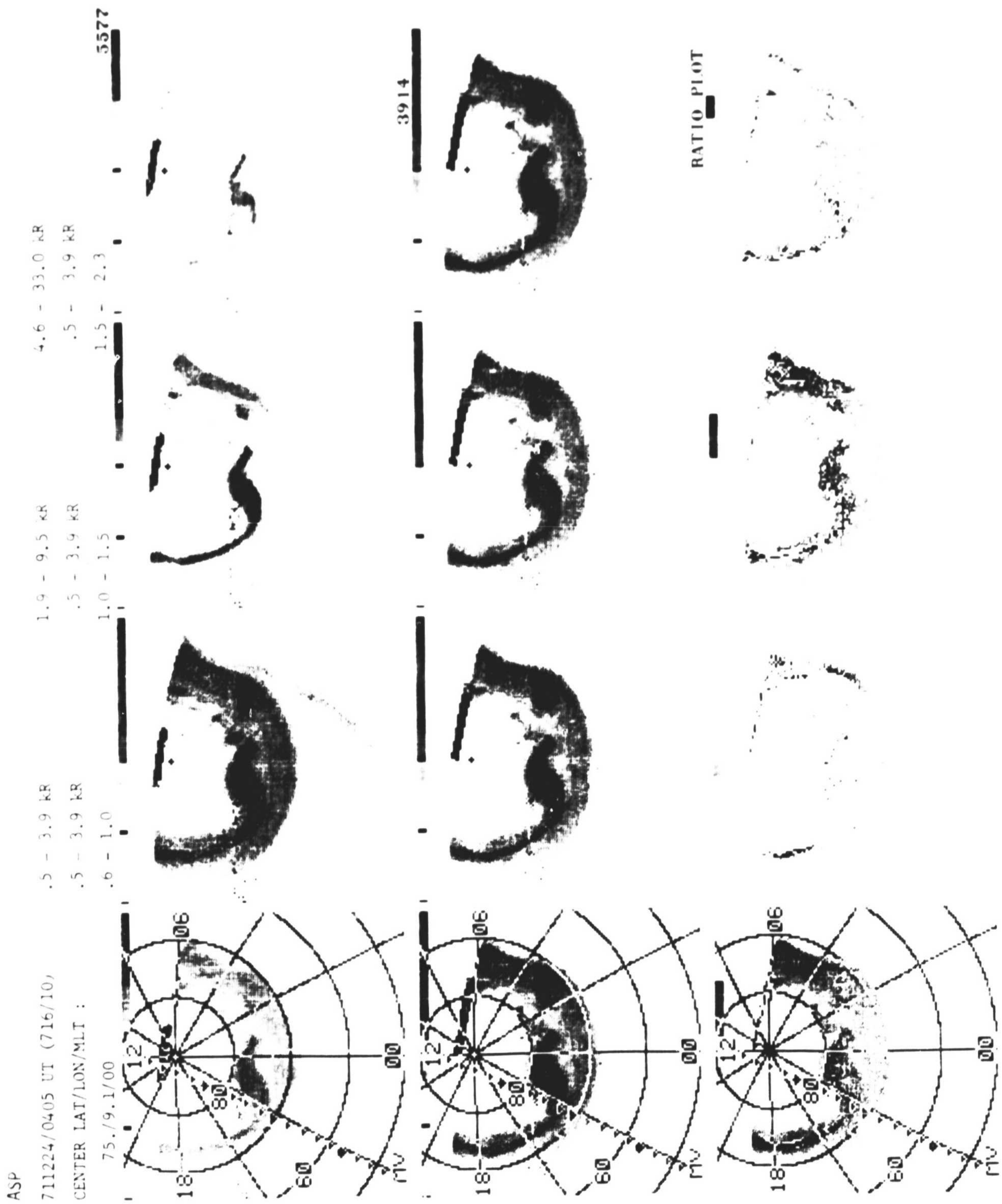

SET 22, FORMAT 7

ORIGINAL PAGE IS
OF POOR QUALITY

ORBIT 3383 (71/DEC/24)
DAY 358 OF YEAR 1971

6300 ANGSTROM INTENSITY

DATE PROCESSED: 80/SEP/09
INVARIANT COORDINATES (250 KM.)

FIRST SPIN U.T. $4^{H}5^{M}$
LAST SPIN U.T. $4^{H}37^{M}$

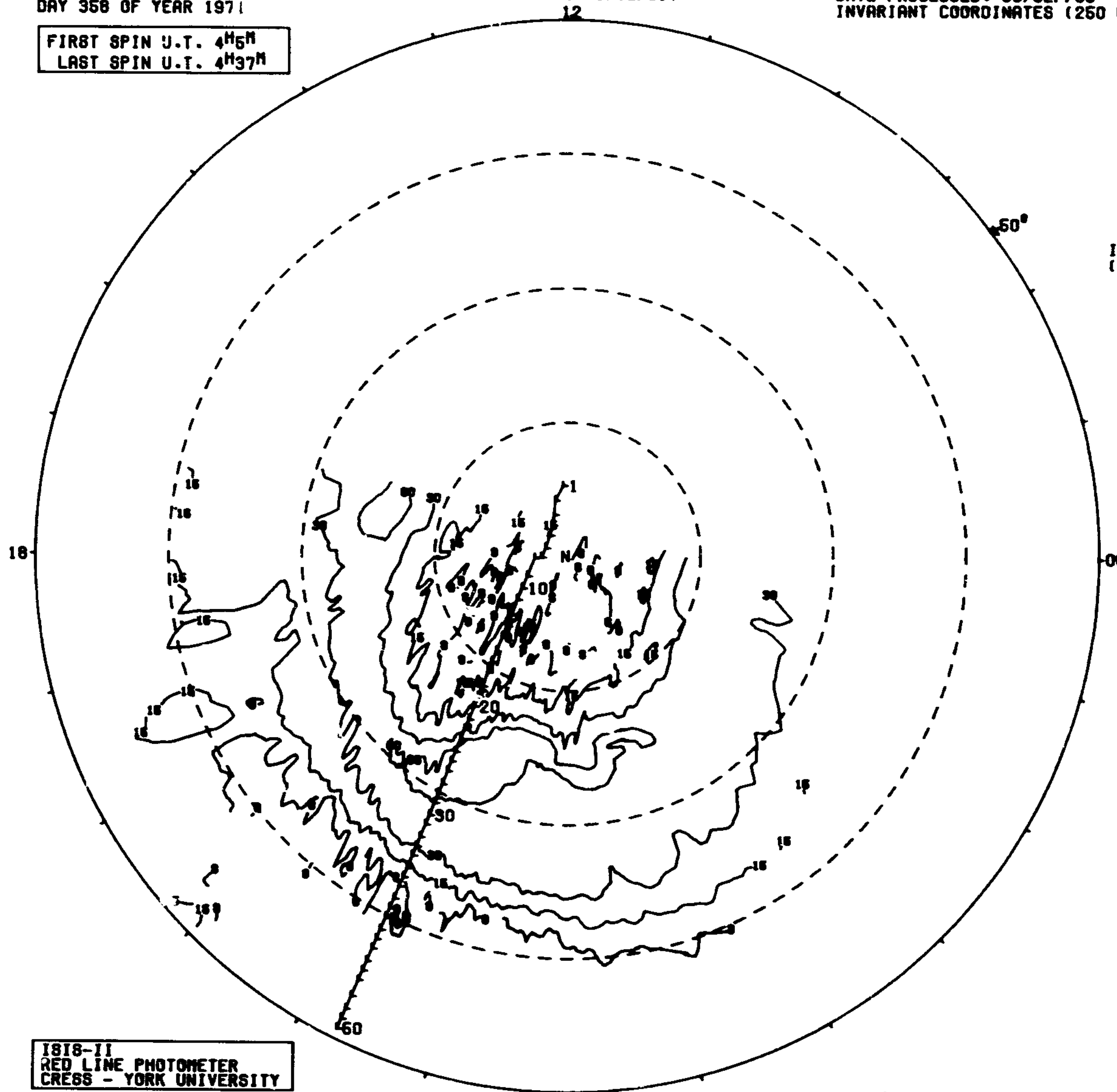

CONTOURS PLOTTED

80
150
300
600
1200
2400
ZENITHAL INTENSITIES (RAYLEIGHS)

SPACECRAFT INFORMATION

SPIN NUMBER	ORBIT TIME (HRMNSC)	INVARIANT LATITUDE (DEGREES)
1	040534	84.0
2	040558	84.3
3	040622	84.3
4	040640	84.3
5	040658	84.3
6	040722	84.2
7	040740	84.2
8	040758	84.3
9	040822	84.3
10	040840	84.3
11	040858	84.3
12	040922	83.9
13	040940	83.4
14	040958	82.8
15	041022	81.9
16	041040	81.2
17	041058	80.3
18	041122	79.2
19	041140	78.5
20	041158	77.7
21	041222	76.7
22	041240	75.9
23	041258	75.1
24	041322	74.1
25	041340	73.3
26	041358	72.5
27	041422	71.4
28	041440	70.6
29	041458	69.8
30	041522	68.7
31	041540	67.9
32	041604	66.8
33	041622	66.0
34	041640	65.2
35	041704	64.1
36	041722	63.3
37	041740	62.5
38	041804	61.4
39	041822	60.6
40	041840	59.7
41	041904	58.6
42	041922	57.8
43	041940	57.0
44	042004	55.9
45	042022	55.1
46	042040	54.3
47	042110	52.9
48	042134	51.8
49	042152	51.0
50	042210	50.2
51	042234	49.2
52	042252	48.4
53	04231[illegible]	47.6
54	04[illegible]4	46.5
55	042352	45.7
56	042410	45.0
57	042434	43.9
58	042452	43.2
59	042510	42.4
60	042534	41.4

ISIS-II
RED LINE PHOTOMETER
CRESS - YORK UNIVERSITY

HRT Y00270
FILE 16

SPACECRAFT TRACK TRACED DOWN TO 250 KM. (NUMBERS DENOTE SPINS)

RX = 0.50
DATA FILTERED
ZERO SUBTRACTION NOT PERFORMED

SET 22, FORMAT 8

ORBIT 3383
DATE 711224
DAY 358

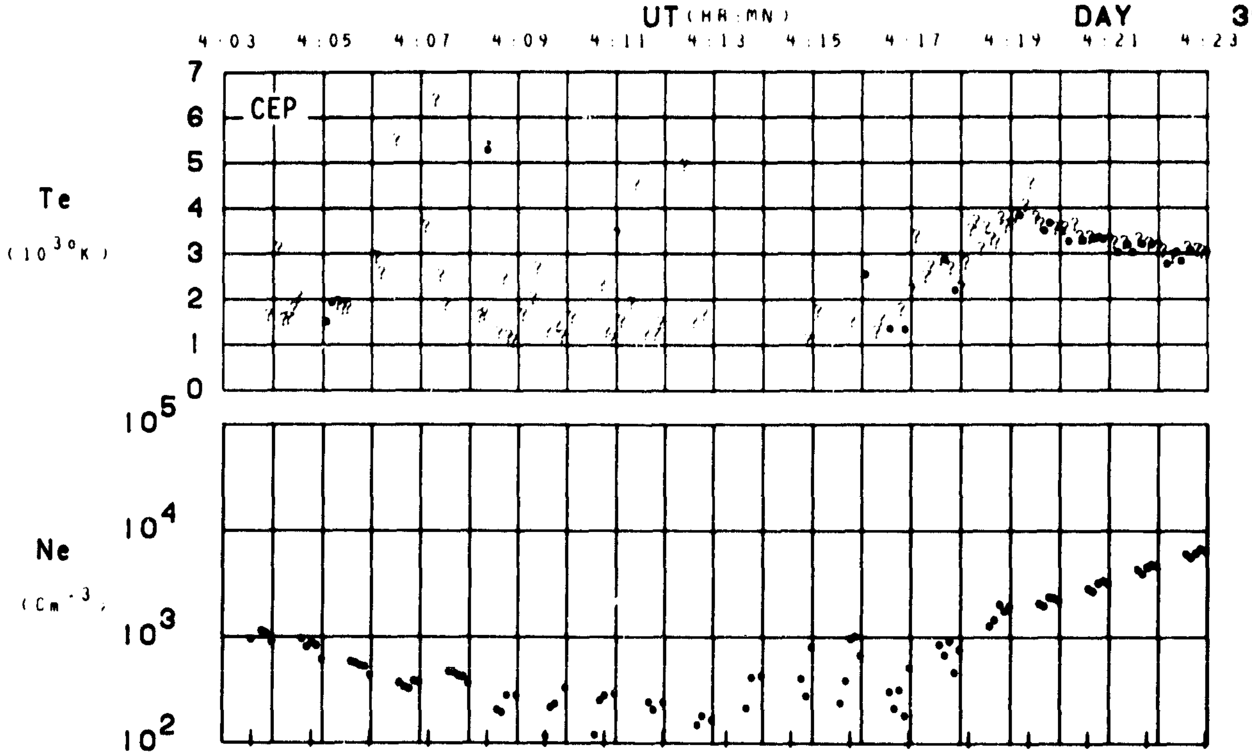

LAT	87	87	84	80	77	73	69	65	61	57	53	50	46	42	38	34	31
LONG	134	-139	-102	-94	-91	-89	-89	-88	-88	-87	-87	-87	-87	-87	-88	-88	-88
LT	18:03	18:47	21:15	21:48	22:02	22:10	22:15	22:18	22:21	22:23	22:25	22:26	22:27	22:28	22:29	22:29	22:30
DIP	88	88	89	-89	89	88	87	87	86	85	84	82	81	80	78	76	74
DIPLAT	87	88	89	89	88	87	86	84	82	80	78	76	74	71	68	65	61
L	30.9	65.1	99.6	99.7	102.4	80.9	40.0	22.2	13.7	9.3	6.9	5.3	4.3	3.5	3.0	2.6	2.2
INVLAT	79	82	84	84	84	83	80	77	74	70	67	64	6'	57	54	51	48
ZA	110	113	117	120	124	127	131	134	138	141	144	147	1[illegible]0	153	155	157	158

SET 22, FORMAT 10

72/008/0551

Excerpts of VLF Spectral film for the period 0551 - 0607

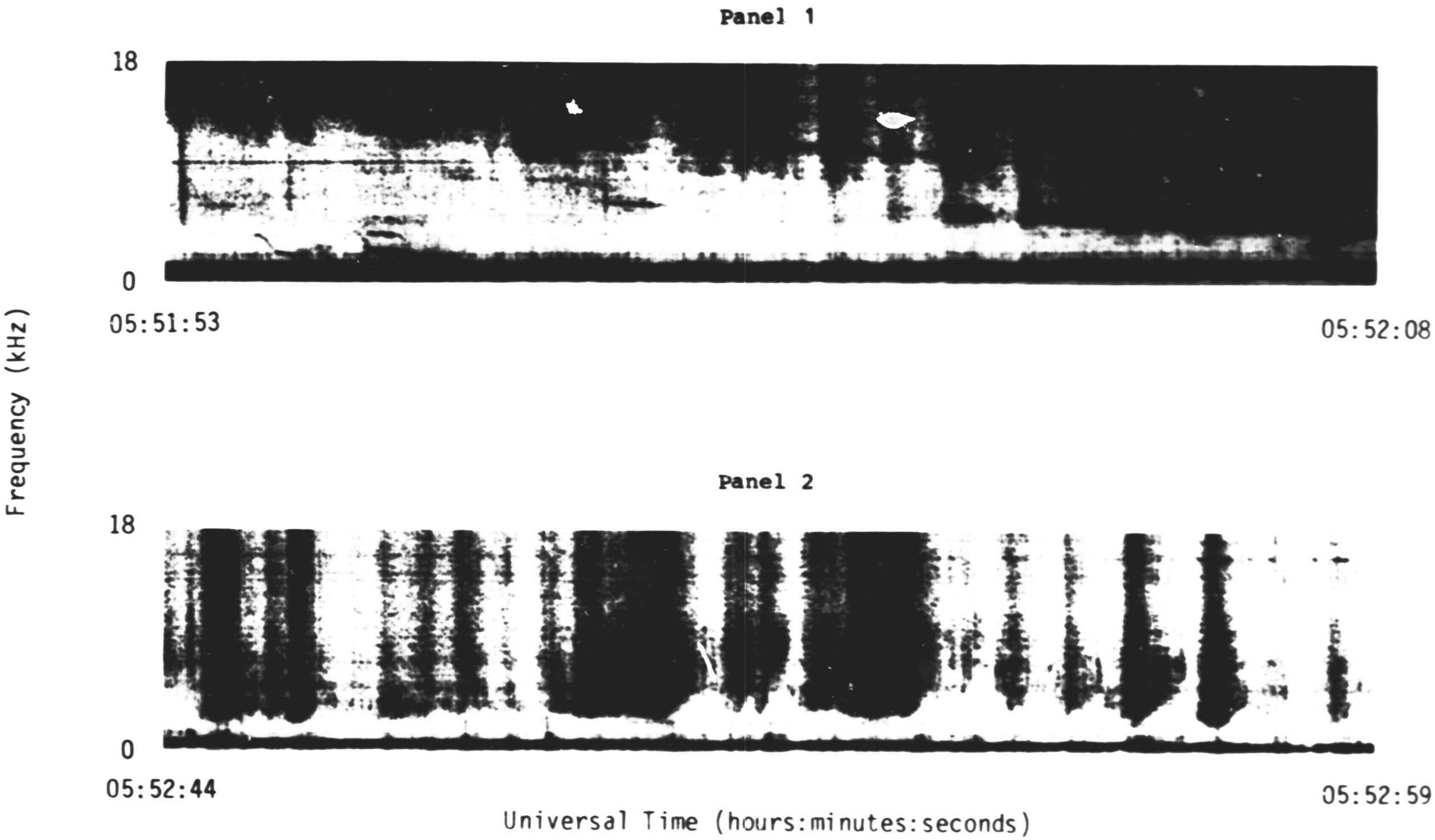

SET 23, FORMAT 11

72/008/0551

Excerpts of VLF Spectral film for the period 0551 - 0607

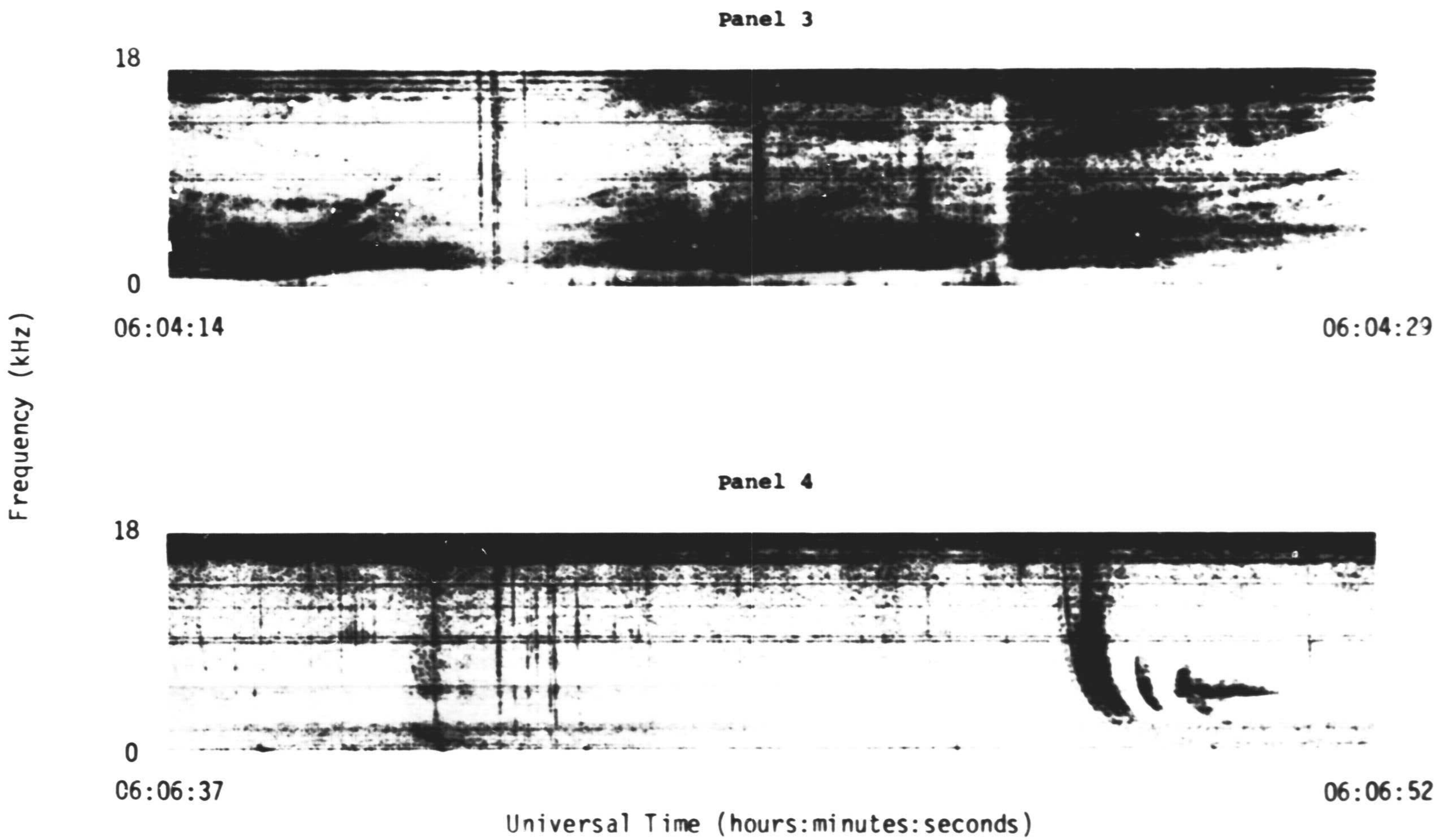

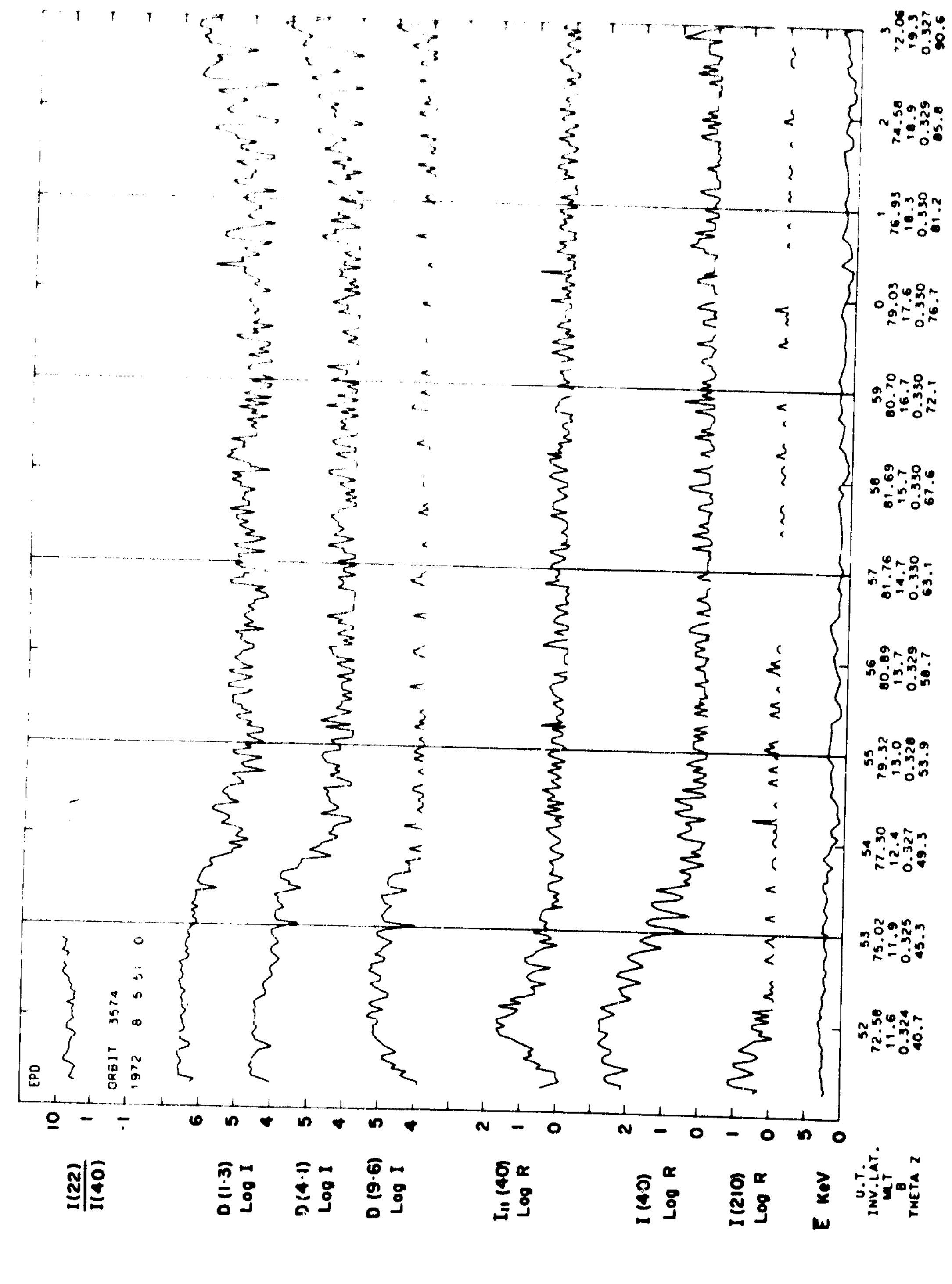

SET 23, FORMAT 3

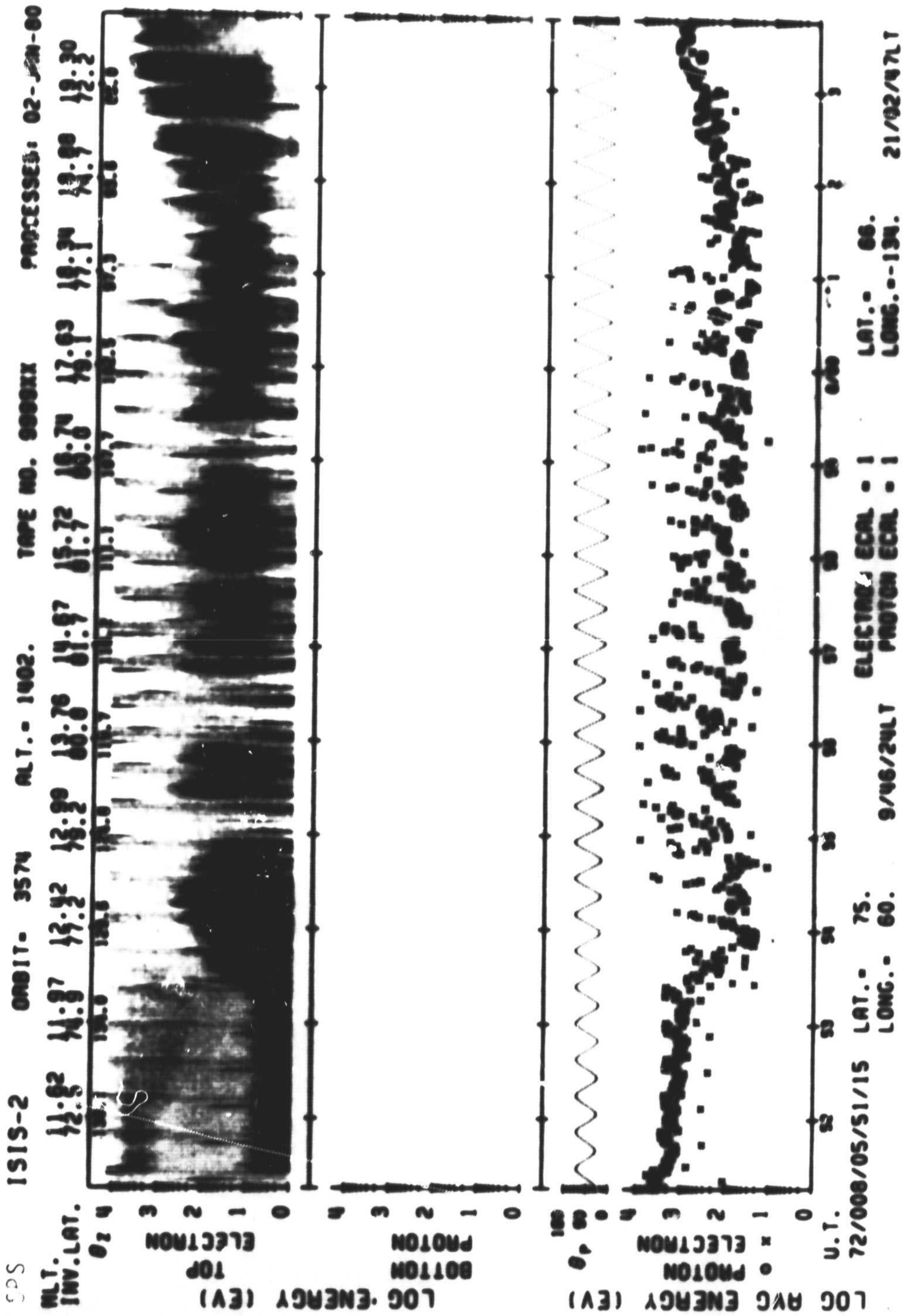

SET 23, FORMAT 6

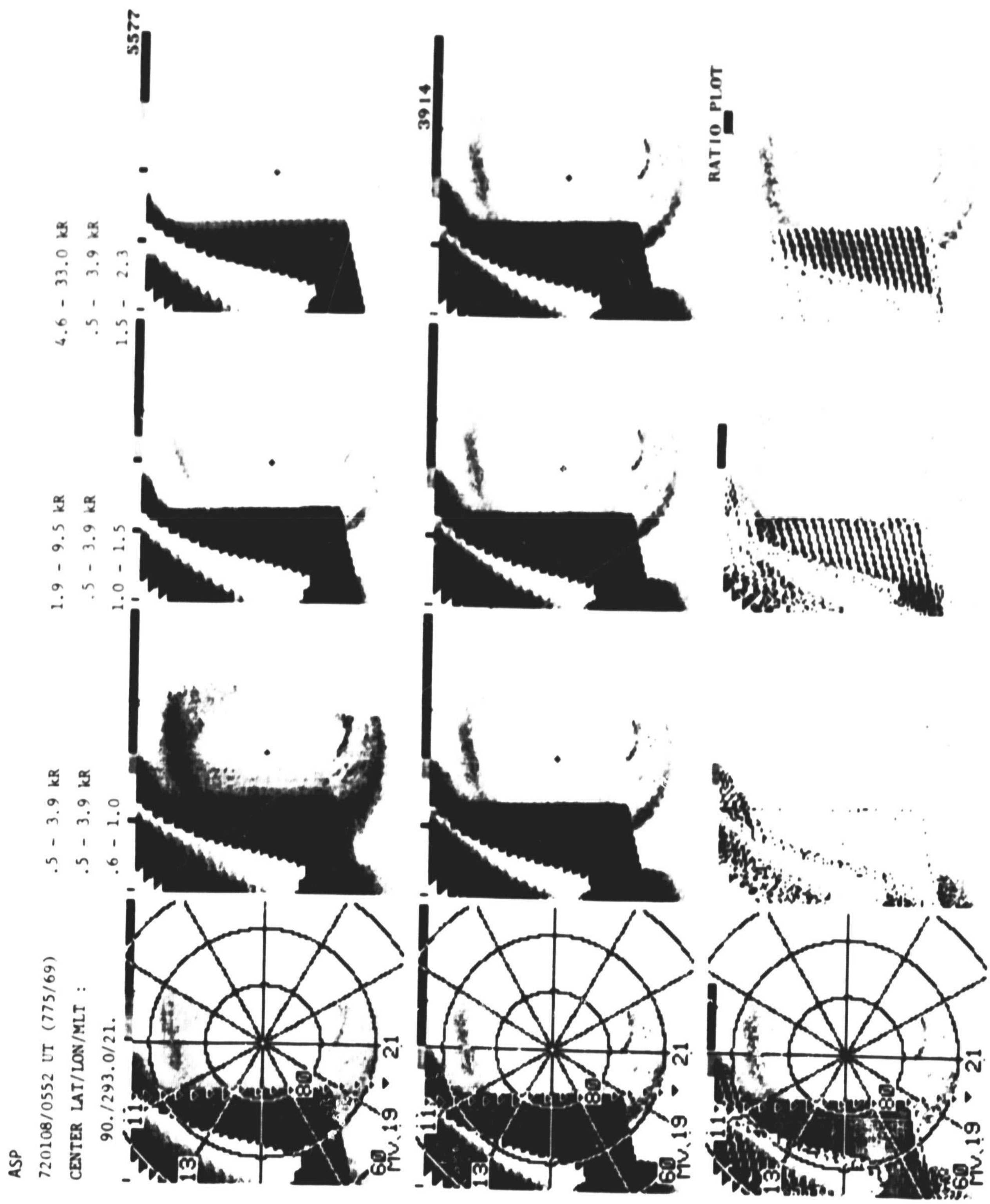

SET 23, FORMAT 7

ORBIT 3574 (72/JAN/8)
DAY 8 OF YEAR 1972

FIRST SPIN U.T. $5^{H}52^{M}$
LAST SPIN U.T. $6^{H}7^{M}$

6300 ANGSTROM INTENSITY

DATE PROCESSED: 79/NOV/01
INVARIANT COORDINATES (250 KM.)

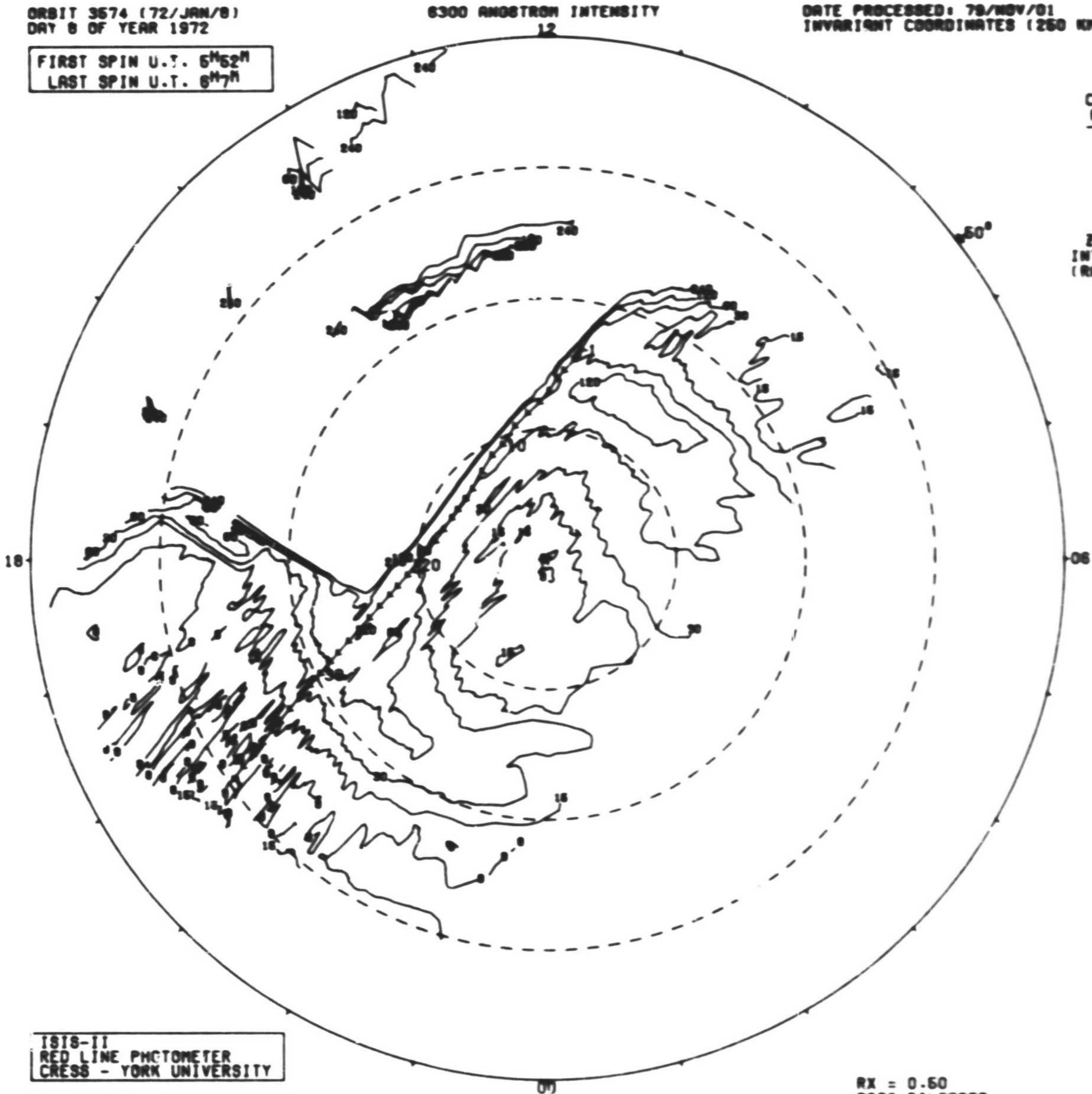

CONTOURS PLOTTED

80
150
300
600
1200
2400
ZENITHAL INTENSITIES (RAYLEIGHS)

SPACECRAFT INFORMATION

SPIN NUMBER	ORBIT TIME (HRMNSC)	INVARIANT LATITUDE (DEGREES)
1	055245	74.4
2	055309	75.4
3	055333	76.3
4	055351	77.0
5	055415	77.8
6	055439	78.7
7	055503	79.4
8	055527	80.1
9	055551	80.7
10	055609	81.1
11	055633	81.5
12	055657	81.7
13	055721	81.8
14	055745	81.8
15	055809	81.6
16	055827	81.4
17	055851	80.9
18	055915	80.3
19	055939	79.7
20	060003	78.9
21	060[illegible]	78.1
22	060[illegible]	77.3
23	0[illegible]	76.6
24	0[illegible]3	75.7
25	[illegible]7	74.7
26	[illegible]21	73.7
27	[illegible]245	72.7
28	[illegible]309	71.7
29	060327	70.9
30	060351	69.8
31	060415	68.8
32	060439	67.7
33	060503	66.6
34	060527	65.5
35	060545	64.7
36	060609	63.6
37	060633	62.5
38	060657	61.4
39	060721	60.3

ISIS-II
RED LINE PHOTOMETER
CRESS - YORK UNIVERSITY

MRT Y00506
FILE 41

SPACECRAFT TRACK TRACED DOWN TO 250 KM. (NUMBERS DENOTE SPINS)

RX = 0.60
DATA FILTERED
ZERO SUBTRACTION NOT PERFORMED

SET 23, FORMAT 8

ORBIT 3574
DATE 720108
DAY 8

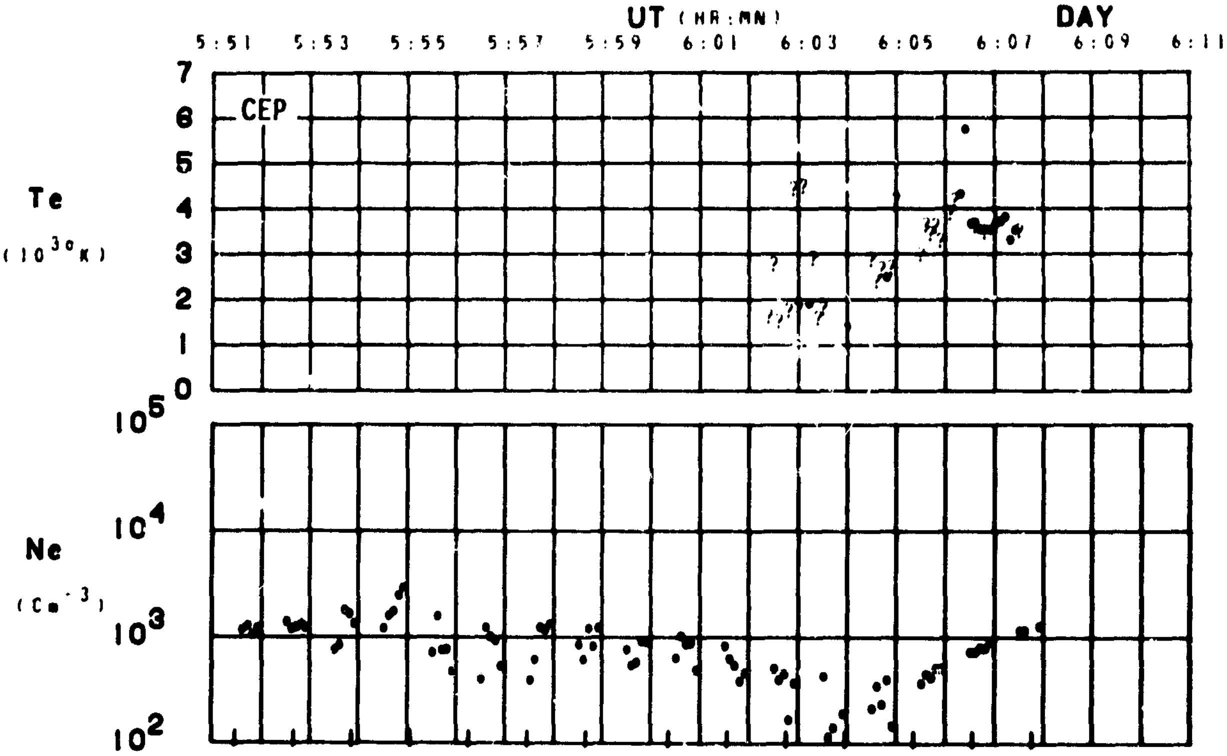

LAT	75	79	83	86	87	84	81	75	72	68	64	60	56	52
LONG	60	63	68	85	163	-147	-140	-136	-134	-134	-133	-133	-133	-133
LT	9:47	9:58	10:21	11:32	16:42	20:01	20:30	20:49	20:56	21:00	21:03	21:06	21:07	21:09
DIP	81	83	85	86	87	87	86	84	82	81	79	76	74	71
DIPLAT	74	78	81	82	85	85	83	79	76	72	69	64	60	56
L	9.6	13.5	19.7	29.7	42.7	49.7	42.3	24.5	16.3	11.3	8.2	6.0	4.7	3.8
INVLAT	71	74	76	79	81	81	81	78	75	72	69	65	62	59
ZA	100	103	106	108	111	114	117	121	124	126	129	131	133	135

SET 23, FORMAT 10

71/226/0409

Excerpts of VLF Spectral film for the period 0410 - 0425

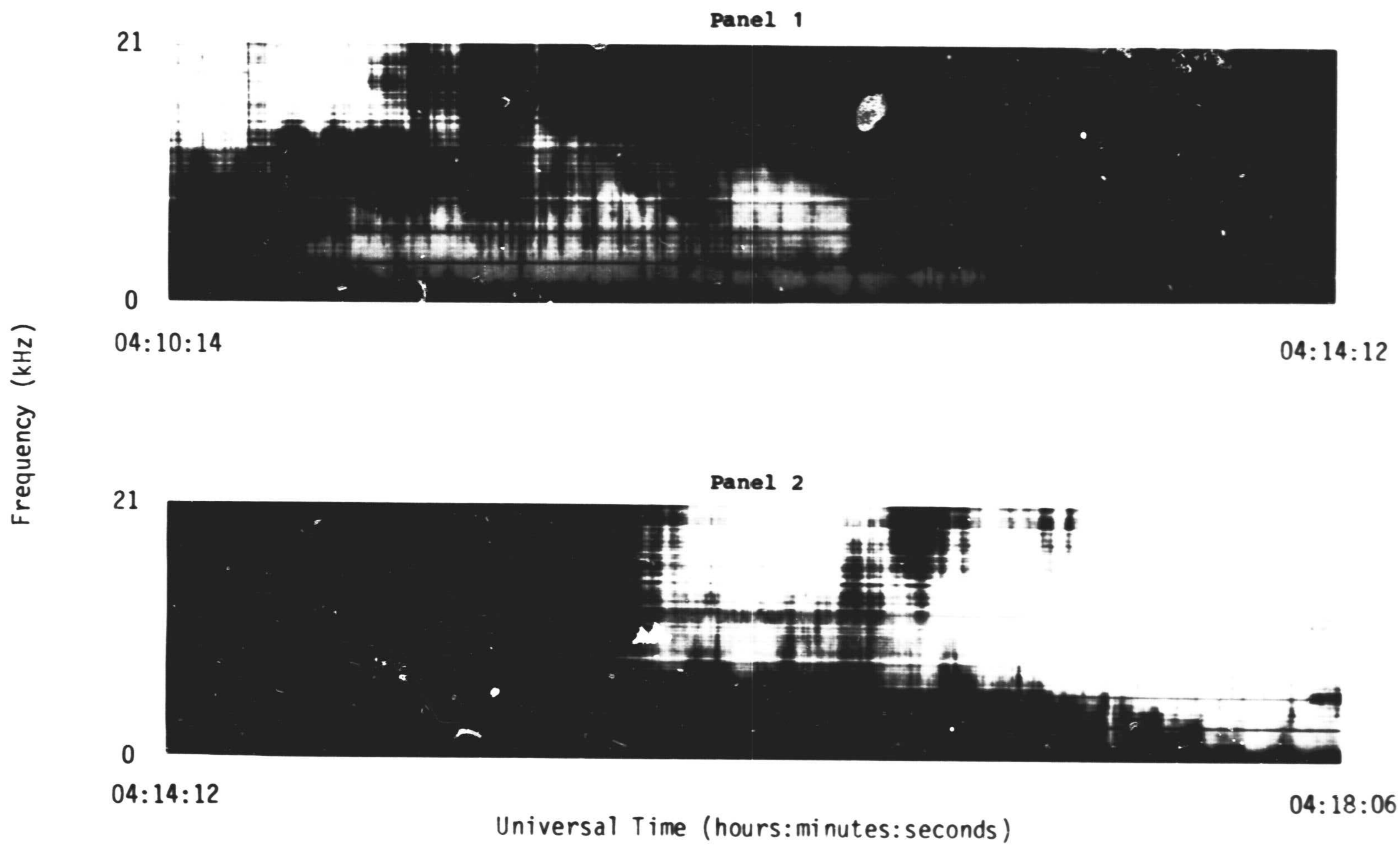

71/226/0409

Excerpts of VLF Spectral film for the period 0410 - 0425

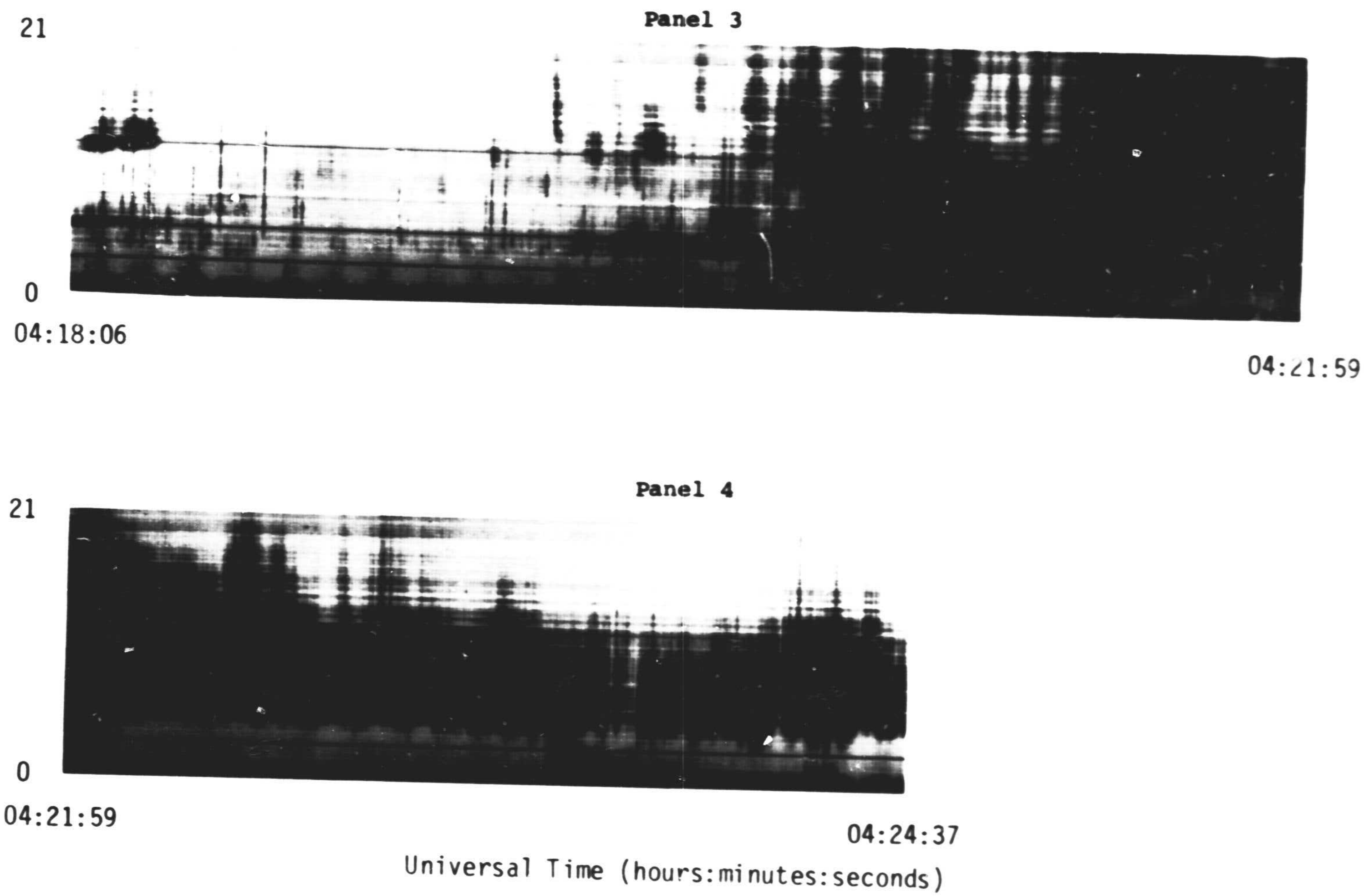

SET 24, FORMAT 11

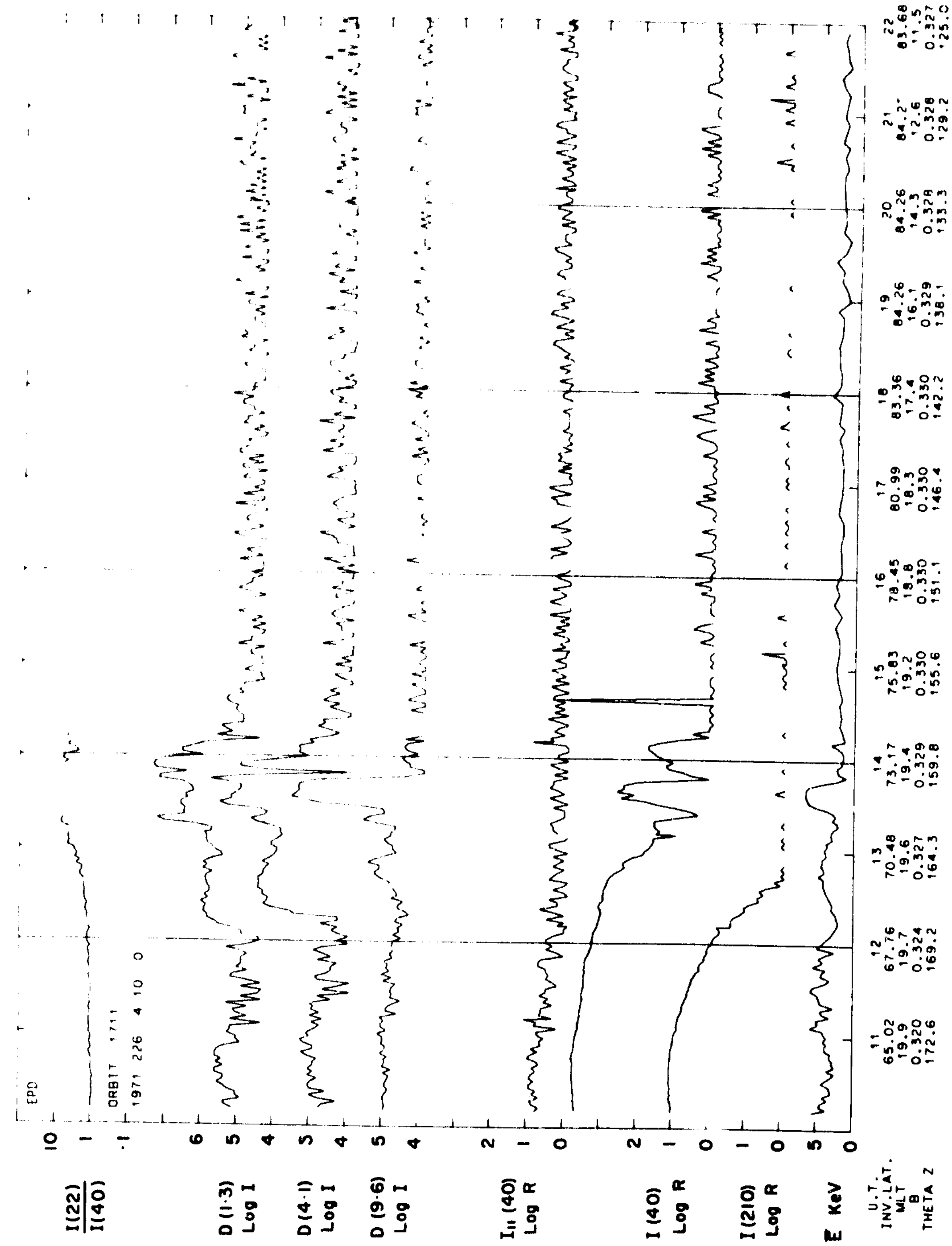

SET 24, FORMAT 3

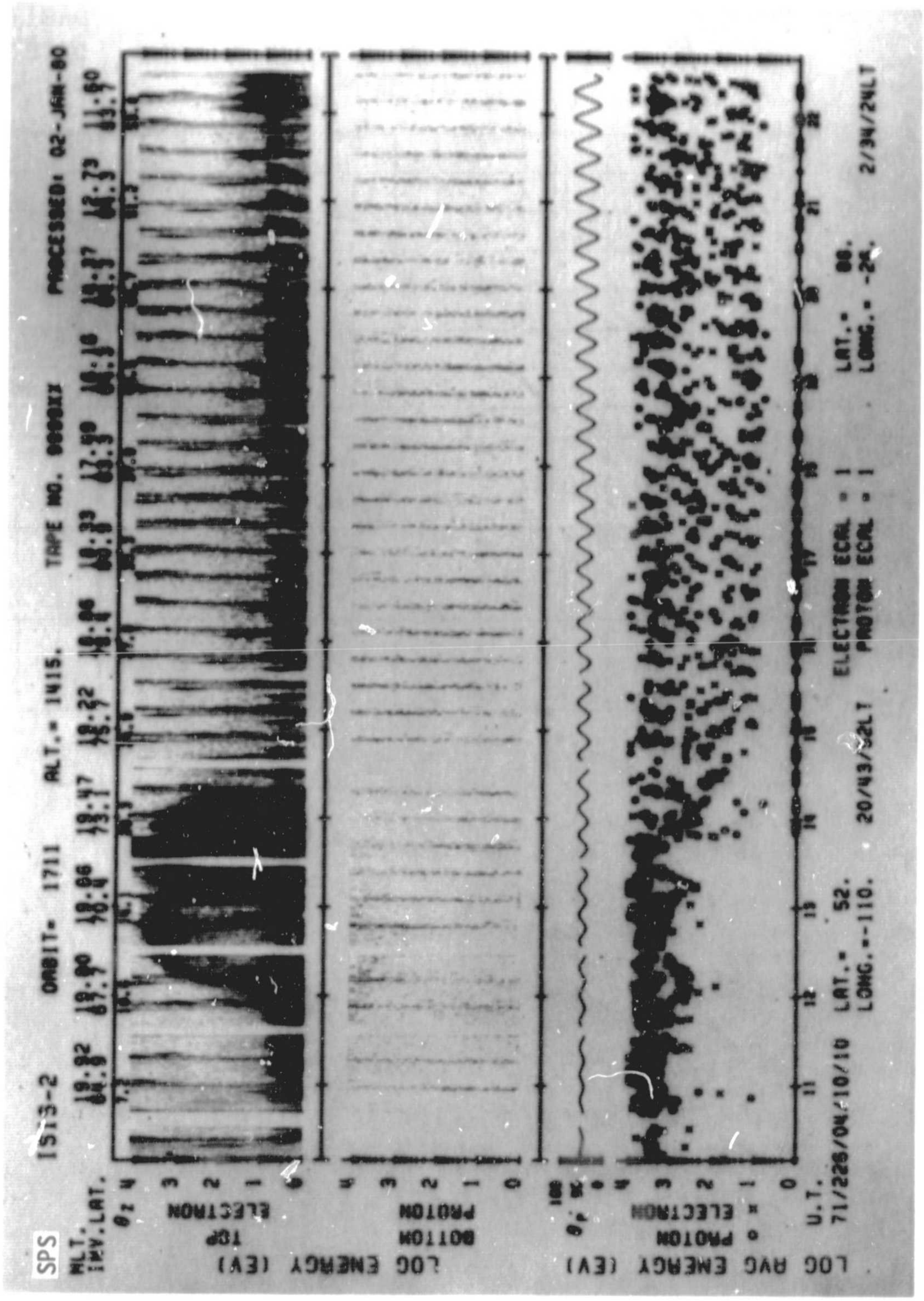

SET 24, FORMAT 6

ORBIT 1711
DATE 710814
DAY 226

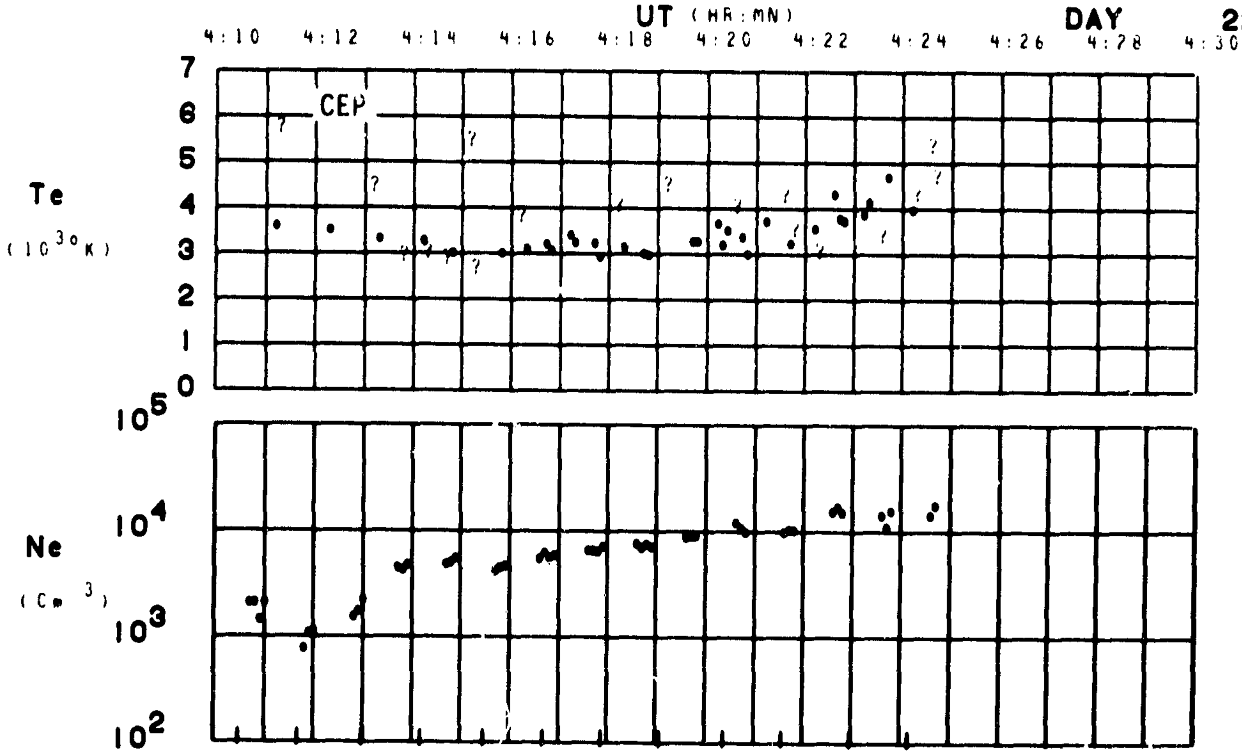

LAT	52	56	60	64	68	72	75	79	83	87	87	83
LONG	-110	-110	-110	-109	-109	-108	-107	-104	-99	-76	21	46
LT	20:44	20:45	20:47	20:49	20:53	20:57	21:03	21:14	21:37	23:09	5:44	7:24
DIP	75	78	80	82	84	86	87	88	89	88	86	85
DIPLAT	63	67	71	75	79	82	85	88	89	87	83	80
L	5.0	6.5	8.9	12.6	20.0	33.6	70.5	100.8	100.6	93.3	45.0	24.8
INVLAT	63	66	70	73	77	80	83	84	84	84	81	78
ZA	100	98	95	93	90	88	85	83	80	78	75	73

SFT 24, FORMAT 10

The following is a list of past and present contributors to the Alouette-ISIS Program. The list has been compiled to give credit to the many individuals who have participated significantly in the planning, growth, development, or management of the Alouette-ISIS spacecraft, and in the analysis of the resultant data.

The contributors have been listed under their sponsoring agency at the time of their participation in the program. In cases where organizations have changed names, the present name has been used, and former designations are given in parentheses.

An effort has been made to make the list as complete as possible. Any omission is purely unintentional.

LIST OF CONTRIBUTORS TO THE ALOUETTE-ISIS PROGRAM

AUSTRALIA

Ionospheric Prediction Service

P. L. Dyson
C. G. McCue
J. Turner

CANADA

Communications Research Centre (DRTE)

R. E. Barrington
J. S. Belrose
R. J. Bibby
J. D. R. Boulding
R. K. Brown
W. S. Campbell
J. H. Chapman
F. Daniels
C. D. Florida
C. A. Franklin
T. Garrett
R.S. Gruno
E. L. Hagg
T. R. Hartz
L. Herzberg
E. D. Hewens
N. S. Hitchcock
H. G. James
D. H. Jelly
R. C. Langille
G. E. K. Lockwood
M. A. Maclean
J. Mar
J. S. Matsushita
A. R. Molozzi
D. B. Muldrew
G. L. Nelms
I. Paghis
F. H. Palmer
L. E. Petrie
H. R. Raine
R. P. Sharma
R. W. Southern
P. H. Timleck
E. S. Warren
J. H. Whitteker

National Research Council

S. Babey
E. E. Budzinski
J. R. Burrows
J. C. Foster
I. B. McDiarmid
D. C. Rose
P. Venkatranagan
D. D. Wallis
M. D. Wilson

Spar Aerospace Ltd. (DeHaviland Aircraft Co.)

H. S. Kerr
H. R. Warren

Spar Aerospace Ltd. (RCA Victor Company, Ltd.)

T. Fancott
J. McNally
F. J. F. Osborne
J. M. Stewart

University of Calgary

C. D. Anger
L. L. Cogger
R. Elphinstone
S. Ismail
R. Khaneja
A. T. Y. Lui
M. C. Moshupi
J. S. Murphree
W. Sawchuk
R. H. Wiens

University of Victoria

R. E. Horita

University of Western Ontario

P. A. Forsyth
G. F. Lyon
E. H. Tull

York University

F. E. Bunn
B. Gertner
D. Goel
C. F. Martin
G. G. Shepherd
E. Stathopoulos
F. W. Thirkettle

FRANCE

Centre National d'Etudes des Telecommunications

J. Bitoun
F. DuCastel
J. M. Faynot
R. Feldstein
L. Fleury
P. Graff
B. Higel
M. Petit
M. Sylvain
C. Taieb
G. Vasseur
P. M. Vila

GERMANY

Freiburg

R. Kist

HONG KONG

University of Hong Kong

G. O. Walker

INDIA

Physical Research Laboratory

R. Raghava Rao

JAPAN

Radio Research Laboratory

Y. Hakura
H. Hojo
H. Inuki
N. Matuura
M. Nagayama
R. Nishizaki
Y. Ogata
T. Ondoh
H. Oya
K. Tao

NEW ZEALAND

Department of Scientific and Industrial Research

M. K. Andrews
G. J. Burtt
M. R. Deshpande
G. Keys
R. Lobb
F. A. McNeill
C. A. Roper
G. F. Stuart
J. E. Titheridge
R. S. Unwin

NORWAY

Auroral Observatory

O. Holt
B. Landmark

Royal Norwegian Council for Scientific and Industrial Research (NTNF)

K. Melby

UNITED KINGDOM

Appleton Laboratory (RSRS, RRS)

J. D. Burge
D. Eccles
J. W. King
G. W. Luscombe
P. A. Smith

Imperial College

J. O. Thomas

University College

R. L. F. Boyd
A. P. Willmore
G. L. Wrenn

U. K. Scientific Mission Washington, D.C.

H. K. Bourne

UNITED STATES

Air Force Geophysics Laboratory (AFCRL)

R. S. Narcisi
C. Pikes
R. Sagalyn
M. Smiddy

Airborne Instruments Laboratory

S. H. Gross
S. Russell III
F. C. Zimmer

Applied Physics Laboratory

D. Bianco

Batelle Memorial Institute

L. L. Smith
H. Liemohn

NASA Ames Research Center

K. L. Chan
L. Colin
S. W. Dufour
D. S. Willoughby

NASA Goddard Space Flight Center

S. J. Bauer
R. F. Benson
R. E. Bourdeau
L. H. Brace
S. Chandra
J. F. Clark
J. L. Donley
L. L. Dubach
J. A. Findlay
R. J. Fitzenreiter
C. H. Freeman
W. H. Hoggard
R. A. Goldberg
E. J. Gregg
J. E. Jackson
E. J. R. Maier
N. J. Miller
E. D. Nelsen
G. W. Ousley
G. F. Pieper
B. C. Narasinga Rao
R. W. Rhodes
R. S. Sade
R. G. Sanford
J. F. South
N. W. Spencer
R. G. Stone
R. F. Theis
B. E. Troy
R. M. Tysdal

NASA Headquarters

S. Andrews
M. J. Aucremanne
R. Barnes
F. W. Gaetano
D. R. Hallenbeck
J. L. Mitchell
J. R. Morrison
J. E. Naugle
A. G. Opp
E. R. Schmerling
W. E. Williams

NASA John F. Kennedy Space Center

J. Schwartz

National Oceanic and Atmospheric Administration (ESSA-ITSA-CRPL)

W. Calvert
J. A. Fejer
E. E. Ferguson
G. B. Goe
R. G. Green
R. Knecht
E. Marovich
J. R. McAfee
L. Miller
R. B. Norton
E. R. Schiffmacher
T. E. Van Zandt
J. M. Warnock
E. C. Whipple

University of California - Los Angeles

J. D. Barry
P. J. Coleman, Jr.

University of Colorado - Boulder

L. M. Libby
W. F. Libby

University of Texas - Dallas (SCAS)

E. L. Breig
W. H. Dodson
W. J. Heikkila
J. H. Hoffman
D. M. Klumpar
C. R. Lippincott
J. R. Sharber
J. B. Smith
J. D. Winningham

U.S. Army Signal Research and Development Laboratory

P. R. Arendt
V. J. Rosati
H. Soicher

INDEX

VOLUMES 1, 2, 3, AND 4

Date	Day	Time	Vol. No.	5577Å Height Pro-files	5577Å Lat. Pro-files	6300Å Lat. Pro-files	ASP	CEP	EPD	IMS	Magne-tometer	Optical Data and SPS	RLP	RPA	Sounder	SPS	VLF
71 May 15	135	0905	4	-	-	-	-	119	-	-	-	-	-	120	-	-	117
71 Jul. 02	183	0329	4	-	-	-	-	131	129	-	-	-	-	-	-	130	127
71 Aug. 14	226	0409	4	-	-	-	-	168	166	-	-	-	-	-	-	167	164
71 Oct. 13	286	0811	2	-	-	-	-	97	-	-	-	94	-	98	96	95	-
71 Oct. 13	286	0959	2	-	-	-	-	101	-	-	-	99	-	102	-	100	-
71 Oct. 17	290	0850	4	82	81	-	-	84	-	-	-	-	-	85	83	86	-
71 Oct. 19	292	0759	2	-	-	-	-	155	-	155	-	152	-	156	154	153	-
71 Oct. 22	295	0807	2	-	-	-	-	112	-	112	111	109	-	113	111	110	-
71 Oct. 23	296	0642	4	-	-	-	-	159	-	159	-	157	-	160	-	158	161
71 Oct. 23	296	0636	2	-	-	-	-	165	-	165	-	163	-	166	-	164	-
71 Oct. 23	296	0842	2	-	-	-	-	85	-	85	-	83	-	86	-	84	87
71 Oct. 24	297	0725	2	-	-	-	-	92	-	92	91	89	-	93	91	90	-
71 Oct. 29	302	0650	2	-	-	-	-	107	105	107	106	103	-	108	106	104	-
71 Oct. 30	303	0727	2	-	-	-	-	118	116	118	117	114	-	119	117	115	-
71 Nov. 11	315	0727	2	-	-	-	-	57	55	-	56	53	-	58	56	54	-
71 Nov. 16	320	0644	2	-	-	-	-	45	43	45	44	41	-	46	44	42	-
71 Nov. 17	321	0524	2	-	-	-	-	124	122	124	123	120	-	125	123	121	-
71 Nov. 17	321	0718	2	-	-	-	-	150	148	150	149	146	-	151	149	147	-
71 Nov. 17	321	0722	2	-	-	-	-	39	37	39	38	35	-	40	38	36	-
71 Nov. 18	322	0413	2	-	-	-	-	63	61	63	62	59	-	64	62	60	-
71 Nov. 18	322	0600	2	-	-	-	-	138	136	138	137	134	-	139	137	135	-
71 Nov. 18	322	0605	2	-	-	-	-	51	49	51	50	47	-	52	50	48	-
71 Nov. 20	324	0523	2	-	-	-	-	130	128	130	129	126	-	131	-	127	132
71 Nov. 22	326	0445	2	-	-	-	-	144	142	144	143	140	-	145	-	141	-
71 Nov. 22	326	0452	2	-	-	-	-	69	67	69	68	65	-	70	-	66	-
71 Nov. 22	326	0648	4	87	-	-	-	90	93	90	-	-	-	91	89	92	94
71 Nov. 22	326	0648	2	-	-	-	-	81	79	81	80	77	-	82	80	78	-
71 Nov. 23	327	0538	4	98	96	97	-	99	-	99	-	-	-	100	-	101	-
71 Nov. 24	328	0607	2	-	-	-	-	75	73	-	74	71	-	76	-	72	-
71 Nov. 27	331	0414	4	-	-	-	-	141	140	-	-	-	-	142	-	143	138
71 Dec. 15	349	0400	1	-	-	-	77	80	78	-	-	-	-	-	80	79	-
71 Dec. 15	349	0408	1	-	-	-	159	162	160	-	-	-	-	-	162	161	-
71 Dec. 15	349	0600	1	-	-	-	163	166	164	-	-	-	-	-	166	165	-
71 Dec. 17	351	0518	4	-	-	-	-	-	36	-	-	-	35	-	37	-	-
71 Dec. 17	351	0705	4	-	-	-	-	-	38	-	-	-	-	-	40	39	-
71 Dec. 17	351	0717	4	-	-	-	-	-	41	-	-	-	-	-	43	42	-
71 Dec. 18	352	0207	4	-	-	-	44	48	46	-	-	-	45	-	48	47	-
71 Dec. 18	352	0402	4	-	-	-	49	53	51	-	-	-	50	-	53	52	-
71 Dec. 18	352	0556	4	-	-	-	54	58	56	-	-	-	55	-	58	57	-
71 Dec. 19	353	0246	4	-	-	-	59	63	61	-	-	-	60	-	63	62	-
71 Dec. 20	354	0324	4	-	-	-	64	68	66	-	-	-	65	-	68	67	-
71 Dec. 20	354	0518	4	-	-	-	69	73	71	-	-	-	70	-	73	72	-
71 Dec. 21	355	0402	4	-	-	-	74	78	76	-	-	-	75	-	-	77	-
71 Dec. 22	356	0445	1	-	-	-	181	184	182	-	-	-	-	-	184	183	-
71 Dec. 24	358	0403	4	-	-	-	154	156	152	-	-	-	155	-	-	153	150
71 Dec. 24	358	0415	4	-	-	-	147	149	145	-	-	-	148	-	149	146	144
71 Dec. 27	361	0212	1	-	-	-	171	175	173	-	-	-	172	-	175	174	-
71 Dec. 27	361	0406	1	-	-	-	176	180	178	-	-	-	177	-	180	179	-
72 Jan. 08	008	0551	4	-	-	-	161	163	159	-	-	-	162	-	-	160	157
72 Jan. 09	009	0248	1	-	-	-	144	148	146	-	-	-	145	-	148	147	-
72 Jan. 10	010	0325	1	-	-	-	140	143	142	-	-	-	141	-	143	-	-
72 Jan. 11	011	0019	1	-	-	-	185	189	187	-	-	-	186	-	189	188	-
72 Jan. 11	011	0214	1	-	-	-	154	158	156	-	-	-	155	-	-	157	-
72 Jan. 16	016	0325	1	-	-	-	149	153	151	-	-	-	150	-	153	152	-
72 Feb. 06	037	0321	1	-	-	-	116	120	118	-	-	-	117	-	120	119	-

Date	Day	Time	Vol. No.	5577Å Height Pro-files	5577Å Lat. Pro-files	6300Å Lat. Pro-files	ASP	CEP	EPD	IMS	Magne-tometer	Optical Data and SPS	RLP	RPA	Sounder	SPS	VLF
72 Feb. 06	037	0515	1	-	-	-	121	125	123	-	-	-	122	-	125	124	-
72 Feb. 08	039	0629	1	-	-	-	111	115	113	-	-	-	112	-	115	114	-
72 Feb. 10	041	0358	1	-	-	-	126	130	128	-	-	-	127	-	130	129	-
72 Apr. 20	111	0730	4	104	102	103	-	106	-	-	-	-	-	-	105	107	-
72 Apr. 21	112	0610	4	110	108	109	-	112	-	-	-	-	-	113	111	114	-
72 May 12	133	1041	3	-	-	-	-	209	208	209	207	-	-	210	-	206	211
72 May 23	144	0559	3	-	-	-	-	142	141	142	-	-	-	143	140	139	-
72 May 23	144	0807	3	-	-	-	-	86	85	86	-	-	-	87	84	83	-
72 May 31	152	0727	3	-	-	-	-	195	194	-	-	-	-	-	193	192	-
72 June 03	155	0922	3	-	-	-	-	204	203	-	202	-	-	205	202	201	-
72 June 04	156	0806	3	-	-	-	-	190	189	-	188	-	-	191	188	187	-
72 June 05	157	0843	3	-	-	-	-	199	198	199	197	-	-	200	197	196	-
72 June 05	157	0948	2	-	-	-	-	231	229	231	230	227	-	232	230	228	-
72 June 11	163	0843	3	-	-	-	-	91	90	91	89	-	-	92	89	88	-
72 June 11	163	0948	2	-	-	-	-	213	[illegible]	213	212	209	-	214	212	210	-
72 June 12	164	0713	3	-	-	-	-	118	117	118	116	-	-	119	-	115	120
72 June 12	164	0725	3	-	-	-	-	79	78	79	77	-	-	80	-	76	81
72 June 12	164	0920	3	-	-	-	-	96	95	96	94	-	-	97	-	93	98
72 June 13	165	0909	2	-	-	-	-	207	205	207	206	203	-	208	206	204	-
72 June 15	167	1025	2	-	-	-	-	219	[illegible]	219	218	215	-	220	218	216	-
72 June 18	170	0126	2	-	-	-	-	243	241	243	242	239	-	244	242	240	-
72 June 23	175	0635	3	-	-	-	-	239	238	239	237	-	-	240	237	236	-
72 June 23	175	0647	3	-	-	-	-	185	184	185	183	-	-	186	183	182	-
72 June 25	177	0609	3	-	-	-	-	74	73	-	72	-	-	75	72	71	-
72 June 27	179	0712	3	-	-	-	-	234	233	234	232	-	-	235	232	231	-
72 July 03	185	1834	3	-	-	-	-	147	146	147	145	-	-	148	145	144	-
72 July 04	186	1719	3	-	-	-	-	135	134	135	133	-	-	136	-	132	137
72 July 04	186	1731	3	-	-	-	-	47	46	47	45	-	-	48	-	44	49
72 July 07	189	1719	3	-	-	-	-	249	248	249	247	-	-	250	247	246	-
72 July 07	189	1731	3	-	-	-	-	152	151	152	150	-	-	153	150	149	-
72 July 08	190	0048	3	-	-	-	-	244	243	244	242	-	-	245	-	241	-
72 July 08	190	0750	2	-	-	-	-	237	235	237	236	233	-	238	236	234	-
72 July 08	190	2332	3	-	-	-	-	125	124	125	123	-	-	126	123	122	-
72 July 10	192	0712	2	-	-	-	-	225	223	225	224	221	-	226	224	222	-
72 July 10	192	1910	3	-	-	-	-	254	253	254	252	-	-	255	252	251	-
72 July 10	192	1922	3	-	-	-	-	157	156	157	155	-	-	158	155	154	-
72 July 11	193	0750	2	-	-	-	-	201	199	201	200	197	-	202	-	198	-
72 July 13	195	0400	3	-	-	-	-	108	107	108	106	-	-	109	106	105	-
72 July 13	195	0712	2	-	-	-	-	171	169	171	170	167	-	172	170	168	-
72 July 13	195	0751	3	-	-	-	-	113	112	113	111	-	-	114	111	110	-
72 July 14	196	0749	2	-	-	-	-	177	175	177	176	173	-	178	176	174	-
72 July 14	196	1037	3	-	-	-	-	59	58	59	57	-	-	60	57	56	-
72 July 14	196	1231	3	-	-	-	-	54	53	54	52	-	-	55	52	51	-
72 July 15	197	0634	2	-	-	-	-	183	181	183	182	179	-	184	182	180	-
72 July 15	197	1448	3	-	-	-	-	130	129	130	128	-	-	131	128	127	-
72 July 15	197	1500	3	-	-	-	-	42	41	42	40	-	-	43	40	39	-
72 July 16	198	0711	2	-	-	-	-	195	193	195	194	191	-	196	194	192	-
72 July 22	204	0359	3	-	-	-	-	103	102	103	101	-	-	104	101	100	-
72 July 22	204	0607	3	-	-	-	-	69	68	69	67	-	-	70	67	66	-
72 July 22	204	0801	3	-	-	-	-	64	63	64	62	-	-	65	62	61	-
72 July 24	206	1114	3	-	-	-	-	162	161	162	160	-	-	163	160	159	-
72 July 25	207	0359	3	-	-	-	-	228	227	228	226	-	-	-	-	225	229
72 July 25	207	0411	3	-	-	-	-	179	178	179	177	-	-	-	-	176	180
72 July 27	209	0517	3	-	-	-	-	223	222	223	221	-	-	224	221	220	-
72 July 27	209	0529	3	-	-	-	-	174	173	174	172	-	-	175	172	171	-

INDEX (concluded)

Date	Day	Time	Vol. No.	5577Å Height Profiles	5577Å Lat. Profiles	6300Å Lat. Profiles	ASP	CEP	EPD	IMS	Magnetometer	Optical Data and SPS	RLP	RPA	Sounder	SPS	VLF
72 Aug. 01	214	0437	3	-	-	-	-	216	215	216	214	-	-	217	-	213	218
72 Aug. 01	214	0449	3	-	-	-	-	167	166	167	165	-	-	168	-	164	169
72 Aug. 02	215	0631	2	-	-	-	-	189	187	189	188	185	-	190	188	186	-
72 Oct. 11	285	0559	1	-	-	-	42	46	44	-	-	-	43	-	-	43	47
72 Oct. 12	286	0442	1	-	-	-	37	41	39	-	-	-	38	-	41	40	-
72 Oct. 12	286	0636	1	-	-	-	167	170	168	-	-	-	-	-	170	169	-
73 Jan. 13	013	1145	1	-	-	-	65	68	67	-	-	-	66	-	68	-	-
73 Jan. 25	025	0412	1	-	-	-	61	64	63	-	-	-	62	-	64	-	-
73 Jan. 31	031	0412	1	-	-	-	53	56	55	-	-	-	54	-	56	-	-
73 Feb. 04	035	0448	1	-	-	-	57	60	59	-	-	-	58	-	60	-	-
73 Feb. 04	035	0455	1	-	-	-	100	102	101	-	-	-	-	-	102	-	-
73 Feb. 24	055	0749	1	-	-	-	49	52	51	-	-	-	50	-	52	-	-
73 Jun. 18	169	0951	4	-	-	-	-	136	135	136	-	-	-	137	134	-	132
73 Jul. 04	185	0833	4	-	-	-	-	-	124	125	-	-	-	126	123	-	121
73 Dec. 23	357	0058	1	-	-	-	88	91	90	-	-	-	89	-	91	-	-
73 Dec. 31	365	1140	1	-	-	-	131	134	133	-	-	-	132	-	134	-	-
74 Jan. 01	001	1218	1	-	-	-	135	137	136	-	-	-	-	-	137	-	138
74 Dec. 03	337	0931	1	-	-	-	103	-	105	-	-	-	104	-	106	-	-
74 Dec. 14	348	0851	1	-	-	-	107	110	109	-	-	-	108	-	110	-	-
74 Dec. 14	348	1044	1	-	-	-	96	99	98	-	-	-	97	-	99	-	-
75 Nov. 29	333	0721	1	-	-	-	92	95	94	-	-	-	93	-	95	-	-
75 Dec. 03	337	0953	1	-	-	-	85	87	-	-	-	-	86	-	87	-	-
75 Dec. 09	343	2113	1	-	-	-	73	-	75	-	-	-	74	-	76	-	-
75 Dec. 13	347	1032	1	-	-	-	81	84	83	-	-	-	82	-	84	-	-
75 Dec. 13	347	1227	1	-	-	-	69	-	71	-	-	-	70	-	72	-	-